Analysis of the role of the X/Y homologous gene family *Xmr/Sly* in murine spermiogenesis

Louise Nicole Reynard

Division of Stem Cell Biology and Developmental Genetics,
MRC National Institute for Medical Research
and
Department of Anatomy and Developmental Biology,
University College London

A thesis submitted to University College London for the degree of Doctor of Philosophy

April 2008

I, Louise Nicole Reynard, confirm that the work presented in this thesis is my own. Where information has been derived from other sources, I confirm that this has been indicated in the thesis.

……

Louise Nicole Reynard

Abstract

Spermatogenesis is a complex, continuous developmental process that involves the formation of highly differentiated haploid sperm from diploid spermatogonial stem cells. Deletion analysis has established that genes on the Y chromosome are essential for normal sperm production in humans, mice and *Drosophila*. In mice, deletions of the Y chromosome long arm (Yq) are associated with abnormal sperm head formation, reduced fertilising ability, up-regulation of spermatid-expressed sex-linked genes, and an offspring sex ratio distortion in favour of females. The severity of the testicular phenotypes correlates with the extent of the deletion, with mice lacking the Yq being sterile. It has been suggested that deficiency of a Yq-encoded multicopy genetic element (the 'spermiogenesis factor') is responsible for these phenotypes, and one potential candidate gene is *Sly*, a member of the *Xlr* superfamily. This family also includes *Xmr*, an X-linked multicopy gene found to be up-regulated (along with other X- and Y-encoded genes) in the Yq deletion models.

To access the candidacy of *Sly* as the 'spermiogenesis factor', the expression of this gene was examined in the testis at the transcript and protein levels. *Sly* encodes a protein that is expressed in round and early elongating spermatids. SLY interacts with the acrosomal protein DKKL1, suggesting that SLY may be involved in the development or function of the acrosome, a structure that contains digestive enzymes required for fertilisation.

Secondly, the role of *Xmr* in spermatogenesis was investigated. *Xmr* has been reported to encode a meiotic protein that localises to the transcriptionally silent sex body in pachytene spermatocytes. However, evidence is provided that this meiotic protein is not XMR, with the antibody used in previous studies unable to recognise XMR. Instead, *Xmr* is predominantly transcribed in spermatids were it encodes a cytoplasmic protein of unknown function.

Next, the up-regulation of X- and Y-linked genes in spermatids from the Yq deletion mice was studied in detail. This up-regulation is due, at least in part, to increased gene transcription, and this is accompanied by changes to the epigenetic profile of the sex chromosome and centromeric heterochromatin in round spermatids. In addition, the protein levels of the up-regulated genes are also increased in the testis from Yq

deletion mice, and thus the testicular phenotypes exhibited by these mice may be the result of over-expression of one or more X- and Y-encoded proteins, rather than a direct effect of Yq-linked gene deficiency.

Finally, mice transgenic for *Sly* were generated and characterised to determine if loss of this gene alone is responsible for the spermiogenic defects observed in mice with Yq deletions. *Xmr* transgenic mice were also produced to examine any potential regulatory interaction between *Sly* and *Xmr* and investigate if over-expression of *Xmr* contributes to the phenotypes exhibited by Yq deletion mice.

Index of Contents

Chapter 2. Materials and Methods

Index of figures

Chapter 5 Examination of sex chromosome transcription and epigenetic marks in spermatids from mice with MSYq deletion

Chapter 6. Generation and characterisation of *Sly* and *Slx* transgenic mice

List of tables

List of Abbreviations

AD	activation domain
Ade	Adenine
Amp	Ampicillin
APS	ammonium persulphate
BLAST	Basic Local Alignment and Searching Tool
bp	base pair
BSA	bovine serum albumin
cDNA	complementary DNA
cfu	colony forming units
CAM	Chloramphenicol
CMV	cytomegalovirus
CSK	cytoskeletal buffer
Da	Dalton
DAPI	4', 6-diamino-2-phenylindole
DB	DNA binding domain
DIG	Digoxigenin
ddH_20	double distilled water
DMEM	Dulbecco's Modified Eagle's Medium
DMSO	dimethyl sulphoxide
DNA	deoxyribonucleic acid
dNTP	deoxyribonucleotide triphosphate
d*pc*	days *post coitum*
d*pp*	days *post partum*
DSB	double stand break
DTT	dithiothreitol
EDTA	ethylene diamine tetraacetic acid
EGTA	ethylene glycol tetraacetic acid
EST	expressed sequence tag
EtOH	ethanol
FISH	fluorescent *in situ* hybridisation
g	gram
GAPDH	glyceraldehyde-3-phosphate dehydrogenase
GFP	green fluorescent protein

GSK-3	glycogen synthase kinase-3
HEPES	4-2-hydorxyethyl-1-piperazineethanesulfonic acid
His	histadine
Hr	hour
HRP	horseradish peroxidise
ICSI	intracytoplasmic sperm injection
IgG	immunoglobin G
Kan	kanamycin
Kb	kilo base
kDa	kilo Dalton
L	litre
LB	Luria Bertani
Leu	Leucine
M	molar
µg	microgram
µL	microlitre
mg	milligram
min	minute
mL	millilitre
µm	micrometer
mm	millimetre
mM	millimolar
µM	micromolar
MD	meiotic driver
mRNA	messenger RNA
MSCI	meiotic sex chromosome inactivation
MSUC	meiotic silencing of unpaired chromatin
MSY	male specific part of the Y chromosome
NCBI	National Centre for Biotechnology Information
ng	nanogram
NLS	nuclear localisation signal
NP40	Nonidet P40
OCT	optimal cutting temperature
OD	optical density
ORF	open reading frame

PAGE	polyacrylamide gel electrophoresis
PAR	pseudoautosomal region
PBS	phosphate buffered saline
PCR	polymerase chain reaction
PFA	paraformaldehyde
PGC	primordial germ cell
PMSC	post-meiotic sex chromatin
PSCR	post-meiotic sex chromosome repression
RNA	ribonucleic acid
R/T	room temperature
RT-PCR	reverse transcription polymerase chain reaction
rpm	revolutions per minute
SC	synaptonemal complex
SD	synthetic dropout
SDS	sodium dodecyl sulphate
SRD	sex ratio distorter
SSC	standard saline solution
SV40	Simian virus 40
TBE	tris borate EDTA
TEMED	N,N,N',N'-tetra-methyl-ethylenediamine
Tris	tris(hydroxylmethyl)aminomethane
Trp	Tryptophan
w/v	weight to volume
X-α-gal	5-Bromo-4-chloro-3-indolyl α-D-galactopyranoside

Chapter 1

Introduction

Introduction

1.1 The mammalian sex chromosomes

Genetic sex determination is very common and has evolved independently several times in different lineages including plants, birds, reptiles and mammals. The sex chromosomes (XY or ZW) differ phylogenetically and structurally between different taxa, but share many features due to the similar selective pressures shaping their evolution. For example, the hemizygous chromosome (i.e. the Y or W chromosome) tends to be small, heterochromatic and gene poor, while the homozygous chromosomes (the X or Z chromosomes) are similar in size and gene content to autosomes, although they have a propensity to cluster functionally similar genes (reviewed by Vallender and Lahn, 2005). The mammalian X and Y chromosomes are very different in size and gene content, but both chromosomes are enriched for genes involved in sexual differentiation and reproduction.

The eutherian (placental mammal) X chromosome consists of approximately five percent of the haploid genome and encodes for functionally diverse proteins, although it is enriched in genes involved in cognitive function and male fertility. The eutherian X chromosome is conserved in structure, gene content and gene order, except for the mouse and rat X chromosomes which have been rearranged compared to the X of other mammals (Ohno, 1967; Ross et al., 2005; Waters et al., 2007). In contrast, the Y chromosome varies significantly between placental mammals in structure, heterochromatin content, size, gene content and its homology to the X chromosome. The rapid evolution of the eutherian Y chromosome has resulted in the preservation of few genes other than those critical for testis determination (i.e. the sex determining factor *SRY*) and male reproduction, and it has been lost in two species of mammals (Waters et al., 2007). The human Y chromosome is very small (about 60Mb, 1-2% of the haploid genome) and encodes for 27 distinct proteins, leading to the eutherian Y chromosome being described as a 'genetic desert' (Burgoyne, 1998a), and a 'functional wasteland' (Quintana-Murci and Fellous, 2001). The mouse Y chromosome is larger but currently is only known to contain approximately 15 genes or gene families that are specialised for spermatogenesis and fertility.

1.1.1 Origin and evolution of the mammalian sex chromosomes

Although cytogenetically very dissimilar, there is strong theoretical and experimental data suggesting that the mammalian X and Y chromosomes evolved from a single pair of autosomes after one chromosome (the proto-Y) acquired a sex determining allele (Charlesworth, 1991; Muller, 1914; Ohno, 1967). The autosomal origin of the sex chromosomes is demonstrated by the presence of ancient X-Y homologous gene pairs on the marsupial and placental sex chromosomes and the identical gene content of pseudoautosomal region (PAR) regions of the X and Y chromosomes within a species (reviewed by Graves, 2006). The sex chromosomes of birds and snakes also appear to have differentiated from an autosomal pair, and Ohno (1967) suggested that the variation in the size and gene content of W chromosomes between different families of snake represented stages in the divergence of the female limited W chromosome from the Z chromosome.

The mammalian sex chromosomes formed within the last 300 million years, after the mammal, bird and reptile lineages diverged. Differentiation of the sex chromosomes is believed to have begun after the monotreme/therian split, when a single dominant testis determining allele arose by mutation of SOX3 to produce SRY. This formed the nascent or proto-Y chromosome bearing the SRY gene, and the proto-X chromosome containing the original SOX3 gene (Foster and Graves, 1994). Recombination between the proto-X and proto-Y chromosomes was suppressed around the sex-determining region and this resulted in the accumulation of sexually antagonistic male benefit genes surrounding the *SRY* locus. Suppression of recombination spread to encompass these genes, enlarging the male specific region of the Y chromosome (MSY), leading to further divergence of the sex chromosomes. Over time, continual linkage of male benefit genes to the Y chromosome gradually led to a step-wise loss of recombination along the entire Y chromosome except at the small PAR regions where the sex chromosomes pair and undergo recombination during meiosis. Deleterious mutations amassed on the Y chromosome because it was genetically isolated from the X chromosome, so corrupted sequences were not replaced by recombination. This led to the gradual decay of the Y chromosome as a result of 'hitch-hiking' of a degraded gene with a favourable mutation and random genetic drift; this is seen for the W chromosome in different snake families (Ohno, 1967). The evolution of the mammalian sex chromosomes is summarised in Figure 1.1.

Figure 1.1

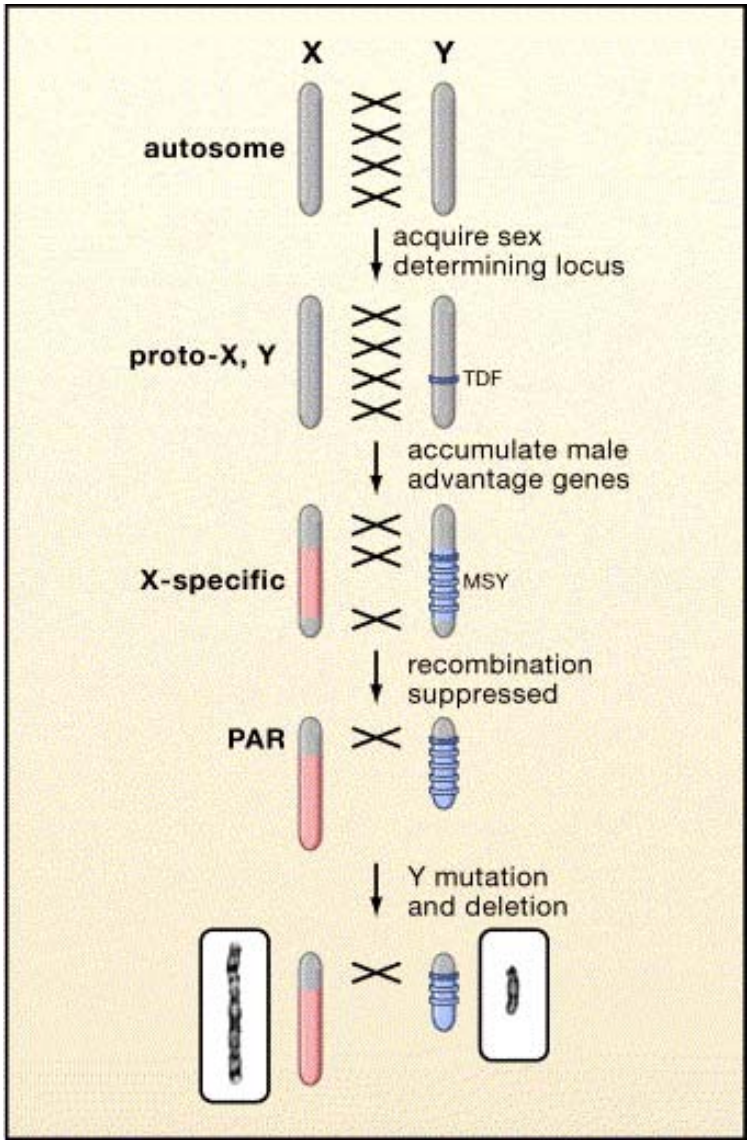

Figure 1.1 Differentiation of the mammalian sex chromosomes from an ancient pair of autosomes

Sex chromosome differentiation began when the Y chromosome acquired the testis determining factor *SRY*. The Y chromosome then accumulated male-specific alleles, leading to suppression of recombination (represented by crosses) between the two chromosomes. This created a male specific region on the Y (MSY). Lack of recombination led to MSY degradation, leaving a small pseudoautosomal region (PAR) of shared homology between the X and Y chromosomes. Genes on the Y chromosome were lost except for male advantage genes such as those involved in spermatogenesis and fertility.

This figure is taken from the review by Graves, 2006.

The eutherian sex chromosomes are thought to have further evolved by several cycles of gene addition and attrition as autosomal regions were added to the PAR of one sex chromosome and gradually degraded on the Y chromosome after the PAR boundaries moved (the addition-attrition model; Graves, 1995; Graves, 1998). The marsupial X chromosome contains genes found on the long arm and pericentric region of the human X chromosome, and thus is thought to represent the ancient X-conserved region (XCR) present on the original autosome before the proto-Y chromosome acquired the testis determining factor; these genes share homology to a region of the chicken chromosome 4p. However, the human X short arm contains several genes found on the X chromosome in other placental mammals but not in monotremes or marsupials, suggesting this X added region (XAR; Graves, 1995) was added after the marsupial/placental split but before the placental radiation. Genes within the XAR map to three autosomal clusters in marsupials and monotremes, suggesting there has been at least three autosomal translocation events onto the PAR during eutherian sex chromosome evolution (Ross et al., 2005; reviewed by Graves, 2006). These added regions were then subject to recombination suppression on the Y chromosome when the PAR boundary moved as a consequence of a chromosome rearrangement event such as an inversion, ultimately resulting in mutation and attrition of the added region.

Evidence for the addition of autosomal regions to the PAR of the eutherian X chromosome comes from sequence comparisons between X-Y homologous genes in humans and mice (Lahn and Page, 1999; Ross et al., 2005; Sandstedt and Tucker, 2004). Lahn and Page (1999) looked at 19 differentiated X-Y homologous genes on the human sex chromosomes, and found that the age of the different gene pairs correlated with the position of the gene on the X chromosome, with age decreasing from the distal tip of the long arm. Based on the degree of sequence divergence, these 19 genes can be subdivided into at least four groups or evolutionary strata; this indicates that divergence of the human sex chromosomes was punctuated by at least four incidences of XY recombination suppression, probably caused by Y chromosome inversions that reduced the size of the PAR. The oldest two strata (strata 1 and strata 2) identified by Lahn and Page (1999) correspond to the XCR identified by Graves (1995), and includes the SOX3/SRY pair, providing evidence that sex chromosome differentiation began when these genes stopped recombining. Sandstedt and Tucker (2004) reported a similar finding for X-Y homologous genes in mice, although the murine sex chromosome lack genes in human strata 4, which are thought to have been

added by a translocation event in the primate lineage (Sandstedt and Tucker, 2004). Human X-Y gene pairs in strata 3 and 4 represent those added after the marsupial/placental split (the XAR of placental mammals) and recent re-evaluation of these strata suggests that these can be redefined into three strata on the X chromosome based on new sequencing data, each one representing an inversion event that prevented recombination between the X and Y homologues (Ross et al., 2005). Furthermore, sequence analysis of the human *AMEL* gene on the Y chromosome suggests that the PAR boundary between strata 3 and 4 may once have been within this gene, because X-Y sequence diversity is three times higher in the 5' region of this gene than in the 3' region (Iwase et al., 2003; Marais and Galtier, 2003).

1.1.2 Accumulation of male benefit genes on the mammalian X chromosome

Genes that assist male reproduction but are unfavourable to females are predicted to be driven off the mammalian X chromosome during evolution because this chromosome spends two-thirds of its time in females (Wu and Xu, 2003). Sexually antagonistic alleles are alleles of the same gene which enhance the reproductive success of one sex but are detrimental to the other sex. Fisher (1931) proposed that sexually antagonistic alleles that are beneficial to females have an increased probability of spreading through a population if they are X-linked than if they were on an autosome. Together, these processes are expected to result in a dearth of male benefit genes on the mammalian X chromosome. However, several studies have demonstrated that this is not the case; the mouse X chromosome is enriched for testis genes expressed before or after meiosis, and there is a three-fold increase in sex or reproduction related genes on the human X chromosomes compared to autosomes (Khil et al., 2004; Mueller et al., 2008; Saifi and Chandra, 1999; Wang et al., 2001).

Wang and colleagues (Wang et al., 2001) suggested that the main evolutionary processes that account for the masculinisation of the mammalian X chromosome are meiotic drive and hemizygous exposure of male benefit genes. During evolution, the sex chromosomes are thought to be much more likely to accumulate genes that favour their own transmission (meiotic drivers) than autosomes, leading to an enrichment of genes involved in spermatogenesis and sperm function on the X chromosome. This hypothesis is supported by the finding that at least 273 genes (out of a total of 1,555 genes) on the mouse X chromosome are expressed predominately or exclusively in

haploid male germ cells, where they are assumed to be involved in sperm development (Mueller et al., 2008). Furthermore, several of these X-encoded spermatid-expressed genes are over-expressed in males that have a distorted offspring sex ratio in favour of females (Ellis et al., 2005).

Rice (1984) postulated that the X chromosome should evolve to carry a disproportionate number of male specific genes that function in male differentiation and fertility due to the hemizygous exposure of male-benefit alleles. If an X-linked gene acquires a recessive sexually antagonistic allele that bestows a male reproductive advantage, the effect of the mutation will be immediately beneficial in males. The mutation will rapidly reach fixation within a population even if the advantage to males is less than the cost to females because the effect will be masked in females (where it is detrimental) by the presence of a second X chromosome. As the mutation increases in frequency, homozygous females will appear in the population and these will have reduced reproductive fitness due to the sexually antagonistic nature of the gene. There will then be strong selective pressure for the spread of new modifier alleles that mitigate the deleterious effect in females by restricting expression of the original gene to the testes. A similar process occurs when the original male-benefit mutation has no effect on female fitness. Over time this will lead to an accumulation of spermatogenesis genes on the mammalian X chromosome. However, sexually antagonistic male benefit alleles that arise on an autosome are unlikely to spread to fixation because the recessive effects are hidden and the disadvantage to females must be less than the advantage to males.

Even X-linked genes not originally involved in reproduction are envisaged to evolve sex-related functions as a result of sex-specific selection (Graves, 2006; Hurst and Randerson, 1999). The predilection of the mammalian X chromosome to accrue reproduction-related genes could assist mammalian speciation by providing pre-mating and post-mating reproductive barriers, leading to Graves and colleagues to label the mammalian X chromosome ‘the engine of speciation’ (Graves et al., 2002).

1.1.3 Attrition and functional specialisation of the Y-linked genes

Genes on the mammalian Y chromosome appear to have three evolutionary fates:

inactivation and loss, functional preservation, or specialisation to a male specific function (see Figure 1.2.A; Lahn et al., 2001). It is clear that the majority of X-Y homologous genes present on the ancestral autosome, as well as those added subsequently by translocations to the PAR, have been mutated and deleted on the Y chromosome in placental mammals due to the lack of recombination on the MSY. Rice and Friberg (2008) suggested that the attrition of the Y chromosome slows down over time and may even stop. They argued that as the number of genes on the Y chromosomes falls, the efficiency of natural selection increases on the remaining genes (Rice and Friberg, 2008). An intermediate step in Y gene attrition may be restriction of expression to the testis, either at the transcription level (e.g. *Zfy*, *Ube1y* and *Usp9y* in mice: Brown et al., 1998; Mardon and Page, 1989; Odorisio et al., 1996) or at the level of translation (e.g. DDX3Y in humans: Ditton et al., 2004).

After being limited to the male germ line, the Y-linked copy of an X-Y homologous gene pair may become amplified, as is the case for *RBMY/Rbmy* in humans and mice. Recently added species-specific Y-linked genes have also become amplified, such as *Ssty* in mice and *DAZ* in humans, suggesting that gene duplication is a common phenomenon during Y chromosome evolution. This may provide a mechanism to protect against harmful gene mutation – although one copy may become mutated, other intact copies remain that can carry out the function of the gene and act as further substrate for amplification (Lahn et al., 2001). The MSY regions of placental Y chromosomes are commonly enriched for repetitive DNA such as retroviral elements and these are thought to mediate frequent duplication of flanking genes (Eicher et al., 1989; Eicher and Washburn, 1986; Fennelly et al., 1996; Foote et al., 1992; Lahn and Page, 1997; Lahn et al., 2001; Vollrath et al., 1992). The male specific region of the human Y chromosome contains eight large palindromes comprising approximately 25% of the euchromatic region, and at least six of these palindromes contain testis-expressed genes (Skaletsky et al., 2003). Multicopy genes within these palindromes have been shown to undergo gene conversion events (non-reciprocal transfer of DNA from one homologous locus to the other) by intra-chromosomal recombination between different copies located within a palindrome, maintaining an intra-palindromic sequence identity of over 99.9% (Rozen et al., 2003; Skaletsky et al., 2003). This gene conversion has been proposed to reduce the mutational load and thus functional decay of the human Y chromosome and it is possible that a similar

mechanism has evolved independently a number of times in different eutherian lineages (Gvozdev et al., 2005; Rozen et al., 2003; Skaletsky et al., 2003).

Several X-Y homologous genes have been retained on the eutherian Y chromosome including *ZFY*, *JARID1D*, *RBMY* and *SRY*. For genes to have been preserved during mammalian evolution, they must have been selected for either because they have dosage critical functions or because they have acquired male-specific functions. In humans, *ZFY* and *JARID1D* are ubiquitously expressed and are thought to have been preserved because they have dosage-critical functions - their X-linked homologues are also ubiquitously expressed and escape somatic X-inactivation (Agulnik et al., 1994a; Agulnik et al., 1994b; Palmer et al., 1990b; Schneider-Gädicke et al., 1989). The mouse *Eif2s3y* gene has also been retained due to haploinsufficiency; loss of this gene in males can be compensated for by an extra copy of the *Eif2s3x* gene, suggesting that these two genes have redundant functions (Burgoyne and Mitchell, 2007; Mazeyrat et al., 2001). Although *Eif2s3y* is expressed in a wide range of tissues, haploinsufficiency of EIF2S only affects the male germline. In addition, the Y-linked copy of an X-Y gene pair may have evolved a specialised role in testis determination (e.g. *SRY*) or male fertility. For example, the Y-linked members of the *RBM* gene family have become testis-specific in humans and mice (Mahadevaiah et al., 1998), while the X-encoded members are expressed in a wide variety of tissues. Moreover, these genes have been amplified on the Y chromosome in humans and mice, and are a candidate for the human AZFb azoospermia factor (Elliott and Cooke, 1997; Najmabadi et al., 1996).

The gene content of the Y chromosome varies between even closely related mammalian species due to different rates of gene attrition, and addition of different genes either directly to the MSY by transposition or via the PAR (Figure 1.2.B). Genes that are important in one species have been lost in others, possibly when their function was replaced by over-expression of the X homologue or by an autosomal retrogene. An example of this is the mouse *Eif2s3y* gene which is vital for type A spermatogonial proliferation – this gene has been lost in humans, perhaps when its function was replaced by the *Eif2s3x*-derived autosomal retrogene (Ehrmann et al., 1998). Alternatively, homologous genes may have evolved separate roles in different mammalian species so are no longer functionally redundant.

Asexual degradation of the Y chromosome predicts that there will be a generalised loss of Y genes over time due to lack of recombination. Inconsistent with this idea is the vast enrichment of male benefit genes on the male-specific part of the Y chromosomes in different eutherian species, despite their divergent structure and gene content. Thus, during the eutherian radiation, the mammalian Y chromosome has become masculinised, and an extreme example of this is the functional specialisation of the mouse Y chromosome. Analysis of XO female mice indicates that the Y chromosome is dispensable for somatic development, in contrast to the situation in humans. Moreover, all MSY-encoded genes are expressed in the testis and examination of deletion variants suggests that the function of the mouse Y chromosome is restricted to testis-determination and spermatogenesis.

One reason for the enrichment of male-advantage genes on the Y chromosome is the preservation of Y genes that have evolved specialised functions in male fertility. However, the placental Y chromosomes are also thought to have accumulated male benefit genes directly onto the MSY such as *CDY* and *DAZ* in humans, and some of these genes may be sexually antagonistic. Although there is no direct evidence of sexually antagonistic genes on the human Y chromosome, it has been noted that approximately 30% of females that carry Y chromosome material develop an ovary tumour known as a gonadoblastoma, and this has been suggested to be a manifestation of sexually antagonistic genes on the Y chromosome (Tsuchiya et al., 1995; Vallender and Lahn, 2005). Male benefit genes on the Y chromosome will immediately be expressed in males and so will be selected for. Moreover, they are restricted to males, and so any costs to female reproductive fitness will be avoided. Constant unidirectional selection will drive any Y-linked male benefit gene to fixation within a population more rapidly than for an autosomal or an X-linked gene, and genes involved in sperm development and function are especially likely to benefit from this (Vallender and Lahn, 2005). However, the effect of random genetic drift is expected to be greater for the Y chromosomes because the effective population size of the Y chromosomes is four fold smaller than that of the autosomes and three times smaller than the X chromosome. In theory, small effective population size decreases the efficiency of selection and increases the role of genetic drift in the extinction and selection of alleles (Ohta, 2002; Vallender and Lahn, 2005).

In conclusion, during their evolution, the sex chromosomes have become specialised

for functions involved in male fertility by a variety of selective processes. This has led to an enrichment of testis-expressed genes on the mouse X and Y chromosomes.

Figure 1.2 The fate of genes on the mammalian Y chromosome

This figure had been adapted from figures 4 and 5 from Graves, 2006.

A) Addition, attrition and specialisation of Y-encoded genes during mammalian evolution.

Genes become restricted to the male specific region of the Y chromosome by suppression of recombination between the X and Y chromosome during meiosis. During evolution, the majority of genes on the mammalian Y chromosome have become inactive (white) and were lost. However, some of the genes on the original proto-Y chromosome remain active (purple) or partially active (lilac), while a few genes acquire a male specific function in sex or spermatogenesis (dark blue). Many of the male specific genes become amplified (indicated by arrows) and amplified copies may be degraded. Some genes originate from autosomes by transposition or retrotransposition (yellow), and become restricted to the male germ line.

B) Gene content of the Y chromosome in different mammals

Schematics of the Y chromosome structure and content in different mammalian species (taken from Graves, 2006). The rapid and independent genetic erosion of the ancestral proto-Y chromosome accounts for the significant variation in the size and structure of the Y chromosome in placental mammals as well as the dissimilar gene content. Genes on the Y chromosome that are critical in one species (e.g. the mouse *Eif2s3y* gene) may have been lost or acquired a different function in another species. Genes that are located within the pseudoautosomal region (PAR) are indicated in purple, active MSY-encoded genes are denoted in blue. Pseudogenes are light blue, and deleted genes are grey. Orange denotes genes that have been transposed from an autosome.

Note that sequence analysis indicates the spermatid-specific *Ssty* and *Sly* genes located on the mouse long arm did not originate directly by transposition from an autosome. Instead, these genes arose by transposition of an X-linked homologue (*Sstx* and *Xlr*/*Xmr* respectively) that was already restricted to spermatids. In both cases, the X-encoded progenitor gene is thought to have evolved from an ancestral gene (the *Spin* gene in the case of *Sstx* and *Sycp3* in the case of *Xlr*/*Xmr*) expressed exclusively in the male and female germlines.

The DAZ gene was not present on the ancestral Y chromosome but arose by retrotransposition of the autosomal DAZL gene in the primate linage 30-40 million years ago.

Figure 1.2

A)

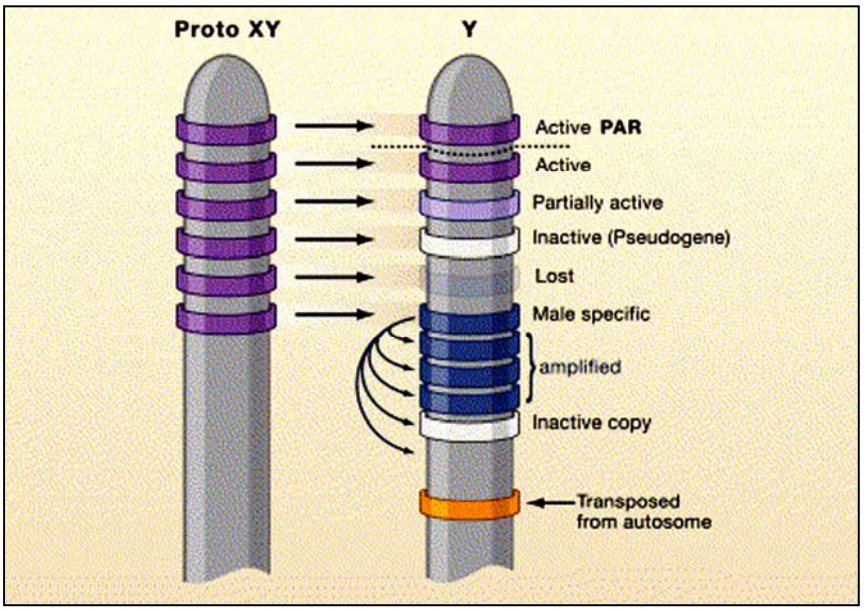
Proto XY
Y
Active PAR
Active
Partially active
Inactive (Pseudogene)
Lost
Male specific
amplified
Inactive copy
Transposed from autosome

B)

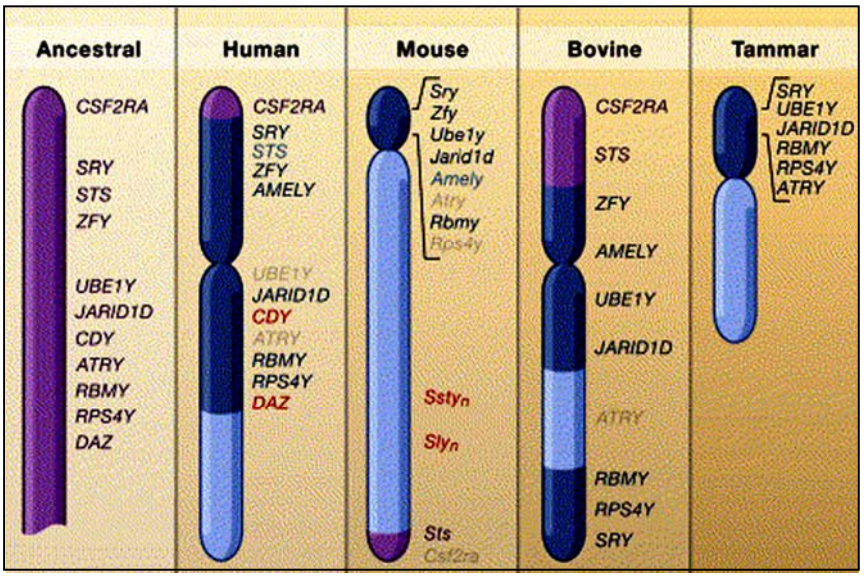
Ancestral
CSF2RA
SRY
STS
ZFY
UBE1Y
JARID1D
CDY
ATRY
RBMY
RPS4Y
DAZ
Human
CSF2RA
SRY
STS
ZFY
AMELY
UBE1Y
JARID1D
CDY
ATRY
RBMY
RPS4Y
DAZ
Mouse
Sry
Zfy
Ube1y
Jarid1d
Amely
Atry
Rbmy
Rps4y
Sstyn
Slyn
Sts
Csf2ra
Bovine
CSF2RA
STS
ZFY
AMELY
UBE1Y
JARID1D
ATRY
RBMY
RPS4Y
SRY
Tammar
SRY
UBE1Y
JARID1D
RBMY
RPS4Y
ATRY

1.2 Spermatogenesis

Spermatogenesis is a term used to describe a series of complex, developmental processes that are involved in the formation of highly differentiated haploid sperm from diploid spermatogonial stem cells. It proceeds in clearly defined stages that can be divided into three phases of approximately equal length; spermatogonial proliferation (spermatogoniogenesis; Hilscher, 1981), meiosis, and spermiogenesis (sperm differentiation). In mammals, the sequence of spermatogenesis is well conserved (Delbridge and Graves, 1999; Russell et al., 1990) and takes place within the seminiferous tubules of the testes. Spermatogenesis is initiated at puberty and is a continuous process that ensures the constant production of sperm in reproductively active adult males. Timing of spermatogenesis is highly controlled, and takes approximately 35 days to complete in mice (Oakberg, 1956b).

1.2.1 The testes

Testis development is initiated by expression of *Sry* in the bi-potential gonad during embryogenesis, which triggers the steroidogenic supporting cell and germ cell lineages to commit to the male pathway. The establishment of the spermatogonial stem cell pool and the initiation of spermatogenesis occur after birth. The testes contains over ten different cells types within a fibrous capsule and can be divided into two physiological compartments, the interstitial compartment and the avascular seminiferous tubules (Bellve, 1993; Bellvé et al., 1977; Eddy, 2002; Guraya, 1980). The interstitial compartment is vascularised and contains steroidogenic Leydig cells, whose principal role is thought to be the synthesis and secretion of androgens, especially testosterone (Mendis-Handagama, 1997). The seminiferous epithelium is divided into the basal and adluminal compartments and consists of the non-dividing somatic Sertoli cells and germ cells undergoing spermatogenesis.

Germ cell differentiation is dependent on complex paracrine interactions with Sertoli cells (Skinner et al., 1991), which are thought to stimulate germ cells by secreting regulatory molecules such as growth factors and proteases (Griswold, 1998). The Sertoli cells comprise approximately 25% of the seminiferous epithelium (Cavicchia and Dym, 1977) and are necessary for maintaining the tubule environment. The Sertoli

cell cytoplasm reaches towards the tubule lumen and is in intimate contact with proliferating and differentiating germ cells, providing nutritional and physical support for spermatogenesis (Griswold, 1998). The seminiferous tubules are surrounded by a limiting membrane which provides physical support and consists of collagen fibres, fibroblasts and contractile myoid cells that are thought to supply the motive power to propel the sperm through the testicular tubules into the epididymis (Guraya, 1980; Guraya, 1987; Maekawa et al., 1996)

Figure 1.3

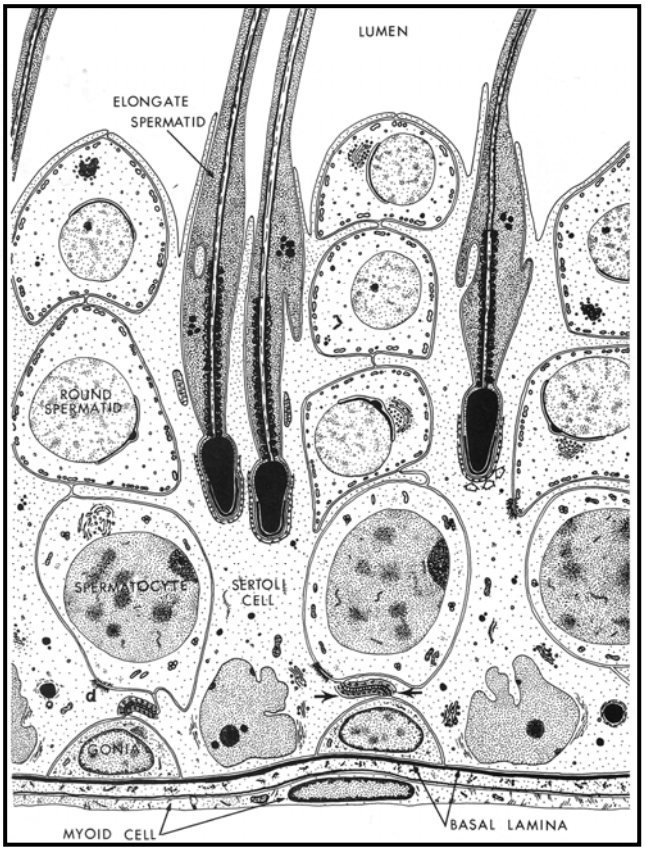

Figure 1.3 A schematic diagram of the seminiferous tubule epithelium in mice

As germ cells mature from spermatogonia to spermatids, they move from the basal lamina towards the lumen of the tubule. Elongating and condensing spermatids reside within crypts of the Sertoli cell and so may appear between other germ cell types. The Sertoli cell cytoplasm extends from the basal lamina to the lumen and makes contact with germ cells of all stages, as well as neighbouring Sertoli cells.

Taken from Russell et al., 1990.

Figure 1.4

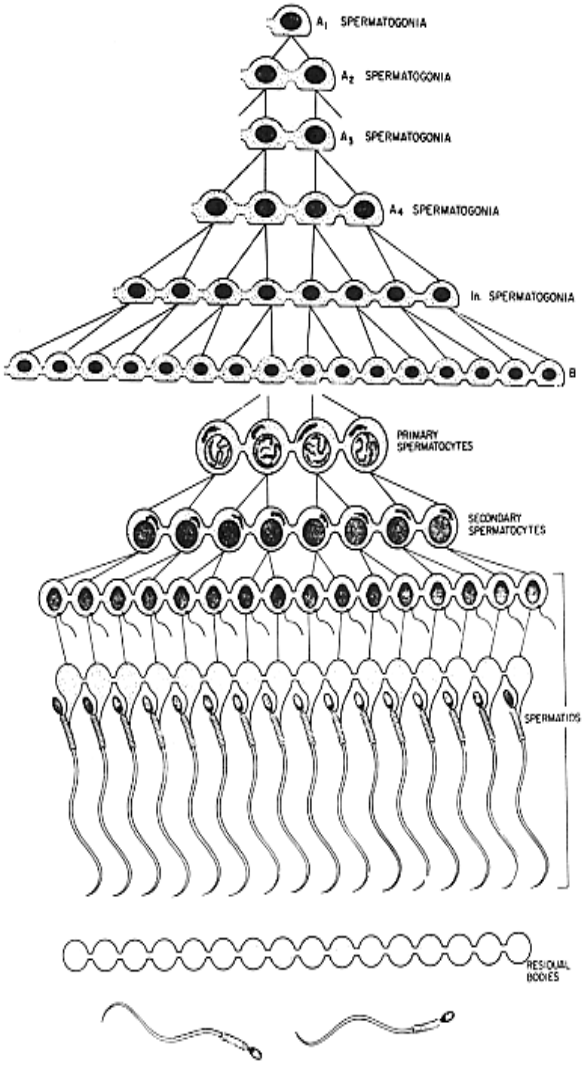

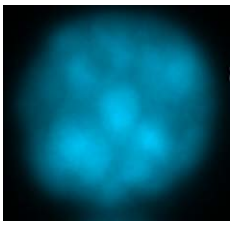

Spermatogonium

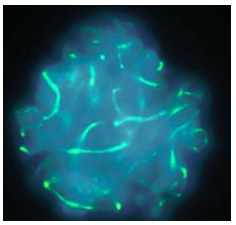

Spermatocyte
(meiotic cell)

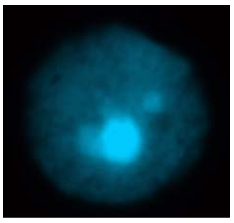

Round spermatid
(post meiotic)

Figure 1.4 Murine Spermatogenesis

Schematic representation of the stages of spermatogenesis, modified from Russell et al. (1990).

The nuclei of different spermatogenic subtypes can be accurately identified using 4', 6-diamino-2-phenylindole (DAPI, shown in blue) and antibody markers (e.g. presence or absence of the synaptonemal complex protein SYCP3, shown in green)

1.2.2 Spermatogonial proliferation

Spermatogonial stem cells are immature germ cells that arise from primordial germ cells (PGCs). These stem cells divide to renew and to produce differentiating spermatogonia that in mice undergo nine to eleven mitotic divisions to form a large number of preleptotene spermatocytes. Preleptotene spermatocytes subsequently go through meiosis to generate the haploid cells (spermatids) that differentiate into mature sperm. Primordial germ cells inhabit the epiblast of the gastrulating embryo and migrate back into the embryo from the extraembryonic mesoderm via the allantois, where they collect (reviewed by McLaren, 2001; McLaren, 2003). The PGCs move into the yolk sac and travel through the newly formed hindgut and up the dorsal mesentery into the genital ridge. They populate the genital ridge from 11*dpc* and there are approximately 2500 to 5000 PGCs in the gonad by 12*dpc*, when sexual differentiation is first apparent (Chiquoine, 1954; Tam and Snow, 1981; Wylie and Heasman, 1993). Once in the gonad, the PGCs grow and divide for approximately three days during gonadal differentiation before becoming arrested at G0/G1 phase of the cell cycle at about 15d*pc*.

Spermatogenesis initiates shortly after birth within the basal compartment of the seminiferous tubule when mitogenic factors secreted by the Sertoli cells trigger arrested prespermatogonial stem cells to divide into undifferentiated $A_{isolated}$ spermatogonia. These $A_{isolated}$ spermatogonia act as stem cells and can undergo mitosis to form A_{paired} spermatogonia. Some $A_{isolated}$ spermatogonia fail to transform into A_{paired} spermatogonia, and instead, undergo self renewal and migrate along the basement membrane to form a constant pool of spermatogonial stem cells which can start the cycle again. A_{paired} spermatogonia divide to form $A_{aligned}$ spermatogonia; together these two cell types are known as proliferative spermatogonia and are thought to be able to self-renew. $A_{aligned}$ spermatogonia divide and differentiate to form differentiating spermatogonia (type A_1 spermatogonia, intermediate and type B spermatogonia). Type B spermatogonia go through a final mitotic division to produce preleptotene spermatocytes (Bellvé et al., 1977; Clermont and Perey, 1957). Spermatogonia reside next to the basal lamina of the tubule and are connected to other spermatogonia of the same sub-type by intercellular bridges that may allow movement of RNA and proteins between cells, leading to synchronous development of cells within a clone.

1.2.3 Meiosis

Meiosis occurs in the adluminal compartment of the seminiferous epithelium and consists of DNA replication followed by two reduction divisions to form four haploid spermatids from each primary spermatocyte. Meiotic prophase I can be subdivided into five stages and commences when preleptotene spermatocytes replicate their DNA to form leptotene spermatocytes. During leptotene, the DNA is uncondensed and chromosomes consist of two sister chromatids joined at the centromere. In mice, the centromeres cluster to form several DNA dense regions of the nucleus and axial elements begin to develop between sister chromatids. Double-strand breaks (DSBs) are initiated in leptotene spermatocytes, and these DSBs are essential for normal pairing of homologous chromosomes. During zygotene, homologous chromosomes begin to align side by side (pairing) and then synapse, forming a synaptonemal complex (Parra et al., 2003). The synaptonemal complex is a proteinaceous 'zipper' like-structure that consists of a central element (the axial element) and two lateral elements joined by transverse filaments. Synapsis of the autosomes is completed by the beginning of pachytene and the chromosomes thicken and condense. The X and Y chromosomes begin to pair via their homologous pseudoautosomal regions (PARs), and form a cytologically distinct sex body (Solari, 1974). Sex chromosome synapsis initially spreads beyond the PAR regions, but this regresses during pachytene so the X and Y chromosomes are unpaired along most of their length.

In pachytene spermatocytes, homologous chromosomes undergo recombination, allowing the exchange of genetic material at sites known as chiasmata or recombination nodules (Carpenter, 1987). Meiotic recombination is initiated at 200-400 sites throughout the genome in mammals but only 10% of these result in exchange of DNA (Baudat and de Massy, 2007). In mice, failure of synapsis or recombination causes complete pachytene arrest and infertility, as demonstrated by male mice with mutations in genes such as *Dmc1, Msh5, Sycp1-3*, and *Syce2* (Bolcun-Filas et al., 2007; de Vries et al., 2005; de Vries et al., 1999; Edelmann et al., 1999; Pittman et al., 1998; Yang et al., 2006; Yoshida et al., 1998; Yuan et al., 2000). In diplotene spermatocytes, the synaptonemal complex disassembles, and homologous chromosomes start to separate except at the chiasmata where recombination took place. During diakinesis, the centromeres move away from each other, the nuclear envelope breaks down and the chromosomes align at the metaphase plate. Homologous

chromosomes separate at anaphase I and the cell divides meiotically to produce two secondary spermatocytes, each containing one chromosome from each pair. Meiotic prophase II is brief and sister chromatids are separated during the second meiotic division to form four genetically distinct haploid round spermatids that are connected by cytoplasmic bridges.

1.2.4 Spermiogenesis

The term spermiogenesis refers to the dramatic morphological differentiation of round spermatids into mature spermatozoa and has been described as 'one of the most phenomenal cell transformations in the body' (Russell et al., 1990). Spermatid remodelling is necessary for the production of functional motile spermatozoa (sperm) and consists of several simultaneous events including chromatin condensation, acrosome formation, and removal of the residual cytoplasm. The sperm is organised into an anterior head structure which contains the DNA and proteins required for fertilisation, and a tail which is important for passage through the female reproductive tract. In mice, spermiogenesis is a regimented and synchronised process that can be divided into 16 stages based on the structure of the acrosome (Oakberg, 1956a; Russell et al., 1990; see figure 1.5). Once spermiogenesis is completed, the cytoplasmic bridges between cells are broken and the sperm are released into the tubule lumen (spermiation), where they are propelled to the epididymis in testicular fluid secreted by the Sertoli cells. The main events that occur during spermatid differentiation are described below.

Flagellum formation

Development of the flagellum is a continuous process which begins at the start of spermiogenesis and is not completed until spermiation occurs. It commences when one of the centrioles develops into the axoneme after they migrate to the spermatid cell surface, causing the protrusion of the spermatid plasma membrane from the cell. During spermiogenesis, the flagellum travels to the nucleus and is found opposite the acrosome, where the mid, principal, and end pieces are formed by the addition of accessory machinery. Cytoplasmic mitochondria are conscripted to the flagellum, where they provide energy for sperm motility. In mammals, outer dense fibres form in the mid and principal piece of the flagellum and a fibrous sheath surrounds the

flagellar axoneme. This sheath is thought to act as a scaffold for the localisation of signal transduction factors and energy-producing enzymes. The fibrous sheath may also function with the outer dense fibres to boost the driving force of the flagellum (Eddy et al., 2003). Sperm motility develops in the epididymis but vigorous movement only occurs in the female reproductive tract.

Development of the acrosome

Acrosome formation is a slow process that is similar in all mammals but the exact shape and content of the acrosome is specific to each species. At stage 2 of murine spermiogenesis, the Golgi produces small proacrosomal vesicles that contain a dense proacrosomal granule. These proacrosomal vesicles fuse to form a single acrosomal vesicle at spermatid stage 3 and this flattens as it makes contact with the nucleus at stage 4. The acrosomal granule remains dense and the developing acrosome increases in size as the Golgi body contributes more material to it. The Golgi moves away from the acrosome as the nucleus progressively elongates and the acrosome stops increasing in size but becomes uniformly dense. At stage 8, the spermatids orientate themselves so that the acrosome faces the basement membrane, initiating the acrosomic phase of development. Between stages 9 and 12, the spermatid nucleus becomes elongated and the cytoplasm is stretched along the flagellum, elongating the cell. The shape of the head and acrosome changes before sperm release, and the acrosome appears as an elongated crescent at spermatid stage 14. The nucleus narrows during stage 15 and the tip of the maturing sperm continues to develop into a sickle shape.

Nuclear DNA condensation

During spermiogenesis, the genome undergoes condensation and changes from a nucleosome based histone-rich chromatin structure to a predominantly protamine based chromatin structure. The pattern of DNA compaction varies between species, and together with the manchette (a cytoskeletal complex formed around the nucleus by microtubules), contributes to the species-specific shape of the sperm nucleus. DNA condensation reduces the volume of the sperm and acts with cytoplasmic elimination to streamline the sperm head, enabling efficient movement through the fluid environment of the female reproductive tract. In elongating spermatids, DNA condensation is initiated by a wave of histone acetylation (Hazzouri et al., 2000) which is followed by replacement of histones with the transition proteins, TP1 and TP2, at spermatid stage 12. This results in heterochromatinisation of the genome, silencing

transcription. These transition proteins are exchanged for protamines at spermatid stage 14 when further nuclear elongation occurs, ensuring tight packaging of the DNA (Meistrich 1989; Alfonso and Kistler, 1993). However, not all histones are replaced, with 10-15% of histones retained in the human sperm nucleus. These histones are enriched at imprinted loci, genes transcribed early in embryogenesis and heterochromatic regions (Gardiner-Garden et al., 1998; Rousseaux et al., 2005; Wykes and Krawetz, 2003). Telomeres and centromeres are enriched in H2B variants and histone H3 variant CENP-A respectively (Churikov et al., 2004; Gineitis et al., 2000; Palmer et al., 1990a; Wykes and Krawetz, 2003; Zalensky et al., 2002). Two recently identified histone variants participate in the formation of nucleoprotein structures specifically in the pericentric heterochromatic regions in mice (Govin et al., 2007).

Elimination of spermatid cytoplasm

During the elongating steps of spermiogenesis, water is thought to be eliminated from the cytoplasm. The cytoplasm itself is discarded just before the mature sperm are released into the tubule lumen. The Sertoli cells phagocytose the cytoplasmic fragments and transport them to the base of the tubule.

Figure 1.5

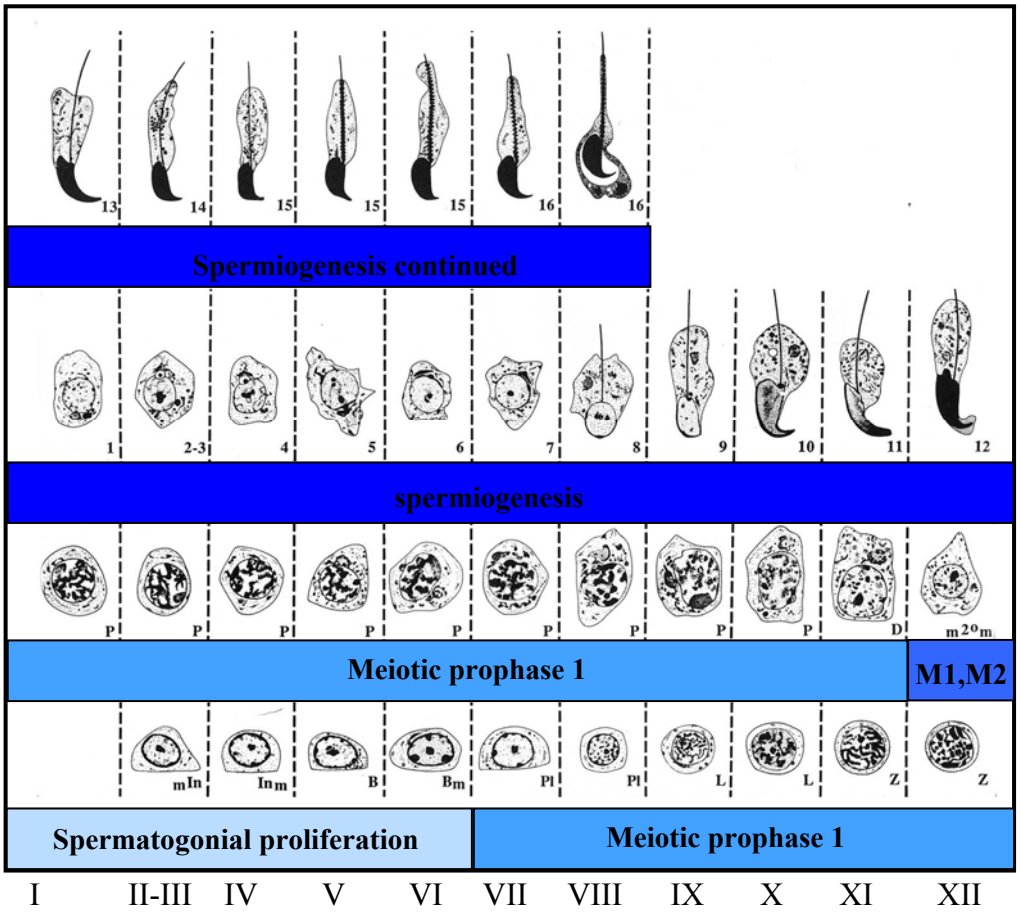

Figure 1.5 The twelve stages of murine spermatogenesis

Oakberg (1956b) divided spermatogenesis into twelve stages in the mouse (represented by vertical columns labelled with roman numerals). Each stage has a specific subset of germ cell types within a cross sectioned tubule segment that are at particular developmental time point. During spermatogenesis, germ cells divide and differentiate from immature spermatogonia (bottom row, left hand corner) into mature sperm (top row) before being released into the lumen of the seminiferous tubule at stage IX. Each spermatogenetic stage will occur in order in a given segment of the seminiferous epithelium (the spermatogenic cycle) before being initiated again. There are sixteen steps of spermiogenesis (dark blue) which are largely defined by the structure of the acrosome (Oakberg, 1956a).

Modified from Russell et al., 1990.

1.3 Sex chromosome gene activity during spermatogenesis

The transition from spermatogonium to mature sperm is accompanied by dramatic changes in X and Y gene transcription. During the spermatogonial divisions, the sex chromosomes are transcriptionally active, with almost all of the genes on the Y short arm (Yp) being transcribed. The Y chromosome plays an essential role during this proliferative period, and male mice lacking a segment of the Y short arm show complete spermatogonial arrest (Burgoyne et al., 1986). This is due to the absence of the Y-linked *Eif2s3y* gene which is required for proliferation of differentiating A spermatogonia (Mazeyrat et al., 2001). The X chromosome also has a major role in the pre-meiotic stages of spermatogenesis and is enriched for genes expressed in spermatogonia in both mice (Khil et al., 2004; Wang et al., 2001) and humans (Lercher et al., 2003; Saifi and Chandra, 1999). This is in agreement with the hypothesis that genes that are beneficial to males will accumulate on the X chromosome during evolution due the hemizygous nature of this chromosome in males (Fisher, 1931; Rice, 1984). Wang and colleagues (Wang et al., 2001) reported that there is an approximately 15-fold enrichment of male germ cell-specific spermatogonially expressed genes on the mouse X chromosome. Further evidence that spermatogonial genes are over-represented on the mouse X chromosome comes from microarray analysis of *Spo11*-/- testes. Spermatogenesis in *Spo11*-/- mice arrests during meiosis at the mid pachytene stage and thus the testes are enriched for pre-meiotic cells including spermatogonia. Genes transcribed before the *Spo11*-/- block are significantly more dense on the X chromosome, as are genes expressed in juvenile mice up to 11 days old (Khil et al., 2004). Targeted inactivation of several spermatogonially expressed genes identified by Wang et al. (2001) has demonstrated that the majority of these cause meiotic defects (reviewed by Wang and Pan, 2007). One such gene is *Nxf2*, an X-linked gene involved in nuclear mRNA export. This suggests that the X and Y chromosome may play an important role in regulation of meiosis as well as being necessary for the proliferative stage of spermatogenesis.

Although active during the leptotene and zygotene stages of meiosis, the sex chromosomes are rapidly silenced at the zygotene-pachytene transition, when autosomal chromosome synapsis is complete. The X and Y chromosomes are compartmentalised into a specialised chromatin domain known as the sex body (Solari, 1974; Turner, 2007). This phenomenon is called Meiotic Sex Chromosome

Inactivation (MSCI; McKee and Handel, 1993) and is a manifestation of MSUC (Meiotic Silencing of Unsynapsed Chromatin; Baarends et al., 2005; Schimenti, 2005; Turner et al., 2004). MSUC is a universal mechanism used to silence the chromatin associated with chromosome axes that remain unsynapsed during the pachytene stage of meiosis. MSCI is initiated when the tumour suppressor protein BRCA1 recruits the kinase ATR to the asynapsed axis of the X and Y chromosomes (Turner et al., 2004). ATR translocates from the axial elements to the chromatin loops, where it rapidly phosphorylates the histone H2A variant, H2AX, at serine-139 to form γH2AX (Fernandez-Capetillo et al., 2003), instigating heterochromatinisation of the sex chromosomes. The XY bivalent subsequently undergoes further chromatin modifications including dimethylation of histone H3, deacetylation of histones H3 and H4 (Khalil et al., 2004), H2A ubiquitylation (Baarends et al., 1999), widespread replacement of the histones H3.1 and H3.2 with the histone variant H3.3 (van der Heijden et al., 2007), and incorporation of specific histone variants such as macroH2A.1 (Hoyer-Fender et al., 2000).

The transcriptional repression of the sex chromosomes during MSCI has been known about for decades (reviewed by McKee and Handel, 1993; Solari, 1974), although the extent of silencing has only recently become apparent (Namekawa et al., 2006; Turner et al., 2006; Turner et al., 2005; Wang et al., 2005a). Wang et al. (2005a) analysed the expression of fourteen X- and Y-linked genes in various spermatogenic subtypes by RT-PCR and found that all 14 genes were subject to MSCI regardless of the function of their encoded protein or location along the sex chromosome. A second group used microarray analysis on purified spermatogenic cells to investigate the extent of X chromosome silencing during MSCI. Almost all genes that were transcribed pre-meiotically were suppressed or down-regulated in pachytene spermatocytes (Namekawa et al., 2006). RNA FISH using gene-specific probes indicates that silencing acts at the level of transcription, and is concurrent with the appearance of γH2AX on the XY bivalent at the zygotene-pachytene transition (Turner et al., 2005; Turner et al., 2006; Mueller et al., 2008). The sex body chromatin domain also excludes RNA splicing factors and the active form of RNA polymerase II, and is negative for Cot-1 signals, a marker of nascent transcription (Namekawa et al., 2006; Richler et al., 1994; Turner et al., 2006). Together, these studies demonstrate that MSCI globally silences virtually all X- and Y-linked genes during meiosis. In mice, there is evidence that MSCI is essential for normal meiotic progression; cells where the

X or Y chromosomes escape MSCI through synapsis (e.g. synapsis of the YY bivalent in XYY spermatocytes or non-homologous synapsis of the X chromosome in T(X:16)16H spermatocytes) are eliminated during mid-pachytene (Turner et al., 2006). This is considered to be a result of the toxic effect of inappropriate expression of one or more X- and Y- linked genes in pachytene spermatocytes.

A number of X-linked genes encode proteins with essential housekeeping functions that may be required for meiosis. One way to overcome the long period of transcriptional silencing induced by MSCI is by stabilisation of either the transcript or the protein, a strategy that the *Hprt* gene appears to have adopted (Shannon and Handel, 1993). Another potential mechanism for the spermatocyte to cope with the silencing of a critical housekeeping gene is by having a 'back-up' copy located on an autosome. Studies revealed that the X chromosome has generated an approximately three-fold excess of retrogenes relative to autosomes in both mice and humans (Betran et al., 2004; Emerson et al., 2004; Wang, 2004). These retrogenes are located on autosomes, and many originate from widely expressed intron-containing house-keeping genes; expression analysis has demonstrated that the retrogenes are transcribed specifically in the testis. Virtually all of these autosomal 'back-ups' begin to be transcribed at the beginning of meiosis and are widely believed to have evolved to compensate for their X-linked progenitors during MSCI – the compensation hypothesis (for details, see review by Wang, 2004). These retrogenes may then have evolved testis-specific functions under the influence of sexual selection. Some of the retrogenes (e.g. *Pgk2*) are ancient, and arose before the eutherian and marsupial divergence about 150 million years ago. Other retrogenes are specific to either the human or mice lineages, implying that the retrotransposition of genes from the X chromosome is an ongoing evolutionary process that actively drives the differentiation of the mammalian X chromosome (Emerson et al., 2004; Wang, 2004). Several of these autosomal retrogenes have been inactivated by mutation or gene-targeting approaches, and while some are crucial for spermatogenesis (e.g. *Utp14b*, *Ant4*; Bradley et al., 2004; Brower et al., 2007; Rohozinski and Bishop, 2004), others appear dispensable (e.g. *Zfa*; Banks et al., 2003).

Numerous X and Y-linked genes are known to undergo post meiotic reactivation in round spermatids (Hendriksen et al., 1995; Odorisio et al., 1996; Wang et al., 2005a) and *de novo* transcription of several genes has been reported (Clotman et al., 2000;

Ellis et al., 2005; Touré et al., 2005). In addition, BRCA and ATR dissociate from sex chromosomes before the first meiotic division (Mahadevaiah et al., 2001; Turner et al., 2004) and these observations imply that MSCI occurs transiently and is restricted to meiosis. However, in round spermatids, the X and Y chromosomes form a heterochromatic chromatin domain known as the PMSC (Post-Meiotic Sex Chromatin; Namekawa et al., 2006), which is located next to the centromeric heterochromatin. The PMSC is enriched for several histone modifications and variants associated with transcriptional inactivation, and Cot-1 RNA FISH suggests that the sex chromosomes remain undertranscribed in round spermatids (Greaves et al., 2006; Khalil et al., 2004; Namekawa et al., 2006; Turner et al., 2006).

Microarray and real-time RT-PCR analysis of sex-linked genes estimates that around 87% of X-linked genes remain repressed in round spermatids (Namekawa et al., 2006), a process known as Post-meiotic Sex Chromosome Repression (PSCR; Turner et al., 2006). In contrast to the X chromosome, microarray analysis demonstrated that Y-linked genes appear to reactivate in round spermatids, in agreement with RT-PCR data from Wang et al. (2005a). X-autosomal translocation studies indicate that PSCR is a downstream consequence of meiotic silencing (Turner et al., 2006). However, unlike MSCI, this post-meiotic repression is imperfect, with RNA FISH studies demonstrating that most X-linked genes show some level of transcription in a small proportion of spermatids (Turner et al., 2006; Mueller et al., 2008).

MSCI and PSCR are thought to provide an evolutionary force that drives genes expressed in late spermatogenesis off the X chromosome (Wu and Xu, 2003), and testis-expressed genes are reported to be under-represented on the mouse X chromosome (Khil et al., 2004). In their analysis of *Spo11*-/- mice, Khil and colleagues (Khil et al., 2004) noticed that the X chromosome was strongly depleted in genes that are down-regulated in the testes of these mice. Furthermore, re-examination of previous microarray studies revealed that testis-expressed genes were 2.5 fold less dense on the X chromosome than expected based on random genomic distribution, with genes expressed at later stages of spermatogenesis being almost completely absent on the X chromosome. However, a recent study has found that approximately 18% of the protein coding genes on the mouse X chromosome are expressed predominantly or exclusively in spermatids. These genes represent 33 gene families which correspond to approximately 273 genes and are located within palindromes or

ampliconic sequences. These multi-copy genes were previously overlooked by Khil and colleagues (Khil et al., 2004), who primarily analysed single copy X genes, explaining the conflicting findings of Khil et al. (2004) and Mueller et al. (2008). RNA FISH analysis demonstrated that there was a correlation between the X-encoded gene copy number, and its escape from PSCR, with the percentage of round spermatids expressing the gene increasing with increasing copy number (Mueller et al., 2008). In addition, re-analysis of microarray data from Namekawa et al. (2006) revealed that the level of expression achieved by multi-copy X-linked genes in round spermatids is similar to that of single-copy autosomal genes (Mueller et al., 2008). A similar finding has been reported for the spermatid-specific Yq-linked multicopy *Ssty1* family based on northern blot analysis; there is as much transcription from two copies of the autosomal *Tcp-1* gene as there is from the *Ssty* gene predicted to be present in over 200 copies (Conway et al., 1994). Both papers suggest that gene amplification may compensate for the repressive effects initiated by MSCI and generate high levels of gene expression required to carry out important functions during spermiogenesis (Conway et al., 1994; Mueller et al., 2008).

To conclude, the X and Y chromosomes are enriched for genes transcribed during the initial stages of spermatogenesis that are required for proliferation of spermatogonia and early meiosis. The asynapsed nature of the XY bivalent in pachytene spermatocytes causes these chromosomes to be transcriptionally silenced by MSCI. This is thought to have led to a depletion of meiotic and post-meiotic genes on the X chromosome, and several X-linked housekeeping genes have evolved autosomally located retrogenes that are expressed exclusively during meiosis. The majority of X-encoded (and possibly Y-encoded) genes remain repressed during spermiogenesis, although a significant minority of sex-linked genes are transcribed in spermatids. Some of these may be indispensable for normal sperm development and differentiation. An overview of the mouse sex chromosome activity during spermatogenesis is shown in Figure 1.6.

Figure 1.6

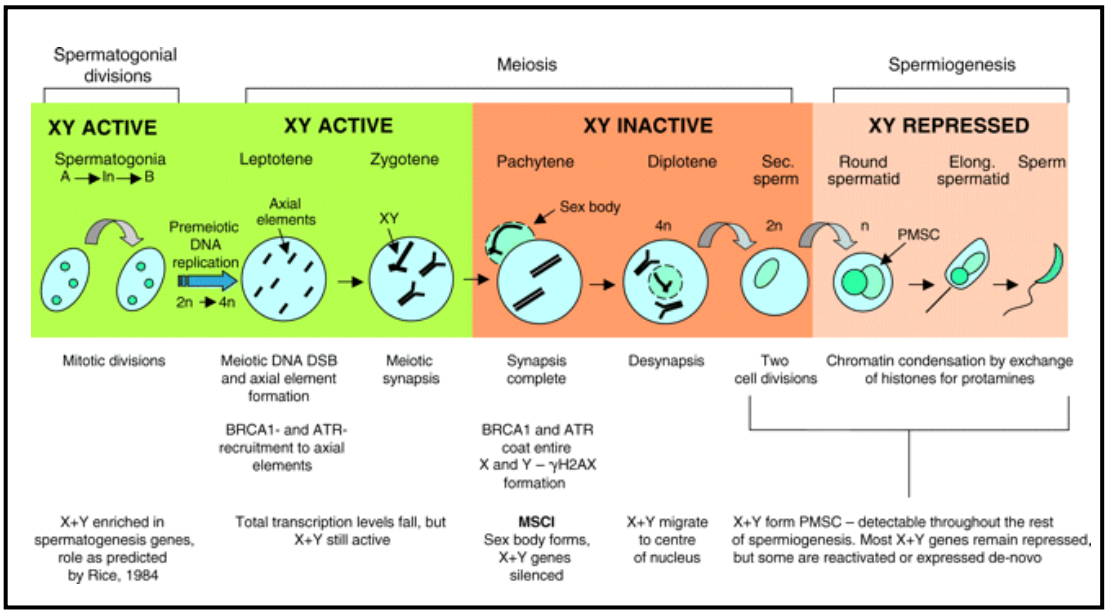

Figure 1.6 The transcriptional activity of the mouse sex chromosomes during spermatogenesis

The X and Y chromosomes are hypertranscribed in germ cells during the spermatogonial divisions and remain transcriptionally active during leptotene and zygotene stages of meiosis when total nuclear transcription is low. Once the autosomes are fully synapsed at the zygotene/pachytene transition, BRCA1 and ATR are recruited to the unsynapsed regions of the X and Y axial elements. ATR then spreads to the chromatin associated with the unsynapsed axes where it phosphorylates the histone variant H2AX to form γH2AX, and MSCI takes place. After meiosis, repression of the X and Y chromosomes is maintained (post-meiotic sex chromosome repression, PSCR). The sex chromosomes form the post-meiotic sex chromatin (PMSC), a heterochromatic domain (represented by the light-turquoise structure) located next to the chromocentre (dark turquoise; contains centromeric heterochromatin) in round and elongating spermatids. PSCR is 'leaky' compared to MSCI, and several sex-linked genes show reactivation or *de novo* transcription in spermatids.
Elong., elongated; sec., secondary.

This figure was taken from a review by Turner (2007).

1.4 The structure of the mouse Y chromosome

In mice, the Y chromosome is small (between 78Mb and 94.7Mb; Bergstrom et al., 1998; Gregory et al., 2002), heterochromatic, and represents 1-2% of the haploid mouse genome (Figure 1.7). Although the role of the Y chromosome in sex determination has been known since 1959 (Welshons and Russell, 1959), it is only in the last 15 years that the view of the Y chromosome as a 'genetic wasteland' has been challenged. Excluding its role as the testis determinant, the mouse Y chromosome encodes a limited number of functions that appear to be restricted to spermatogenesis and male fertility, although the Y chromosome may promote embryonic growth during the preimplantation period (Burgoyne, 1993b). The pseudoautosomal region (PAR) is attached to the distal tip of the Y long arm and mediates pairing and crossing over with the homologous X PAR during meiosis to ensure normal segregation of the sex chromosomes at MI (Burgoyne, 1982). In the absence of PAR pairing and recombination, spermatocytes arrest at MI and are eliminated by apoptosis (Burgoyne et al., 1992)

The male specific region of the Y chromosome (MSY) is structurally divided into a short arm (MSYp) and a highly repetitive long arm (MSYq), which comprises approximately 90% of the total MSY (see Figure 1.7; Burgoyne and Mitchell, 2007). The majority of functional Y-encoded genes reside on the short arm and almost all Yp genes have related sequences on the X and Y chromosomes of other eutherian mammals (Agulnik et al., 1994a; Delbridge et al., 1999; Lahn and Page, 1999; Mitchell et al., 1992; Murphy et al., 2001; Sandstedt and Tucker, 2004) Some of these MSYp genes are also found on the Y chromosome of marsupials (e.g. *Rbmy*, *Smcy*, *Ube1y* and *Jarid1d*) and are thus assumed to have been present on the original autosomes before they acquired the sex-determining function and differentiated into the mammalian sex chromosomes (Agulnik et al., 1999; Delbridge et al., 1999; Foster and Graves, 1994; Mitchell et al., 1992). Other genes (including *Usp9y*, *Eif2s3y* and *Zfy*) appear to be restricted to eutherian mammals and are thought to represent an autosomal translocation event that occurred after the marsupial-eutherian split but before the eutherian radiation. One exception to this is the *H2al2* gene, which evolved after the murine and rat lineages diverged (Ellis et al., 2005). *H2al2* is intronless and may have arisen by a retrotransposition event; two mouse homologues have been identified, one X-linked and the other autosomal. All three genes are intronless and

expressed specifically in spermatids, but the origin and evolutionary relationships between these genes is unknown (Ellis et al., 2005; Govin et al., 2007).

While the genes on the short arm are for the most part long-lasting inhabitants of the mammalian Y chromosome, genes on the MSYq appear to be restricted to the muridae, suggesting that they have arisen by recent retrotransposition and amplification events. The MSYq is comprised of highly repetitive sequences that are dispersed throughout the long arm and include two Y-specific retroviral elements estimated to be present in at least 300-500 copies, MuRVY (murine repeated virus Y-linked) and IAPE-Y (Eicher et al., 1989; Eicher and Washburn, 1978; Eicher and Washburn, 1986; Fennelly et al., 1996). Other sequences include the simple GATA repeat (Jones and Singh, 1981; Singh et al., 1994) and a large number of unidentified elements detected by an assortment of probes (Avner et al., 1987; Baron et al., 1986; Bergstrom et al., 1997; Bishop et al., 1985; Harbers et al., 1990; Harbers et al., 1986; Lamar and Palmer, 1984; Nallaseth and Dewey, 1986; Navin et al., 1996; Nishioka, 1989; Nishioka and Lamothe, 1986; Prado et al., 1992)

Interspersed between these repetitive sequences is the *Ssty* multicopy gene family thought to be present in over 250 copies. A recent microarray study has identified three more MSYq encoded multicopy genes predicted to be present in up to 120 copies each; all four MSYq encoded genes are expressed specifically in spermatids (Conway et al., 1994; Ellis et al., 2007; Touré et al., 2005). These genes are organised into unit of about 500Kb (known as the Huge Repeat Array) that has been amplified as a block (Ellis et al., 2007). The human Y chromosome contains eight massive palindromes which are thought to undergo intra-chromosomal recombination events, maintaining homology between different copies of a gene (Rozen et al., 2003; Skaletsky et al., 2003). It will be interesting to investigate if the repeats of the Huge Repeat Array on the murine MSYq are organised into amplicons or palindromes, which may also allow recombination between genes within these repeats.

Figure 1.7

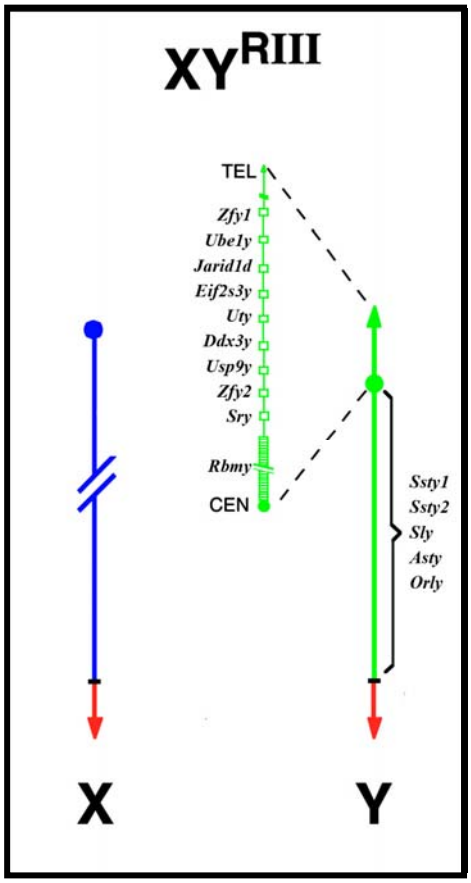

Figure 1.7 The mouse sex chromosomes

A schematic diagram of the male sex chromosome complement. The X chromosome is in blue and the Y chromosome in green. The short arm of the MSY chromosome contains the following genes: *Ube1y*, *Jarid1d*, *Eif2s3y*, *Uty*, *Ddx3x*, *Usp9y*, two copies of the *Zfy* gene (*Zfy1* and *Zfy2*), the testis determining factor *Sry*, two copies of the histone variant *H2al2* and approximately 50 copies of the *Rbmy* gene. The male specific part of long arm contains repetitive sequences including the retroviral element MuRVY, and multiple copies of the *Sly*, *Asty*, *Orly* and *Ssty* gene families. All mouse Y-encoded genes have homologues on the X chromosome except for *Orly*, which is a chimera of other Yq genes. The pseudoautosomal region (red) is located on the distal tip of the Yq and undergoes recombination with its X homologue (also red) during meiosis.

1.5 Spermatogenic functions of genes on the mouse Y chromosome

Effects of the mouse Y chromosome on the efficiency of spermatogenesis have been known for several decades. Studies by Krzanowska indicated that Y-linked factors play an important role in determining the shape of the sperm head and the incidence of sperm head abnormalities, which varies noticeably among inbred mice strains (Krzanowska, 1966; Krzanowska, 1969; Krzanowska, 1971; Krzanowska, 1976; Krzanowska, 1986). The F1 offspring of all types of crosses have a decrease in the proportion of abnormal sperm heads compared to the parental strains (Krzanowska, 1976; Wyrobek, 1979). Furthermore, the percentage of abnormal sperm heads can be reduced significantly by introducing the Y chromosome from an inbred strain with a low level of abnormal heads onto a genetic background associated with a high number of abnormal sperm (Krzanowska, 1971; Krzanowska, 1976). Unfortunately, the identity of these Y linked factors is currently unknown. The lack of recombination along most of the Y chromosome has restricted the study of Y-encoded genes by the conventional methods of meiotic mapping and positional cloning. The localisation of Y-encoded genes has depended on a combination of *in situ* hybridisation to metaphase spreads, chromosome rearrangements and deletion mapping. To date, no mice have been produced that have a targeted mutation of a Y-encoded gene, although this approach has been successful in targeting *Ddx3y* and *Eif2s3y* in ES cells (Rohozinski et al., 2002). Instead, analysis of several naturally occurring deletions has been used to identify the functions of Y-linked genes. These deletion models include deletions of the short arm that are associated with failure of spermatogonial proliferation, and long arm deletions whose effect appears to be restricted to sperm development and function (Burgoyne, 1987; Burgoyne, 1993a; Burgoyne and Mitchell 2007; Eicher et al., 1983).

1.5.1 Deletions of the Y chromosome short arm

The *Sxr^b* deletion

The *Sxr^b* deletion lacks the genetic information for H-Y antigen expression and spermatogonial proliferation. It arose by an unequal crossover involving *Zfy2* and *Zfy1* in a mouse carrying two copies of the short arm derived *Sxr^a* factor (*Sxr^a* encompasses the MSYp from the telomere to the *Rbmy* cluster close to the centromeres; Burgoyne et al., 1986; Cattanach et al., 1971; McLaren et al., 1984; Sutcliffe and Burgoyne, 1989).

This unequal crossover produced a *Zfy2*/*Zfy1* fusion gene with the loss of over 900Kb of DNA that lies between these two genes (Simpson and Page, 1991). The spermatogonial proliferation block in X*Sxr*^{b}O mice is rescued by an *Eif2s3y* transgene and spermatogenesis proceeds to the second meiotic division before arresting (Mazeyrat et al., 2001). If these *Eif2s3y* rescue mice are provided with a meiotic pairing partner, then spermatogenesis proceeds through meiosis to form haploid round spermatids. However, these spermatids fail to elongate or form the axoneme, indicating that one or more genes within the *Sxr*^{b} deletion interval are required for spermatid differentiation (Burgoyne and Mitchell, 2007). Alternatively, this spermiogenic block may be due to *Zfy* haploinsufficiency.

The Y^{d1} deletion

This deletion arose by unequal crossing over within the *Rbmy* cluster in an X*Sxr*^{a}Y male and removes at least 3-4Mb of the *Rbmy* gene cluster (Capel et al., 1993; Laval et al., 1995; Mahadevaiah et al., 1998). XY^{d1} mice have a 10-fold reduction in the copy number of *Rbmy* and are sex reversed due to transcriptional silencing of the flanking *Sry* gene (Capel et al., 1993; Laval et al., 1995). XY^{d1} mice carrying a *Sry* transgene are fertile but produce an increased incidence of grossly abnormal sperm (Mahadevaiah et al., 1998). *Rbmy* mRNA is barely detectable in these mice by northern blot analysis, suggesting that reduced expression of this gene during spermiogenesis may be responsible for the sperm phenotype seen in the XY^{d1}*Sry* mice. Surprisingly, replacement of RBMY in round spermatids using an *Rbmy* transgene was unable to rescue the XY^{d1}*Sry* sperm head defects (Szot et al., 2003), and there is conflicting data on whether *Rbmy* is actually expressed in spermatids (Mahadevaiah et al., 1998; Szot et al., 2003). So far, no additional gene has been identified as a candidate for the sperm head abnormalities within the Y^{d1} deletion interval. Alternatively, the increase in sperm head defects in XY^{d1}*Sry* mice may be caused by transcriptional repression of a gene outside this deletion interval. It has been suggested that the silencing of *Sry* in the XY^{d1} mice is due to *Sry* being brought close to the repressive effects of centromeric heterochromatin (Burgoyne and Mitchell, 2007). Since a copy of *H2al2* maps between *Sry* and the *Rbmy* cluster, it may be similarly repressed and members of the *H2al* family have been implicated in the remodelling of the developing sperm head.

1.5.2 Deletions of the Y chromosome long arm

Although the mouse Y chromosome long arm is highly repetitive and transcriptionally silent in all cells except spermatids, deletion analysis has demonstrated that it is indispensable for normal spermatogenesis. Four mice variants with deletions of the male specific part of the Y chromosome have been identified that have defective spermiogenesis; three of these arose by large interstitial deletions probably as a result of unequal crossing over between repeats, and the fourth deficiency lacks all Yq material as a result of chromosome rearrangement. Analysis of these mice indicates that the MSYq contains genetic elements that are required for normal development of the sperm head, epididymal maturation of sperm, sperm motility and fertilising capacity.

The Y^{del} and Y^{RIII}del deletions

Two deletions, Y^{del} and Y^{RIII}del, have been reported that remove approximately two-thirds of the Y long arm and are associated with increased sperm head abnormalities, reduced fertility and defective sperm motility (Conway et al., 1994; Grzmil et al., 2007; Moriwaki et al., 1988; Styrna et al., 2002; Styrna et al., 1991a; Styrna et al., 2003; Styrna et al., 1991b; Styrna and Krzanowska, 1995; Ward and Burgoyne, 2006; Xian et al., 1992). The Y^{del} deletion arose in the B10.Br strain of mice and is associated with an approximately three-fold increase in the incidence of epididymal sperm with abnormally shaped sperm heads (Styrna et al., 2002; Styrna et al., 1991a; Styrna et al., 1991b). The majority of these sperm have flat acrosomal caps, which is never seen in mice without the deletion. Furthermore, there is a higher proportion of severely deformed sperm from the epididymis of Y^{del} mice, an effect also seen in F1 hybrids (Styrna et al., 1991a; Styrna et al., 1991b). Analysis of the acrosome reveals that the acrosomal cap forms normally in round spermatids from Y^{del} mice, but they often lack the acrosomal granule and have little or no acrosomal material (Styrna et al., 1991a). This suggests that formation of the acrosome cap is independent of the synthesis of acrosomal material, and that one or more factors on the MSYq are involved in this. Analysis of the forming acrosome demonstrated that elongating spermatids from Y^{del} mice frequently contain small, round vesicles which are not present in spermatids from normal males. The majority of these vesicles are retained in mature sperm, and may account for the flattened acrosomal caps in Y^{del} sperm (Siruntawineti et al., 2002; Styrna et al., 2003). In addition, Y^{del} sperm frequently have

a reduction in level, distribution and enzymatic activity of the acrosomal proteinase acrosin (Styrna et al., 1991a; Styrna et al., 2003). Although Y^{del} mice are fertile, there is a four-fold decrease in the fertilising rate of Y^{del} sperm by IVF compared to control males, possibly due to poor capacitation and reduced levels of acrosin (Xian et al., 1992). Moreover, most matings are sterile in Y^{del} mice, and there is a reduced fertilising capacity of Y^{del} sperm that reach the eggs compared to males without the deletion (Styrna et al., 2002). The Y^{del} mice also have a greater frequency of degenerated seminiferous tubules, increased numbers of epididymal sperm with the cytoplasmic droplet still attached indicative of delayed maturation, and decreased sperm velocity (Styrna et al., 2002; Grzmil et al., 2007). Y^{del} mice have an improved fertilising ability on the CBA genetic background but the percentage of epididymal sperm with a damaged or absent acrosome, and dead sperm is increased on this background compared to control males (Styrna et al., 2003).

Cytogenetically, the Y^{RIII}del chromosome (also known as the 2/3MSYq-; Figure 1.8.A) appears to be less than half its normal length and arose in a mouse carrying the Y^{RIII} chromosome. This deletion is associated with a 3.5 fold rise in the incidence of abnormal sperm heads on the inbred C57BL/10 and the random bred MF1 backgrounds (Conway et al., 1994). Although the number of grossly abnormal sperm is increased in mice carrying the 2/3MSYq- deletion, the most common sperm abnormality is a flattening of the acrosomal cap similar to that seen in the Y^{del} mice (Conway et al., 1994). Furthermore, although males carrying the Y^{RIII}del chromosome are fertile, they have a slight distortion in their offspring sex ratio in favour of females, from 43% in XY^{RIII} males to 54% in 2/3MSYq- males on the inbred C57BL/10 background. This distortion is also observed on an MF1 background, with the percentage of male offspring falling from 51% in control males to 38% in 2/3MSYq- males; a similar sex ratio distortion is seen with IVF using sperm from the 2/3MSYq- males (Conway et al., 1994; Ward and Burgoyne, 2006). However, the 2/3MSYq- deletion does not affect the production of Y-bearing gametes based on the transmission frequency of the 2/3MSYq- chromosome by intracytoplasmic sperm injection (ICSI; Ward and Burgoyne, 2006). ICSI involves the injection of sperm directly into the egg and so the progeny obtained reflects the frequency of X- and Y-bearing sperm in the epididymis. This indicates that the sex ratio distortion seen in the offspring of 2/3MSYq- males by copulation and IVF is due to poorer fertilising ability of 2/3MSYq- bearing sperm compared to their X counterparts (Ward and Burgoyne,

2006). This reduction in 2/3MSYq-sperm quality is also observed in males with a mixture of XY and 2/3MSYq- sperm. These mosaic mice have a significant reduction in the transmission of the 2/3MSYq- chromosome to offspring even though both Y^{RIII} and 2/3MSYq- bearing sperm are present in the ejaculate (Burgoyne, 1998b).

Y^{Tdym1}qdel deletion

The Y^{Tdym1}qdel deletion removes approximately nine-tenths of the MSYq including all copies of the *Ssty* family (see below), but the distal PAR and short arm (aside from the deletion of *Sry*) remain intact (Figure 1.8.B). Males carrying this deletion are commonly referred to as 9/10MSYq- mice, and have normal sized testes but spermiation is delayed. Males carrying the 9/10MSYq- chromosome are virtually sterile and have significantly reduced sperm counts compared to controls, although these are still within the fertile range. All of the epididymal sperm produced by 9/10MSYq- males are abnormal, and the majority (up to 92%) are classified as having severely deformed heads (Touré et al., 2004b). When 9/10MSYq- sperm were injected by ICSI, the number of eggs reaching the two-cell stage was significantly reduced, from 84% in the control to 71% in the 9/10MSYq- mice, but the transmission of the 9/10MSYq- chromosome was unaffected (Ward and Burgoyne, 2006). This indicates that infertility in the 9/10MSYq- is the result of an inability to fertilise the egg, probably caused by defective sperm morphology and reduced sperm motility (Ward and Burgoyne, 2006).

X*Sxr*^{a}Y^{*x} and XY^{*x}*Sxr*^{a} mice variants

Total absence of the Y long arm occurs in mice with the X*Sxr*^{a}Y^{*x} (Figure 1.8.C) and XY^{*x}*Sxr*^{a} genotypes, which are collectively called MSYq- mice. These mice have the Yp-derived *Sxr*^{a} factor attached to the PAR of either the X chromosome or the Y^{*x} chromosome. The Y^{*x} chromosome is composed of a pseudoautosomal region attached to an X centromere and acts as a paring partner for the X chromosome during meiosis, although X*Sxr*^{a}Y^{*x} spermatocytes show reduced levels of sex chromosome synapsis (Burgoyne and Evans, 2000; Burgoyne et al., 1998; Burgoyne et al., 1992; Eicher et al., 1991). MSYq- males produce nearly normal levels of sperm and testis histology from these mice demonstrated that germ cells of all spermatogenic stages are present (Burgoyne et al., 1992). Analysis of sperm from the testes and vas deferens of MSYq- mice reveals that they have 100% grossly abnormal sperm heads. These mice are sterile, almost certainly due to defects in spermiogenesis that are reflected by the

distortion in the sperm head shape (Burgoyne et al., 1992). Sperm from MSYq- mice are more severely affected than 9/10MSYq- sperm (see above), potentially because MSYq- mice also have reduced expression of *Rbmy* as well as lacking the whole MSYq. Alternatively, the less severe sperm abnormalities in 9/10MSYq- mice may be due to the retention of a MSYq-linked genetic element that has a role in controlling sperm head shape which is absent in the MSYq- mice.

Figure 1.8 Schematic representations of the sex chromosome pair in the three MSYq deletion models

The X chromosome and X chromosome derived segments are in blue, Y chromosome sequences are in green and the pseudoautosomal (PAR) segment is in red.

A) A schematic of the sex chromosomes in the 2/3MSYq- mouse variant. Approximately two-thirds of the male specific region of the Y long arm has been deleted from the Y^{RIII} chromosome, removing copies of the Yq-encoded genes including *Ssty* and *Sly*. The Y chromosome PAR and short arm are unaffected by the deletion.

B) Schematic diagram of the 9/10MSYq- model sex chromosome complement. The *Sry* gene on the Yp has been deleted in these mice and so 9/10MSYq- males carry an *Sry* transgene. Cytogenetically, this deletion variant has lost nine-tenths of the MSYq sequence, although the PAR is intact. All copies of *Ssty*, *Asty* and *Orly* are deleted, although a few copies of the *Sly* gene are thought to remain.

C) The sex chromosome complement of the MSYq- mouse model. In this mouse, there is no Y chromosome long arm derived sequences. Instead, the Yp derived Sxr^a fragment is attached to the distal tip of the X chromosome PAR. This fragment contains all known Yp genes, although only seven of the 50 copies of *Rbmy* remain. The tiny Y^{*x} chromosome is a highly deleted X chromosome containing the centromere and PAR regions. This provides a second PAR region, allowing the two sex chromosomes to pair and recombine during meiosis. $XY^{*x}Sxr^a$ mice also lack all MSYq sequences and were produced by ICSI using sperm from $XSxr^aY^{*x}$ males which had undergone recombination between the PARs of the $XSxr^a$ and Y^{*x} chromosomes (Ward and Burgoyne, unpublished).

Figure 1.8

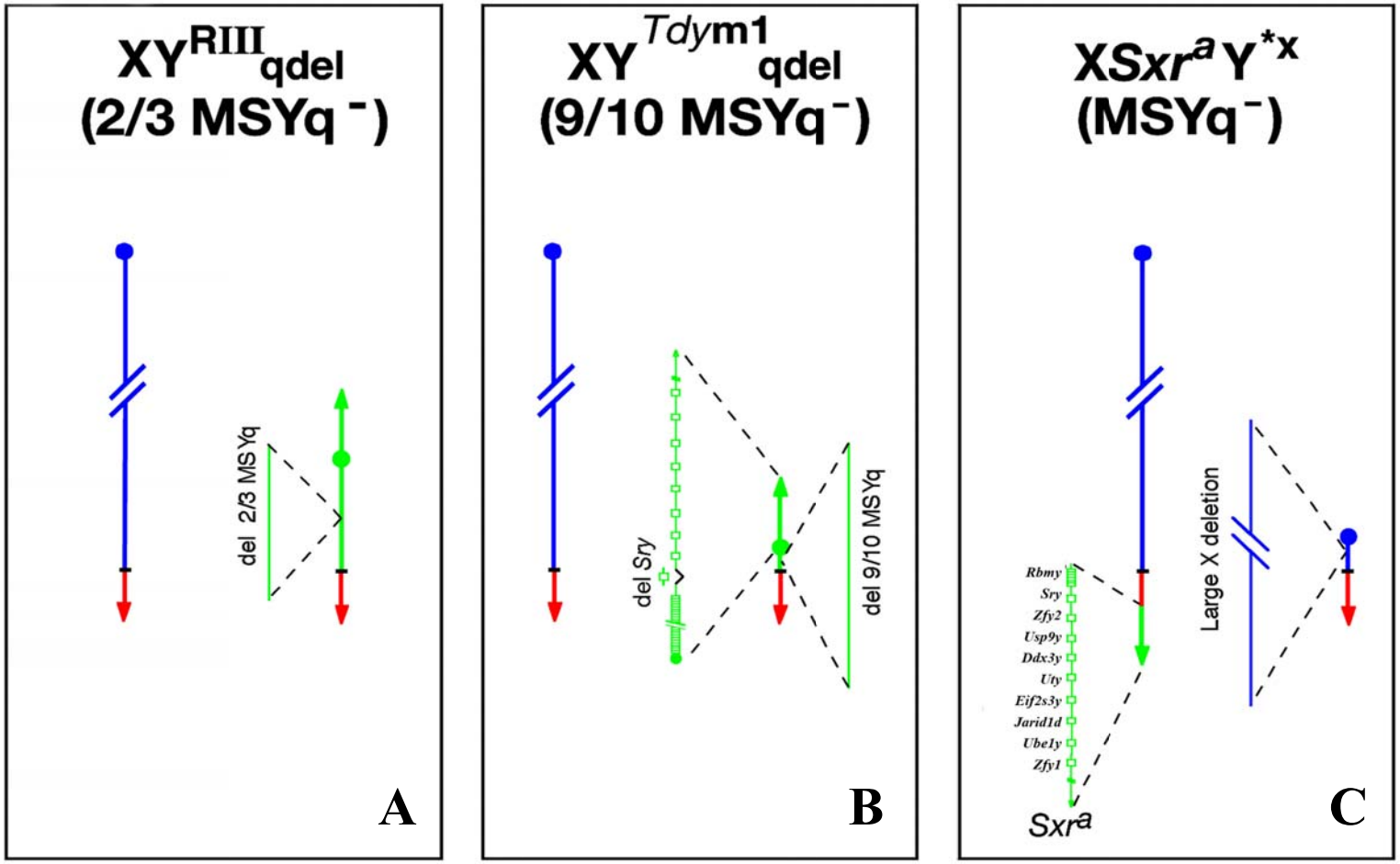
XY^RIIIqdel
(2/3 MSYq⁻)
del 2/3 MSYq
A
XY^Tdym1qdel
(9/10 MSYq⁻)
del Sry
del 9/10 MSYq
B
XSxr^aY^*x
(MSYq⁻)
Rbmy
Sry
Zfy2
Usp9y
Ddx3y
Uty
Eif2s3y
Jarid1d
Ube1y
Zfy1
Sxr^a
Large X deletion
C

1.5.3 The *Ssty* gene family is a candidate for the Yq-linked spermiogenesis factor

Analysis of mice with long arm deletions has indicated that this region contains one or more factors involved in sperm differentiation and function. The fact that mice with partial deletions of the MSYq have a less severe sperm phenotype than those with larger deletions suggests that this 'spermiogenesis factor' is present in multiple copies on the mouse Y long arm (Burgoyne et al., 1992). The *Ssty* gene family is estimated to be present in over 200 copies on the mouse Y chromosome long arm and represents at least two distinct subfamilies (*Ssty1* and *Ssty2*: Bishop et al., 1985; Bishop and Hatat, 1987; Conway et al., 1994; Prado et al., 1992). The *Ssty1* and *Ssty2* subfamilies share a high degree of similarity between their ORFs, but have different 5' and 3' untranslated regions and so they may be processed differently (Ellis et al., 2007; Touré et al., 2004a). These genes are presumed to be derived from the related X-linked spermatid-specific *Sstx* gene family (Mueller et al., 2008; Touré et al., 2004) which itself is believed to have originated by retrotransposition of the autosomal *Spin* gene. Orthologues of the mouse *Spin* gene are present in humans, fish, frogs and chickens (Itoh et al., 2001; Wang et al., 2005b; Wang et al., 2005c), and the protein encoded by the *Spin* gene localises to the metaphase spindle in mouse oocytes (Oh et al., 1998).

Ssty1 and *Ssty2* are expressed specifically in round spermatids (Conway et al., 1994), and *Ssty2* appears to be the most abundant MSYq transcript (Burgoyne and Mitchell, 2007). However, only a subset of *Ssty1* transcripts are thought to be translated and no SSTY2 protein has been identified to date (Touré et al., 2004a). Although there is a two- to three-fold reduction in *Ssty1/2* sequences in 2/3MSYq- mice (Conway et al., 1994), there is no decrease in *Ssty1* transcription and the protein level is increased by approximately two-fold (Touré et al., 2004b). The *Ssty* gene family is absent in 9/10MSYq- and MSYq- males, indicating that there are no copies of this gene elsewhere in the mouse genome (Burgoyne et al., 1992; Touré et al., 2004b). The function of *Ssty1* and *Ssty2* remains unknown, and no rescue of the sperm head defects is seen in MSYq- mice transgenic for *Ssty1* or *Ssty2*, possibly because these transgenes were not translated (Burgoyne and Mitchell, 2007; Touré et al., 2004a).

1.5.4 Identification of three new multicopy Y long arm genes

To identify additional candidate genes for the MSYq encoded 'spermiogenesis factor', the testis transcriptomes of 2/3MSYq-, 9/10MSYq- and MSYq- mice were analysed by microarray analysis (Touré et al., 2005) This study used a custom made testis cDNA library enriched for spermatogenic cell transcripts and was greatly facilitated by accumulating sequence data resulting from the Mouse Chromosome Y Mapping Project (Jessica E Alfoldi, Helen Skaletsky, Steve Rozen and David C Page at the Whitehead Institute for Biomedical Research, Cambridge, MA, USA, and the Washington University Genome Sequencing Centre, St. Louis, MO, USA). Three new spermatid-specific MSYq-encoded multicopy genes were identified; *Sly*, *Asty* and *Orly*, each of which is a contender for the 'spermiogenesis factor' (Ellis et al., 2007; Touré et al., 2005).

Based on sequence analysis, there are approximately 65 copies of *Sly* present on the MSYq, although only 34 copies retain an open reading frame (Touré et al., 2005). The putative SLY protein is related to the chromatin associated nuclear proteins XLR and XMR, which are encoded by the related X-linked multicopy *Xlr* superfamily (Ellis et al., 2005; Touré et al., 2005). Sequence analysis indicates that *Sly* was created by the fusion of the 5' region of the *Xmr* gene to the 3' portion of the *Xlr* gene followed by an internal duplication of two *Xmr*-derived exons (Ellis et al., 2007). *Sly* is highly transcribed specifically in the testes, where it is present in spermatid stages 1 to 12 (Touré et al., 2005). Furthermore, northern blot analysis demonstrated that *Sly* is down-regulated in the testes of 2/3MSYq- and 9/10MSYq- males in proportion to the deletion size, and is absent in MSYq- males. Touré et al. (2005) and Ellis et al. (2005) suggested that the putative SLY protein could be involved in chromatin remodelling, and deficiency of this protein may disturb chromatin organisation resulting in the abnormal sperm heads observed in the three MSYq deletion models (Ellis et al., 2005; Touré et al., 2005).

Asty was identified through binding of its transcripts to the X-linked *Astx* gene on the microarray chip. *Asty* and *Astx* have an identical genomic organisation and share between 92-94% sequence identity across introns and exons. Sequence data suggests the *Asty* gene is present in over 120 copies on the MSYq, and these are absent in the 9/10MSYq- and MSYq- mouse models (Touré et al., 2005). *Asty* transcription is

restricted to the testis, were it appears to be transcribed at very low levels in round spermatids. However, these transcripts are not thought to be translated as none of the copies of *Asty* have the open reading frame present in *Astx*.

Unlike the other MSYq encoded genes, *Orly* does not have a multicopy X-linked homologue but is composed of sequences derived from other MSYq-encoded genes (Ellis et al., 2005; Touré et al., 2005). *Orly* has a functional promoter at either end and this allows bidirectional transcription of the gene to give a range of splice variants, none of which appear to encode a protein. *Orly* is a chimera of *Ssty1*, *Asty* and *Sly* and arose by exon shuffling before these genes became amplified on the MSYq (Ellis et al., 2007). RT-PCR data indicates that both sense and antisense *Orly* transcripts are restricted to the testis where they are predominantly transcribed in spermatids (Ellis et al., 2007).

1.6 The MSYq regulates transcript levels of several sex-linked genes during spermiogenesis

In addition to identifying new genes, the microarray analysis of the three MSYq deletion models led to the identification of an unexpected function of the mouse Y chromosome in spermatogenesis. Fourteen spermatid-expressed X- and Yp-linked genes were found to be significantly up-regulated in the three MSYq- models (Ellis et al., 2005), signifying that the MSYq modulates the transcription of other genes expressed during spermiogenesis. This is similar to the regulatory role the Y chromosome appears to play in *Drosophila melanogaster*. Transcriptional analysis among different *D. melanogaster* lines that varied only in Y chromosome origin demonstrated that this chromosome mediates the expression of genes on other chromosomes, particularly those on the X chromosome. Moreover, most of these genes are more strongly expressed in males, and include those involved in spermatogenesis and temperature adaptation (Lemos et al., 2008).

The majority of the X- and Yp-encoded genes affected by deletion of the mouse MSYq are present in multiple copies or are members of a multigene family. Almost all of the affected genes are transcribed exclusively in the testis during spermiogenesis and therefore these up-regulated genes may contribute to the sex ratio distortion and sperm

head abnormalities seen in the MSYq deletion models. Several of the up-regulated genes have autosomally located homologues that are expressed in the testes, but these showed no change in their mRNA levels in the three MSYq deletion models. This indicates that the transcriptional up-regulation affects only the sex chromosomes, in contrast to the genome wide effect of the *D. melanogaster* Y chromosome. Moreover, the up-regulation of the affected X- and Yp-linked genes was found to increase with the deletion size, implying that a multicopy gene on the MSYq represses transcription of specific sex-linked genes during spermiogenesis.

One promising candidate for the MSYq-encoded transcriptional repressor is *Sly*, deficiency of which may affect sperm head shape indirectly by up-regulating the expression of a gene(s) involved in sperm head morphogenesis. *Sly* retains at least one transcribed copy in the 9/10MSYq- testes in contrast to the other three MSYq encoded genes and this could explain why the sperm head abnormality is less penetrant in the 9/10MSYq- mice compared to the MSYq- mice that lack *Sly* (Ellis et al., 2007; Touré et al., 2005; Touré et al., 2004b). The putative SLY protein contains a COR1 domain that is predicted to facilitate chromatin binding and this domain is also found in the synaptonemal complex protein SYCP3. Furthermore, the X-linked homologue of *Sly* encodes the spermatocyte protein XMR that locates to the sex body during MSCI and is hypothesised to be involved in gene silencing (Calenda et al., 1994; Escalier and Garchon, 2005; Escalier and Garchon, 2000). Ellis and colleagues (Ellis et al., 2005) predicted that the putative SLY protein binds to the X and Y chromosomes in spermatids, where it could regulate their chromatin conformation and expression in a way analogous to XMR during meiotic prophase.

1.7 Intragenomic conflict between the X and Y chromosomes during spermatogenesis

Intriguingly, two of the genes up-regulated in the MSYq deletions models are *Xmr* and the related X-linked gene *AK015913,* which are both related to *Sly*. This was surprising because *Xmr* was not thought to be expressed in spermatids, and it is unknown if these spermatid transcripts are translated (Ellis et al., 2005). The level of *Xmr* transcription increased in proportion to the decrease in *Sly* levels in the three MSYq deletion models, suggesting that there may be regulatory interactions between *Sly* and *Xmr* in

normal males (Ellis et al., 2005; Touré et al., 2005). Intragenomic conflict theories have envisaged the existence of such interactions between multicopy X- and Y-linked gene families, which may potentially lead to a distorted sex ratio when disturbed (Hurst, 1992; Partridge and Hurst, 1998). The sex chromosomes are predicted to accumulate and express genes that drive their own transmission (meiotic drivers or selfish genes), thus disturbing the 1:1 sex ratio, and this appears to be very common in species where females are the heterogametic sex, such as butterflies and moths (Burt and Trivers, 2006).

In mammals, genomic conflict may arise between the sex chromosomes if the X chromosome acquires a meiotic driver that increases its transmission to offspring. The ratio of male to female offspring would then deviate from the evolutionary stable 1:1 sex ratio, leading to the automatic selection of suppressor alleles that counteract this distortion. This suppression mechanism could involve the Y chromosome acquiring a gene or mutation that acts to rebalance the sex ratio. Duplication of the X-encoded distorter will once again unbalance the sex ratio, leading to a duplication of the Y-linked suppressor. Over time, the 'evolutionary arms race' between the X-linked distorted and Y-linked suppressor genes will lead to massive amplification of both genes. Ellis et al. (2005) proposed that such intragenomic conflicts may underlie the massive amplification of all four MSYq-encoded genes. They went on to suggest that the extensive blocks of heterochromatin that are characteristic of the Y chromosome in various mammalian species including humans and mice may represent the 'genomic scars left at the sight of past intragenomic battles' (Ellis et al., 2007; Ellis et al., 2005). Although predicted to be common, the effects of mutations that distort transmission ratios are rarely observed because of the rapid fixation of meiotic drivers and suppressors that mask their effects. However, genomic conflict between distorter and suppressor genes is seen in crosses between different subspecies due to the unbalancing of these complexes in F1 hybrids. This leads to hybrid sterility and is observed in crosses of *Mus musculus* with *Mus molossinus* (Oka et al., 2004). Amplification of the distorter gene or deletion of the suppressor gene (e.g. in the 2/3MSYq- mice) also exposes the consequence of intragenomic conflict between the sex chromosomes by distorting the sex ratio.

One well characterised X-Y 'genomic conflict' phenomenon has been described in *Drosophila melanogaster*, between the X-linked *Ste* genes, and the Y-linked *Su(Ste)*

genes. The *Su(Ste)* gene arose from the *Ste* gene by the insertion of a transposon with an active promoter in the reverse orientation and is transcribed from both strands to produce dsRNA (Aravin et al., 2001; Belloni et al., 2002; Stapleton et al., 2001). The dsRNA targets the *Ste* transcripts for degradation by RNA interference (RNAi), regulating the level of *Ste* encoded protein (Aravin et al., 2001). Deletion of the majority of *Su(Ste)* tandem repeats localised in the *Crystal* locus on the Y chromosome (*cry1*Y chromosome) results in over-expression of *Stellate* in testes. This leads to a variety of meiotic phenotypes including the accumulation of crystalline aggregates of *Stellate* encoded protein in primary spermatocytes and sex ratio distortion in favour of females.

Xmr and *Sly* may be involved in a similar intragenomic conflict in mice, either at the RNA or protein level, and this could explain the dramatic amplification of these genes on the sex chromosomes. Alternatively, *Sly* and *Xmr* may have evolved to reciprocally repress the expression of meiotic drivers by their effect on sex chromatin, thereby maintaining the one-to-one sex ratio (Ellis et al., 2005). Unlike the *Ste/Su(Ste)* model, the potential conflict between the mouse X and Y chromosomes does not affect the primary sex ratio in the MSYq deletion mice, since equal numbers of X and Y bearing sperm are being produced based on ICSI with sperm from 2/3MSYq- and 9/10MSYq- males (Ward and Burgoyne, 2006). Instead this conflict seems to increase the fertilising ability of X-bearing gametes compared to those carrying the deleted Y chromosome.

1.8 Thesis Aim

Ellis et al. (2005) proposed that *Sly* and *Xmr* may play an important role in spermiogenesis by regulating sex chromatin structure and gene expression in spermatids. *Sly* is therefore a contender for the multicopy Yq-encoded 'spermiogenesis factor', deficiency of which may lead to de-regulation of sex linked gene expression and abnormal head formation in the MSYq deletion models. Data from Ellis and colleagues (Ellis et al., 2005) also suggests that disturbances in the equilibrium between *Sly* and *Xmr* transcripts could underlie the offspring sex ratio distortion in 2/3MSYq- males. The aim of this thesis is to investigate the role of the *Sly* and *Xmr* multicopy gene families in spermatogenesis and examine their potential contribution to

the testicular phenotypes observed in mice with deletions of the Y chromosome long arm. Firstly I will analyse the expression and function of *Sly* in spermiogenesis. I will then re-examine the transcription and translation of *Xmr* in the testis, paying specific attention to whether the spermatid transcripts identified by Ellis et al. (2005) encode a functional protein. The over-expression of X- and Y-linked spermatid expressed genes will be studied in more detail and finally, an *Sly* transgene will be introduced in the MSYq deletion mice to assess whether *Sly* is able to complement any of the phenotypes associated with these deletions.

Chapter 2

Materials and Methods

Materials and Methods

2.1 Mouse lines

XY mice

These mice have an R^{III} strain Y chromosome and are the appropriate controls for the 2/3MSYq- and MSYq- mice models.

2/3MSYq- mice

These mice have an R^{III} strain Y chromosome with a deletion removing approximately two-thirds of the MSYq and were derived from a stock originating from the mice described by Conway et al, (1994).

9/10MSYq- mice

These mice have a 129 strain Y chromosome with a deletion removing approximately nine-tenths of MSYq and also a small deletion removing the testis determinant *Sry* from the short arm, which is complemented by an autosomally located *Sry* transgene. The mice used in this study were produced by Monika Ward (University of Hawaii) by ICSI of cryopreserved 9/10MSYq- sperm samples using B6D2F1 females as oocyte donors and CD-1 females as surrogate mothers as previously described (Ward and Burgoyne, 2006).

MSYq- (X*Sxr*^{a}Y*^{x} and XY*^{x}*Sxr*^{a}) mice

These mice lack the entire Y-specific (non-PAR) gene content of MSYq, and the only Y-specific material is provided by the Y short arm derived factor *Sxr*^{a}. These mice also have a 7.5-fold reduction in copies of the *Rbmy* gene family located on the short arm adjacent to the centromere. The Y*^{x} chromosome provides a second PAR, thus allowing fulfilment of the requirement for PAR synapsis. X*Sxr*^{a}Y*^{x} males (Burgoyne et al., 1992) were produced by mating XY*^{X} females (Burgoyne et al., 1998; Eicher et al., 1991) to XY*Sxr*^{a} males (Cattanach, 1987; Cattanach et al., 1971). XY*^{x}*Sxr*^{a} mice were produced by Monika Ward by ICSI of sperm from X*Sxr*^{a}Y*^{x}.

D4/XEGFP mice

D4/XEGFP mice (Hadjantonakis et al., 2001; Hadjantonakis et al., 1998) were obtained from Andras Nagy (Samuel Lunenfeld Research Institute). Hemizygous

EGFP transgenic XX females were bred with either XY^{RIII} or 2/3MSYq- MF1 males to produce XY-GFP and 2/3MSYq-GFP mice, with non-transgenic littermates used as controls.

2.1.1 Animal care

Animals were kept on a 12 hour light-dark cycle, and food and water were provided at all times. All mice were produced on an MF1 random-bred background at the MRC National Institute for Medical Research. All methods were carried out in accordance with the Animals in Scientific Procedures Act 1986 and subject to local ethical review. Adult males were processed at the age of 2 to 3 months.

2.1.2 Genotyping

Tail pieces or ear pieces were digested overnight at 55°C in 100µL of tail lysis buffer (50mM KCL, 1.5mM $MgCl_2$, 10mM Tris-HCL, 0.45% NP40, 0.45% Tween20; Sigma) and 2µL proteinase K (20mg/mL; Roche). Samples were boiled for 15min at 95°C and centrifuged using a desktop centrifuge (Heraeus) at 13,200rpm for 5min at R/T. One microlitre was used per 25µL PCR reaction containing 5µL 5X PCR buffer (250mM Tris pH 9.0, 75mM ammonium sulphate, 35mM magnesium chloride, 0.85mg/mL BSA, 0.25% NP40), 5µL 7.5mM dNTPs (GE Healthcare), 1µL 250µM forward primer, 1µL 250µM reverse primer and 0.5µL 5U/µL Taq polymerase (Thermo Scientific). The standard PCR cycling procedure was 95°C for 10min (1 cycle), 95°C for 30sec, annealing temperature for 30sec, 72°C for 42sec (35 cycles), followed by 72°C for 10min (1 cycle).

The primers used for genotyping are given in Table 2.1.

Table 2.1

Transgenic line	PCR name	Forward primer	Reverse primer	Annealing temperature	Product size
Ylr BAC	*Sly* 5'	GTGTGGGTGGTGGTGGTAGTTCAT	TTTCCTCCGTGTATGCCATTTATC	57°C	409bp
Ylr BAC	*Sly* middle	CCTCTTTGTTTGCTGGCTTCGTC	AGTGTGCATGTTTCCGTCCTT	57°C	396bp
Ylr BAC	*Sly* 3'	TGTCCAAATGTAGTCAGA	GGTCCCCAAGTTCATCA	50°C	445bp
Ylr BAC	pTARBAC zone A	AACGGCGCCCTCGGTATCAT	AGTATCGGCATTTTCTTTTTG	57°C	519bp
Ylr BAC	pTARBAC zone B	CGCAGCCGTGTAACCGAGCATAG	AAAAAGAAAGGCCGCCAGACGACT	60°C	400bp
Ylr BAC	pTARBAC zone D	CGCCTGGTTGCTACGCCTGAA	TCGACCGATGCCCTTGAGAGC	60°C	353bp
Ylr BAC	5' *Asty*	GGTTGGGGACATTAAGCAGACT	CAATAGACACAGGGAGAAGAGGAA	60°C	489bp
Ylr BAC	3' *Asty*	TCAGGTCATTTGGAAGAT	CACCCTGAGCATTGTTAA	60°C	354bp
mP1-*Sly*	*Sly*-SV40	GGGGTATTAATTAAGAGAAGAATGGCTCTTAAGAAA	GCAGTGCAGCTTTTTCCTTT	60°C	1Kb
mP1-*Slx*	*Slx*-SV40	GGGTTGGATCCTTAATTAAGAGAAAAATGTCTATAA	GCAGTGCAGCTTTTTCCTTT	60°C	1Kb
mP1-*Slx* cDNA	*Slx* cDNA-SV40	GGGGTATTAATTAACAGGAATCTCTGCTGACAAC	GCAGTGCAGCTTTTTCCTTT	60°C	1.2Kb
	myogenin	TTACTCCATCGTGGACAGCAT	TGGGCTGGGTGTTAGTCTTAT	60°C	245bp

Table 2.1 Primers used for genotyping of transgenic mice lines

2.2 RNA techniques

2.2.1 Reverse Transcriptase - Polymerase Chain Reaction

Total RNA extraction from testis

Total testis RNA was extracted using TRIzol® (Invitrogen) in accordance to the manufacturer's instructions. Adult testis samples were homogenised in 2mL TRIzol® using a 1mL syringe (BD Plastipak) and a 19G X 1.5'' needle (Terumo). The homogenates were allowed to stand for 5min at R/T and 0.4mL of chloroform was added. Samples were mixed by inversion, left at R/T for 3 minutes before being centrifuged at 12,000g for 15min at 4°C using a benchtop centrifuge (Eppendorf 5415R). The resulting aqueous supernantant was transferred to a fresh Eppendorf tube and RNA was precipitated by adding 1mL of isopropanol (Fisher Scientific). After mixing gently, samples were left at R/T for 10min and then centrifuged as described above. The resulting pellet was washed in 75% ethanol and centrifuged for 5min at 7,500g at 4°C. Ethanol was removed and pellets were air-dried at R/T before being re-dissolved in 50µl RNase-free water. The RNA was then quantified using the NanoDrop ND-1000 spectrophotometer (Labtek) and samples were stored at -80°C until use.

DNAse treatment and reverse transcription of total RNA

Three micrograms of total RNA were treated with 5 units RQ DNAse 1 (Promega) for 1 hour at 37°C according to the manufacturer's instructions. The enzyme was inactivated by heating to 95°C for 5 mins. RNA samples were then ethanol precipitated and eluted in RNase-free water.

One microgram of DNAse-treated RNA was reverse transcribed with 1µL of oligo dT primers (Invitrogen) in a 20µL reaction using the Superscript II reverse transcriptase (150 U; Invitrogen) at 42°C for 1.5hours according to the manufacturer's instructions. For negative RT control samples, RNAse-free water was added to the RNA sample instead of Superscript II reverse transcriptase. The reactions were stored at -20°C until use.

PCR procedure

PCRs were carried out using 1µL of cDNA derived as described in section 2.1.2 above

in 25µL reactions containing 5µL 5X PCR buffer (250mM Tris pH 9.0, 75mM ammonium sulphate, 35mM magnesium chloride, 0.85mg/mL BSA, 0.25% NP40), 5µL 7.5mM dNTPs (GE Healthcare), 1µL 250µM forward primer, 1µL 250µM reverse primer and 0.5µL 5U/µL Taq polymerase (Thermo Scientific). The standard PCR cycling procedure was 95°C for 5min (1 cycle), 95°C for 30sec, annealing temperature for 30sec, 72°C for 30sec (35 cycles), followed by 72°C for 8min (1 cycle).

The annealing temperature for each primer pair is given in Table 2.2.

PCR products were run on a 2% agarose gel (Invitrogen) in Orange G loading buffer (Searle Diagnostic) and sized using the 200bp smart ladder (Eurogentec).

Table 2.2

Gene/primer pair	Reference	Forward primer	Reverse primer	Annealing temperature	Product size
Sly	Ellis et al., 2005	CTGGAGATGACATTTATAAGACGC	TCCTCCATGATGGCTCTTTC	60°C	405bp
AB	Calenda et al., 1994	CTTGAGAGACAACAATGGAAAAC	AGTCTGAAGATGGGAAACTAGAAG	56°C	*Xlr*=630bp, *Xmr*=427bp
DC	Calenda et al., 1994	ATTGAGGAGTTGAGCACGCAA	TAACTTGCTGTTCACCACTTAACAAATT	56°C	*Xmr*=421bp, *AK015913*=287bp
DB	Calenda et al., 1994	ATTGAGGAGTTGAGCACGCAA	AGTCTGAAGATGGGAAACTAGAAG	56°C	*Xmr*=813, *AK015913*=623bp
Xmr	Ellis et al., 2005	TTCAGATGAAGAAGAAGAGCAGG	TCCATATCAAACTTCTGCTCACAC	60°C	372bp
AK015913	Ellis et al., 2005	TTGGAGGACGCTCATTCTG	ACGACTTGTTGTTGATCATCTCC	60°C	237bp
Xlr	Ellis et al., 2005	ATGGGAATGCTCCAGAATTG	TGTTTGTTCGTTTTCAAAGTTG	60°C	244bp
Hprt	Melton et al., 1984	CCTGCTGGATTACATTAAAGCACTG	GTCAAGGGCATATCCAACAACAAAC	60°C	352bp
pACT2	Clontech	CTATTCGATGATGAAGATACCCCACCAAACCC	GTGAACTTGCGGGGTTTTTCAGTATCTACGA	68°C	variable

Table 2.2 Primers used for Reverse Transcriptase – Polymerase Chain Reaction (RT-PCR)

2.2.2 RNA FISH on surface spread spermatogenic cells

The probes used for RNA and DNA FISH are given in Table 2.3

Purification of BAC/fosmid probes

Bacteria containing the BAC or fosmid were streaked onto LB plates containing 12.5μg/mL chloramphenicol and grown overnight 37°C. A single colony was inoculated into 10mL LB medium containing 12.5μg/mL and grow overnight at 37°C. Bacteria was pelleted by centrifuging at 4,000rpm for 15min at 15°C and then resuspended in 300μL P1 solution (15mM Tris pH 8, 10mM EDTA, 100 μg/mL RNAse A) by vortexing. Three hundred microlitres of P2 solution (0.2M NaOH, 1% SDS), was added, gently shaken to mix and incubated at room temp for 5min. 300 μL P3 solution (3M potassium acetate, pH 5.5) was then added, mixed, incubated on ice for 5min and centrifuged at 13,000rpm for 10min at R/T. The supernatant (800μL) was transferred into a fresh Eppendorf tube, and 480μL (0.6vol) of ice-cold isopropanol was added before being mixed by inversion. The solution was then centrifuged at 13,000rpm for 15min at R/T, and the supernatant discarded. The BAC DNA pellet was washed in 500μL 70% ethanol by inverting and centrifuge at 13,000rpm for 5min at R/T. The 70% ethanol was then removed from the pellet, and the pellet allowed to air dry before being resuspended in 60μL TE_8 (10mM Tris-HCl, 1mM disodium EDTA, pH 8.0). The BAC DNA was then incubated with 1μL 10mg/mL RNAse A (Sigma) overnight at 37°C. After treatment with RNase A, the BAC DNA solution was supplemented to 400μL using TE_8 and then the protein was removed by extraction in equal volume of phenol, phenol:chloroform:isoamyl alcohol and finally chloroform:isoamyl alcohol. In each case the solutions were mixed by inversion, centrifuged at 13,000rpm for 5min a R/T and the upper phase transferred to a new Eppendorf tube. The final volume of BAC DNA was estimated and precipitated using 0.6 volumes ice-cold isopropanol followed immediately by centrifugation at 13,000rpm for 15min at 4°C. The supernatant was discarded and the BAC DNA pellet was washed in 500μl 70% ethanol by inverting before being centrifuged at 13,000rpm for 5min at R/T. The 70% ethanol was aspirated, the BAC DNA pellet air dried and resuspended in 30μL TE_8. DNA was stored at 4°C until ready for probe labelling.

Long-range PCR product preparation

PCR primers were designed using the Primer3 algorithm with the following parameters: primer T_m [min = 68°C, opt = 70°C, max = 71°C], primer length [min = 25bp, opt = 28bp, max = 31bp]. For each primer pair, a 50µL long range PCR reaction was performed using the KOD XL polymerase kit (Novagen) according to manufacturer's instructions, with either 100ng genomic DNA or 50ng BAC DNA as template. The following conditions were used for PCR: 1 cycle of 95°C for 1min, 30 cycles of 94°C for 30secs and 68°C for 10mins. The PCR products were electrophoresed through a 0.8% agarose gel and excised using a sterile blade. The long range PCR product was then gel purified using the PCR Gel Extraction kit (Qiagen) according to manufacturer's instructions. The DNA concentration was quantified using the NanoDrop ND-1000 spectrophotometer (Labtek).

Probe labelling

1µg of BAC DNA or purified long range PCR product was labelled using the BioNick DNA Labeling System (Invitrogen) for biotin labelling or the DIG-Nick Translation Mix (Roche) for digoxigenin labelling according to manufacturer's instructions. The reaction was stopped when the probe length reached 50-200bp. One-tenth of the reaction volume was combined with 3µL Cot1 DNA (1µg/µL; Invitrogen) and 1µL salmon sperm DNA (10mg/mL) before being precipitated by adding 100% ethanol and storing at -80°C for 10min. The DNA was pelleted by centrifuging at 13,000rpm for 10min at 4°C. The supernatant was discarded and the pellet washed in 100µL 70% ethanol by inverting several times before being centrifuged at 13,000rpm for 5min at 4°C. The 70% ethanol was aspirated, and the pellet air dried before being resuspended in 10µL deionised formamide (Sigma). Probes were stored at -20°C until use.

RNA FISH

A cell suspension was made from freshly harvested or frozen (stored at -80°C) testis material in ice-cold RPMI + L-glutamine using sterile scalpel blades. Sterile Superfrost slides (BDH) were placed on an ice cold, horizontal platform and two drops of cell suspension were added to each slide. Cells were permeabilised by adding ice-cold CSK buffer (100mM NaCl, 300mM sucrose, 3mM $MgCl_2$, 10mM PIPES, 0.5% Triton X-100, 1mM EGTA, 2mM Vanadyl Ribonucleoside) to the slide for 10min. The CSK solution was drained from the slide and cells fixed for 10min with ice-cold 4%

paraformaldehyde (PFA) diluted in tissue-culture grade PBS. After draining off the PFA solution, slides were rinsed in ice-cold PBS and transferred into ice-cold 70% ethanol. The slides were dehydrated through an ice-cold ethanol series (70%, 80%, 95%, 100%, 3min each) followed by air drying. Biotin-labelled probes were denatured at 80°C for 10min. Following denaturation, 10µL 2X hybridization buffer (4XSSC, 50% dextran sulphate, 2 mg/mL BSA, 2mM Vanadyl Ribonucleoside) was added to the probe and vortexed to mix. Probes were then prehybridised at 37°C for 30min. The prehybridised probe was added directly onto the slide, placed into a humid chamber and incubated overnight 37°C. Slides were washed at R/T on a shaker three times in stringency wash solution A (50% formamide, 1XSSC; pH 7.2-7.4) preheated to 42°C, and three times in stringency wash solution B (2XSSC, pH 7-7.2) preheated to 42°C, for 5min each wash. The slides were the rinsed briefly in stringency wash solution C (4XSSC, 0.1% Tween-20, pH 7; kept at R/T) before being drained, and placed horizontally in a humid chamber. Slides were blocked by adding 100µL blocking buffer (4XSSC, 4mg/mL BSA, 0.1 % Tween-20) to each slide, a coverslip applied and the slides incubated at 37°C for 30min. Afterwards, the coverslip was removed from the slide, the blocking buffer drained and 100µL of streptavidin AlexaFluor 555 conjugate (Invitrogen) diluted 1:100 in detection buffer (4XSSC, 1mg/mL BSA, 0.1 % Tween-20) added to each slide before being incubated at 37°C for 30min. The coverslip was then removed and the slides washed three times in stringency wash solution C for 2min each, with shaking. Next, 100µL of biotinylated anti-streptavidin (Vector) diluted 1:100 in detection buffer was added to the slide, a coverslip applied followed by incubation at 37°C for 30min. After removing the coverslip, the slides were washed three times in stringency wash solution C at room temp for 2min, with shaking and 100µL diluted streptavidin AlexaFluor 555 conjugate added to each slide. Slides were incubated at 37°C for 30min before being washed three times in wash solution C for 2min each. Slides were then drained and mounted in Vectorshield mounting media with DAPI (Vector), ready to be observed. Slides were stored at -20°C.

Antibody staining after RNA FISH

Coverslips were removed, and slides were washed in PBS twice for 10min each. Next, slides were re-fixed for 10min in 4% PFA, and washed once in PBS for 5min. Slides were then ready for immunostaining as described in section 2.3.3.

DNA FISH post-RNA FISH

After removing the coverslips, the RNA FISH slides were washd two times in PBS at R/T for 10min each. Slides were then dehydrated in the following ethanol gradient; two washes in 70%, two washes in 90%, two washes in 100%, each wash for 3min. Slides were air dried and then denatured for 8min at 80°C in denaturation solution (70% deionised formamide: 30% 2xSSC). After quenching the slides in ice cold 70% EtOH for 4min, the ethanol gradient described above was repeated. DIG-labelled probes were denatured at 80°C for 10min before adding 10µL 2X hybridization buffer (as described above) to each probe. Probes were vortexed to mix and rehybridised at 37°C for 30min. The prehybridised probes were added to the denatured, air dried slides and then incubated overnight at 37°C. Stringency washes were carried out as described for RNA FISH. After incubating slides in blocking buffer for 30min at 37°C, the coverslip was removed from the slide and the blocking buffer drained. Next, 100µL FITC-conjugated anti-digoxigenin (Chemicon) diluted 1:10 in detection buffer was added to each DNA FISH slide, a coverslip applied and the slides incubated a 37°C for 60mins. The slides were washed after removing the coverslip three times in stringency wash solution C for 2min each before being drained and mounted in Vectashield mounting medium with DAPI.

Chromosome painting post-RNA FISH

Coverslips were removed from the RNA FISH slides, which were then washed once in PBS for 10min. Next, the slides were dehydrated, denatured, dehydrated again and air dried as described for DNA FISH. Cy3 or FITC StarFISH© mouse X or Y chromosome paint (Cambio) was incubated at 65°C for 10min followed by prehybridisation for 30min at 37°C according to the manufacturers' instructions. Chromosome paint was added to the slide, a coverslip applied followed by an overnight incubation at 37°C. Following the overnight incubation, stringency washes were performed as described for RNA FISH before mounting the slides in Vectashield mounting medium with DAPI.

Table 2.3

Gene	BAC/Fosmid identifier	Source	Long range FP	Long range RP	Product size	Reference
Xmr/Slx	RP23-470D15	CHORI	N/A	N/A	N/A	Reynard et al., 2007
Slxl1	RP24-170G23	CHORI	TCATTCCCACCTCCTGAAAACTCCCTTA	TTTGTGATCATTCAGGCATAGTGCCAAC	8088bp	Mueller et al., 2008
	RP24-170G23	CHORI	TTCCTGAAGAAATCGTTGGAGATACACG	TCCGTACAAAAGGACTATTTGCCACTCA	9038bp	Mueller et al., 2008
Satl1	RP24-209010	CHORI	N/A	N/A	N/A	N/A
Vsig1	RP24-291J23	CHORI	N/A	N/A	N/A	N/A
Ube1y	B65	Research Genetics	N/A	N/A	N/A	N/A
Uty	CITB-246A22	Research Genetics	N/A	N/A	N/A	Turner et al., 2006
Ott	RP24-278F7	CHORI	GGGTTCCTTTCTTCTTGATCTGTGTTTCC	GTCATTCACATGGATTGCTTTTGTGCAT	8893bp	Mueller et al., 2008
Fmr1	G135P65476A4	CHORI	CTGTCAGCAGGCAGCTTTTACATCCTGT	CTTGTGCGTGGACAGCATTTTGAGAGTA	12225bp	Mueller et al., 2008
	G135P65476A4	CHORI	ATGCCACCAAGTTCCCTACCTTCCAATA	GTGACAAATATCTCCTCCAACCCCAACA	12797bp	Mueller et al., 2008
Ddx3x	CITB-551M19	Research Genetics	N/A	N/A	N/A	Turner et al., 2006
Grhpr	RP24-460J15	CHORI	N/A	N/A	N/A	N/A
Prkdc	RP24-354G13	CHORI	N/A	N/A	N/A	N/A
Brca1	BMq-359C01	Gene Services	N/A	N/A	N/A	N/A
Atr	RP24-3994J4	CHORI	N/A	N/A	N/A	N/A
Adam3	RP24-103I8	CHORI	N/A	N/A	N/A	N/A
Xiap		CHORI	N/A	N/A	N/A	N/A
Sly	RP24-402P5	CHORI	N/A	N/A	N/A	N/A

Table 2.3 BAC/Fosmid identifiers and long range PCR primer sequences used for gene-specific RNA FISH

2.2.3 Northern blot

Sample Preparation

RNA was extracted from testes as described in 2.2.1. Twenty micrograms of RNA was diluted in sample buffer (40mM morpholinopropanesulfonic acid (MOPS) pH 7.0, 10mM sodium acetate, 1mM EDTA pH 8.0, 50% deionised formamide, 5.9% formaldehyde) and incubated at 65°C for 5min. 1μL of loading buffer (50% glycerol, 1mM EDTA, 0.4% bromophenol blue) was added to each RNA sample just prior to loading.

Electrophoresis of RNA samples and transfer to Hybond-N membrane.

RNA samples were loaded onto a 1.4% formaldehyde/agarose gel (1.4% agarose, 6.66% formaldehyde, 40mM MOPS pH 7.0, 10mM sodium acetate, 1mM EDTA). The RNA was then separated by electrophoresis at 80V for 4hrs in running buffer (40mM MOPS pH 7.0, 10mM sodium acetate, 1mM EDTA). After electrophoresis, the gel was rinsed three times in water, incubated in 50mM sodium hydroxide for 20min at R/T, rinsed in water three times and incubated twice in 20xSSC for 20min each. The RNA was then transferred to a Hybond-N membrane (Amersham) overnight in 20xSSC as previously described (Maniatis et al., 1982). The membrane was rinsed twice in 2xSSC for 5min each, allowed to air dry and then baked for 2hrs at 80°C.

Probe hybridisation and detection

The probes used for northern analysis were the *Sly* cDNA probe (Touré et al., 2005), and the *Xmr*, *AK005922* and *Mgclh* probes previously used by Ellis et al, (2005). An actin probe that recognises α and β actin transcripts (Minty et al., 1981) served as a loading control. After baking, the membrane was incubated for 2hrs at 60°C in hybridisation buffer (6xSSC, 5x Denhardt's solution, 0.1% SDS, 50mM sodium phosphate, 10μg/mL salmon sperm DNA). Next, 25ng of probe DNA was labelled with dATP α^{32}P using the Prime-It II Random Primer labelling Kit (Stratagene) according to the manufacturers instructions, followed by probe denaturation at 95°C for 5min. The membrane was then incubated overnight at 60°C with the denatured probe in hybridisation buffer. After probe hybridisation, the membrane was rinsed three times with 2xSSC, 0.1% SDS at R/T and once at 57°C for 5min each. The membrane was then washed twice in 0.5xSSC, 0.1% SDS for 30min each at 57°C before being exposed to X-ray film (Kodak) at -80°C for 5hrs. Subsequently, the

membrane was exposed to a phosphorimager screen overnight at R/T to allow quantitation of hybridisation using ImageQuant software. For multiple hybridisations, the membrane was stripped for 1hr in stripping solution (50% deionised formamide, 10mM sodium phosphate pH 6.8) at 60°C and then washed once in 2xSSC for 20min at R/T before being reprobed.

2.3 Immunohistochemistry

The preparation of material for immunohistochemistry is described below, and the antibodies used in this thesis are listed in table 2.4.

2.3.1 Preparation of spermatogenic cells for immunostaining

Testis squash procedure

Squashes of spermatogenic cells were carried out according to the procedure of Page et al (1998). Freshly harvested testis material was placed in PBS. Following removal of the tunica albuginea, the seminiferous tubules were gently shaken in order to remove the adherent extratubular remnants. The tubules were then placed in fresh 2% formaldehyde (TAAB) in PBS containing 0.05% Triton X-100 at R/T for 10min. Small pieces of tubule were teased apart using forceps on ethanol-cleaned Superfrost slides. The resulting suspension was squashed by applying a 22 X 50mm coverslip over the slide and pressing down briefly. The slides were then immersed in liquid nitrogen, after which coverslips were removed and slides were washed three times in PBS for 5min each. Immunostaining was then performed as described in section 2.3.3.

Surface spread procedure

Frozen testis material from three mice per genotype was placed in R/T RPMI medium with added L-glutamine and allowed to defrost. After defrosting, a single cell suspension was made for each genotype using sterile scalpel blades and the resulting suspension transferred to a 15mL round bottomed tube. The cells were fixed for 5min at R/T in fixation solution (2.6mM sucrose, 1.86% formaldehyde in PBS), and centrifuged at 1000rpm for 5min at R/T in an Eppendorf 5804 centrifuge. The fixative was removed and the cells resuspended in PBSA. Three drops of the cell suspension were added to Superfrost Plus slides (BHD) and allowed to air dry at R/T. The cells

were permeabilised by adding 0.5% Trition X-100 to the slides for 10min at R/T. The slides were then drained and washed once in PBS for 5min, before continuing with immunostaining staining protocol as described in section 2.3.3

2.3.2 Preparation of testis sections for immunohistochemistry

Preparation of testis cryosections

Freshly dissected mouse testes were fixed in 4% PFA diluted in PBS overnight at R/T. Testes were then rinsed twice in PBS by inversion, placed in 30% sucrose solution at 4°C and allowed to sink. Testes were then positioned in optimal cutting temperature (OCT) in Dispomoulds and frozen in place using dry ice. Frozen samples were stored at -80°C until ready for sectioning. Ten micrometre sections were cut with a Cryostat (Leica) and transferred onto Superfrost Plus slides (BDH). Slides were stored at -80°C until required. Slides were removed from -80°C and allowed to defrost at R/T before being rinsed twice in PBS, 0.1% Triton to remove the OCT. The sections were then fixed in 4% PFA for 2min at R/T and rinsed twice more in PBS, 0.1% triton. Immunostaining was then performed as described in section 2.3.3

Preparation of paraffin-embedded testis sections

After dissection, mouse testes were either fixed in 4% PFA overnight at R/T, or pre-fixed in 4% PFA for 4hrs at R/T before being fixed in dilute Bouin's solution (0.675% picric acid, 9.25% formaldehyde, 4.9% glacial acetic acid diluted in miliQ water) overnight at 4°C. Testes were then rinsed in 70% ethanol for 30min and then stored in fresh 70% ethanol overnight at 4°C. Next, the testes were dehydrated through an ethanol series (85%, 90%, 95% for 30min each and 3x30min in 100% ethanol). Testes were washed in 1:1 xylene:100% ethanol for 20min at R/T and then rinsed three times in xylene for 20min each. Before embedding the testes in paraffin wax, they were incubated in 1:1 xylene:paraffin wax at 60°C for 20min, in paraffin wax for 30min, and finally 1hr in paraffin wax at 60°C. Testes were embedded in paraffin wax and stored at 4°C until sectioning. 3μm sections were cut by a Cambridge Rotary Rocking microtome and mounted onto Superfrost slides. Slides were stored at 4°C until required. Slides were then heated to 60°C for 15min before being allowed to cool to R/T. Next, the sections were de-waxed by rinsing the slides twice in histoclear (National Diagnostics) for 5min each and once in 1:1 histoclear:100% ethanol. The slides were rehydrated through an ethanol series (two 5min washes in 100% ethanol

followed by one 5min wash in 95%, 80%, 70% and 50% ethanol) before being rinsed twice in PBS for 5min each. The slides were then boiled for 10min in 0.01M sodium citrate solution pH 6.0 using a microwave oven to retrieve antigens. After boiling, the slides were rinsed twice for 5min each in PBS before continuing the antibody staining protocol described in section 2.3.3.

2.3.3 Antibody staining

Primary and secondary antibodies used for immunostaining are listed in Table 2.4. Slides were incubated in PBT (PBS, 0.15% BSA, 0.1% Tween-20) for 1hr at R/T. Following draining of excess PBT, 100µL of the appropriate primary antibody diluted in PBT was added and a 22 X 64mm coverslip placed over the slide. Slides were then incubated in a humid chamber overnight at 37°C (or 4°C for cryosections). Following primary incubations, coverslips were removed and slides were washed three times in PBS for 5min each. Slides were drained and 100µL of the secondary antibody diluted in PBS was applied. After incubating at 37°C for 1hr in a humid chamber, slides were washed in PBS three times for 5min each. One drop of Vectorshield mounting media with DAPI was added and a coverslip added. Slides were kept in the dark at -20°C until viewing.

2.3.4 Examination

Immunostained slides were examined and digitally imaged on an Olympus IX70 inverted microscope with a 100W Mercury arc lamp, using a 40X, 0.85 NA UPL APO dry objective for low power images or a 100X 1.35 U-PLAN-APO oil immersion objective for high power images. Each fluorochrome image was captured separately as a 12-bit source image using a computer-assisted (Deltavision) liquid-cooled CCD (Photometrics CH350L; Sensor: Kodak KAF1400, 1317x1035 pixels). A single multiband dichromic mirror was used to eliminate shifts between different filters. Captured images were processed using Adobe Photoshop CS2.

2.4 Gel electrophoresis and protein analysis

The antibodies and their relevant concentration used for western blot analysis are listed in Table 2.4.

2.4.1 Testis protein extraction prior to gel electrophoresis

Testis protein lysates were obtained by homogenisation on dry ice and resuspended in Laemmli buffer (Sigma) at 10% w/v. Lysates were vortexed and denatured for 10min at 95°C. Samples were vortexed again and samples passed several times throught a small gauge needle to reduce viscosity caused by DNA and RNA.

2.4.2 Sodium dodecyl sulphate - polyacrylamide gel electrophoresis (SDS-PAGE)

SDS-PAGE was performed using Min-PROTEAN II gel apparatus (Bio-Rad Laboratories, UK) with 1mL spacers. Protein samples and protein standards (Bio-Rad low range or broad range molecular markers) were loaded onto the stacking gel (5.33% acrylamide, 0.125M Tris-HCL pH 6.8). The proteins were then separated through a 12% acrylamide separating gel (12% acrylamide, 5% glycerol, 0.375M Tris-HCL pH 8.8) by electrophoresis in running buffer (25mM Tris pH 8.3, 200mM glycine, 0.1% SDS) at 50mA until the desired separation of protein standards was achieved.

2.4.3 Western blotting and detection of protein on membranes

After protein samples were electrophoresed through an SDS-PAGE denaturing gel, the separated proteins were transferred to a Hybond C+ membrane (Amersham, UK) using the Mini Transfer Blot system (Bio-Rad, UK) at 100V for 1hr in transfer buffer (25mM Tris-HCL pH 8.3, 200mM glycine, 20% (v/v) ethanol). Membranes were blocked for 1hr at R/T in blocking solution (PBS, 5% Marvel milk powder, 0.1% v/v Tween20), then incubated with primary antibody diluted in blocking solution overnight at 4°C. Membranes were washed three times in PBSA, 0.1% Tween20 for 10min each at R/T with agitation and then incubated at R/T for 45min with the corresponding secondary antibody coupled to peroxidise as described by the

manufacturer (Dako, Carpintaria, CA). After 3 washes (as above), the signal was revealed by chemiluminescence (SuperSignal, Pierce, Rockford, IL) and recorded on X-ray film.

2.5 Immunoprecipitation

2.5.1 Covalent coupling of antibody to protein A sepharose beads

Protein A sepharose beads (50µl; GE Healthcare) were washed twice in binding buffer (PBS, 1% NP-40) and centrifuged at 2000rpm for 5min to remove ethanol. For antibody coupling, the beads were resuspended in 1mL of binding buffer with 5µg of antibody overnight at 4°C to allow the antibodies to bind. Beads were washed twice in 0.2M sodium borate (pH 9.0) by centrifuging as described above. Beads were resuspended in 1mL of this buffer and solid dimethyl pimelimidate (DMP) was added to a concentration of 30mM. The mixture was rotated at R/T for 30min and the reaction was stopped by washing the beads in 0.2M ethanolamine (pH 8.0) by centrifugation as before. Beads were resuspended in 1mL of fresh 0.2M ethanolamine buffer and rotated for 2hrs at R/T. Beads were then washed twice in PBS by centrifugation at 2000rpm for 5min, and suspended in PBS, 0.5% NP40. Antibody coupled beads were stored in PBS, 0.5% NP40 at 4°C until use.

2.5.2 Preparation of native testicular lysates for immunoprecipitation

Testis material was homogenised on dry ice, placed in an Eppendorf tube and 10% w/v cell lysis buffer (300mM NaCL, 10mM Tris pH 7.4, 5mM EDTA, 1% Triton-100, 0.2mM PMSF, 0.2mM sodium vanadate) was added. The testis material was resuspended by vortexing and then incubated at 4°C for 30min on an end-over-end rotor (Stuart Scientific). Samples were centrifuged at 13,000rpm for 15min at 4°C and the cell lysate supernatant collected. The lysates were then passed through a small gauge needle several times before being incubated with 50µL protein A sepharose beads for 3hrs at 4°C. Following the incubation, the lysates were centrifuged at 4°C for 5min at 2000rpm and the supernatant transferred to a new tube. This supernatant (the cleared testis lysate) was stored at -80°C until use.

2.5.3 Preparation of denatured testicular lysates for immunopreciptitation

Testis material was homogenised on dry ice and resuspended in 10% w/v denaturing lysis buffer (1% SDS, 10mM Tris pH 7.4, 1mM sodium vanadate) preheated to 95°C. Samples were boiled at 95°C for 5min before being allowed to cool to R/T. The lysates were then passed several times through a small gauge needle and centrifuged at 13,000rpm for 15min at 4°C. Next, the denatured cell lysates were incubated with 50µL protein A sepharose beads on an end-over-end rotor for 4hrs at 4°C before being centrifuged at 2000rpm for 5min at 4°C. The supernatant was transferred into a fresh Eppendorf tube and stored at -80°C until required.

2.5.4 Immunoprecipitation using covalently-coupled antibodies

Beads that had been coupled to antibodies as described in section 2.5.1 were washed once in 1mL PBS, 0.5% NP40 and incubated at 4°C overnight on an end-to-end rotor with 500µL of native or denatured testis protein lysates. The beads were then centrifuged at 2000rpm for 5min at 4°C and the supernatant removed. Beads were washed three times in PBS, 0.5% NP40 at 4°C. The beads were then resuspended in 40µL of PBS, 0.5% NP40 and 20µL of 5x Laemmli sample buffer (Sigma). The beads were boiled for 5min at 100°C to elute the proteins before being centrifuged for 5min at 2000rpm. The protein supernatant was removed and visualised by SDS-PAGE and western blotting as described in section 2.4.

Table 2.4

Primary antibodies

Antibody	Source	Catalogue number	Western blot dilution	Immunostaining of testis section dilution	Immunostaining of spread cells dilution
rabbit anti-SLY SK97	Eurogentec	N/A	1:5000	1:100	1:100
rabbit anti-SLY SK98	Eurogentec	N/A	1:5000	1:100	1:100
rabbit anti-XMR69-81	Eurogentec	N/A	1:2500	1:100	1:100
rabbit anti-XMR96-106	Eurogentec	N/A	1:2000	1:100	1:100
rabbit anti-XMR1-93	Christer Hoog	N/A	1:2000	1:100	N/A
mouse anti-XLR	HJ Garchon (Garchon and Davis, 1989)	N/A	1:1000	1:100	N/A
mouse anti-γH2AX	Upstate	16-193	1:1000	1:200	1:100
rabbit anti-γH2AX	Upstate	07-164	N/A	1:100	N/A
rabbit anti-SYCP3	Abcam	ab15092	N/A	N/A	1:100
rabbit anti-PrBPδ	R Cote (Norton et al., 2005)	N/A	1:300	1:100	N/A
goat anti-DKKL1	R and D systems	AF1508	1:500	1:100	N/A
rabbit anti TIP60 chromodomain	John Lough (McAllister et al., 2002)	N/A	N/A	1:100	N/A
mouse anti-Flag m5	Sigma	F4042	10µg/mL	N/A	1:100
rat anti-CBX1	Prim Singh	N/A	N/A	1:200	1:200
rabbit anti-H3K9me3	Upstate	07-442	N/A	1:300	1:300
rabbit anti-H3K9me2	Upstate	07-212	N/A	1:100	1:100
rabbit anti-H4K8Ac	Upstate	06-760	N/A	1:100	N/A
mouse anti-actin	Sigma	A5441	1:10,000	N/A	N/A

2.4 A list of antibodies used in this study

Secondary antibodies

Antibody	Source	Catalogue number	Western blot dilution	Immunostaining of testis section dilution	Iimmunostaining of spread cells dilution
Alexa 488 chicken anti-mouse IgG	Molecular probes	A-21200	N/A	1:500	1:500
Alexa 488 chicken anti-rabbit IgG	Molecular probes	A-21441	N/A	1:500	1:500
Alexa 488 goat anti-rat IgG	Molecular probes	A-11006	N/A	1:500	1:500
Alexa 594 chicken anti-mouse IgG	Molecular probes	A-21201	N/A	1:500	1:500
Alexa 594 chicken anti-rabbit IgG	Molecular probes	A-21442	N/A	1:500	1:500
Alexa 568 donkey anti-goat IgG	Molecular probes	A-11057	N/A	1:500	1:500
HRP-conjugated goat anti-mouse IgG	Dakocytomation	P0447	1:1000	N/A	N/A
HRP-conjugated goat anti-rabbit IgG	Dakocytomation	P0448	1:1000	N/A	N/A
HRP-conjugated rabbit anti-goat IgG	Dakocytomation	P0449	1:1000	N/A	N/A
HRP-conjugated rabbit anti-rat IgG	Dakocytomation	P0450	1:1000	N/A	N/A

2.6 Assessment of sperm morphology by silver staining

2.6.1 Preparation of sperm samples

The right epididymis was dissected from an adult male and separated into the caput 1 and caput 2 regions. Four drops of PBS were added separately to caput 1 and caput 2 and a cell suspension made using sterile scalpel blades. The cell suspension was pipetted up and down for two minutes to suspend the sperm and two drops of the cell suspension were added to sterile Superfrost slides. After spreading the cell suspension across the slide, the slides were left to air dry before being fixed for 5min in 3:1 methanol:glacial acetic acid solution. The slides were then air dried and rinsed twice in 0.4% Photo-Flo (Kodak) pH 8.3 for 5min each. The slides were air dried before proceeding with the silver staining protocol.

2.6.2 Silver staining of epididymal sperm

Two drops of developer solution (1% w/v gelatine in distilled water) were mixed with two drops of silver solution (50% w/v silver nitrate in distilled water) on a coverslip and the coverslip added to the slide. The slide was placed on a 60°C hotplate for 1min to 3min until it turned golden-brown. The slide was rinsed in distilled water and washed for 3min with several changes of water before being allowed to air dry. The slide was then mounted and viewed under 100X magnification using a light microscope (Olympus BH2).

2.6.3 Scoring of sperm abnormalities

For each genotype, sperm was analysed from 7 adult males. Slides were coded and randomised. One hundred sperm from the caput 1 and 100 sperm from the caput 2 were analysed per mouse, and the sperm were classified as described previously (Mahadevaiah et al., 1998).

2.7 Generation of DNA constructs

The plasmids used in this study are the pGBKT7 vector (Clontech; Appendix 1), the pCMV/SV Flag1 plasmid constructed by Y Kamachi (Kamachi et al., 1999; Appendix 2), and the mP1 construct (Braun, 1990).

2.7.1 Amplification of cDNA and incorporation of restriction sites using PCR

Sly, *Xmr* and *AK015913* cDNA sequences were amplified from XY adult testis cDNA by RT-PCR as described in section 2.2.1. PCR primer pairs used are listed in Table 2.5 and were designed to incorporate a unique restriction endonuclease site at each end of the amplified sequence. A 6 base pair (bp) restriction endonuclease site was added at the 5'-end of the 5'-primer and the 3'-end of the 3'-primer with a 4bp-6bp flanking region to aid enzymatic restriction digests.

For each construct, four 25µL PCR reactions were performed. Each reaction contained 1µL Pfx50 DNA polymerase (Invitrogen), 2.5µL 10X Pfx50 PCR buffer (Invitrogen), 5µL 7.5mM dNTPs (GE Healthcare), 1µL 250µM forward primer, 1µL 250µM reverse primer, 3.5µL 20mM magnesium sulphate, and 2µL cDNA template. The standard PCR cycling procedure was 95°C for 10min (1 cycle), 95°C for 30sec, annealing temperature for 40sec (see Table 2.5), 68°C for 1min (35 cycles), followed by 68°C for 10min (1 cycle).

2.7.2 Gel purification of PCR products

PCR products were run on a 1% agarose gel made with 1X TAE to which a suitable volume of ethidium bromide had been added. The PCR product was excised from the gel using sterile scalpel blades and purified using the QIAquick Gel Extraction Kit (Qiagen) in accordance to the manufacturer's instructions.

2.7.3 Digestion of DNA with restriction endonucleases

Purified PCR products and DNA vectors were digested with the appropriate restriction endonucleases using the supplied buffer (Roche, New England Biolabs) for 4hrs at

37°C. DNA digestion was confirmed by running a small sample of the digest product on a 1% agarose gel. Protein and salt contaminants were removed using the QIAquick Gel Extraction Kit (Qiagen), and the digested DNA eluted in 15µl of sterile double-distilled water (ddH_2O). DNA was quantified using the NanoDrop ND-1000 spectrophotometer (Labtek).

2.7.4 Ligation of insert into vector

Isolated digested DNA fragments were ligated into prepared vector using the Rapid DNA Ligation Kit (Baker et al.) for 1hr at 16°C according to the manufacturer's guidelines.

2.7.5 Transformation of *E. coli* by plasmid DNA

For each construct, 50µl of One Shot TOP10 chemically competent *E. coli* (Invitrogen) were transformed with DNA in accordance with the maufacturer's instructions. Briefly, the TOP10 cells were thawed on ice and 1-4 µl of DNA solution was added. After incubating on ice for 15min, the cells were heat-shocked for 30sec at 42°C and placed on ice for 5min. 250µl of R/T SOC medium was added and the cells were incubated at 37°C for 1hr with agitation. 50µl of cells were plated onto pre-warmed Luria-Bertani (LB) agar plates containing the appropriate antibiotic (50µg/mL ampicillin for pCMV/SV Flag1 and mP1 constructs, 50µg/mL kanamycin for pGBKT7 constructs). Bacterial plates were incubated overnight at 37°C.

2.7.6 Colony selection following transformation

Single bacterial colonies were picked with sterile 20µl pipette tips and used to inoculate 12µl of LB broth with the appropriate antibiotic. One microlitre of colony cell suspension was used as template in a 25µl PCR reaction (as described in section 2.1.2) and amplified for 20 cycles using the primers listed in Table 2.5. PCR products were run on a 1% agarose gel and bacterial colonies with the correct sized insert were used to inoculate 3mL of LB broth containing the appropriate antibiotic.

2.7.7 Purification of plasmid DNA from *E. coli*

After growing overnight at 37°C at 200rpm, 3mL of the resulting bacterial culture was pelleted by centrifugation at 6000rpm for 5min using a desktop centrifuge. The supernatant was removed by aspiration and the DNA isolated using the Nucleospin Plasmid Kit following the manufacturer's protocol. DNA was eluted with 20-50µl of RNase/DNase free water and stored at -20°C.

2.7.8 Long term storage of *E. coli* cultures

250µl of sterile glycerol was added to an equal volume of bacterial culture and mixed by pipetting. Glycerol stocks were stored at -80°C. When required, glycerol stocks were thawed on ice and 8µl used to inoculate 3mL LB broth with the appropriate antibiotic. Bacterial cultures were then grown and the plasmid DNA extracted as described above.

2.7.9 DNA sequencing and sequence analysis

Sequencing was performed by Lark Technologies. Approximately 1µg of DNA was sent for sequencing with 30µM of the appropriate sequencing primer. DNA sequence analysis and alignments and translated protein sequence alignments were performed using the ClustalW sequence alignment algorithm (www.ebi.ac.uk/**clustalw**/).

2.7.10 Preparation of DNA for microinjection

mP1-*Sly*, mP1-*Slx* and mP1-*Slx* cDNA constructs were synthesised as described above. The constructs were linearised by digesting with NaeI and ApaII restriction endonucleases in 10x buffer I (New England Biolabs) at 37°C overnight. The digestion products were then run on a 0.8% TAE and the appropriate band extracted from the gel. After purifying the linear plasmid DNA using the QIAquick Gel Extraction Kit, the DNA was eluted in 30µl of elution buffer (Qiagen). Next, the plasmid DNA was quantified and diluted to 5ng/µl in RNase/DNase free water and stored at -20°C until required. Microinjection was performed by Sophie Woods.

Table 5.4

Construct	Forward primer	Reverse primer	Annealing temperature	Product size	Restriction endonucleases
Flag-*Sly*	ATGGACGAATTCATGGCTCTTAAGAAATTGAAGGT	ATGGACGCGGCCGCTTAGTTCTTGGTCCCCAAGTTCATC	60°C	696bp	EcoRI+NotI
Flag-*Xmr*	ATGGAAGAATTCATGTCTATTAAGAAACTCTGGGTG	ATGGAAGCGGCCGCTCATAATGTCTCTTCACCATCTA	60°C	668bp	EcoRI+NotI
Flag-*AK015913*	ATGGAAGGAATTCATGGCTCTTAAGAAACTGTGG	ATGGAAGCGGCCGCTCATTTTCTCAATTCACCATCTACATCA AAAAG	60°C	495bp	EcoRI+NotI
pGBKT7-*Sly*	GGGGGGAATTCATGGCTCTTAAGAAATTGAAGG	GGGGGGATCCTTCTTGGTCCCCAAGTTCAT	60°C	690bp	EcoRI+ BamH1
pGBKT7-XMR	GGGGGGAATTCATGTCTATTAAGAAACTGTGGG	GGGGGGGATCCTCATAATGTCTCTTCACCATCT	60°C	660bp	EcoRI+BamHI
pGBKT7-XMR N terminal	GGGGGGAATTCATGTCTATTAAGAAACTGTGGG	GGGGGGGATCCAAGGTCCAATTCTGAAGCATT	58°C	317bp	EcoRI+BamHI
pGBKT7-XMR COR1	GGGGGGAATTCATGGAAGTACAGAATCCAGTAA	GGGGGGGATCCTCATAATGTCTCTTCACCATCT	58°C	320bp	EcoRI+BamHI
mP1-*Sly*	GGGGTATTAATTAAGAGAAGAATGGCTCTTAAGAAATTG	AAGATCGCATGCTTAGTTCTTGGTCCCCAAGTTCAT	60°C	680bp	PacI+SphI
mP1-*Slx*	GGGTTGGATCCTTAATTAAGAGAAAAATGTCTATTAAGAAAC TGTGGGT	AAGGTTCCTTCACAAAGATCGCATGCTCATAATGTCTCTTCA CCATCTAC	60°C	694bp	PacI+SphI
mP1-*Slx* cDNA	GGGGTATTAATTAACAGGAATCTCTCTGACAAC	AAGATCGCATGCGTTAGTGAATTTTTTATTAGGTTA	58°C	932bp	PacI+SphI

Table 2.5 Primers used for generating DNA constructs

2.8 Yeast-two-hybrid analysis

2.8.1 Generation of bait constructs

The bait plasmids analysed in this thesis contain the following inserts: the full length *Sly* ORF (designated pGBKT7-*Sly*), *Xmr* ORF (pGBKT7-*Xmr*), the first 106 amino acids of XMR (pGBKT7-XMR N-terminal) and the COR1 domain of XMR (pGBKT7-XMR COR1). The bait plasmids were constructed by PCR amplification of the required DNA sequence using the primers listed in Table 2.4 followed by insertion of the BamHI-EcoRI PCR fragments into the pGBKT7 vector (Appendix 1) as described in section 2.7. Approximately 100ng of bait vector was transformed into the *S. cerevisiae* AH109 reporter strain (see section 2.8.2 for more details) according to the TRAFO protocol (http://home.cc.umanitoba.ca/~gietz/Quick.htmL: Gietz and Woods, 2002) and positive transformants were selected by plating onto Synthetic Dropout (SD) agar plates lacking tryptophan. Positive clones where then tested for autoactivation of the reporter genes, toxicity and synthesis of the GAL4-DB-bait fusion proteins as described in the manufacturer's protocol.

2.8.2 Library screening

The Matchmaker Two-Hybrid System 3 (Clontech) was used to screen a pretransformed mouse adult testis Matchmaker cDNA library. The library was pretransformed into *S. cerevisiae* host stain Y187 and the construct expressing the bait was transformed into the reporter strain AH109, which contains three reporters – HIS3, ADE2 and MELI – under control of the distinct GAL4 upstream activating sequences and TATA boxes. The pretransformed library was screened according to the manufactures' instructions. Briefly, a single colony carrying the pGBKT7-bait plasmid in the AH109 stain was used to inoculate 5mL of SD medium lacking tryptophan (SD/-Trp), and the culture grown for at 30°C for 8hrs at 175rpm. 1mL of this preculture was then added to 50mL of SD/-Trp media and grown overnight at 30°C at 250rpm until the OD_{600} reached 0.8. The overnight culture was centrifuged at 1,000g for 5min, the supernatant discarded and the pellet resuspended in 5mL of SD/-Trp medium. A frozen aliquot of the library was thawed at R/T and added to a flask containing 45mL of 2X YPD medium (20g/l yeast extract, 40g/l bacto-peptone, 20g/l dextrose) supplemented with with 50µg/mL kanamycin. The 5mL culture containing the bait was then added

to the flask, and the resulting culture grown at 30°C for 20-24hrs at 40rpm until diploids were present (determined by examination under a light microscope). Next, the yeast were pelleted by centrifugation at 1000rpm for 10min and resuspended in 10mL of 0.5x YPD medium (5g/l yeast extract, 10g/l bacto-peptone, 5g/l dextrose). 200µL aliquots were plated onto 14cm diameter plates containing SD –Trp/-Leu/-His agar and incubated for 5 days at 30°C. Cells were also plated on SD –Trp, SD –Leu and SD –Trp/-Leu plates to calculate the number of library clones screened and mating efficiency.

Colonies growing on SD –Trp/-Leu/-His plates after 5 days were picked and restreaked three times onto SD -Trp/-Leu/-His agar plates to obtain clones with only one library vector. These colonies were then picked and streaked onto SD –Trp/-Leu/-His/-Ade agar containing 5-Bromo-4-chloro-3-indolyl α-D-galactopyranoside (X-α-Gal; glycosynth) and grown for 8 days at 30°C to check for expression of all three reporter genes. Colonies that were Ade+, His+ and Mel+ were considered positive interactors.

2.8.3 Isolation and sequencing of library plasmids.

Single Ade+, His+, Mel+ colonies were used to inoculate 10mL of SD –Leu/-His/Ade medium and grown overnight at 30°C and 200rpm. The cells were pelleted by centrifuging at 3000rpm for 6min in a Centra MP4 centrifuge (International Equipment Company). The pellet was resuspended in 250µL P1 lysis buffer (Qiagen) and purification of plasmid DNA was performed using the Qiagen plamid miniprep kit (Qiagen) following the manufacturer's instructions, with an additional lysis step of adding 5µL of 10mg/mL zymolase to buffer P1, incubating at 37°C for 1hr at 250rpm and vortexing vigorously for 5 min. Plasmid DNA was eluted in 20µL elution buffer (Qiagen) and quantified. The library insert was amplified using 1µL of plasmid DNA as a template and the pACT2 MATCHMAKER 5' and 3' AD LD-Insert Screening Amplifiers (Clontech; Table 2.2) used as primers in a 25µL PCR reaction as described in section 2.1.2. The PCR conditions used were 94°C for 8min (1 cycle), 94°C for 30sec, 68°C for 3min (28cycles) and 68°C for 10min (1 cycle). PCR products were electrophoresed on a 1% TAE/agarose gel and extracted as described in section 2.7.2. Approximately 2µg of purified plasmid DNA or 300ng of PCR product was sent for sequencing as described in section 2.7.9.

2.9 Commonly used buffers and solutions

PBS (Phosphate buffered saline)

1% (w/v) NaCl, 0.025% (w/v) KCl, 0.14% (w/v) Na_2HPO_4, 0.025% (w/v) KH_2PO_4. The pH was adjusted to 7.4 with concentrated HCl.

2X LaemmLi's buffer without β mercaptoethanol

4% (w/v) SDS, 20% (w/v) glycerol, 0.12M Tris, 1mM DTT pH 8, containing a trace of bromophenol blue.

Luria-Bertani (LB) medium

1% (w/v) Tryptone, 0.5% (w/v) yeast extract, 1% (w/v) NaCl. The pH was adjusted to 7.0 with 5N NaOH.

LB agar

LB medium containing 2% (w/v) Bacto agar.

SDS-PAGE running buffer

25mM Tris base, 192mM glycine, 0.1% SDS.

Western blot transfer buffer

30mM Tris base, 240mM glycine, 20% ethanol.

50X TAE

242g Tris base, 57.1 mL glacial acetic acid, 18.6g EDTA made up to 1L with ddH_2O. For 1X TAE, dilute in ddH_2O.

SOC medium

20g Bacto Tryptone, 5g Bacto Yeast Extract, 10mM NaCl, 2.5mM Kcl, 10mM $MgCl_2$, 10mM $MgSO_4$, 20mM glucose.

20X SSC

3M NaCl, 300mM trisodium citrate in distilled H_2O. Adjust pH to 7-7.2 with 1M HCl and sterilise by autoclaving.

Chapter 3

Analysis of the expression and function of *Sly* in the testis

Analysis of the expression and function of *Sly* in the testis

3.1 Introduction

Partial deletion or absence of the mouse Y chromosome long arm (Yq) is associated with up-regulation of X- and Yp-linked genes expressed during spermiogenesis, sex ratio distortion and impaired fertility (Burgoyne et al., 1992; Conway et al., 1994; Ellis et al., 2005; Grzmil et al., 2007; Styrna et al., 2003; Touré et al., 2004b; Ward and Burgoyne, 2006; Xian et al., 1992) Mice with MSYq deletions also have sperm head abnormalities, the severity of which correlates with the extent of the deletion, indicating that a multicopy gene is responsible (Burgoyne et al., 1992; Conway et al., 1994; Styrna et al., 1991a; Styrna et al., 2003; Touré et al., 2004b). Recently, microarray analysis of these MSYq deletion models identified a new multicopy Yq gene, *Sly*, deletion of which may be responsible for one or more of these phenotypes. This chapter describes the characterisation of *Sly* in the testis.

Sly (*Sycp3*-like Y-linked) is a MSYq-linked gene present in at least 65 copies (given the incompleteness of the Yq sequencing, there may be more copies), and is closely related to the X-linked multicopy *Xlr* gene family named after the founding member *Xlr* (Touré et al., 2005). *Xlr* encodes a 30kDa nuclear protein that is expressed in lymphoid cells (Siegel et al., 1987), foetal thymocytes during the rearrangement of the T-cell receptor genes (Escalier et al., 1999) and oocytes during meiotic prophase (Escalier et al., 2002). Southern blot analysis detected multiple *Xlr* related sequences on the X and Y chromosomes but it was concluded that these mostly represented non-transcribed pseudogenes (Garchon et al., 1989). However, another X-linked member was subsequently identified that was expressed in the testis during meiosis and named *Xmr* (Calenda et al., 1994); since then transcription of numerous family members has been described (Bergsagel et al., 1994; Davies et al., 2005; Ellis et al., 2005; Touré et al., 2005).

Recent bioinformatics analysis suggests that *Sly* is a chimeric gene, and was created by the fusion of the 3' region of *Xlr* and 5' region of *Xmr* together with an internal duplication of two *Xmr*-derived exons (Ellis et al., 2007). The putative SLY protein (along with other XLR family members) contains a COR1 domain, which is also found

in the synaptonemal complex protein SYCP3, from which these genes are thought to have evolved (Touré et al., 2005). Sequence analysis showed that 34 of the 65 *Sly* loci have retained protein coding potential and that the putative SLY protein is most similar to XMR, a meiosis-specific protein that localises to the sex body in pachytene spermatocytes (but see Chapter 4). The COR1 domain of the predicted SLY protein shares 79% identity to that of XLR (Touré et al., 2005); XLR co-localises with SATB1 in foetal thymocytes, a protein that binds to particular AT rich sequences at the base of chromatin loops and is proposed to regulate the expression of many genes (Dickinson et al., 1992; Escalier et al., 1999). Thus, it has been predicted that the putative SLY protein will associate to chromatin loops (Touré et al., 2005) and may regulate sex chromosome chromatin conformation and expression during spermiogenesis (Ellis et al., 2005).

Northern blot analysis of multiple mouse tissues revealed that *Sly* mRNA is restricted to the testis (Touré et al., 2005), where it is present from 20d*pp*, suggesting *Sly* is transcribed in late meiotic or post-meiotic cell types. This observation was confirmed by *in situ* hybridisation, which demonstrated that *Sly* expression is restricted to spermatids, with high mRNA levels in stage 1-7 spermatids, and lower levels of transcripts in stage 8-12 spermatids (Touré et al., 2005). Transcription of *Sly* is decreased in the three MSYq deletion models in proportion to the extent of the deletion and no *Sly* band is detectable by RT-PCR in the MSYq- model lacking the Y chromosome long arm, indicating that no copies of *Sly* reside elsewhere in the genome (Touré et al., 2005).

Of the four multicopy Yq-linked genes so far identified, Touré et al. (2005) and Ellis et al. (2005) have suggested that *Sly* deficiency is the most likely cause for the sperm head abnormalities and gene up-regulation seen in the MSYq- models for several reasons. Firstly, one or more copies of *Sly* are transcribed in the 9/10MSYq- testis (unlike *Asty* or *Ssty*), which potentially explains the less severe sperm head abnormalities seen in these mice compared to MSYq- mice which lack all copies of *Sly*. Secondly, *Sly* is the most strongly transcribed of all known MSYq genes. Thirdly, it is predicted to encode a chromatin-associated protein which may localise to the sex chromosome in spermatids in a way analogous to that of its X-linked relative, XMR, during pachytene. SLY may thus regulate sex chromosome transcription and chromatin conformation, and *Sly* deficiency could affect sperm head shape by

disturbing chromatin organisation within the spermatid nucleus. Although the transcription of *Sly* is reduced or absent in the MSYq deletion models, there is an up-regulation of the related X-linked genes, *Xmr* and *AK015913* in spermatids, the increase in transcription correlating with the decrease in *Sly* transcription. All three genes are highly amplified and these observations suggest that there is an intragenomic conflict between the X- and Y-encoded copies of this gene family during spermiogenesis, a theory known as the *Sly/Xmr* conflict hypothesis (Ellis et al., 2005). Ellis and colleagues (Ellis et al., 2005) went on to proposed that the sex ratio distortion seen in the offspring of 2/3MSYq- males is due to an underlying post-meiotic X-versus-Y intragenomic conflict that has been uncovered by the reduction in MSYq encoded transcripts resulting from the deletion. *Sly* and *Xmr* may be important players in this conflict, perhaps due to their putative antagonistic effects on sex chromatin and gene transcription (Ellis et al., 2005).

In order to determine if loss of *Sly* contributes to any of the phenotypes seen in mice lacking the Y chromosome long arm, the expression of *Sly* at the transcript and protein level was analysed in the testis.

3.2 Results

3.2.1 Transcriptional analysis of *Sly* during spermatogenesis

Northern blot and *in situ* hybridisation analysis by Touré et al. (2005) indicates that transcription of *Sly* occurs specifically after meiosis in round spermatids. However, neither technique is sensitive enough to detect low level transcription of *Sly* which may be occurring prior to this point. To address this issue, the expression of *Sly* was investigated by performing RT-PCR analysis on testis samples taken during the first spermatogenic wave using *Sly*-specific primers designed by Ellis et al. (2005). In prepubertal mice, the first wave of spermatogenesis is a synchronised process whereby progressively more mature spermatogenic cell types populate the seminiferous tubules at defined time points after birth. This allows the correlation of gene expression with the appearance of a specific cell type. *Sly* mRNA was weakly detectable at 18.5d*pp*, which corresponds to the meiosis-spermiogenesis transition, with transcription increasing by 21.5d*pp* and remaining high thereafter (Figure 3.1.A). This suggests that predominant *Sly* expression occurred from 21.5d*pp*, when spermatids are present, in agreement with previous data (Touré et al., 2005).

Northern blot, *in situ* hybridisation and RT-PCR analysis all detect mature transcripts, and thus it is feasible that *Sly* transcription may initiate prior to 18.5d*pp*, but that the transcripts are not processed until this time. To precisely determine which spermatogenic cell types actively transcribe *Sly*, RNA FISH was performed using a *Sly*-containing BAC as a probe. This probe detects nascent *Sly* transcripts in the nucleus before they are processed and exported to the cytoplasm. *Sly*-specific RNA FISH signals were seen in round spermatid nuclei (Figure 3.1.B.i). Approximately one half (49.5%, 1199/2422) of round spermatids analysed had RNA FISH signals and these were multiple in nature, as expected from the multicopy nature of *Sly*. *Sly* RNA was not detected in meiotic cells (n=143; Figure 3.1.B.ii) or spermatogonia (0/112). To verify that the RNA FISH signals originated from the *Sly* gene, DNA FISH was performed using the same probe; RNA and DNA FISH signals co-localised in round spermatids, confirming these transcripts originated from the *Sly* gene. Y chromosome paint also showed 100% concordance with the presence of the RNA FISH signal, confirming that the signal originates from the Y chromosome (Figure 3.1.C). These

data suggest that *Sly* is transcribed predominantly or exclusively in round spermatid nuclei, agreeing with previous data (Ellis et al.,2005; Touré et al., 2005).

Figure 3.1 Transcriptional analysis of *Sly*

A) RT-PCR analysis of testis RNA samples taken at time points during the first spermatogenic wave using *Sly* specific primers from Ellis et al. (2005), which are designed to sequences within exon 7. The band corresponding to *Sly* mRNA is present from 18.5d*pp*.

B) Detection of *Sly* nascent transcripts by RNA FISH on

(i) a Y-bearing round spermatid nucleus
(ii) a pachytene spermatocyte

Far left panel; DAPI (blue) staining of the cell nuclei.
Left panel; *Sly* RNA FISH (red). The pachytene spermatocyte is also stained for the meiosis-specific synaptonemal complex protein SYCP3 (green).
Right panel; *Sly* DNA FISH (green).
Far Right panel; overlay of *Sly* RNA and DNA FISH signals. The nucleus is stained with DAPI (blue)

C) Y chromosome painting of a round spermatid nucleus expressing *Sly*.
Far left panel; spermatid nucleus stained with DAPI. The arrow points to the DAPI-dense Y chromosome domain, which is adjacent to the chromocentre.
Left panel; *Sly* RNA FISH signal (red).
Right panel; Y chromosome paint (green).
Far right panel; overlay of *Sly* RNA FISH and Y chromosome paint signals

Figure 3.1

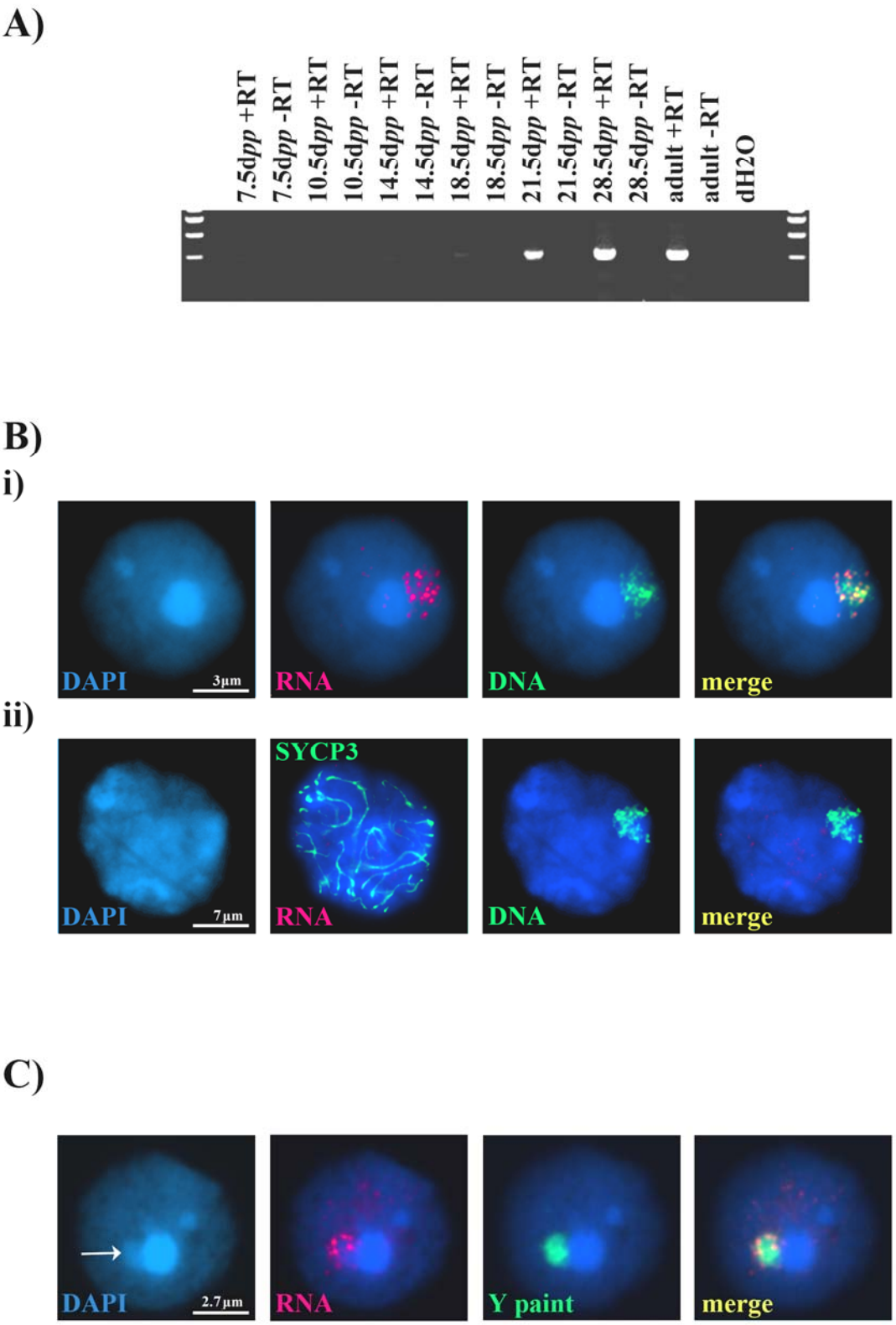
A)
7.5dpp +RT
7.5dpp -RT
10.5dpp +RT
10.5dpp -RT
14.5dpp +RT
14.5dpp -RT
18.5dpp +RT
18.5dpp -RT
21.5dpp +RT
21.5dpp -RT
28.5dpp +RT
28.5dpp -RT
adult +RT
adult -RT
dH2O
B)
i)
DAPI
3µm
RNA
DNA
merge
ii)
DAPI
7µm
SYCP3
RNA
DNA
merge
C)
DAPI
2.7µm
RNA
Y paint
merge

3.2.2 Design and characterisation of anti-SLY antibodies

Of the 65 copies of *Sly* identified based on predicted DNA sequence, 34 have retained protein coding potential, suggesting that the *Sly* mRNA is translated to produce a functional protein related to three chromatin-associated proteins, XLR, XMR (but see chapter 4) and SYCP3. To investigate the expression and localisation of the putative SLY protein, antibodies were raised against the putative SLY protein. A ClustalW alignment of XLR, XMR and SYCP3 with the predicted SLY amino acid sequence (Figure 3.2) identified a 14 amino acid SLY-specific peptide which was used to generate two SLY antibodies (the SK97 and SK98 antibodies) To determine if these antibodies could detect the putative SLY protein, COS7 cells were transiently transfected with the *Sly* ORF fused to a FLAG tag. Both antibodies were able to detect the fusion protein by immunofluorescence (Figures 3.3.A), indicating that they are able to detect the protein encoded by the *Sly* gene.

Figure 3.2

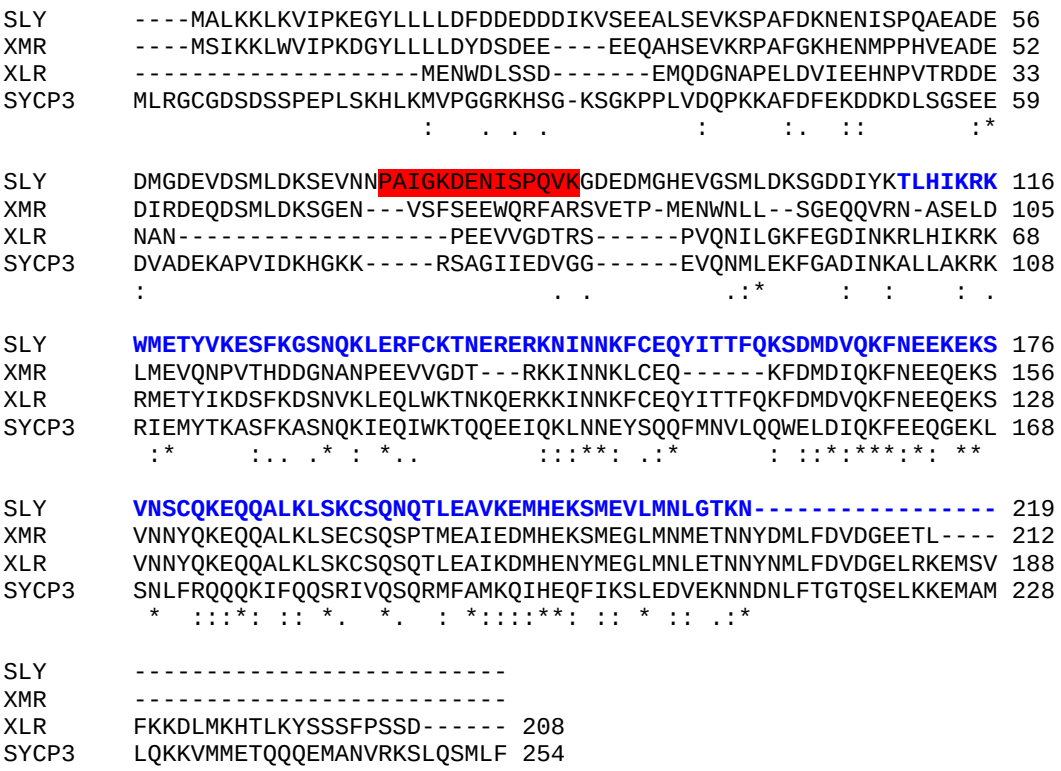

Figure 3.2 A ClustalW alignment of the putative SLY protein with XLR, XMR and SYCP3 amino acid sequences

The 14 amino acid SLY specific peptide PAIGKDENISPQVK (highlighted in red) was used to immunise two rabbits, producing two SLY antibodies, SK97 and SK98. The COR1 domain of SLY is in blue font.

Figure 3.3 Transfection of COS7 cells with a *Sly-Flag* fusion construct

A) Immunofluorescence staining of *Sly-Flag* transfected cells with
   i) anti-FLAG antibody
   ii) anti-SLY SK97 antibody and
   iii) anti-SLY SK98 antibody (bottom row).

B) Immunofluorescence staining of non-transfected COS-7 cells with
   i) anti-SLY SK97 antibody
   ii) anti-SLY SK98 antibody

Left panel; nuclei of COS7 cells stained with DAPI.
Middle panel; antibody staining (red).
Right panel; overlay of DAPI and antibody staining.

All three antibodies detect the SLY-FLAG fusion protein, which localises to both the nucleus and cytoplasm of transfected cells.

Figure 3.3

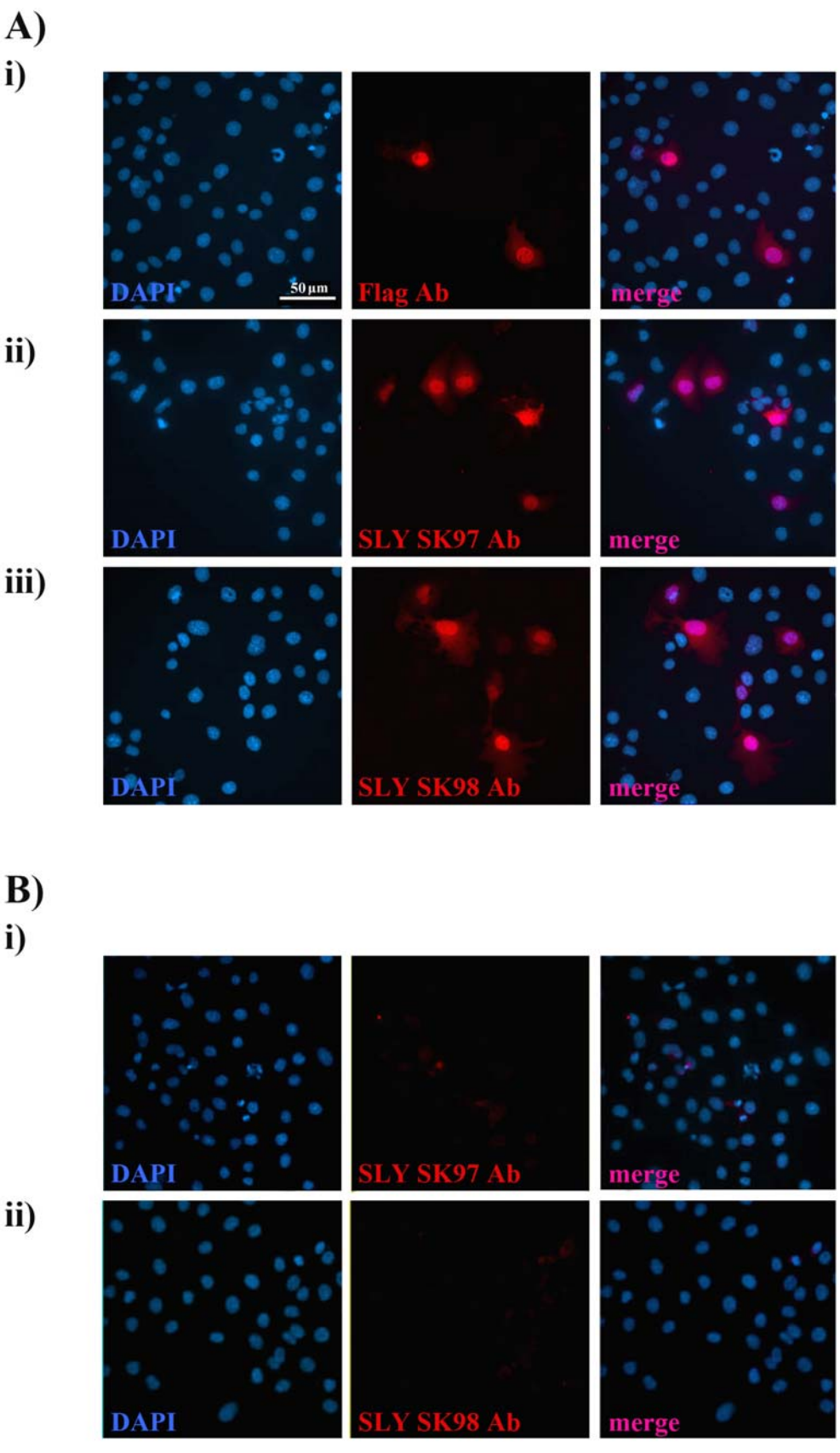
A)
i)
DAPI
50 µm
Flag Ab
merge
ii)
DAPI
SLY SK97 Ab
merge
iii)
DAPI
SLY SK98 Ab
merge
B)
i)
DAPI
SLY SK97 Ab
merge
ii)
DAPI
SLY SK98 Ab
merge

3.2.3 Expression of SLY in the testis

Northern blot analysis of multiple tissues detected *Sly* transcription only in the testis (Touré et al., 2005), and so the putative SLY protein is expected to be testis-specific. Western blot analysis of kidney and testis samples with the two antibodies detected a testis-specific protein of approximately 40kDa (Figure 3.4.A). This protein was not detected by the pre-immune serum (Figure 3.4.A) or after pre-absorption of the antibody with the peptide to which it was raised (Figure 3.4.B). Immunoprecipitation with both antibodies followed by detection with the SLY SK97 antibody confirmed that both antibodies detected the same 40kDa protein (Figure 3.4.C).

If this 40kDa protein is encoded by the *Sly* gene, it should be reduced or absent when copies of *Sly* are deleted in the three MSYq deletion models. These models lack varying lengths of the Y chromosome long arm but produce near-normal levels of sperm. Western analysis showed a clear decrease in the 40kDa protein in the 2/3MSYq- testis, suggesting that it is encoded by a multicopy gene on the Y long arm (Figure 3.4.D). The protein was undetectable in the 9/10MSYq- or MSYq- samples (Figure 3.4.D), but a faint 40kDa protein band was detected in MSYq- mice carrying an *Sly* transgene, confirming that this protein is SLY. Quantification of protein levels with Image J software suggests that there is a 75% decrease in SLY levels in the 2/3MSYq- testes compared to controls.

3.2.4 Analysis of SLY expression during spermatogenesis.

To identify which spermatogenic cells express SLY, western blot analysis was performed on testes harvested at different ages during the first wave of spermatogenesis. SLY was first detected at low levels at 21.5d*pp*, and reached adult levels by 28.5d*pp*, suggesting the protein is restricted to spermatids (Figure 3.5.A). The timing of SLY expression was further refined by analysis of daily time points between 18.5d*pp* and 22.5d*pp* which confirmed that SLY was present from 21.5d*pp* (Figure 3.5.B).

To verify that SLY is expressed exclusively in spermatids, immunostaining of adult testis cryosections was performed using both SLY antibodies. No staining was seen

with the pre-immune serum (Figure 3.6.A) or after the antibody had been preincubated with the peptide to which it had been raised (Figure 3.6.B). SLY staining was seen in most tubules and appeared to be limited to spermatids (Figures 3.6.C). No co-localisation was seen between SLY and γH2AX, a protein present in the nucleus of leptotene and zygotene cells, and the sex body domain of pachytene cells (Mahadevaiah et al., 2001), confirming that SLY was not present during meiotic prophase (Figure 3.6.D and 3.6.E). These data indicate that SLY is a spermatid-specific protein, in agreement with the transcriptional data.

Closer analysis of SLY immunostaining indicated that SLY was not nuclear as expected but was present in the cytoplasm (Figure 3.7.A). As it was possible that epitope masking may have prevented detection of nuclear SLY protein, western blot analysis of cytoplasmic and nuclear testis fractions from adult testis was performed. The 40kDa band corresponding to SLY was present in the cytoplasmic and whole testis fractions but not the nuclear fraction (Figure 3.7.B). Analysis of the SLY amino acid sequence showed that it lacked a nuclear localisation signal (NLS), due to mutation of the ancestral NLS found in XLR, potentially explaining why SLY is cytoplasmic and not nuclear as expected. The protein is also predicted to be cytoplasmic by the PSORT II bioinformatics program (http://psort.nibb.ac.jp/form2.html). Together these data indicate that SLY is predominantly if not exclusively cytoplasmic.

Figure 3.4 Western blot analysis of SLY in the testis

A) Western blot of kidney and testis protein lysates from an 8 week old male mouse. Membranes were probed with either the pre-immune serum for anti-SLY antibody SK97 (far left panel), purified anti-SLY SK97 antibody (left panel), the pre-immune serum for anti-SLY SK98 antibody (right panel) or purified anti-SLY SK98 antibody (far right panel). Anti-SLY SK97 and anti-SLY SK98 antibodies both detect a testis-specific protein of approximately 40kDa (arrowed) that is presumed to be SLY.

B) Analysis of testis and kidney lysates incubated with the following:
   i) purified anti-SLY SK98 antibody
   ii) purified anti-SLY SK98 antibody that was pre-incubated for 4hrs with the peptide to which it was raised
   iii) purified anti-SLY SK98 antibody that was pre-incubated for 4hrs with the non-specific ATR peptide.

   The 40kDa testis specific band is not detected by the anti-SLY SK98 antibody after pre-absorption with the peptide to which it was raised, but is present after pre-absorption of the antibody with a non-SLY peptide.

C) Immunoprecipitation of SLY from the testis followed by western blot with the anti-SLY SK97 antibody.

   The 40kDa protein (arrowed) is present in the imput lysate (lane 1), and is immunoprecipitated with both anti-SLY antibodies (lanes 3 and 4), but is not immunoprecipitated by the pre-immune serum (lane 2).

D) Analysis of testis protein lysates from XY, 2/3MSYq-, 9/10MSYq-, MSYq- and MSYq- *Sly* hemizygous transgenic males. Blots were probed with the anti-SLY SK97 antibody (top row), the anti-SLY SK98 antibody (middle row) and an anti-actin antibody as a loading control.

   The 40kDa protein (arrowed) detected by the anti-SLY antibodies is reduced in the 2/3MSYq- sample (lane 2) and absent in the 9/10MSYq- and MSYq- samples (lanes 3 and 4). The protein is faintly detected in MSYq- sample carrying an *Sly* transgene (lane 5; see chapter 6), confirming that the protein is SLY.

Figure 3.4

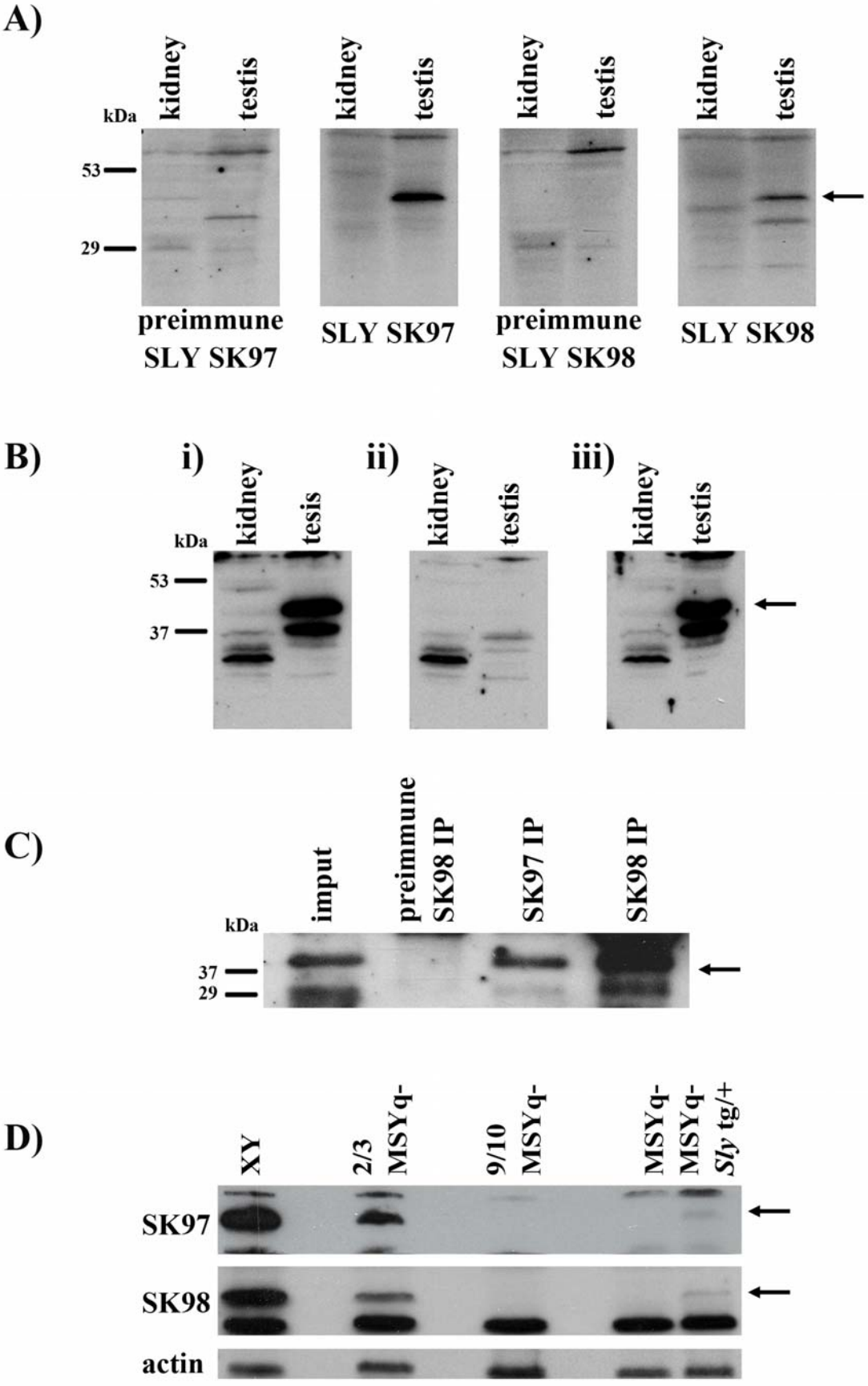
A)
kDa
kidney
testis
53
29
preimmune SLY SK97
SLY SK97
preimmune SLY SK98
SLY SK98
B)
i)
ii)
iii)
kidney
tesis
testis
kDa
53
37
C)
imput
preimmune SK98 IP
SK97 IP
SK98 IP
kDa
37
29
D)
XY
2/3 MSYq-
9/10 MSYq-
MSYq-
MSYq- Sly tg/+
SK97
SK98
actin

Figure 3.5

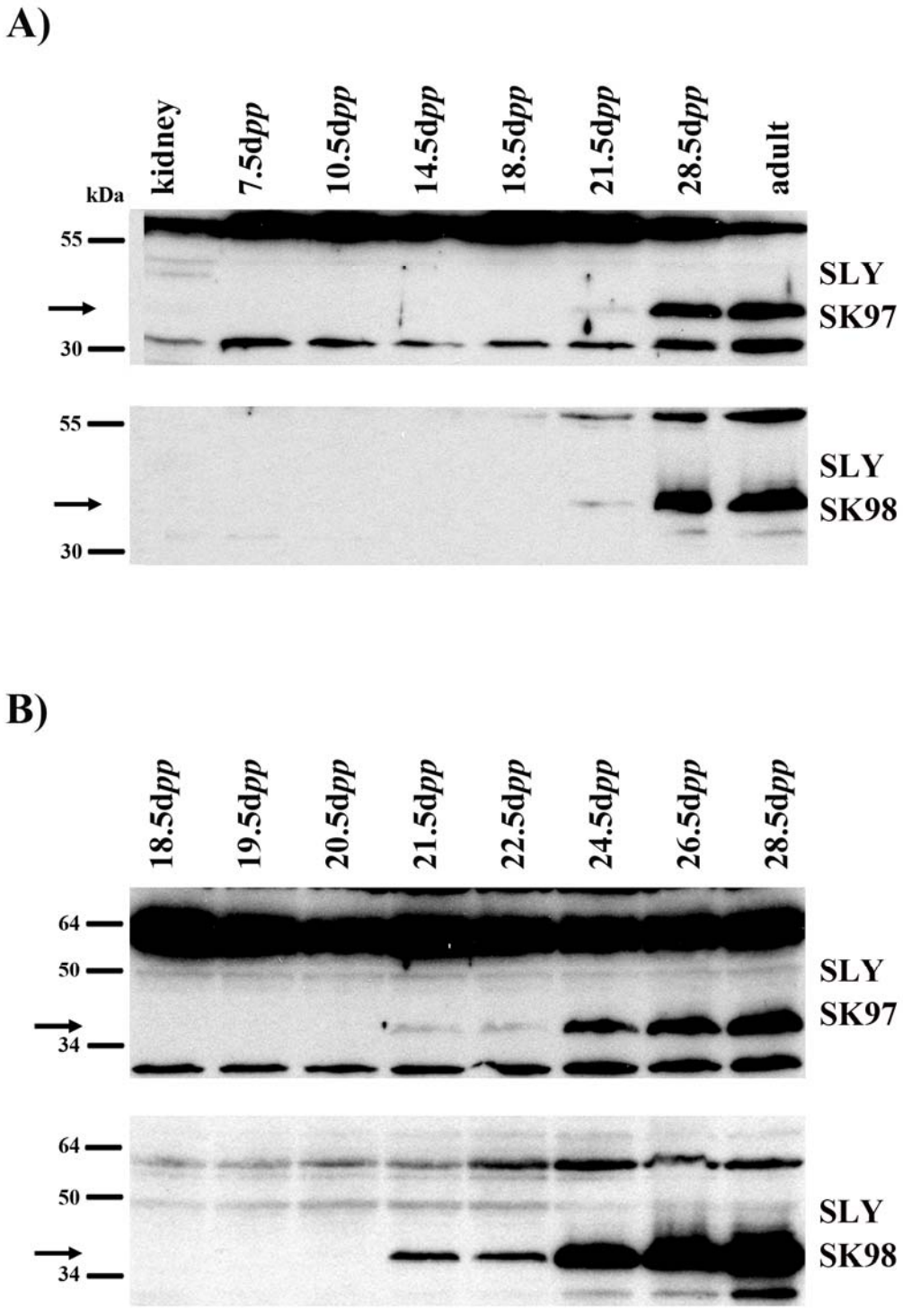

Figure 3.5 SLY expression during the first spermatogenic wave

Western blot analysis of XY testis samples from
A) 7.5d*pp* to adult males
B) 18.5d*pp* to 28.5d*pp*
The anti-SLY SK97 (top row) and anti-SLY SK98 (bottom row) antibodies detect a band corresponding to SLY (arrowed) from 21.5d*pp*

Figure 3.6 SLY localisation in the adult testis

Antibody staining of testis cryosections with;

A) anti-SLY SK97 pre-immune serum (red)
B) anti-SLY SK97 antibody preincubated with the peptide to which it was raised (red)
C) anti-SLY SK97 antibody (red)
D) anti-SLY SK97 antibody (red) and anti-γH2AX antibody (green)
E) anti-SLY SK98 antibody (red) and anti-γH2AX antibody (green)

Left panel; DAPI staining of cell nuclei (blue).
Middle panel; SLY (red)
Right panel; overlay of DAPI, SLY and γH2AX.

Figures A-C are 20X magnification and D-E are 100X magnification. The anti-γH2AX antibody stains the whole nucleus of leptotene and zygotene spermatocytes and the sex body domain of pachytene spermatocytes. Anti-SLY staining is seen in round spermatids

Note
The anti-rabbit secondary antibody (red) detects a non-specific signal in the interstitial cells (seen in A and B). The anti-mouse secondary antibody (green) also stains the basal lamina of the seminiferous tubules.

Figure 3.6

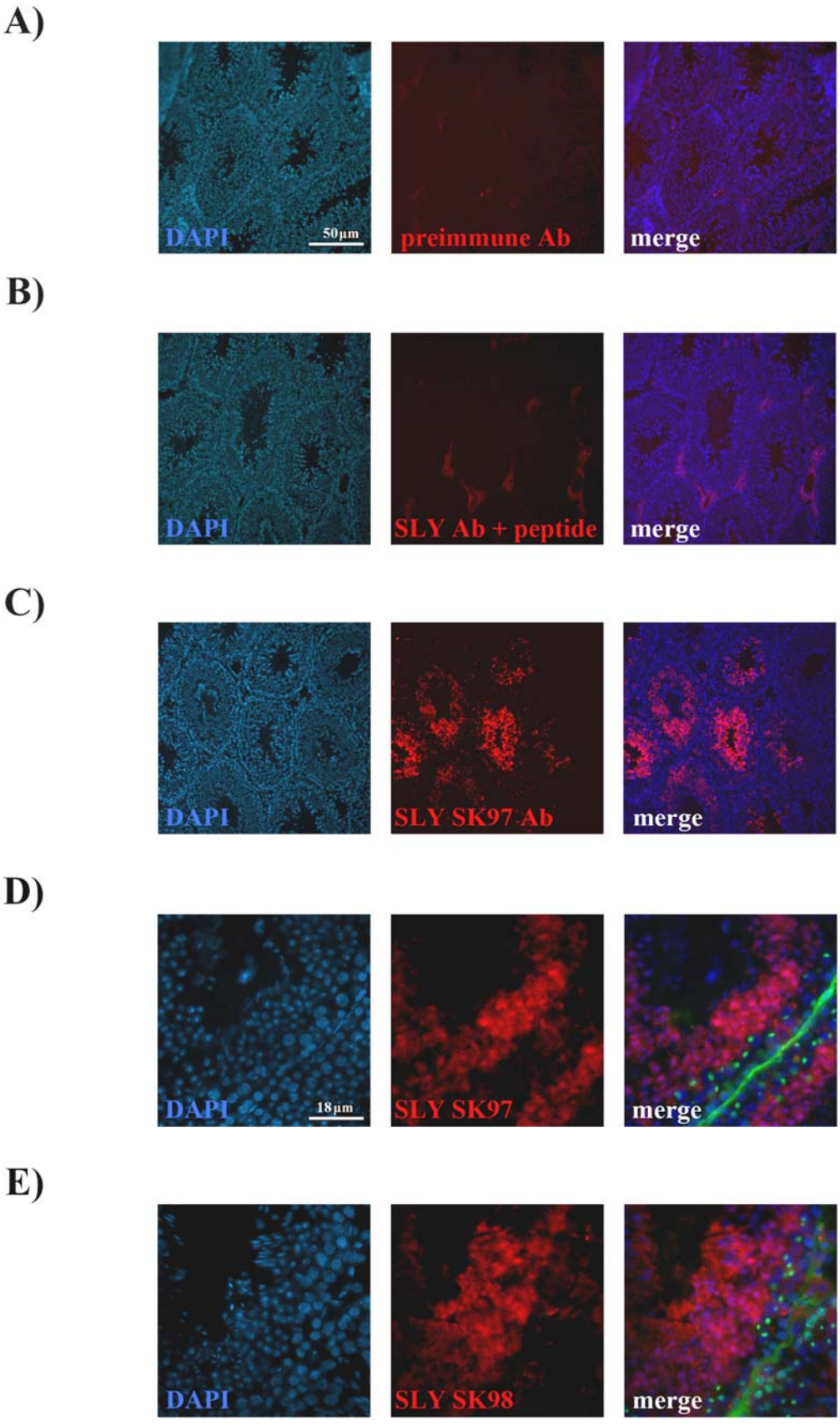
A)
DAPI
50µm
preimmune Ab
merge
B)
DAPI
SLY Ab + peptide
merge
C)
DAPI
SLY SK97 Ab
merge
D)
DAPI
18µm
SLY SK97
merge
E)
DAPI
SLY SK98
merge

Figure 3.7 Cellular localisation of SLY

A) Antibody staining of XY adult testis cryosections with the anti-SLY SK97 antibody under X40 magnification (upper row) and X100 magnification (lower row). Left panel; DAPI staining of cell nuclei (blue). Middle panel; anti-SLY SK97 antibody (red). Right panel; overlay of SLY and DAPI.
SLY staining is seen in the cytoplasm of spermatids.

B) Western blot analysis of cytoplasmic and nuclear fractions from adult testis with the anti-SLY SK97 and anti-SLY SK98 antibodies. SLY is present in the cytoplasmic but not nuclear fraction. A whole testis sample (overloaded relative to the nuclear and cytoplasmic fractions) is included a positive control. The anti-γH2AX antibody (lower panel) is a nuclear control; no γH2AX band is seen in the cytoplasmic fraction, indicating that there is no nuclear contamination of the cytoplasm.

Figure 3.7

A)

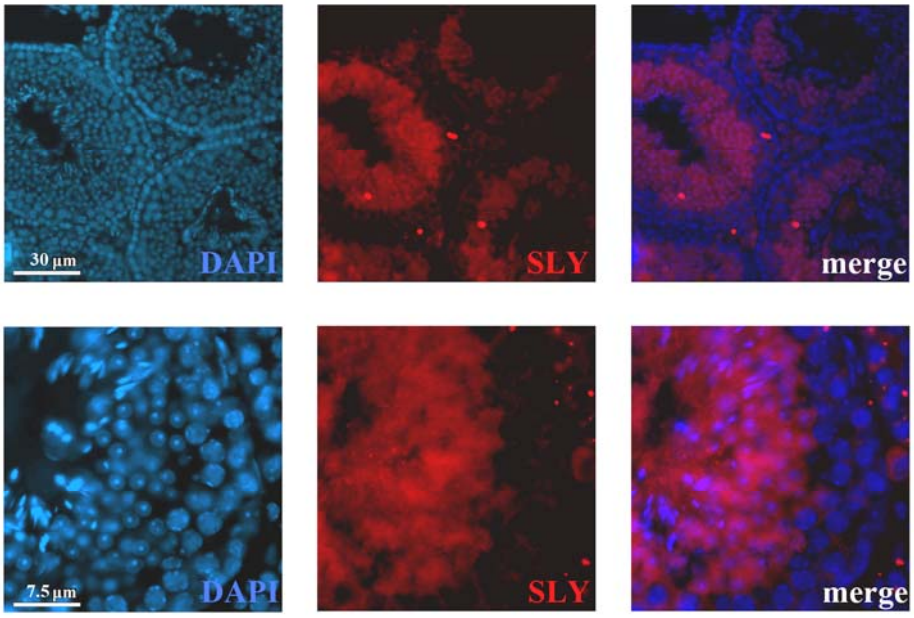
30 µm
DAPI
SLY
merge
7.5 µm
DAPI
SLY
merge

B)

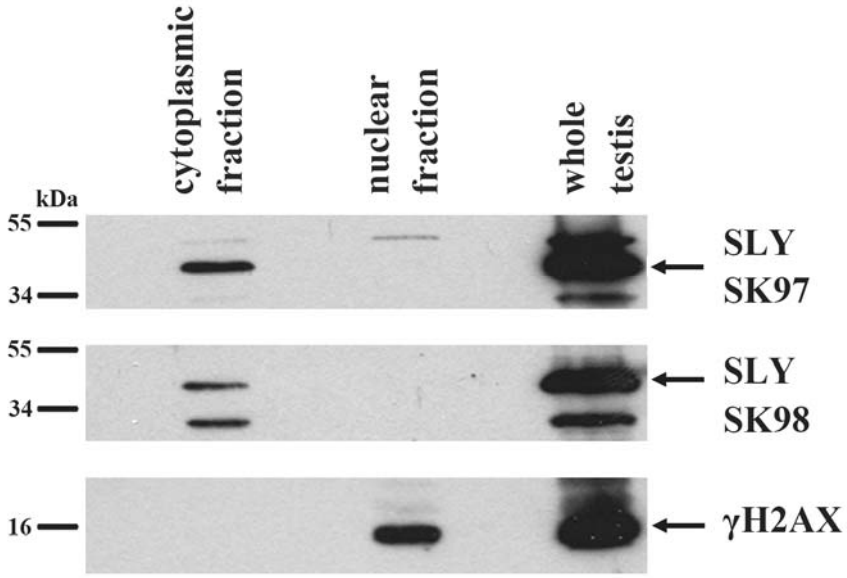
cytoplasmic fraction
nuclear fraction
whole testis
kDa
55
34
SLY
SK97
55
34
SLY
SK98
16
γH2AX

3.2.5 Yeast-two-hybrid analysis of SLY

To investigate the function of SLY during spermiogenesis, potential interacting proteins were identified. A yeast-two-hybrid analysis was carried out using a pre-transformed *S. cerevisiae* mouse testis cDNA library as prey. Initial control experiments indicated that SLY was not toxic to the yeast, and was unable to activate the *MEL1* reporter gene, allowing the library to be screened. The bait and prey yeast were mated and plated out on the highest stringency medium with X-α-gal (QDO/ X-α-gal) to select for colonies strongly expressing the reporter genes. Approximately 1.5 $x10^8$ library clones were screened and positive colonies were re-streaked to confirm the phenotype. The library plasmids responsible for activation of the reporter genes were isolated and 85 clones were sent for sequencing. These prey plasmids represented 23 proteins that could potentially interact with SLY (see Table 3.1). They were retested to determine if they generated genuine interactions with SLY. False positives (where the prey plasmid can activate the reporter genes in the absence of the SLY bait) were identified by transforming the prey plasmids into AH109 yeast containing the pGBKT7-SLY or pGBKT7 vector alone. For 14 of the proteins identified in the screen, the SLY bait plasmid was necessary to activate the reporter genes, indicating that these proteins were able to interact with SLY, at least in a two-hybrid assay (Table 3.2). As the testis library screened in the yeast-two-hybrid analysis contained cDNA expressed in all germ cell subtypes as well as testicular somatic cells, it is possible that the proteins encoded by these cDNAs may not be present in the same cell as SLY. Microarray analysis and literature searches indicated that 10 of the genes identified by the yeast-two-hybrid analysis were transcribed in spermatocytes or spermatids, and thus encode a protein that is potentially present in spermatids (Table 3.2).

3.2.6 Confirmation of SLY interactions

The majority of the genes identified in the yeast-two-hybrid screen have not been previously characterised in the testis, and some are predicted genes, so very few antibodies are available for co-immunoprecipitation studies. However, antibodies against three potential interacting proteins are available. Immunohistochemistry on adult testis sections with antibodies against HIV-1 tat interactive protein (TIP60, a histone acetyltransferase), Dickkopf-like 1 (DKKL1, also known as SOGGY1) and Prenyl binding protein delta (PrBP/δ, encoded by the *Pde6d* gene) verified that these

proteins are present in spermatids. PrBP/δ is present in the nucleus and cytoplasm of spermatocytes and spermatids (Figure 3.8.B), and DKKL1 localises to the cytoplasm of spermatids (Figure 3.8.C), the same cellular compartment as SLY. However, TIP60 is a nuclear protein (Figure 3.8.D) and therefore may not interact with SLY in the testis.

To confirm if DKKL1 and PrBP/δ interact with SLY *in vivo*, co-immunoprecitation experiments were performed. Adult testis extracts were incubated with either the two anti-SLY antibodies or pre-immune serum and analysed by SDS-PAGE and western blot. As expected, SLY was precipitated with both SLY antibodies but not the pre-immune serum, and was only detected in the input sample after longer exposure of the membrane (Figure 3.9). DKKL1 was co-immunoprecipitated with both SLY antibodies, but was not present in the pre-immune serum control, verifying that DKKL1 and SLY interact in spermatids. Although PrBP/δ co-immunoprecipitated with SLY, it was also present in the pre-immune control sample, indicating that this interaction is not specific to SLY.

Table 3.1

Gene	accession number	name	no of clones
Sin3B	NM_009188.2|	transcriptional regulator, SIN3B (yeast) (Sin3b),	18
Cops5	NM_013715.1|	COPs5 AKA Jab1, CSN5	17
RanBPM	NM_019930.1|	Ranbp9	7
PEST PCNP	NM_001024622.2|	PEST proteolytic signal containing nuclear protein Pcnp	6
Ubc	XM_001479835	Ubiquitin C like protein	4
4933400C05RIK	NM_177801.3|	4933400C05RIK ??	4
Atp1B3	NM_007502.2	ATPase, Na+/K+ transporting, beta 3 polypeptide Atp1b3	4
DKKL1	NM_015789.2|	Dickkopf-like 1 (Dkkl1)	3
Yod1	NM_178691.3|	YOD1 OTU deubiquitinating enzyme 1 homologue (Yod1), mRNA	2
D130059P03RIK	NM_177185.3|	Mus musculus RIKEN cDNA D130059P03 gene (D130059P03Rik), mRNA	2
1110019N10RIK	NM_026753.2|	RIKEN cDNA 1110019N10 gene (1110019N10Rik),	1
Appbp2	NM_025825.3|	amyloid beta precursor protein (cytoplasmic tail) binding protein 2 (Appbp2)	1
D930010J01RIK	NM_134147.3|	RIKEN cDNA D930010J01 gene (D930010J01Rik	1
DnaJb4	NM_025926	DnaJ (HSP40) homologue subfamily B, member 4	1
Gnl3	NM_153547.3|	guanine nucleotide binding protein-like 3 (nucleolar) (Gnl3	1
IK cytokine	NM_011879.1|	Mus musculus IK cytokine (Ik), mRNA	1
Irak1	NM_008363.2|	interleukin-1 receptor-associated kinase 1 (Irak1),	1
Itgb3bp	NM_026348.3|	integrin beta 3 binding protein (beta3-endonexin Itgb3bp	1
Pde6d	NM_008801.2|	phosphodiesterase 6D, cGMP-specific, rod, delta (Pde6d), mRNA	1
Setd2	NM_001081340.1|	SET domain containing 2 (Setd2	1
Ssty 2	NM_001025241.2|	similar to spermiogenesis specific transcript on the Y 2 (LOC434960), mRNA	1
Tip60	NM_178637.1|	HIV-1 tat interactive protein, homolog (human) (Htatip)	1
Ube2m	NM_145578.1|	ubiquitin-conjugating enzyme E2M (UBC12 homolog, yeast) (Ube2m), mRNA	1
Chromosome 10	N/A	N/A	2
chromosome 18	N/A	N/A	2
chromosome 11	N/A	N/A	1

Table 3.1 A full list of clones identified in the *Sly* yeast-two-hybrid screen

Table 3.2

Gene	genuine interaction with SLY?	testis expression	Antibody available?
Sin3B	no	N/A	N/A
Cops5	no	N/A	N/A
Ubc	no	N/A	N/A
Atp1B3	no	N/A	N/A
D130059P03RIK	no	N/A	N/A
1110019N10RIK	no	N/A	N/A
DnaJb4	no	N/A	N/A
Gnl3	no	N/A	N/A
IK cytokine	no	N/A	N/A
RanBPM	yes	spermatocytes, spermatids	yes
PEST PCNP	yes	spermatogonia, spermatocytes	yes
4933400C05RIK	yes	no information	no
DKKL1	yes	spermatocytes, spermatids	commercial
Yod1	yes	spermatogonia, spermatocytes	no
Appbp2	yes	germ cells	no
D930010J01RIK	yes	spermatocytes, spermatids	no
Irak1	yes	spermatogonia	no
Itgb3bp	yes	spermatocytes, spermatids	no
Pde6d	yes	spermatocytes, spermatids	yes
Setd2	yes	no information	no
Ssty 2	yes	spermatids	yes
Tip60	yes	spermatocytes, spermatids	yes
Ube2m	yes	spermatocytes, spermatids	no

Table 3.2 A list of genes whose encoded proteins interact with SLY in yeast, and their testis expression pattern based on microarray data

Figure 3.8 Localisation of PrBP/δ, DKKL1 and TIP60 in the testis

Immunofluorescence staining of adult XY testis sections with

A) anti-SLY SK97 antibody (red) and anti-γH2AX antibody (green)
B) anti-PrBP/δ antibody (red) and anti-γH2AX antibody (green)
C) anti-DKKL1 antibody (red) and anti-γH2AX antibody (green)
D) anti-TIP60 antibody (red) and anti-γH2AX antibody (green)

The nuclei of cells are stained with DAPI (blue).

Figure 3.8

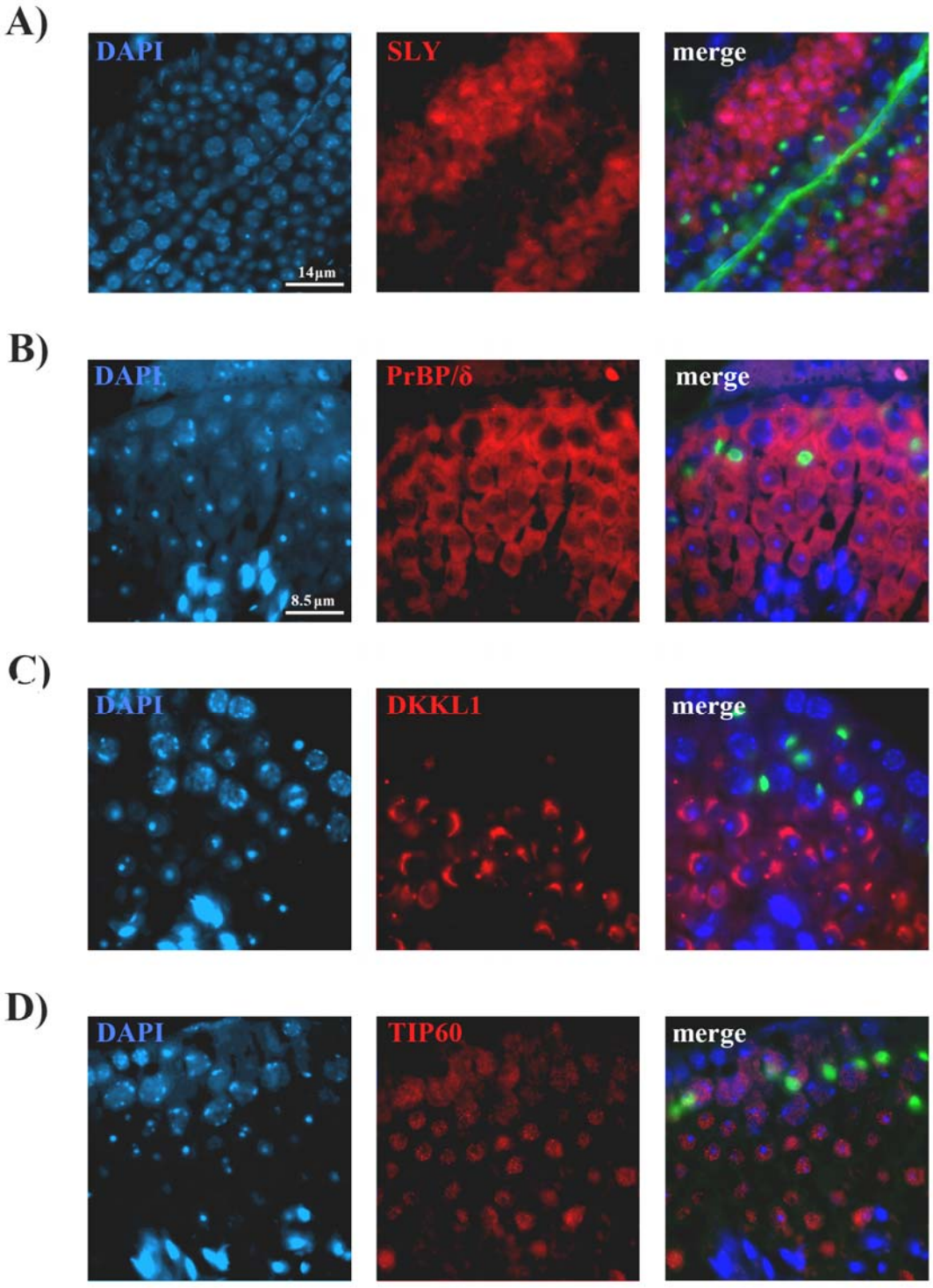
A)
DAPI
SLY
merge
14µm
B)
DAPI
PrBP/δ
merge
8.5µm
C)
DAPI
DKKL1
merge
D)
DAPI
TIP60
merge

Figure 3.9

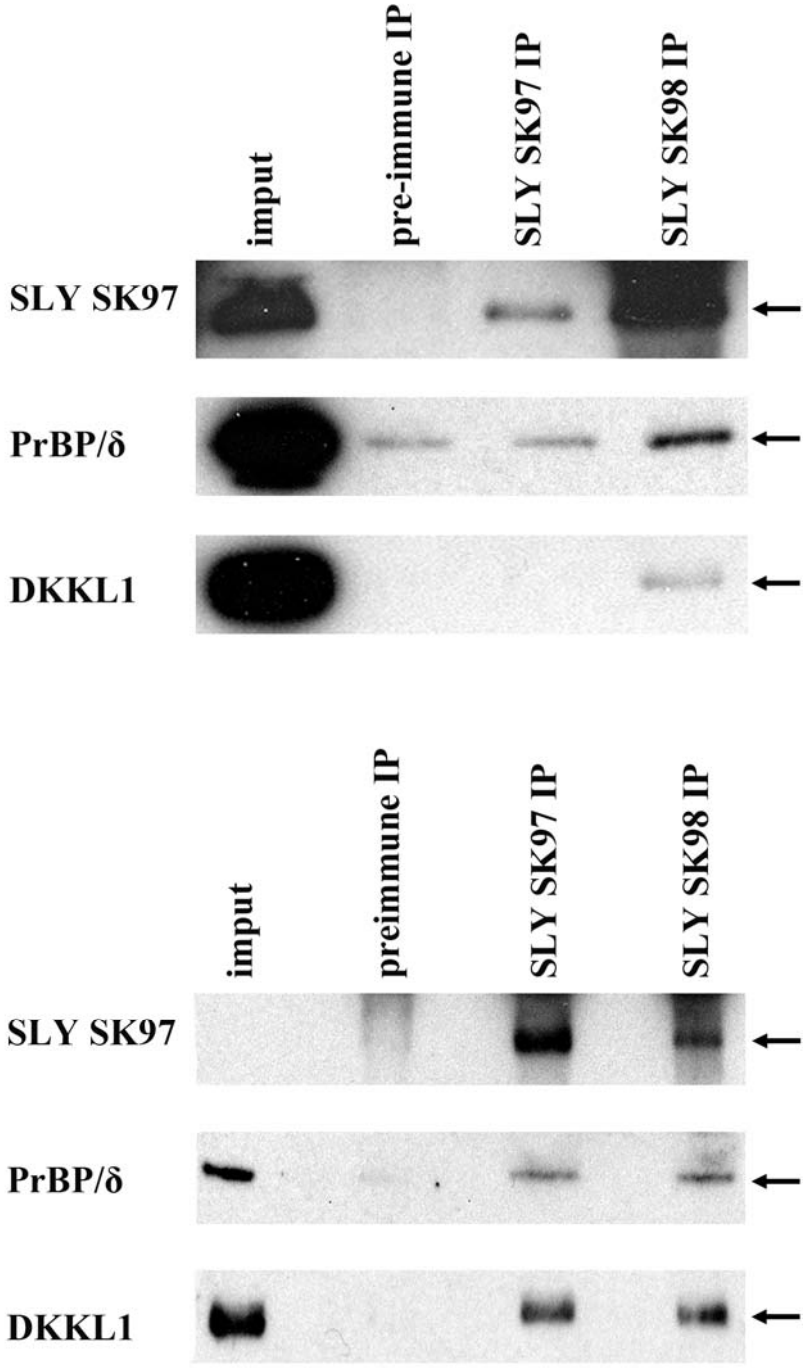

Figure 3.9 Co-Immunoprecipitation of PrBP/δ and DKKL1 with SLY.

Protein lysates from adult XY testis (imput; lane 1) were immunoprecipitated with the anti-SLY SK97 and SK98 pre-immune serum antibody (lane 2), the anti-SLY SK97 antibody (lane 3) and the anti-SLY SK98 antibody (lane 4). Samples were analysed by western blot with the anti-SLY SK97 antibody, anti-PrBP/δ antibody and anti-DKKL1 antibody. SLY (arrowed) was immunoprecipitated with both anti-SLY antibodies but not with the pre-immune serum. DKKL1 (bottom panel, arrowed) was co-immunoprecipitated with SLY only (lanes 3 and 4) but PrBP/δ (middle panel, arrowed) was present in all three immunoprecipitation samples.

3.3 Discussion

In this chapter, I have examined the expression and function of *Sly*, a multicopy MSYq-encoded gene that may be responsible for one or more of the phenotypes observed in MSYq deletion mutants. Transcription analysis validated previous reports that *Sly* is expressed primarily in spermatids (Ellis et al., 2005; Touré et al., 2005). In accordance with the transcriptional data, SLY protein was found in the testis from 21.5d*pp*. However, SLY localised to the cytoplasm of spermatids; this is unexpected as SLY belongs to the XLR family of nuclear proteins and had been predicted to localise to the sex chromosome domain of round spermatids (Ellis et al., 2005; Touré et al., 2005). The ancestor of *Sly* may have been nuclear, but prior to amplification of the gene, the nuclear localisation signal of SLY was lost due to mutation. To gain insight into the function of SLY, a testis cDNA library was screened by yeast-two-hybrid analysis to identify proteins that interact with SLY. One protein isolated in the screen was the acrosomal protein DKKL1 (SOGGY1), and this interaction was verified *in vivo* by co-immunoprecipitation.

Identification of the interaction between SLY and the acrosomal protein DKKL1 suggests a possible function for SLY in acrosome formation or function. The acrosome is a crescent-shaped structure composed of several compartments that develops over the anterior half of the sperm head. It contains proteases and hydrolases (including hyaluronidase and acrosin) that are exocytotically released enabling the sperm to penetrate the zona pellucida of the egg upon fertilisation. Although the structure of the acrosome is well characterised, the mechanisms involved in the assembly and function of the acrosome remain obscure. DKKL1 is a 34kDa protein that is related to the *Dickkopf* gene family of secreted antagonists of WNT signal transduction and has been shown to localise to the acrosome (Kohn et al., 2005). *Dkkl1* is transcribed at low levels in several tissues, but in adult mice it is detected at high levels only in testis, where it is restricted to spermatocytes and round spermatids (Kaneko and DePamphilis, 2000; Kohn et al., 2005). DKKL1 protein localises to the developing acrosome in spermatids, and the acrosome of mature sperm. Unlike related proteins, DKKL1 is not secreted but is N-glycosylated, and glycosylation is thought to be necessary for proper trafficking of proteins through the Golgi complex to the developing acrosome during spermiogenesis (Kohn et al., 2005; Tulsiani, 2003;

Wassarman et al., 2004; Yoshinaga and Toshimori, 2003). The function of DKKL1 in spermatids is unknown but several possibilities have been suggested. Firstly, it has been proposed that DKKL1 may not be active in mature sperm but could facilitate formation of the acrosome during spermiogenesis. Another suggestion is that DKKL1 suppresses motility in developing spermatids, thus preventing their premature spermiation; it should be noted that spermiation in the 9/10MSYq- and MSYq- mice is delayed (Touré et al., 2004b). Thirdly, DKKL1 may play a role in guiding the mature sperm through either the seminiferous tubules, epididymis or during fertilisation (Kohn et al., 2005).

Abnormal acrosome development, structure and enzymatic content have been reported in mice with MSYq deletions, and this is thought to contribute to the increased incidence of abnormal epididymal sperm in these mice. Acrosomal defects in B10.BR-Y^{del} mice include the lack of the pro-acrosomal granule in round spermatids, distortion of the acrosome shape, decreased levels of the acrosomal protease acrosin, and increased numbers of epididymal sperm with damaged or absent acrosomes (Siruntawineti et al., 2002; Styrna et al., 1991a; Styrna et al., 2003). Together, these data suggest there is an MSYq-encoded gene involved in controlling acrosome development during spermiogenesis, and *Sly* is a very good candidate for the 'acrosomal factor' in light of the interaction between DKKL1 and SLY. Nonetheless, further analysis is required to determine if SLY is involved in acrosome formation or maturation. Firstly, other acrosomal proteins such as Sp56 (an acrosomal matrix protein involved in egg recognition; Kim et al., 2001; Kim and Gerton, 2003) should be analysed by co-immunoprecipitation to see if they interact with SLY. In addition, the localisation of acrosomal proteins should also be examined in our three MSYq deletion models and in mice carrying an *Sly* transgene (see chapter 6). SLY is not detectable in condensing spermatids by immunofluorescence based studies, suggesting that the putative acrosomal function of SLY may be restricted to the initial stages of acrosome development. However, it is possible that condensation of the spermatid head causes masking of the SLY epitope at latter stages of spermiogenesis and western blot analysis should be performed on epididymal sperm to see if SLY is present in mature sperm.

SLY shows uniform localisation to the cytoplasm of spermatids, and so it is feasible that SLY has other functions besides its potential role in the acrosome. Verification of

other proteins identified in the yeast-two-hybrid screen is ongoing and may eventually lead to a better understanding of the role of SLY in spermiogenesis. Although several proteins were isolated in the yeast-two hybrid screen, it is possible that some of the proteins that interact with SLY in the testis were not identified. One reason for this may be because not all genes expressed in the testis were represented in the mouse testis cDNA library that was screened. Alternatively, the SLY-GAL4 DNA binding domain fusion protein may fold differently from SLY, and so proteins that can interact with the native SLY *in vivo* are unable to interact with this fusion protein.

Intriguingly, western blot analysis demonstrates that the SLY protein migrates at approximately 40kDa on an SDS-PAGE gel, rather than 25.6kDa, the predicted size of the protein based on amino acid sequence. Protein conformation can affect migration through the gel, and both XLR and XMR have a higher molecular weight than predicted based on amino acid sequence. Alternatively, SLY could be post-transcriptionally modified in spermatids. For instance, SLY may be phosphorylated and *in silico* analysis of the amino acid sequence using the NetPhos 2.0 (http://www.cbs.dtu.dk/services/NetPhos/) and Scan Prosite (http://www.expasy.ch/tools/scanprosite/) bioinformatics programs reveals several motifs that may be recognised by kinases such as Casein kinase 2 (CK2). However, no difference in the size of SLY was seen after treatment with lambda phosphatase, which removes phosphate groups from proteins. Other potential modifications include prenylation, suggested by the interaction of SLY with the prenyl-binding protein PrBP/δ, which interacts with other prenyl binding proteins such as GRK1 and GRK7 (Zhang et al., 2004). However, SLY does not contain a C terminal CaaX motif found in most prenylated proteins. Instead, SLY could be N-glycosylated; this modification is common in acrosomal proteins and may be needed for intracellular trafficking of proteins to the acrosome from the Golgi. Treatment of testicular lysates with a glycosidase such as Peptide:N-glycosidase-F (PNGaseF) would confirm if SLY is N-glycosylated.

In light of the finding that SLY is predominantly, if not exclusively cytoplasmic rather than nuclear, it is unlikely that this protein is directly involved in the increased transcription of X- and Yp-linked genes seen in the MSYq- models, as predicted previously (Ellis et al., 2005; Touré et al., 2005). However, this can not be ruled out at the present time. It is also improbable that SLY interacts with the mRNA of these

genes as it does not contain any motifs usually found in RNA binding proteins. It remains possible that SLY has a role in cytoplasmic RNA processing, but there is no evidence to support this.

Chapter 4

Investigation of the role of *Xmr* during spermatogenesis

Investigation of the role of *Xmr* during spermatogenesis

4.1 Introduction

Results from the previous chapter demonstrated that SLY localises to the cytoplasm of spermatids, where it has an unknown function. It is thus unlikely to be directly responsible for the transcriptional up-regulation of X- and Yp-linked genes that occurs when *Sly* is deleted in the MSYq deletion models. However, a candidate gene for this role is *Xmr*, the multicopy X-linked homologue of *Sly*, which has been reported to encode a testis-specific chromatin-associated protein. In this chapter, the expression and function of *Xmr* during spermiogenesis is explored.

Xmr (*Xlr*-related, meiosis regulated), together with related loci encoding similar testis-expressed transcripts such as *AK015913*, form a subgroup of the complex *Xlr* superfamily of genes. The *Xlr* superfamily has been reported to contain approximately 50-75 genes which are located on the proximal half of the mouse X chromosome, and the mouse Y chromosome (now know to be *Sly*) in regions that show little or no conservation between mice and humans (Garchon et al., 1989). The *Xlr* genes, along with the autosomally encoded *Sycp3* gene and the putative FAM9 proteins encoded by the human X chromosome, all contain a conserved COR1 domain (Touré et al., 2005). Sequence comparison of the mammalian COR1 proteins indicates that *Sycp3* is the ancestral gene, and that this gene came onto the X chromosome before the divergence of the mouse and human lineages. Once on the X chromosome, the *Sycp3*-derived gene was duplicated several times to give multiple copies which then evolved rapidly and independently.

In mouse, the X-linked members of this *Xlr* superfamily can be divided into five distinct groups based on sequence analysis, the closely related *Xlr* (*Xlr1*) and *Xmr* (*Xlr2*) subfamilies, which encode acidic proteins, and the more distantly related *Xlr3*, *Xlr4* and *Xlr5* subfamilies, which encode relatively basic proteins. Orthologues of the *Xlr*, *Xlr3*, *Xlr4* and *Xlr5* genes have been found in the rat, but the *Xmr* subgroup is only found in the mouse lineage, suggesting that it evolved from the closely related *Xlr* genes after these lineages split. A testis expressed chimeric *Xlr-Xmr* sequence then translocated onto the Y chromosome to form the spermatid-specific *Sly* gene and this

new X-Y homologous family became massively amplified on both the X and Y chromosomes, possibly as a result of genomic conflict between sex linked meiotic drivers and suppressors (Ellis et al., 2007; Touré et al., 2005).

Although the precise function of the COR1 domain-containing proteins remains unknown, the expression and localisation of SYCP3 and XLR has been characterised in detail in the mouse. *Sycp3* encodes a structural component of the meiosis-specific synaptonemal complex, and contains a nucleotide binding motif A that is not found in the other COR1 proteins (Dobson et al., 1994; Lammers et al., 1994). *Xlr* is expressed in lymphocytes and foetal thymocytes and encodes a 30kDa acidic nuclear protein (Escalier et al., 1999; Garchon and Davis, 1989; Siegel et al., 1987). Immunofluorescence-based studies of thymus cells have shown that XLR co-localises with SATB1, a protein that binds to AT-rich DNA sequences associated with the nuclear matrix, where it appears to orchestrate the temporal and spatial expression of genes during T-cell development (Alvarez et al., 2000; Dickinson et al., 1992; Escalier et al., 1999). Although XLR is not thought to be expressed in the testis or adult ovary, it is present in the foetal ovary during meiotic prophase I (Escalier et al., 2002).

Staining of foetal ovary cryosections showed that XLR localises to the whole nucleus except the nucleoli of oocytes at leptotene, and increases at the leptotene-zygotene transition. The strongest XLR staining is seen in pachytene oocytes, where XLR concentrates on the condensed chromosomes. XLR staining fades at diplotene before disappearing in dictyate oocytes. Analysis of XY^{Tdym1} oocytes found that the protein recognised by the anti-XLR antibody coats the axis and surrounding chromatin of the asynapsed X chromosome from early pachytene (Turner, 2000). Furthermore, analysis of oocytes from females heterozygous for the autosomal translocation T(2;5)72H demonstrates that XLR accumulates on the axes of asynapsed autosomes, suggesting that it localises to the X chromosome in XY^{Tdym1} oocytes in response to asynapsis (Turner, 2000).

Currently nothing is known about the proteins encoded by the *Xlr3*, *Xlr4* and *Xlr5* subgroups, although the *Xlr3a* and *Xlr3b* genes are transcribed in multiple tissues including the testis, lymphoid cells, and brain, where they are imprinted (Bergsagel et al., 1994; Davies et al., 2005; Raefski and O'Neill, 2005). The *Xlr4* genes are also expressed in lymphocytes and various subregions of the brain, where *Xlr4b* and *Xlr4c*

are imprinted in a complex tissue and stage specific pattern that is independent of somatic X chromosome inactivation (Raefski and O'Neill, 2005).

Xmr was originally identified by northern blot using a full length *Xlr* cDNA probe that hybridised to an abundant testis-specific transcript of 1kb (Calenda et al., 1994). Through screening of a testis cDNA library, an 812bp transcript was identified which shared extensive homology to *Xlr* over the latter two thirds of the transcript. This transcript encoded a putative 212 amino acid protein that contained an N-terminal acidic stretch of 45 amino acids, suggestive of a role in transcriptional activation, and a C terminal coiled-coil domain indicative of the ability to dimerise (Calenda et al., 1994; Gill and Ptashne, 1987; Ma and Ptashne, 1987). Northern analysis of RNA from the first spermatogenic wave detected transcripts from 3 weeks postpartum, suggesting that *Xmr* was expressed in spermatids. However, low level transcription of *Xmr* was detected by RT-PCR from 6d*pp*, two to three days before meiosis begins.

Calenda et al. (1994) then assayed for XMR protein expression in the testis using an antibody raised against the related full length XLR protein (they believed *Xlr* was not expressed in the testis). Immunostaining was seen exclusively in the basal meiotic compartment where it was restricted to the nuclei of primary spermatocytes, in a pattern reminiscent of XLR localisation in primary oocytes. This immunostaining (putatively XMR) was first detected at low levels throughout the nucleus during preleptotene and increased in intensity until zygotene when meiotic recombination is initiated (Mahadevaiah et al., 2001). At zygotene, the putative XMR protein began to preferentially localise to the asynapsed X and Y chromosomes as the sex chromosomes undergo the chromatin changes that result in the formation of the transcriptionally silent sex body (Handel, 2004; Solari, 1974). In early pachytene, the whole nucleus staining became fainter but 'XMR' accumulated on the XY body until staining was only seen on the sex chromosomes by mid-late pachytene, where it was enriched on the chromosome axes (Escalier et al., 2002). When the nucleolus becomes associated with the XY body in mid pachytene spermatocytes, 'XMR' concentrated on the nucleolus granular component, and to a lesser extent, on the fibrillo-granular component of the nucleolus (Escalier and Garchon, 2005). During diplotene, 'XMR' staining decreased and became diffuse throughout the nucleus, eventually becoming preferentially enriched around centromeric heterochromatin at MI (Turner, 2000). 'XMR' was also found to associate with the chromatin of asynapsed autosomal axes in

pachytene spermatocytes carrying the reciprocal T[X:16]16H translocation, indicating that 'XMR' localisation to the sex chromosomes in pachytene is a response to asynapsis (Escalier and Garchon, 2005; Escalier and Garchon, 2000). Immunostaining of human testis sections with the same mouse monoclonal anti-XLR antibody detected a protein in the nuclei of type B spermatogonia and primary spermatocytes despite no *Xlr* or *Xmr* related sequence being identified by Southern or northern blot analysis. However, this protein did not localise to the sex chromosomes (Allenet et al., 1995).

As both *Xmr* and *Xlr* encode nuclear proteins that are expressed at times of genome rearrangement, it has been suggested that they could play important roles in 'genomic metabolism' (Calenda et al., 1994; Escalier et al., 1999). The localisation of 'XMR' to the autosomes in early prophase followed by progressive accumulation on the sex body led to speculation that it may be involved in chromosome condensation (Escalier et al., 1999). XMR shares distant homology to the *Saccharomyces cerevisiae MER2* protein, which is essential for formation of meiotic DNA double-strand breaks (Li et al., 2006), and an alternative hypothesis is that XMR may serve a role in meiotic recombination (Escalier et al., 1999). A recombination-related role is supported by the fact that XLR is highly expressed just prior to T-cell rearrangement (Escalier et al., 1999). In addition, XMR shares significant amino acid homology with the synaptonemal complex protein SYCP3, and male mice that are homozygous for a null mutation of *Sycp3* are sterile due to massive apoptotic cell death during meiosis (Yuan et al., 2000). Proteins involved in recombination and DNA repair (e.g. RAD51 and RPA) are mis-localised in SYCP3 deficient spermatocytes, as are other synaptonemal complex proteins such as SYCP1. In the absence of SYCP3, the synaptonemal complex does not form and chromosomes fail to synapse during meiosis. SYCP3 mutations are also associated with azoospermia in humans (Miyamoto et al., 2003). Nevertheless, the precise functions of XMR and other XLR superfamily members remain unknown and are a matter of debate.

Recent microarray analysis of testes from mice with MSYq deficiencies identified the multicopy Y-encoded *Sly* gene (characterised in the previous chapter) which shares substantial nucleotide and amino acid similarity with *Xmr*. In a linked microarray study, Ellis et al. (2005) made the intriguing finding that the deletion of the mouse MSYq leads to up-regulation of multiple spermatid-expressed X- and Yp-encoded transcripts. The authors concluded that in normal males, the X and Y chromosomes are

specifically repressed in spermatids and that the gene complement of MSYq has a role in maintaining this repressed state. The up-regulated genes included *Xmr* and the related transcript *AK015913*, and unexpectedly, RNA *in situ* hybridisation revealed that *Xmr* was expressed in round and early elongating spermatids but was undetectable in meiotic cells. Furthermore, *Xmr* transcripts appeared between 15d*pp* and 23d*pp* by real-time PCR, consistent with spermatid-derived expression (Ellis et al., 2005).

SLY and XMR contain a COR1 chromatin binding domain, and these observations led Ellis and colleagues (Ellis et al., 2005) to propose that both proteins may have a role in control of chromatin conformation and gene expression of the sex chromosomes during spermiogenesis. The amplified copy number and inverse transcription levels of *Xmr* and *Sly* seen in the MSYq deletion models have been used to support the idea that there is an intragenomic conflict between the X- and Y-linked members of this gene family. This *Sly/Xmr* conflict hypothesis states that one or more of the up-regulated X-linked genes in the MSYq deletion models are responsible for the sex ratio distortion seen in the offspring of 2/3MSYq- males, and *Xmr* and *Sly* act as opposing regulators of this gene via their antagonistic affect on sex chromatin.

The data collected in the previous chapter about the cellular localisation and potential function of SLY does not support this hypothesis. However, given the evidence from the RNA *in situ* hybridisation that *Xmr* is highly transcribed in spermatids together with prior evidence that it encodes a nuclear protein (at least during meiotic prophase), it is feasible that *Xmr* may play an important role in transcriptional regulation during spermiogenesis. Ellis et al. (2005) suggested that the persistence of sex chromosome silencing established in pachytene by MSCI is modulated by *Xmr* and other *Xlr* family members. It should be noted several copies of *Xmr* map to a region of the X chromosome that is associated with sperm head abnormalities similar to those seen in 9/10MSYq- males (Oka et al., 2004). In order to determine what role, if any, *Xmr* plays during spermiogenesis, this chapter re-analyses the expression of *Xmr* in mouse testis in detail. Particular attention is paid to establishing if the abundant *Xmr* transcripts present in spermatids are translated.

4.2 Results

4.2.1 Transcriptional analysis of *Xmr*

Northern blot and *in situ* hybridisation data indicate that *Xmr* is expressed after meiosis, in round spermatids (Calenda et al., 1994; Touré et al., 2005). However, the more sensitive technique of RT-PCR detected transcripts from 6d*pp*, suggesting that transcription of *Xmr* occurs before meiosis (Calenda et al., 1994), and analysis of embryonic gonads using the same primers amplified *Xmr* mRNA from 14.5d*pc* (Turner, 2000). In an attempt to resolve the conflicting transcriptional data for *Xmr*, RT-PCR analysis using multiple primer sets was carried out on testes harvested at different ages during the first spermatogenic wave. The positions of the primers used for RT-PCR analysis are given in Figure 4.1.A.

A faint *Xmr* product was seen from 7.5d*pp* using primer pairs A/B, which also strongly detected *Xlr* at all ages assayed (Figure 4.1.B.i), although an earlier study indicated that *Xlr* was not expressed in the testis (Escalier et al., 2002). Primer pair D/C designed by Calenda et al. (1994) detected a faint *Xmr* band from 7.5d*pp* consistent with their findings; however a clear increase in *Xmr* transcripts was seen from 18.5d*pp* when the meiosis-spermiogenesis transition occurs (Figure 4.1.B.ii). Primer pairs A/B and D/C may also detect related *Xmr* transcripts such as *AK015913*, and to separately assess *Xmr* and *AK015913* transcription, RT-PCR was then carried out using primer pair D/B (Calenda et al., 1994), which gives distinct product sizes for these two genes. *AK015913* was weakly detected by these primers from 21.5d*pp*, and a faint *Xmr* product was detected at 18.5d*pp*, but expression was predominantly from 21.5d*pp* (Figure 4.1.B.iii). Direct sequencing confirmed the identity of these products. However, multiple bands were amplified using primers D/B which may derive from other *Xmr* related sequences in addition to *Xmr* and *AK015913*, so RT-PCR was repeated using primers specific to *Xmr* or *AK015913* sequences (Ellis et al., 2005). RT-PCR using *Xmr*-specific primers gave a product from 21.5d*pp*, suggesting that expression is restricted to spermatids (Figure 4.1.B.iv). RT-PCR for *AK015913* gave a product from 18.5d*pp*, corresponding to the spermatocyte-spermatid transition (Figure 4.1.B.v). Primers specific to *Xlr* designed by Ellis et al. (2005) amplified a product at all ages (Figure 4.1.B.vi), confirming the results seen using primer pair A/B.

To confirm that *Xmr* was transcribed in spermatids, RNA FISH was used to examine

the expression of *Xmr* in different spermatogenic cell types. *Xmr* RNA FISH signals were observed exclusively in round spermatids (Figure 4.2.A.i). Approximately 42% (472/1120) of all round spermatids examined were positive for an *Xmr* RNA signal, and many had multiple signals. This is consistent with *Xmr* being a multicopy gene with several *Xmr* clusters on the X chromosome. X chromosome paint verified that the *Xmr* RNA FISH signals were restricted to X-bearing round spermatids and originated from the X chromosome chromatin domain (Figure 4.2.B, arrowed), which appears as a characteristic DAPI-dense body located next to chromocentre (Turner et al., 2006). Despite detailed examination, *Xmr*-specific RNA signals were not detected in meiotic cells (n=147, figure 4.2.A.ii) or spermatogonia (n=45). To exclude the possibility that chromatin accessibility problems influenced the ability to detect *Xmr* RNA in these cell types, DNA FISH was subsequently carried out with the same probe, which gave clear FISH signals. The RNA and DNA FISH signals co-localised in round spermatids, confirming that these X-encoded transcripts originated from the *Xmr* gene.

Finally, I re-examined the raw data sets from several microarray studies carried out on either purified spermatogenic cells (Namekawa et al., 2006; figure 4.3.A) or on samples taken at time points during the first spermatogenic wave (Ellis et al., 2004; Schultz et al., 2003; Shima et al., 2004; figures 4.3.B, 4.3.C and 4.3.D respectively). In all four studies, *Xmr* transcript levels only increased above background values in purified round spermatids or at time points when spermatids are present in the germinal epithelium. Together, these results show that *Xmr* is predominantly transcribed in round spermatids, with a little transcription occurring prior to this.

Figure 4.1 RT-PCR analysis of *Xmr*, *Xlr* and *AK015913*

A) Schematic diagram of *Xmr* (blue), *AK015913* (green) and *Xlr (*purple) gene structures. Rectangles denote exons, and introns are shown by a line (introns are not to scale). For *AK015913* and *Xlr*, homology to *Xmr* is represented by filled areas. The position of RT-PCR primers used to assay transcription are indicated by arrows.

B) RT-PCR on testis RNA samples taken at time points during the first spermatogenic wave using primers A-D from Calenda et al. (1994) and primers specific to *Xmr*, *AK015913* or *Xlr* designed by Ellis et al. (2005). The blank lanes are for the corresponding –RT samples. For primer pairs AB, DC, and DB, the PCR products corresponding to *Xmr*, *AK015913* and *Xlr* are indicated by arrows. The sizes of the PCR products are indicated below;

i) primer pair AB

Xlr	630bp (upper band)
Xmr	427bp (lower band)

ii) primer pair DC

Xmr	421bp (upper band)
AK015913	287bp (lower band)

iii) primer pair DB

Xmr	813bp (upper band)
AK015913	623bp (lower band).

iv) *Xmr* 372bp

v) *AK015913* 237bp

vi) *Xlr* 244bp (arrowed)

Figure 4.1

A)

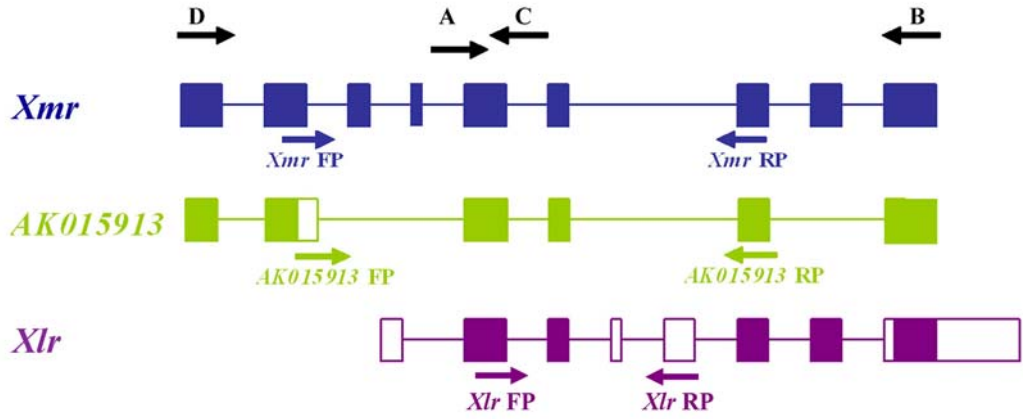
D
A
C
B
Xmr
Xmr FP
Xmr RP
AK015913
AK015913 FP
AK015913 RP
Xlr
Xlr FP
Xlr RP

B)

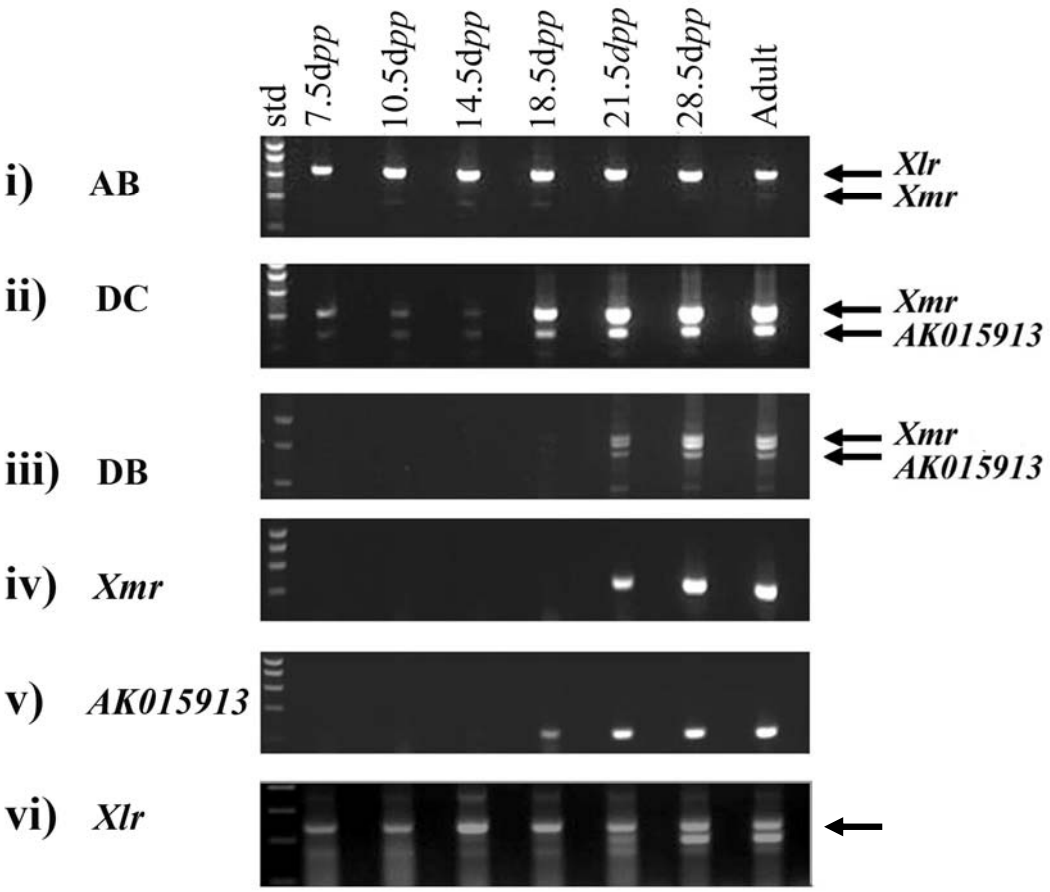
std
7.5dpp
10.5dpp
14.5dpp
18.5dpp
21.5dpp
28.5dpp
Adult
i) AB
Xlr
Xmr
ii) DC
Xmr
AK015913
iii) DB
Xmr
AK015913
iv) Xmr
v) AK015913
vi) Xlr

Figure 4.2 *Xmr* RNA FISH on spermatogenic cells

A) RNA FISH for *Xmr* nascent transcripts on

(i) an X-bearing round spermatid nucleus and
(ii) a pachytene spermatocyte nucleus.

Xmr transcripts originate from the DAPI-dense sex chromosome (arrowed) in round spermatids but are not present in meiotic cells.

Far left panel; nuclei stained with DAPI (blue).
Left panel; *Xmr* RNA FISH (red). The pachytene spermatocyte is also stained for phosphorylated H2AX (γH2AX, green), which localises to the sex body domain.
Right panel; *Xmr* DNA FISH signal (green).
Far right panel; overlay of *Xmr* RNA and DNA FISH signals. The nuclei are stained with DAPI (blue)

B) An *Xmr*-expressing round spermatid nuclei with X chromosome paint.
Far left panel; spermatid nucleus stained with DAPI (blue). The arrow points to the DAPI-dense sex chromosome next to the chromocentre
Left panel; *Xmr* RNA FISH (red).
Right panel; X chromosome paint (green).
Far right panel; overlay of *Xmr* RNA FISH and X chromosome paint signals.

Figure 4.2

A)

i)

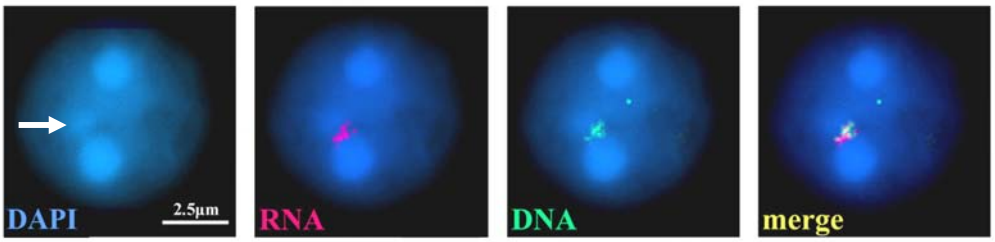

ii)

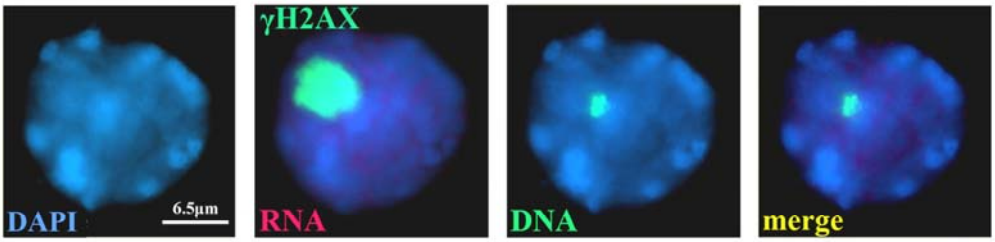

B)

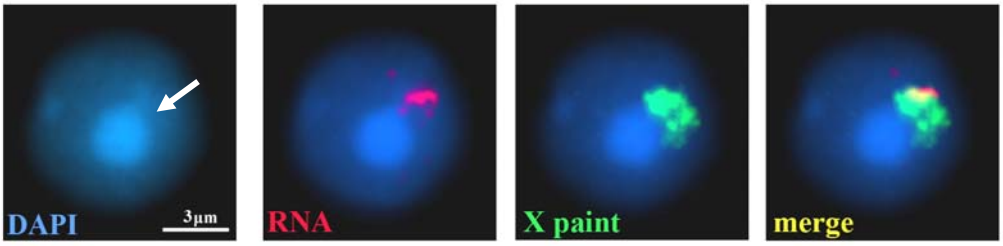

Figure 4.3 Graphical representation of *Xmr* transcript levels in the mouse testis assayed by microarray studies

Graphs representing *Xmr* transcript levels from microarray analysis of testis RNA by

A) Namekawa et al. (2006) on purified spermatogenic cells
B) Ellis et al. (2004) on samples harvested from prepubertal mice at different time points during the first spermatogenic wave
C) Schultz et al. (2003) from time points during the first spermatogenic wave
D) Shima et al. (2004) from the first spermatogenic wave.

Xmr transcript levels only increase above background values in purified round spermatids (Namekawa et al., 2006; graph A), or at time points after round spermatids appear in the germinal epithelium (Ellis et al., 2004; Schultz et al., 2003; Shima et al., 2004; graphs B, C and D)

Figure 4.3

A)

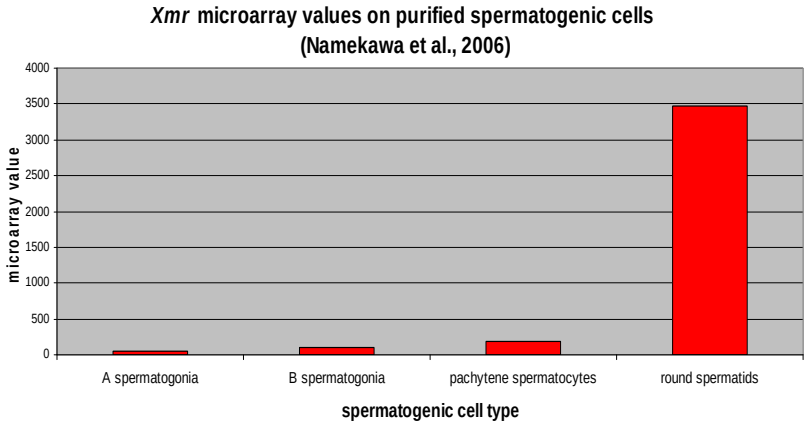

B)

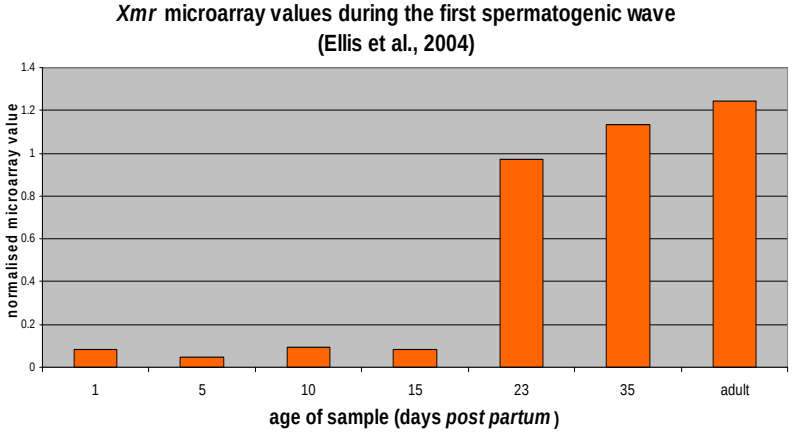

C)

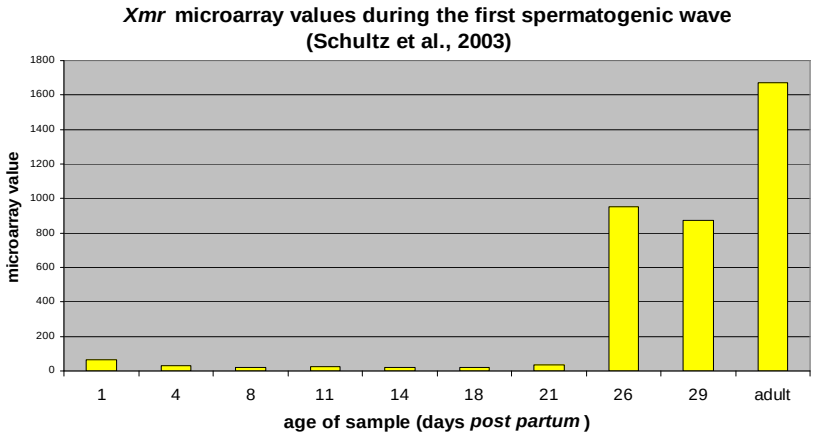

D)

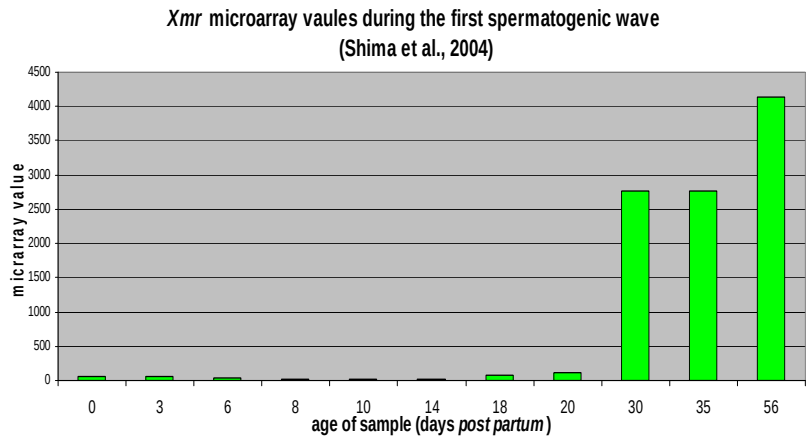

4.2.2 Design and characterisation of XMR-specific antibodies

Previous immunofluorescence-based studies using an antibody raised to the related XLR protein indicated that XMR is a meiotic protein which localises to the nuclei of primary spermatocytes, where it becomes concentrated within the sex body domain during pachytene (Calenda et al., 1994; Escalier and Garchon, 2000). This is difficult to reconcile with the above findings that *Xmr* and *AK015913* transcription is largely confined to spermatids. I therefore decided to re-analyse the expression and cellular localisation of XMR using antibodies designed to be specific to XMR. Three antibodies were synthesised, one against the first 93 amino acids of XMR (XMR^{1-93}) and the others against two XMR-specific peptides (XMR^{69-81}, XMR^{96-106}) identified by a ClustalW alignment of XMR and related proteins (Figure 4.4). To determine if these antibodies are specific to XMR, COS-7 and HEK293 cells were transiently transfected with either the *Xmr* or *AK015913* ORFs. Although very few cells were transfected, immunostaining (Figure 4.5.A) and western blot analysis (figure 4.5.B) indicated that the anti-XMR^{69-81} and anti-XMR^{1-93} antibodies were able to detect both proteins, whereas the anti-XMR^{96-106} antibody only detected the XMR protein, demonstrating that it is specific for XMR.

Figure 4.4

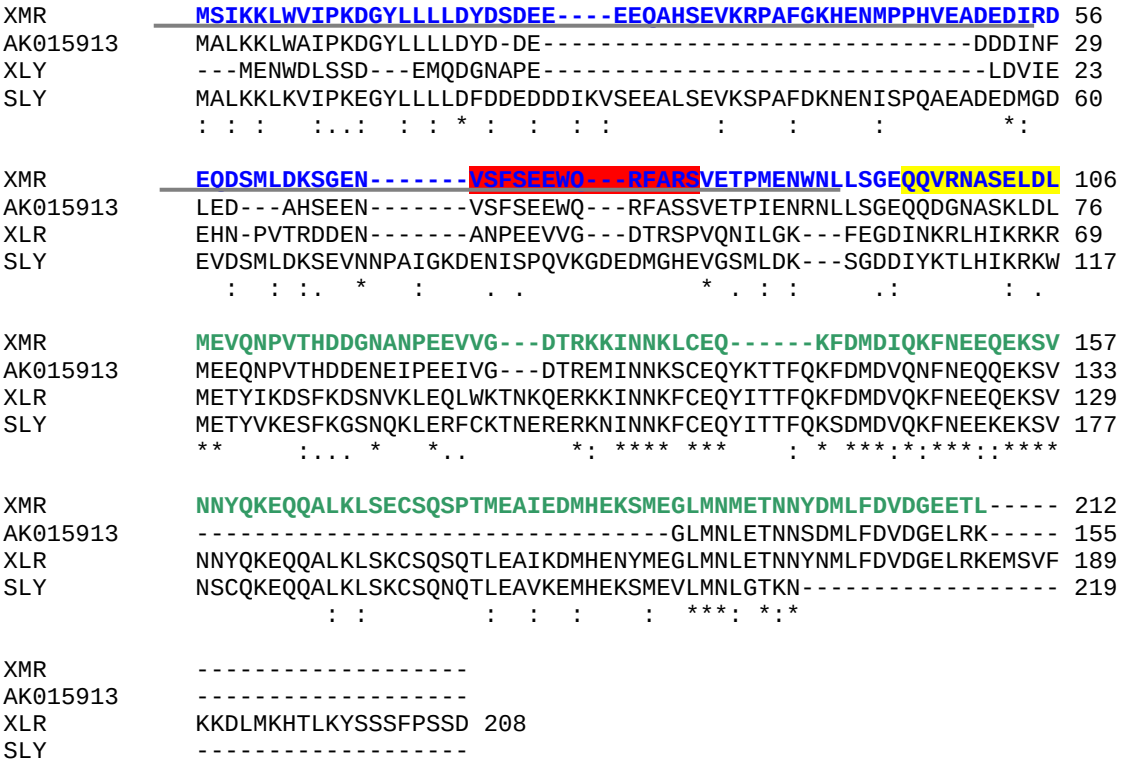

Figure 4.4 A ClustalW alignment of XMR, AK015913, XLR and SLY amino acid sequences

The anti-XMR$^{69\text{-}81}$ antibody was raised against the XMR-specific peptide VSFSEEWQRFARS (highlighted in red).

The anti-XMR$^{96\text{-}106}$ antibody was raised against the QQDGNASKLDL peptide (highlighted in yellow).

The first 93 amino acids of XMR (underlined) were used to generate the anti-XMR$^{1\text{-}93}$ antibody.

The N-terminal domain of XMR (amino acids 1-106) is in blue font and the XMR COR1 (amino acids 107-212) domain is in green font.

Figure 4.5 Transfection of COS7 and HEK 293 cells with the *Xmr* and *AK015913* ORFS

A) Immunofluorescence staining of COS7 cells transiently transfected with the *Xmr* ORF (top row), *AK015913* ORF (middle row) or mock transfected (bottom row). Cells were stained using the anti-XMR$^{69-81}$ antibody (far left panel), the anti-XMR$^{96-106}$ antibody (left panel), the anti-XMR$^{1-93}$ antibody (right panel) or an antibody raised to the related XLR protein (far right panel).

B) Western blot analysis of HEK 293 cells transfected with the *Xmr* ORF (lane 1), mock transfected cells (lane 2) and *AK015913* ORF transfected cells (lane 3). Blots were detected with the anti-XMR$^{69-81}$ (far left panel), anti-XMR$^{96-106}$ (left panel), anti-XMR$^{1-93}$ (right panel) or anti-XLR (far right panel) antibodies. The top arrow indicates the AK015913 protein (in lane 3) and the bottom arrow points to the XMR protein (present in lane 1).

The anti-XMR$^{69-81}$ and anti-XMR$^{1-93}$ antibodies detect both XMR and AK015913 proteins, whereas the anti-XMR$^{96-106}$ antibody is specific to XMR. Despite previous reports (Calenda et al., 1994), the anti-XLR antibody is unable to detect XMR or the related AK015913 protein *in vitro*.

Figure 4.5

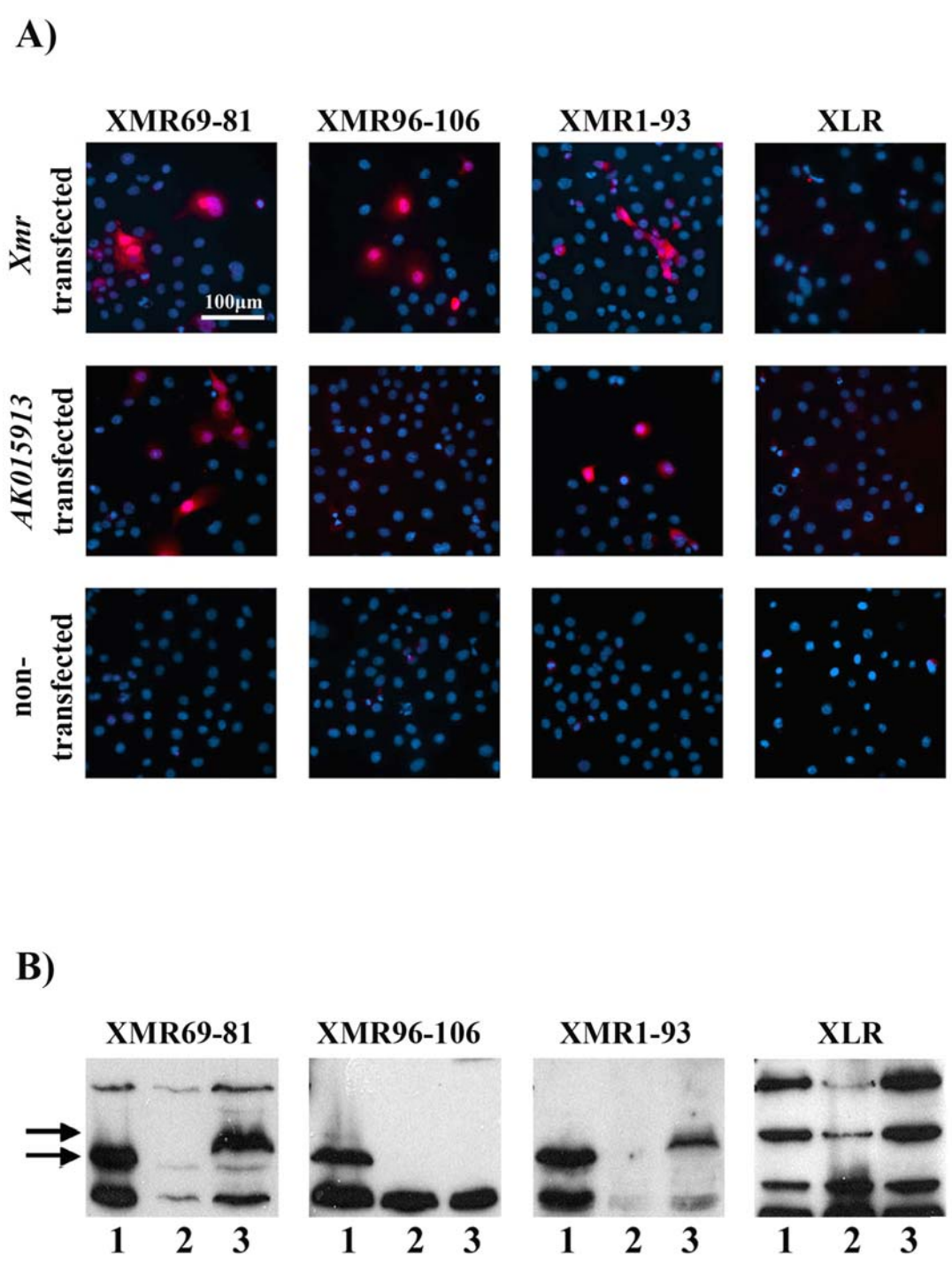
A)
XMR69-81
XMR96-106
XMR1-93
XLR
Xmr transfected
AK015913 transfected
non-transfected
100µm
B)
XMR69-81
XMR96-106
XMR1-93
XLR
1 2 3
1 2 3
1 2 3
1 2 3

4.2.3 Expression of XMR in the testis

Microarray analysis and northern blot data (Calenda et al., 1994) indicate that *Xmr* is expressed specifically in the testis, and western blot analysis of multiple tissues detected a 35kDa testis-specific band with all three XMR antibodies (figure 4.6.A). This protein was not detected by the pre-immune serum or after pre-absorption of the antibody with an excess of the peptide to which it was raised (Appendix 4). The 35kDa protein was detected by all three antibodies after immunoprecipitation with the XMR-specific anti- XMR^{96-106} antibody, confirming that these antibodies detect the same protein (Figure 4.6.B)

To confirm that this protein corresponds to XMR, western blot analysis of testis from MSYq- mice was performed. These mice have increased transcription of *Xmr* and *AK015913* (Ellis et al., 2005); as expected, all three antibodies detected an increase in intensity of the 35kDa protein in MSYq- samples compared to wild type samples (Figure 4.6.C). This confirms that the 35KDa protein seen by western blot analysis is XMR. This is the first time that the up-regulation of mRNA from X- and Yp-linked genes observed in the MSYq deletion models has been shown to result in an increase of the corresponding protein.

4.2.4 Analysis of XMR expression during spermatogenesis

To determine which spermatogenic cell types express the XMR protein, western blot analysis was performed on testis protein samples from the first spermatogenic wave. XMR was detected at low levels from 21.5d*pp*, reaching adult levels by 28.5d*pp* with no protein detectable at 18.5d*pp* or earlier (figure 4.7.A). Western analysis of daily time points between 18.5d*pp* to 22.5d*pp* further refined the timing of expression, confirming that XMR was first present at 21.5d*pp* (figure 4.7.B). This is consistent with spermatid-specific expression and the absence of XMR prior to 21.5d*pp* confirms that XMR is not a meiotic protein as previously published (Calenda et al., 1994; Escalier et al., 2000; Escalier et al., 2002; Escalier et al., 2005). It is not clear if *AK015913* is translated, as no testis-specific protein of the predicted size was detected. However, if *AK015913* is translated, it must have the same pattern of expression as XMR.

To confirm that XMR is spermatid-specific, immunostaining of testis sections was

performed using all three anti-XMR antibodies. Staining was observed exclusively in round spermatids in some but not all tubules (Figure 4.8.A). To identify which tubule stages expressed XMR, sections were co-stained with either the anti-XMR$^{69-81}$, anti-XMR$^{96-106}$ or anti-XMR$^{1-93}$ antibody together with an antibody against γH2AX, which labels the nucleus of leptotene and zygotene cells, and the sex body domain in the nucleus of pachytene cells (Mahadevaiah et al., 2001). XMR staining was seen at high levels in spermatid stages 2 to 9 and at low levels in stage 10-11 spermatids. No co-localisation of XMR and γH2AX was seen (Figure 4.8.A), confirming that the XMR antibodies do not cross react with the meiotic protein detected by the anti-XLR antibody of Calenda et al. (1994). Furthermore, dual labelling of XMR, together with the anti-XLR antibody used by Calenda et al. (1994), gave mutually exclusive staining patterns (Figure 4.8.B). As expected, there is co-localisation of the XLR and γH2AX staining patterns in the pachytene sex body, confirming that the anti-XLR antibody detects a meiotic protein (Figure 4.8.C).

Surprisingly, all three XMR antibodies labelled the spermatid cytoplasm (Figure 4.9.A), and not the nucleus as expected based on published data on the *Xlr* superfamily. In order to see whether epitope masking may have prevented detection of any nuclear XMR protein, cytoplasmic and nuclear fractions from adult testis were analysed by western blot. The 35kDa XMR protein was present in whole testis and cytoplasmic fractions but not the nuclear fraction (Figure 4.9.B). Together, these data indicate that XMR is predominantly, if not exclusively a cytoplasmic protein expressed only in spermatids.

Figure 4.6 Western blot analysis of XMR expression in the testis

A) Examination of brain, kidney and testis protein lysates from an adult XY male mouse. Blots were probed with the anti-XMR$^{69-81}$ antibody (far left panel), the anti-XMR$^{96-106}$ antibody (left panel), the anti-XMR$^{1-93}$ antibody (right panel) or an antibody raised against the related XLR protein (far right panel). A testis-specific protein of approximately 35kDa (arrowed) is detected by all three anti-XMR antibodies, but not the anti-XLR antibody.

B) Immunoprecipitation of XY testis lysates with the anti-XMR$^{96-106}$ antibody under native (left panel) and denatured (right panel) conditions. XMR is present as a doublet in the whole testis lysate (the input, lane 1) and is immunoprecipitated by the anti-XMR$^{96-106}$ antibody (lane 3) but not by the pre-immune serum antibody (lane 2). Membranes were detected with the anti-XMR$^{69-81}$ (far left panel), the anti-XMR$^{96-106}$ (left panel), anti-XMR$^{1-93}$ (right panel) or anti-XLR (far right panel) antibodies. All three anti-XMR antibodies are able to detect the XMR protein precipitated by the anti-XMR$^{96-106}$ antibody, but the anti-XLR antibody cannot.

C) Analysis of XY (lane 1) and MSYq- (lane 2) protein lysates from adult testis. Blots were probed with the anti-XMR and anti-XLR antibodies (upper panel) and an anti-actin antibody as a loading control (bottom panel). The MSYq- samples have an increase in XMR levels relative to the XY control and this is detected with the three anti-XMR antibodies but not the anti-XLR antibody.

Figure 4.6

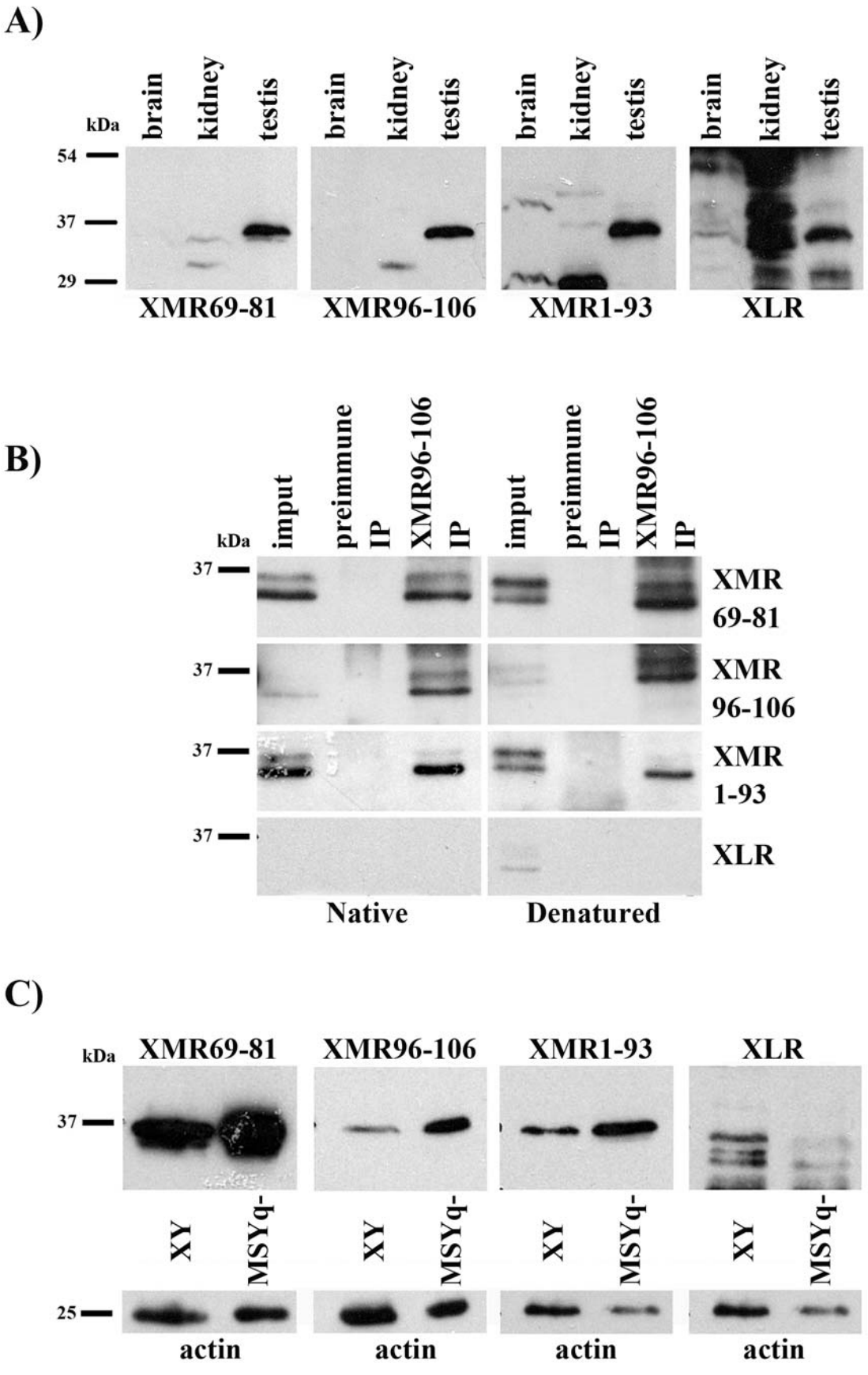
A)
kDa
brain
kidney
testis
54
37
29
XMR69-81
XMR96-106
XMR1-93
XLR
B)
kDa
imput
preimmune IP
XMR96-106 IP
37
XMR 69-81
XMR 96-106
XMR 1-93
XLR
Native
Denatured
C)
kDa
XMR69-81
XMR96-106
XMR1-93
XLR
37
XY
MSYq-
25
actin

Figure 4.7 XMR expression during spermatogenesis

Western blot of XY testis samples taken at time points during the first spermatogenic wave from

A) 7.5d*pp* to adult
B) 18.5d*pp* to 28.5d*pp*

Membranes were probed with the anti-XMR$^{69-81}$ antibody (top panel), the anti-XMR$^{96-106}$ antibody (middle panel) and the anti-XMR$^{1-93}$ antibody (bottom panel). All three antibodies detect XMR from 21.5d*pp*.

Figure 4.7

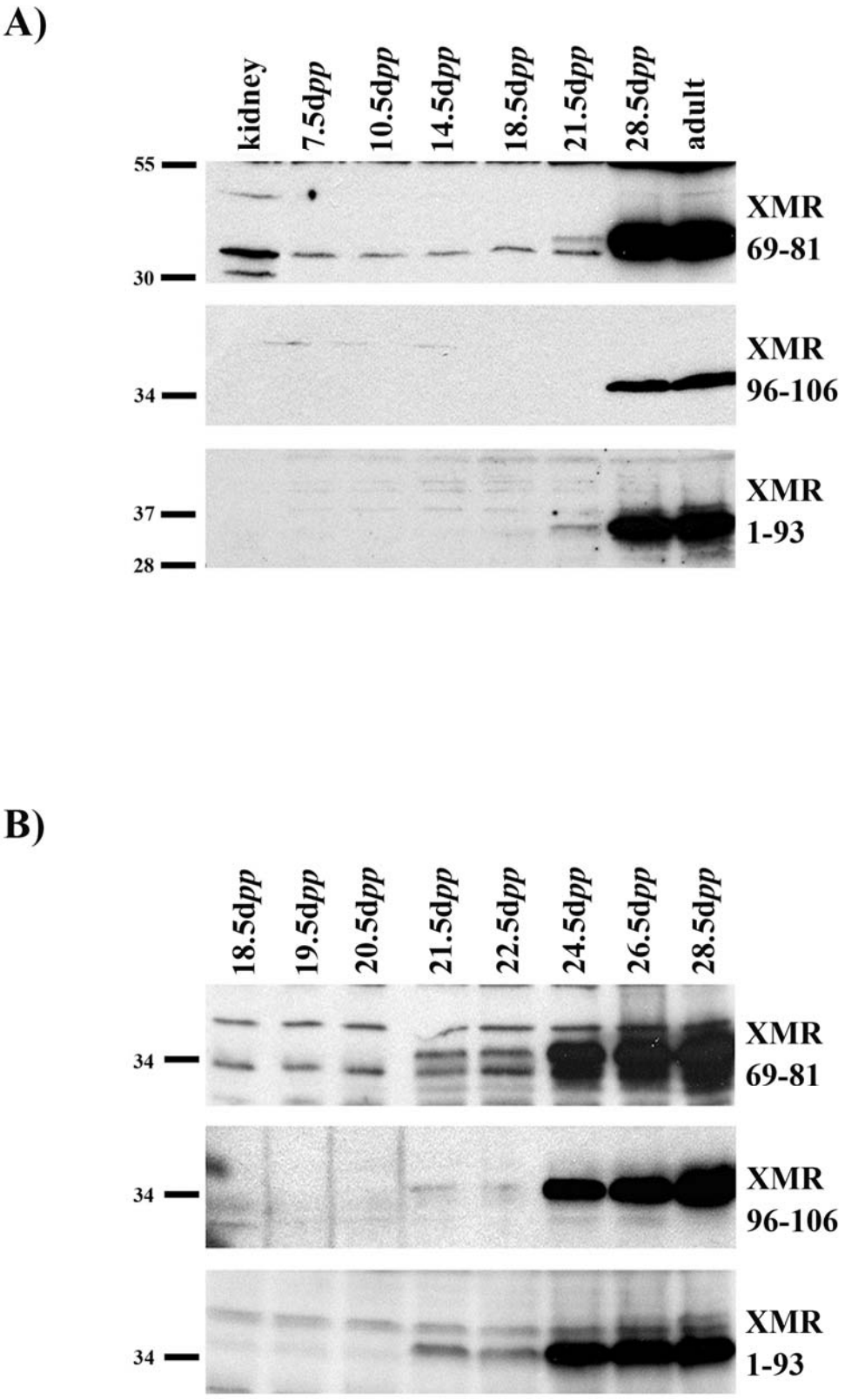
A)
kidney
7.5dpp
10.5dpp
14.5dpp
18.5dpp
21.5dpp
28.5dpp
adult
55
30
34
37
28
XMR
69-81
XMR
96-106
XMR
1-93
B)
18.5dpp
19.5dpp
20.5dpp
21.5dpp
22.5dpp
24.5dpp
26.5dpp
28.5dpp
34
34
34
XMR
69-81
XMR
96-106
XMR
1-93

Figure 4.8 Immunostaining of XY adult testis sections

Immunofluorescence staining of adult testis sections with;

A) anti-XMR$^{69\text{-}81}$ (red) and anti-γH2AX (green) antibodies.
The anti-γH2AX antibody stains the nucleus of meiotic cells. XMR and γH2AX do not co-localise, indicating that XMR is not present in meiotic cells

B) anti-XMR$^{69\text{-}81}$ (red) and anti-XLR (green) antibodies.
The proteins detected by the anti-XMR and anti-XLR antibodies show mutually exclusive expression patterns

C) anti-γH2AX (red) and anti-XLR (green) antibodies.
XLR and γH2AX co-localise, confirming that the anti-XLR antibody detects a meiotic epitope.

The cell nuclei are stained with DAPI (blue).

Figure 4.8

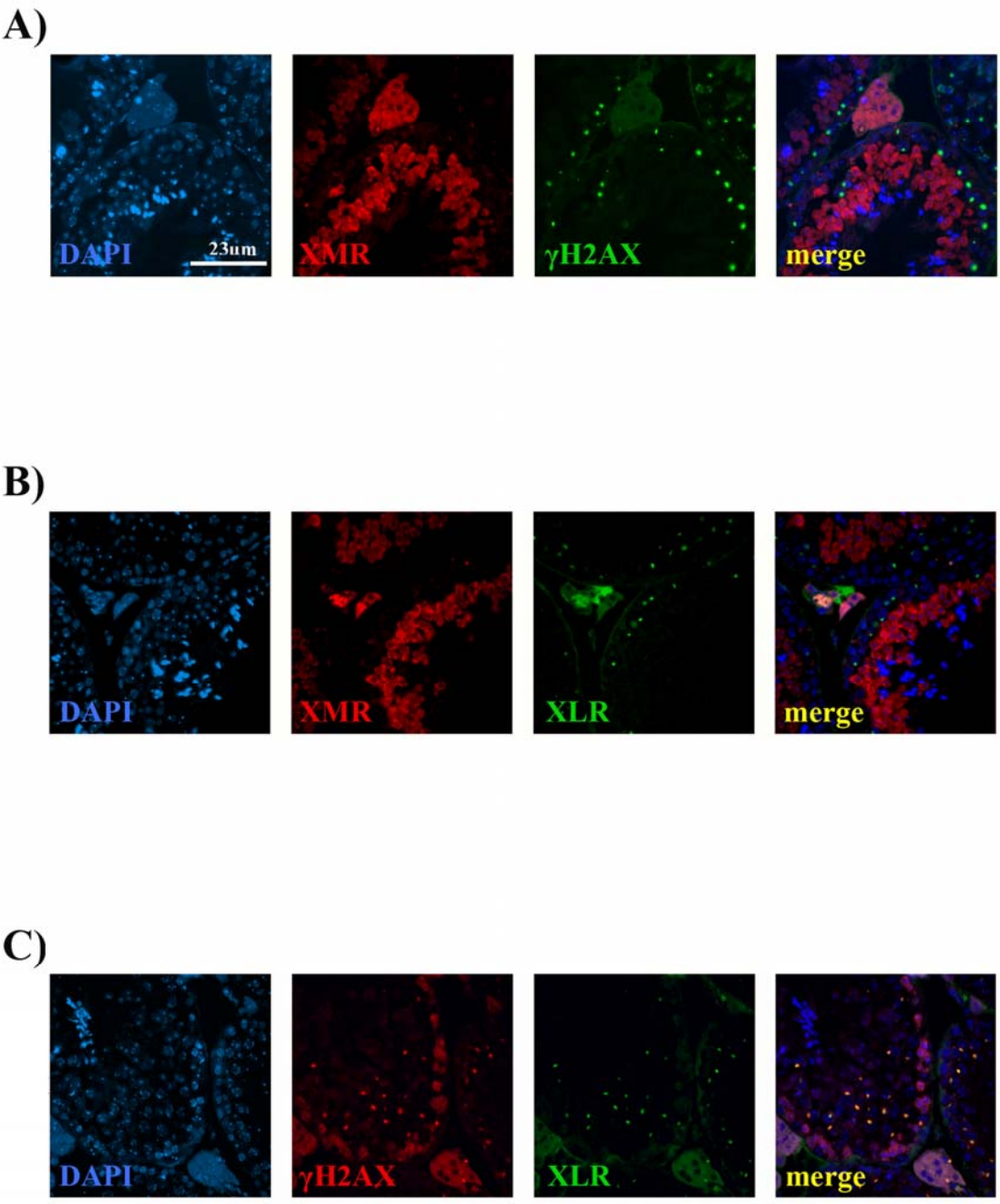
A)
DAPI
23um
XMR
γH2AX
merge
B)
DAPI
XMR
XLR
merge
C)
DAPI
γH2AX
XLR
merge

Figure 4.9 Cytoplasmic localisation of XMR in spermatids

A) XMR staining of XY testis sections under 100X magnification reveals that XMR is restricted to spermatids and appears to be cytoplasmic. Sections were stained with the anti-XMR$^{69-81}$ antibody (top panel; red), the anti-XMR$^{96-106}$ antibody (middle panel; red) and anti-XMR $^{1-93}$ antibody (bottom panel; red). DNA is stained with DAPI (blue)

B) Western blot analysis of cytoplasmic and nuclear fractions from adult XY testis using the three XMR antibodies and the XLR antibody, with the γH2AX antibody as a nuclear control. XMR is present in the cytoplasmic fraction, whereas the testicular protein recognised by the anti-XLR antibody is nuclear. A whole testis sample (overloaded relative to the nuclear and cytoplasmic fractions) is included for each as a positive control.

Figure 4.9

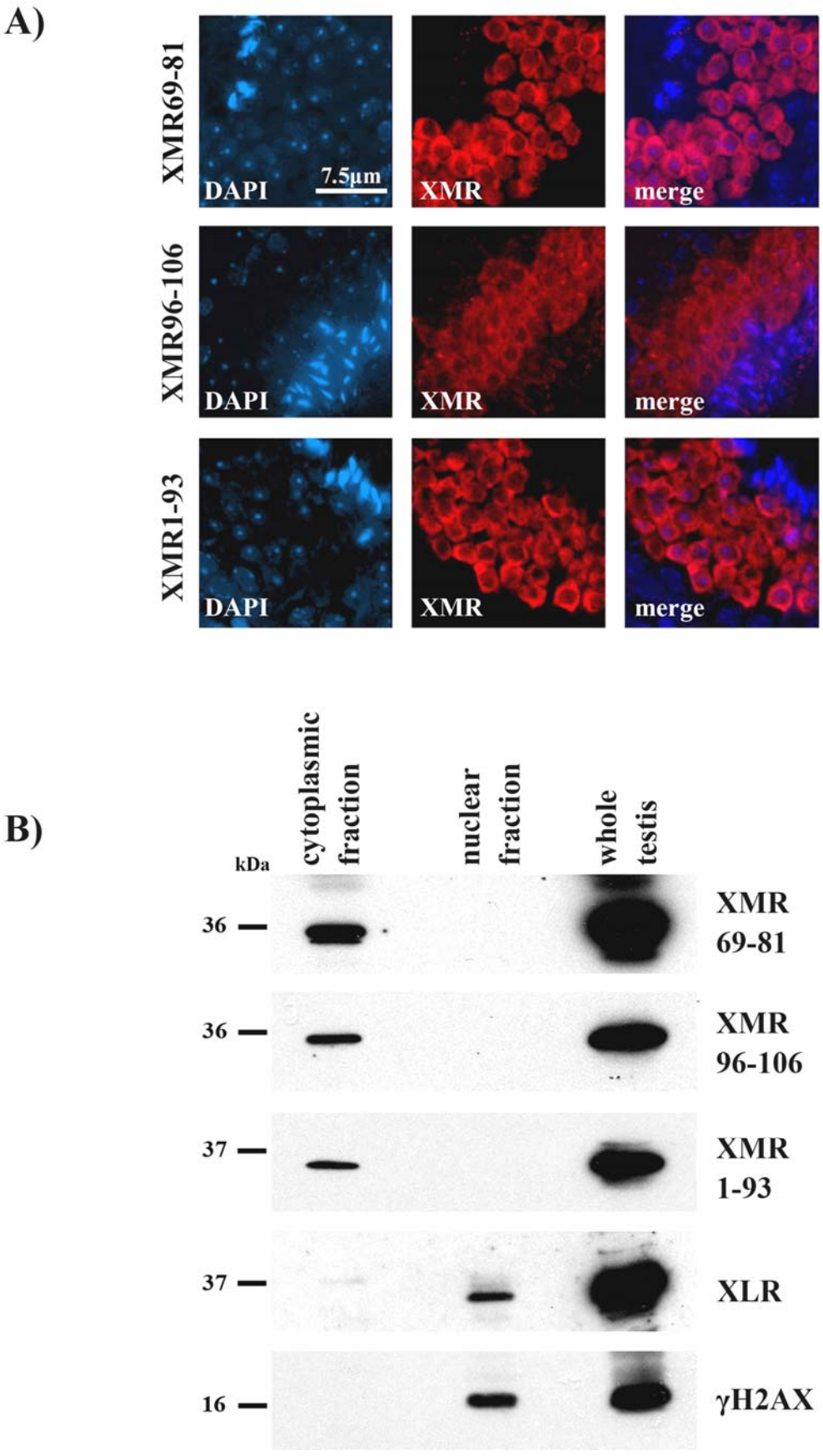
A)
XMR69-81
XMR96-106
XMR1-93
DAPI
7.5µm
XMR
merge
B)
cytoplasmic fraction
nuclear fraction
whole testis
kDa
36
36
37
37
16
XMR 69-81
XMR 96-106
XMR 1-93
XLR
γH2AX

4.2.5 The anti-XLR antibody does not detect XMR

The co-staining experiments described above demonstrate that the mouse monoclonal anti-XLR antibody previously used fails to detect the spermatid XMR protein. Formally speaking, this may have been due to the masking of the XMR/AK015913 epitope recognised by the anti-XLR antibody in testis sections. I therefore decided to characterise this antibody in greater detail. The XLR antibody was unable to detect the XMR or AK015913 proteins in transfected cells by either immunostaining or western blot (figures 4.5.A, 4.5.B). Although a protein of approximately the same size as XMR was detected in the testis on a multi-tissue western blot, closer analysis revealed that it was too small to be XMR and was also present in the brain (figure 4.6.A). Furthermore, the anti-XLR antibody was unable to detect a difference in the band intensity on western blots between control testis and MSYq- testis, although the latter is known to have a marked increase in XMR protein (figure 4.6.C). Finally, the anti-XLR antibody was unable to detect the XMR protein immunoprecipitated with the $XMR^{96\text{-}106}$ antibody, which was detected by all three anti-XMR antibodies (Figure 4.6.B). However, the anti-XLR antibody detected a nuclear protein on a western blot of nuclear and cytoplasmic testis fractions (figure 4.9.B), consistent with previous data (Calenda et al., 1994); this protein is probably the same protein as that detected on testis sections using the same antibody. In conclusion, these data suggest that the anti-XLR antibody cannot detect XMR, and therefore the meiotic epitope detected by Calenda et al. (1994) results from cross reaction of the anti-XLR antibody with another unidentified protein(s).

4.2.6 XMR yeast-two-hybrid analysis

To identify the function of XMR in spermiogenesis, I performed a yeast-two-hybrid analysis using the full length XMR ORF cloned into the pGBKT7 vector as bait and a pre-transformed testis cDNA library as prey. In initial control experiments, the AH109 strain of *S. cerevisiae* was transformed with either the pGBKT7-XMR plasmid or the control pGBKT7 plasmid and grown on selective medium. Yeast colonies containing the pGBKT7-XMR plasmid were significantly smaller than those containing either the empty pGBKT7 or pGBKT7-SLY plasmids, indicating that the XMR is toxic to the yeast. The pGBKT7-XMR colonies also turned blue in the presence of X-α-gal,

indicating that XMR has transcriptional activation activity and is able to express the reporter genes without interacting with another protein, ruling out the possibility of screening the library with the complete XMR ORF.

To determine which part of the XMR protein was responsible for the toxicity and transcriptional activity, the XMR ORF was expressed in two separate segments that specify either the acidic N-terminal domain (amino acids 1-106) or the C-terminal coiled-coil COR1 domain (amino acids 107-212). These domains were separately expressed from the pGBKT7 plasmid in the AH109 strain of *S. cerevisiae* (Figure 4.10). The results are summarised in Figure 4.11. Activation of the *MEL1* reporter gene, assayed by the ability of the colony to turn blue in the presence of the chromatogenic substrate X-α-Gal, occurred with pGBKT7-XMR COR1, and to a lesser extent, pGBKT7-XMR N-terminal containing yeast, indicating that both domains possess transcriptional activation ability (Figure 4.10.B, C). However, yeast colonies containing the pGBKT7-XMR plasmid (Figure 4.10.D) were a more intense blue colour than either the pGBKT7-XMR N-terminal or pGBKT7-XMR COR1 colonies, suggesting that these two domains act in an additive manner in the full length protein. The pGBKT7-XMR N-terminal plasmid had no effect on initial colony growth, but after 5 days, the pGBKT7-XMR N-terminal colonies (Figure 4.10.B) were slightly smaller than the control pGBKT7 colonies (Figure 4.10.A), suggesting that the N-terminal domain of XMR may be slightly toxic to the yeast. The pGBKT7-XMR COR1 colonies (Figure 4.10.C) were also significantly smaller than the pGBKT7 colonies, but were approximately the same size as those containing with the full length XMR (Figure 4.10.D). These results indicate that the COR1 domain of XMR is responsible for most, if not all of the toxicity caused by this protein in yeast.

Figure 4.10 Photographs of XMR-containing *S. cerevisiae* colonies

S. cerevisiae of the AH109 stain were transformed with pGBKT7 plasmids containing the GAL4 DNA binding domain and grown on selective media in the presence of X-α-gal for 5 days. Activation of the MEL1 reporter gene causes the colonies turn blue in the presence of X-α-gal. Photographs are at 1X magnification

A) Photograph of yeast containing the pGBKT7 plasmid alone. The colonies show normal growth and are white in colour (the MEL1 gene is not activated).

B) Photograph of yeast containing the pGBKT7-XMR N-terminal plasmid. The DNA encoding the first 106 amino acids of XMR is fused to the GAL4 DNA BD, forming a fusion protein. The colonies are slightly smaller than those containing the pGBKT7 plasmid alone. The colonies are pale blue, indicating that the MEL1 reporter gene has been activated by the fusion protein.

C) A photograph of yeast containing the pGBKT7-XMR COR1 plasmid. The colonies are smaller than the pGBKT7 control. The DNA BD-XMR COR1 fusion protein causes strong activation of the MEL1 reporter gene indicated by the colony colour.

D) A photograph of yeast colonies containing the pGBKT7-XMR plasmid. The full length XMR protein is fused to the DNA BD of GAL4. The colonies are 2-3X smaller than those containing the control pGBKT7 plasmid, indicating the fusion protein causes growth retardation. The colonies are also dark blue, implying that the fusion protein also causes very strong activation of the MEL1 reporter gene.

Figure 4.10

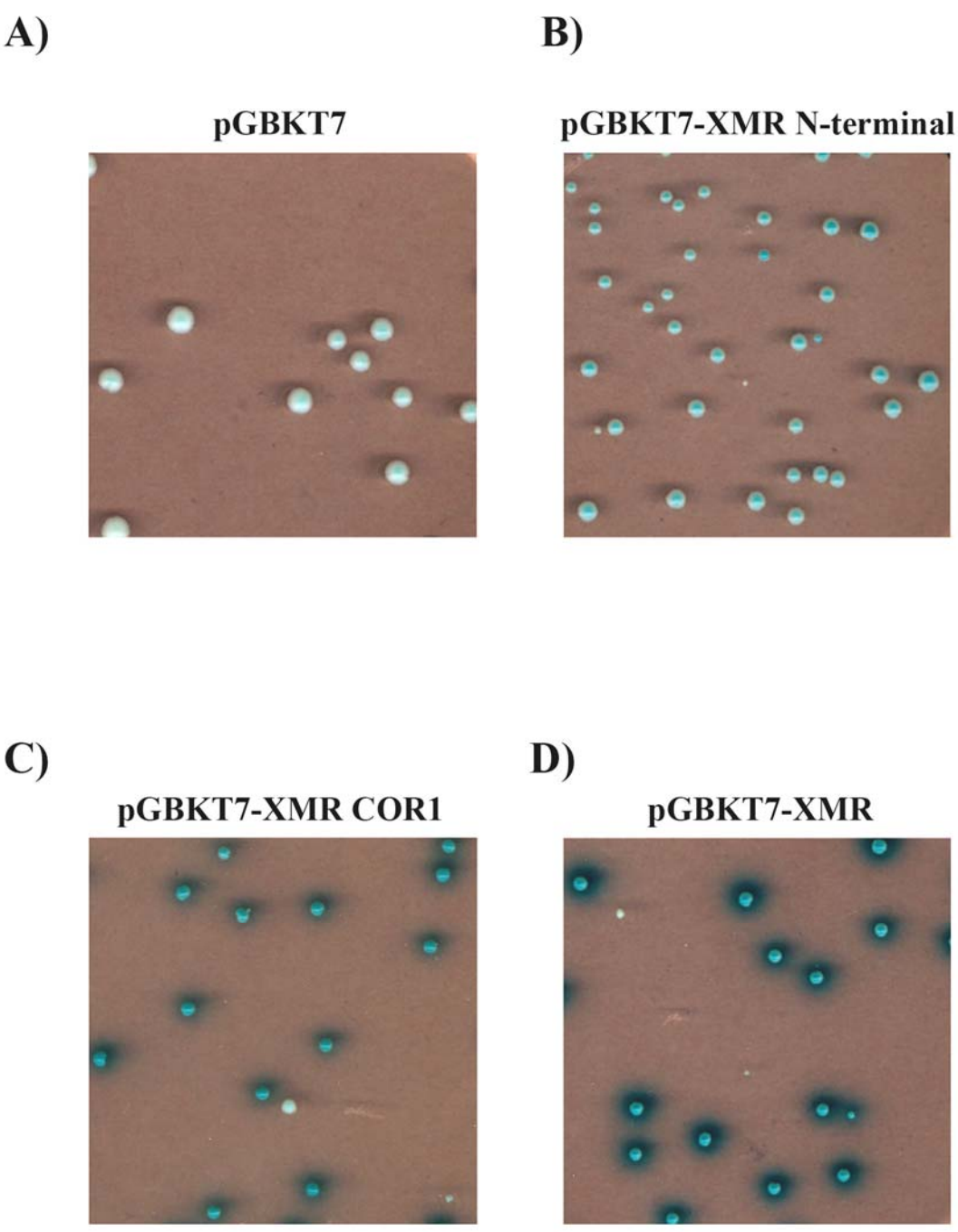
A)
B)
pGBKT7
pGBKT7-XMR N-terminal
C)
D)
pGBKT7-XMR COR1
pGBKT7-XMR

Figure 4.11

A)

B)

construct	colony size	colony growth	colony colour	Activation of MEL1 reporter gene?
pGBKT7	2-3mm	normal	white	no
pGBKT7-XMR N-terminal	1.5-2.5mm	slight retardation	pale blue	yes
pGBKT7-XMR COR1	1-1.5mm	slow, 2-3X smaller than control	blue	yes
pGBKT7-XMR	1-1.5mm	slow, 2-3X smaller than control	dark blue	yes

Figure 4.11 Transformation of *S. cervisiae* with different *Xmr* constructs

A) Schematic representation of the fusion proteins encoded by the different pGBKT7 constructs. The GAL4 DNA binding domain is in yellow, the XMR N-terminal domain is in pale blue and the XMR COR1 domain is in dark blue.

B) A summary of the *S. cerevisiae* colony growth and colour after transformation with the pGBKT7, pGBKT7-XMR N-terminal, pGBKT7-XMR COR1 and pGBKT7-XMR constructs.

4.3 Discussion

In this chapter, I have used RT-PCR and RNA FISH to further substantiate the growing evidence that the multicopy *Xmr* gene is predominantly transcribed in spermatids. Western blot and immunostaining analysis was carried out using antibodies raised specifically to XMR and this demonstrated that XMR it is a cytoplasmic protein present in stage 2–11 spermatids. These findings are inconsistent with previous studies that used an antibody raised to the related XLR, and concluded that XMR is a nuclear protein expressed during meiosis (Calenda et al., 1994; Escalier and Garchon, 2005; Escalier and Garchon, 2000). To explain this discrepancy, I have also demonstrated that this anti-XLR antibody is unable to recognize either XMR or the related protein AK015913. In light of these findings, the name *Xmr* (*Xlr*-related, meiosis regulated) is misleading, and the gene has been renamed *Slx* (*Sycp3*-like, X-linked) to reflect its homology to the Y-encoded multi-copy *Sly* (Reynard et al., 2007). *AK015913* is now named *Slxl1* (*Slx*-like 1).

The identity of the protein recognized by the monoclonal anti-XLR antibody is at present unknown. A candidate for this protein is XLR, although previous data suggests that the *Xlr* gene is not transcribed in the testis (Escalier and Garchon, 2005; Escalier and Garchon, 2000). However, I detected *Xlr* mRNA in the testis by RT-PCR, and this is substantiated by microarray studies (Namekawa et al., 2006; Shima et al., 2004) and data from Turner (2000), which detected *Xlr* mRNA in the testis from 11.5d*pc*. The anti-XLR antibody also recognizes an ovarian meiotic protein reported to be XLR (Escalier et al., 2002). The staining pattern observed in oocytes is reminiscent of the testicular expression pattern observed with the same antibody, with XLR localising to the whole nucleus of leptotene and zygotene oocytes, before reaching its highest levels in pachytene oocytes. In both the XY testis and XY^{Tdym1} ovary, the protein(s) recognised by the anti-XLR antibody localise to sex chromosomes during pachytene (Calenda et al., 1994; Turner, 2000) and this protein(s) also accumulates on the axes of asynapsed autosomes in oocytes and spermatocytes (Escalier and Garchon, 2005; Escalier and Garchon, 2000; Turner, 2000). It is feasible that the anti-XLR antibody detects two different meiotic proteins which are expressed in a sex specific manner, as concluded by Escalier et al. (2002). However, a more parsimonious explanation for the identical staining pattern observed in oocytes and spermatocytes' using the anti-XLR antibody is that this antibody detects the same protein in male and female meiosis. The

observations that *Xlr* is transcribed in the testis as well as the foetal ovary, together with the knowledge that the antibody was raised against the full length XLR protein, suggest that the meiotic protein is XLR. One way to test this hypothesis is by raising an antibody to a peptide sequence specific to XLR and observing if this antibody detects the same meiotic protein as the full length anti-XLR antibody. Alternatively, to examine if the staining pattern detected by the anti-XLR antibody is altered in meiotic cells that have reduced or absent XLR, RNAi could be used to decrease *Xlr* expression levels in germ cells. This approach would also help to elucidate the potential function of XLR during mouse meiosis.

Another possibility is that the anti-XLR antibody recognises a different member of the *Xlr*-superfamily in meiotic cells. RT-PCR and microarray studies show that *Xlr3*, *Xlr4*, and *Xlr5* subfamily members are transcribed in spermatogenic cells, and for *Xlr3* this has been confirmed by Northern blot analysis (Lammers et al., 1994). Transcription of all three subfamilies begins before MSCI takes place (Namekawa et al., 2006; Schultz et al., 2003; Shima et al., 2004). A transcriptional study of ovary development by microarray analysis indicates that the *Xlr3*, *Xlr4*, and *Xlr5* genes are also transcribed during meiosis in females (Small et al., 2005), and could therefore account for the appearance of the protein detected by the anti-XLR antibody. The putative XLR3, XLR4, and XLR5 proteins all contain classical nuclear localization signal motifs (Hicks and Raikhel, 1995; Hicks et al., 1995), and are predicted to be nuclear using Psort II bioinformatics program (http://psort.nibb.ac.jp/form2.html). The protein recognised by the anti-XLR antibody is enriched axes of the X and Y during pachytene and the putative XLR4 protein was identified in a yeast-two-hybrid screen as a potential interactor of SYCE2, a synaptonemal complex central element protein (Y. Costa, personal communication). Transfection of cells with the *Xlr3*, *Xlr4* and *Xlr5* ORFs tagged with a reporter gene could be used to see if the fusion protein is recognised by the anti-XLR antibody. However, this approach would not help to establish the identity of the meiotic protein detected by the antibody, but rather demonstrate if the antibody can recognise other *Xlr* superfamily proteins besides XLR. Alternatively, transgenic mice carrying tagged versions of these genes could be generated to examine if their encoded proteins have the same expression pattern as the protein detected by the anti-XLR antibody. Finally, it is conceivable that the anti-XLR antibody cross-reacts with an unrelated meiotic protein.

The SLX protein contains a COR1 domain, which is hypothesized to facilitate chromatin binding, and so the cytoplasmic localisation of SLX in spermatids is surprising. Transformation of *S. cervisiae* with the *Slx* ORF demonstrates that SLX has transcriptional activation activity when the protein localises to the nucleus. Further analysis in yeast found that the COR1 and N-terminal domains of SLX both contain transcriptional activity (assayed by the ability to activate the *MEL1* reporter gene, which turns the yeast colony blue in the presence of X-α-gal), although the majority of this activity in the full length protein is due to the COR1 domain. SLX was also found to be toxic to yeast, with colonies containing the plasmids encoding SLX being smaller than those transformed with the control plasmid. This toxicity may be related to the transcriptional activity of SLX in yeast, with SLX potentially affecting the transcription of genes involved in cell cycle progression or apoptosis. SLX could also be toxic in mammalian cells when present in cells that do not normally express it, and this may explain the small number of SLX-containing cells when HEK 293 and COS7 cells are transfected with the *Slx* ORF. It should be noted that SLX localises to the nucleus in both cell types, where it may affect transcription, potentially leading to cell death when high levels of SLX are present.

The cellular location of SLX in the testis can be explained by loss of the putative nuclear localization signal motif KRKR found in the COR1 domain of XLR and SYCP3, and by the lack of other identifiable nuclear localization signal motifs. It remains conceivable that in spermatids, a small proportion of SLX protein is present in the nucleus where it is involved in transcriptional regulation during spermiogenesis, with chromatin binding facilitated by the COR1 domain. However, western blot analysis and immunofluorescence studies found no evidence to support this idea. It is more likely that SLX has developed a new role in the cytoplasm of spermatids. One possibility is that SLX is involved in mRNA metabolism, with the COR1 domain evolving to allow binding to cytoplasmic RNAs rather than chromatin. If this is found to be the case, *Slx* may still play a role in the up-regulation of spermatid expressed sex linked genes seen in the MSYq deletion models.

Ellis et al. (2005) have reported that mice with deletions of the MSYq up-regulate a number of X- and Yp-linked transcripts, including *Slx*. Our present results are important because they are the first to show that, at least for *Slx*, the increase in transcription seen in MSYq- mice leads to a corresponding increase in protein levels.

Aside from an increase in sperm head defects seen in MSYq deletion mice models, the fertile 2/3MSYq- mice generate offspring with a distorted sex ratio in favour of females (Conway et al., 1994). Ellis and colleagues (Ellis et al., 2005) proposed that this is because of an underlying post-meiotic X-versus-Y intragenomic conflict that has been uncovered by the reduction of MSYq-encoded transcripts resulting from the deletion. It has further been suggested that *Slx* and *Sly* may be important players in this genomic conflict (Ellis et al., 2005; Touré et al., 2005), perhaps due to the predicted mutually antagonistic action of SLY and SLX on the transcriptionally repressed X and Y chromatin domains of spermatids (Greaves et al., 2006; Namekawa et al., 2006; Turner et al., 2006). However, the findings of chapters 3 and 4 of this thesis indicate that SLX and SLY do not localize to the nucleus, so any potential genomic conflict between these two proteins is unlikely to occur by effects on sex chromatin. It is more likely that any potential interaction between *Slx* and *Sly* is mediated at the post-transcriptional level, perhaps in a manner similar to that described for the multicopy sex-linked *Ste*/*Su(Ste)* genes in *Drosophila* (Aravin et al., 2001; Belloni et al., 2002). Alternatively, the reduction of other MSYq-encoded transcripts such as *Ssty* may be responsible for the distorted sex ratio in offspring of the 2/3MSYq males. The up-regulation of X- and Yp-linked genes in the MSYq deletion models is investigated further in the next chapter.

To conclude, in this chapter I have reanalysed the expression of *Slx* (previously *Xmr*) during spermatogenesis at the RNA and protein level. I have discovered that SLX is expressed in a different cell type and cellular compartment than previously published (Calenda et al., 1994; Escalier and Garchon, 2005; Escalier and Garchon, 2000). However, I was unable to identify the role of this protein during spermiogenesis. Due to the toxicity and effects of SLX on *S. cervisiae* transcription, a yeast-two-hybrid screen could not be performed to identify proteins that interact with SLX. It will be interesting to see if the proteins found to interact with SLY (for example DKKL1, see chapter 3) also interact with SLX. However, I think this is unlikely due to the divergence in protein sequence between SLX and SLY and the observation that unlike SLX, SLY does not have transcriptional effects nor is it not toxic to *S. cervisiae*. I believe that *Slx* transgenic analysis remains the best approach to elucidate the specific role of this gene in spermiogenesis and this is the topic of chapter 6.

Chapter 5

Examination of sex chromosome transcription and epigenetic marks in spermatids from mice with MSYq deletions

Examination of sex chromosome transcription and epigenetic marks in spermatids from mice with MSYq deletions

5.1 Introduction

The results of chapters 3 and 4 demonstrated that SLY and SLX are cytoplasmic proteins, and are thus unlikely to have a direct role in regulating spermatid chromatin conformation and gene expression, as previously hypothesised (Ellis et al., 2005; Touré et al., 2005). It has been assumed that the rise in X- and Yp-linked transcripts observed in mice with MSYq deletions result from the de-repression of these genes in spermatids. However, it is feasible that this up-regulation is a post-transcriptional effect, and may be due to disturbances in mRNA processing or stability. The aim of this chapter is to investigate if the increase in X- and Yp-derived transcripts observed in the three MSYq deletion models is the result of a chromatin mediated effect or a post-transcriptional effect. If the latter is found to be the case, *Sly* and *Slx* remain potential candidate genes for this phenotype in the MSYq deletion models.

Incomplete synapsis of the mammalian X and Y chromosomes during male meiotic prophase triggers the formation of the transcriptionally silent heterochromatic XY or sex body domain, a process known as meiotic sex chromosome inactivation (MSCI). The silencing of the sex chromosomes in MSCI is accompanied by exclusion of the active form of RNA polymerase II (Pol-II) and changes in epigenetic marks from those associated with active chromatin to those associated with transcriptional inactivation (Khil et al., 2004; Namekawa et al., 2006). For a long time, MSCI was assumed to be transient, the sex chromosomes being transcriptionally reactivated at the end of meiotic prophase as proteins associated with silencing were lost. However, recently it was shown that a substantial degree of sex chromosome silencing persists through the meiotic divisions into spermatids (Namekawa et al., 2006; Namekawa et al., 2007; Turner et al., 2006). This phenomenon is termed post-meiotic sex chromosome repression (PSCR; Turner et al., 2006) and microarray studies on purified mouse spermatogenic cells indicate that up to 87% of X-linked genes remain transcriptionally suppressed in round spermatids (Namekawa et al., 2006). Unlike MSCI, PSCR is incomplete, and a number of genes display some level of post-meiotic reactivation (Mueller et al., 2008; Namekawa et al., 2006). There is also *de novo* transcription of

several sex linked genes that are expressed specifically in spermatids (e.g. *Mgclh*, *Slxl1*; Ellis et al., 2005).

In the spermatid nucleus, the sex chromosome is adjacent to the chromocentre and assembles into a DAPI-dense heterochromatic structure known as the post-meiotic sex chromatin (PMSC; Namekawa et al., 2006). This domain is depleted of Cot1 RNA (a marker of nascent transcription) and RNA polymerase II (Namekawa et al., 2006; Turner et al., 2006). The epigenetic status of the spermatid PMSC has been well characterised and includes a number of histone modifications and heterochromatin-associated proteins present on the meiotic sex body, including CBX1 (previously known as HP1β) and dimethylated Histone $H3_{k9}$ (Baarends et al., 2007; Greaves et al., 2006; Khalil et al., 2004; Namekawa et al., 2006; Turner et al., 2006). However, the X and Y chromosomes are continually remodelled during the transition between meiosis and spermiogenesis, and histone modifications associated with transcriptionally active chromatin (e.g. $H4_{K8}$ acetylation and $H3_{K4}$ dimethylation) are also enriched on the PMSC in round spermatids (Baarends et al., 2007; Greaves et al., 2006; Khalil and Driscoll, 2006). These epigenetic changes could explain why PSCR is less complete than MSCI, and may reflect a need to retain expression of some X- and Y-encoded genes that are essential for spermiogenesis.

Deletions of the MSYq are associated with problems in sperm development and function in mice. A number of downstream transcriptional effects secondary to MSYq deficiency were identified by microarray analysis of testes from the 2/3MSYq-, 9/10MSYq- and MSYq- mice models (Ellis et al., 2005). Twenty five spermatid-expressed genes showed at least a 1.5 fold transcriptional change in the MSYq-samples relative to the XY control. Only two of these genes were down-regulated, suggesting that the main effect of the MSYq on testis transcription is the repression of a set of downstream genes. Real-Time RT-PCR analysis confirmed that 15 of the 23 genes were up-regulated, and also identified five additional genes that showed a significant rise in transcript levels in the MSYq-testis compared to the XY control (Table 5.1). For the most highly up-regulated genes, *in-situ* hybridisation confirmed that these genes were expressed predominantly or specifically in spermatids in normal mice. Additionally, the expression pattern of the up-regulated genes was unaltered in the 9/10MSYq- and MSYq- testes. This indicates that elevated spermatid transcript

levels were responsible for the up-regulation rather than additional ectopic gene expression in other cell types.

Of the fifteen genes confirmed as up-regulated by real time PCR and microarray analysis, fourteen of these map to either the X or Y chromosome and include *Slx* and *Slxl1* (see Table 5.1 for a full list up-regulated genes). Many of the genes identified in the array are members of highly homologous gene families, and Ellis and colleagues (Ellis et al., 2005) demonstrated that while X- and Yp-encoded genes were significantly up-regulated in the MSYq deletion models, their autosomal homologues were not. The authors concluded that loss of MSYq-encoded transcripts is associated with a de-repression of specific sex-linked genes in spermatids. They went on to predict that SLX and SLY play a role in the persistence of sex chromosome silencing in spermatids by modulating their chromatin conformation. Furthermore, Ellis et al. (2005) suggested that the up-regulation of spermatid transcription in the MSYq deletion models was potentially due to SLY deficiency. It was also speculated that the up-regulated genes may contribute to the spermiogenic phenotypes in mice with MSYq deletions, with the two most highly affected genes, *AK005922* and *Mgclh,* being good candidates.

It is possible that the initiation or maintenance of PSCR is defective in the three MSYq deletion models. However, any failure of PSCR would be expected to lead to increased transcription of all spermatid-expressed sex-linked genes. This does not appear to be the case, since a moderate increase in transcript levels was only observed for a small number of X- and Yp-encoded genes. Ellis et al. (2005) suggested that the multicopy nature of the up-regulated genes and their location within ampliconic and palindromic regions may permit them to self-synapse during pachytene. This would allow them to escape recognition as unsynapsed chromatin, and so the genes would not be subject to MSCI or PSCR, allowing their expression in spermatids. Although there is no evidence to support the idea that palindromic regions undergo intrachromosomal synapsis during MSCI in mice, Namekawa et al. (2006) did notice that genes expressed in spermatids tend to cluster into specific regions on the X chromosome. They suggested that there are domain-specific features that allow escape from post-meiotic silencing. It is possible that the X and Y genes that are up-regulated in the MSYq deletion models are located within these domains. Furthermore, deletions of the MSYq could lead to

localised disruption of the chromatin structure that is restricted to these domains, resulting in increased transcription of genes residing within these regions.

It is presumed that the up-regulation in the three MSYq deletion models is the result of increased transcription of the affected genes. However, it is possible that the effect may be due to post-transcriptional changes in the processing of these transcripts. During the late stages of spermiogenesis, chromatin compaction occurs in the nucleus and this leads to inhibition of gene transcription. As a result of this, mRNA storage and translational regulation are very important in controlling protein production in spermatids and spermatozoa. Many post-meiotic transcripts are subject to translational repression, with transcripts being stored in the spermatid cytoplasm for 4-5 days before being translated (reviewed by Kleene, 2003). In the MSYq deletion models, translation of some X- and Y-linked transcripts may be delayed due to changes in RNA processing, causing these mRNAs to accumulate and appear up-regulated by microarray analysis. Such translational delays would be expected to cause a decrease in the level of the proteins encoded by these genes. This may explain why the sperm head abnormalities in the MSYq deletion models are similar to those observed in mice and humans that have reduced or absent levels of MGCL1, a protein encoded by the autosomal homologue of the up-regulated X-linked *Mgclh* gene (Kimura et al., 2003; Kleiman et al., 2003; Maekawa et al., 2004). Unfortunately this theory does not explain why the effect is limited to a small number of sex-linked transcripts, with the levels of related autosomal transcripts being unchanged. One explanation for this may be that the affected transcripts share a common motif not present in their autosomal homologues. Alternatively, the autosomal genes may not be expressed in spermatids, and this is known to be the case for *Mgcl1*.

In this chapter, the X- and Y-linked gene up-regulation exhibited by the MSYq deletion mice is investigated to see if it is a chromatin-mediated effect. While SLX and SLY are unlikely to be directly involved in a chromatin-mediated effect, these proteins could act post transcriptionally to regulate mRNA levels.

Table 5.1

Name	Ellis et al., 2005 identifier	Up-regulated by microarray	Up-regulated by RT-PCR	chromosome	copy number
Xmr/Slx	NM_009529	yes	yes	X A2	25*
Slxl1	AK015913	yes	yes	X	14*
Ube1y	NM_011667	no	yes	Y A1	1 and 2 pseudogenes
Ube1x	NM_009457	no	yes	X	1
	XM_358268	no	yes	Y	4
H2al1	AK005922	yes	yes	X A1.1	14*
Ckt1/Cypt2	XM_142014	no	yes	X D	?
Ckt1r1/Cypt3	NM_173367	no	yes	X F3	?
	AK005630	yes	yes	X	3*
	AK005817	yes	yes	X C3	2*
	XM_141928	yes	yes	X	?
Mgclh	AB055854	yes	yes	X A1.1	21*
	AK015451	yes	yes	X	1?
Vsig1	AK006251	yes	yes	X F1	1?
	AA183442	yes	yes	X A1.1	?
SatL1	AK015086	yes	yes	X E1	?
Tgifx1	NM_153109	yes	yes	X E1	2
Grhpr	NM_080289	yes	yes	4 B2	?
Gm362	XM_141720	yes	yes	X	?
	AK006152	yes	yes?	Y	?

Table 5.1 Genes reported by Ellis et al. (2005) to show a minimum 1.5-fold increase in testis mRNA levels in 9/10MSYq- or MSYq- mice

Fifteen genes were identified by microarray analysis and confirmed as up-regulated by real-time RT-PCR. Five additional genes were identified by real-time RT-PCR analysis alone. Genes highlighted in the same colour (e.g. *Slx*, *Slxl1*) belong to the same gene family. The chromosomal location of each gene is given, as is the gene copy number when known.

* gene copy number estimated by Mueller et al., 2008
? unknown gene copy number, presumed to have only one copy.

5.2 Results

5.2.1 Up-regulation of X- and Yp-linked genes in the MSYq deletion models is due to an increase in nascent transcription

In the MSYq deletion models, Ellis et al. (2005) used microarray studies, northern blot and real-time RT-PCR analysis to detect an increase in the transcript levels of a small proportion of X- and Yp-linked genes. All three techniques assay the level of mature RNAs, and so it is unknown if the up-regulation of transcripts observed in the three MSYq deletion models is a consequence of an increase in gene transcription or if this is a post-transcriptional effect. In order to address whether there is increased transcription, I used gene-specific RNA FISH. This also allows the monitoring of nascent transcription specifically in spermatids, the cell type of interest.

Gene-specific RNA FISH was performed on spermatogenic cells from XY, 2/3MSYq- and MSYq- mice. For each gene, RNA FISH was replicated three times using three different mice for each genotype, and the presence of an RNA FISH signal was examined in approximately 100 round spermatids per mouse. Although RNA FISH signals are not normally used to quantitate the levels of gene expression in individual cells, this approach can be employed to identify if there is an increase in the frequency of round spermatids expressing a specific gene. Four X-linked genes (*Slx*, *Slxl1*, *Vsig1*, and *Satl1*) were chosen for investigation, along with the Yp-linked *Ube1y* gene and the autosomal *Grhpr* gene; all six genes were identified as up-regulated in the initial microarray and confirmed to be significantly up-regulated in either the 9/10MSYq- or MSYq- models by RT-PCR analysis (Ellis et al., 2005). Consistent with previous data (Ellis et al., 2005), *Slx*, *Slx1l*, *Vsig1* and *Ube1y* RNA FISH signals were observed in a higher proportion of round spermatids from MSYq- mice compared to the XY control mice (Tables 5.2, 5.3, Graphs 5.1 A-D); in each this was found to be statistically significant at $P<0.05$ using the ANOVA test. The most dramatic difference was seen for *Vsig1*, with the number of RNA FISH positive spermatids increasing more than two-fold, from an average of 16.5% in XY mice to 38.2% in MSYq- mice. Trends of increased RNA FISH signal intensity and the number of signals per cell were also observed in the MSYq- spermatids compared to both XY controls and 2/3MSYq- spermatids. This was most noticeable for *Slx* and *Slxl1* (Figure 5.1.A and 5.1.B). For

the autosomal *Grhpr* gene, no significant difference was observed between the genotypes in the percentage of spermatids with an RNA FISH signal (Tables 5.2, 5.3, Graphs 5.1.E). *Satl1* signals were not observed by RNA FISH, possibly due to rapid processing of nascent transcripts.

In addition to the up-regulated genes assayed above, RNA FISH was performed for eight control spermatid-expressed genes that showed no difference in testis transcript levels between normal and MSYq deletion mice by microarray analysis (Ellis et al., 2005). These were the X-linked *Ott*, *Fmr1* and *Ddx3x* genes, the Y-linked *Uty* gene and four autosomal genes, *Brca1*, *Atr*, *Adam3* and *Prkdc*. The non-spermatid expressed X-linked *Xiap* gene was included as another control; this gene is active in spermatogonia before being silenced by MSCI in pachytene spermatocytes and remains silent in spermatids (Mueller et al., 2008; Namekawa et al., 2006). Unexpectedly, the sex-linked *Ott*, *Fmr1*, *Ddx3x* and *Uty* genes were all expressed in a significantly higher percentage of spermatids from the MSYq- males than the XY controls ($P<0.05$; Tables 5.2, and 5.3, Graphs 5.1.F-I). There was no significant difference between genotypes with respect to the percentage of spermatids with RNA FISH signals for the autosomally located *Brca1*, *Atr*, *Adam3* and *Prkdc* genes (Table 5.2, Graphs 5.1.I-K). As in XY controls, *Xiap* was silent in spermatids from the MSYq- mice (Tables 5.2, and 5.3).

In conclusion, all six X-linked and both Y-linked spermatid expressed genes assayed by the presence of an RNA FISH signal were found to be transcribed in a significantly higher percentage of round spermatids from MSYq- mice compared to the XY control mice. No statistically significant difference was seen between the genotypes for any of the five autosomal genes assayed, including *Grhpr*; this gene was previously reported to be significantly up-regulated in MSYq- mice by microarray and qRT-PCR studies (Ellis et al., 2005). Taken together, these data indicate that the up-regulation of X- and Y-linked genes detected in the MSYq deletion mice is due, at least in part, to an increase in spermatid transcription of these genes. This may be a consequence of a global disruption in the maintenance of sex chromosome gene silencing post-meiosis.

Table 5.2

Gene	chromosome	% of expressing round spermatids			significant at 95% CI?	fold change
		XY	2/3MSYq-	MSYq-		
Slx	X	40.3	43.0	50.3	yes, P=0.005733	1.3
Slxl1	X	34.6	40.0	48.0	yes, P=0.020062	1.4
Vsig1	X	16.5	26.3	38.2	yes, P=0.011006	2.3
Ott	X	19.7	23.2	28.8	yes, P=0.044671	1.5
Fmr1	X	9.3	11.4	22.5	yes, P=0.000252	2.4
Ddx3x	X	18.5	23.0	34.7	yes, P=0.010805	1.9
Ube1y	Y	35.0	37.8	48.8	yes, P=0.002228	1.4
Uty	Y	15.1	16.8	27.0	yes, P=0.033384	1.8
Grhpr	4	57.3	59.0	56.2	no, P=0.891192	1.0
Adam3	8	5.7	3.6	4.6	no, P=0.952326	0.8
Atr	9	9.5	9.3	16.0	no, P=0.099294	1.7
Brca1	11	70.2	70.4	74.5	no, P=0.264541	1.0
Prkdc	16	28.0	29.1	26.5	no, P=0.802551	0.9
Xiap	X	0.0	0.0	0.0	N/A	

Table 5.2 A list of genes analysed by gene-specific RNA FISH in round spermatids from XY, 2/3MSYq- and MSYq- males

For each genotype, three different males were analysed for the presence of an RNA FISH signal, with approximately 100 round spermatids counted per male. Spermatids with an RNA FISH signal were considered to be expressing the gene. For each gene, the mean percentage of spermatids with an RNA FISH signal is given for the three genotypes.

A one way analysis of variance (ANOVA) test (after angular transformation of percentages) was used to determine if the results were statistically significant. The probability that there is no difference between the XY and MSYq- genotypes in the number of spermatids expressing a particular gene is indicated. The fold change in the number of spermatids with an RNA FISH signal is given, and is calculated as the MSYq-/XY ratio. For sex-linked genes, the proportion of round spermatids expressing a particular gene increases with the MSYq deletion size, although this is not statistically significant between the XY and 2/3MSYq- genotypes.

It should be noted that for sex-linked genes, only half of the spermatids carry the gene and so the maximum number of spermatids that can express each gene is 50%. For autosomal genes, all spermatids have a copy of the gene and so these genes can be expressed in up to 100% of spermatids. The chromosomal location of the genes is indicated.

Table 5.3 Number of spermatids with RNA FISH signals

The table shows the raw RNA FISH values. For each gene, RNA FISH was performed on surface-spread spermatogenic cells from XY, 2/3MSYq- and MSYq- testis material, and replicated three times. Values are given as the number of spermatids with an RNA FISH signal over the total number of spermatids counted. Within each replicate, the RNA FISH was performed under the same conditions using a probe labelled at the same time and so the values are comparable.

Table 5.3

Gene	replicate	XY	2/3MSYq-	MSYq-
Slx	replicate 1	39/101	40/103	50/100
	replicate 2	66/156	48/106	57/112
	replicate 3	40/100	45/100	50/100
Slxl1	replicate 1	37/101	45/106	69/135
	replicate 2	35/116	42/112	48/115
	replicate 3	37/100	40/100	51/100
Vsig1	replicate 1	13/102	17/101	35/104
	replicate 2	19/101	32/102	42/100
	replicate 3	18/101	31/101	39/100
Ott	replicate 1	21/101	23/100	30/106
	replicate 2	19/102	22/102	24/103
	replicate 3	20/101	25/100	35/101
Fmr1	replicate 1	8/101	13/105	21/101
	replicate 2	11/101	11/100	21/101
	replicate 3	9/100	11/101	53/206
Ddx3x	replicate 1	16/102	17/100	32/105
	replicate 2	20/100	27/103	38/100
	replicate 3	20/101	26/101	36/101
Ube1y	replicate 1	33/105	39/100	47/101
	replicate 2	37/101	35/102	51/102
	replicate 3	37/100	40/100	50/100
Uty	replicate 1	9/101	13/101	27/107
	replicate 2	17/100	18/101	29/101
	replicate 3	20/103	23/100	27/100
Grhpr	replicate 1	61/101	N/A	52/100
	replicate 2	58/101	66/100	65/102
	replicate 3	54/100	52/100	54/102
Adam3	replicate 1	10/100	5/102	9/102
	replicate 2	0/101	0/100	0/100
	replicate 3	7/103	6/100	5/101
Atr	replicate 1	8/100	6/100	12/100
	replicate 2	12/103	13/100	21/100
	replicate 3	9/101	9/101	15/100
Brca1	replicate 1	72/103	71/100	73/100
	replicate 2	71/102	72/101	82/102
	replicate 3	71/100	71/103	70/100

Gene	replicate	XY	2/3MSYq-	MSYq-
Prkdc	replicate 1	31/100	33/100	31/100
	replicate 2	27/100	27/103	N/A
	replicate 3	26/100	28/100	27/100
Xiap	replicate 1	0/101	0/100	0/100
	replicate 2	0/100	0/103	0/103
	replicate 3	0/102	0/103	0/102

Chart 5.1 Graphical representations of the RNA FISH data

For each gene, the mean percentages of spermatids positive for an RNA FISH signal were plotted per genotype. It should be noted that the maximum number of spermatids that can express a sex-linked gene is approximately 50% due to the haploid nature of these cells. The graphs are for the following genes.

A) *Slx*
B) *Slxl1*
C) *Vsig1*
D) *Ube1y*
E) *Grhpr*
F) *Ott*
G) *Fmr1*
H) *Ddx3x*
I) *Uty*
J) *Brca1*
K) *Atr*
L) *Adam3*
M) *Prkdc*

The percentages of expressing spermatids were transformed into angles and the transformed data were analysed by a one way analysis of variance (ANOVA) test using the NCSS statistical package.

* The number of spermatids with an RNA FISH signal is significantly ($P<0.05$) increased in spermatids from MSYq- mice compared to XY mice

** The number of spermatids with an RNA FISH signal is significantly increased in spermatids from MSYq- mice compared to XY and 2/3MSYq- mice.

Chart 5.1

A)

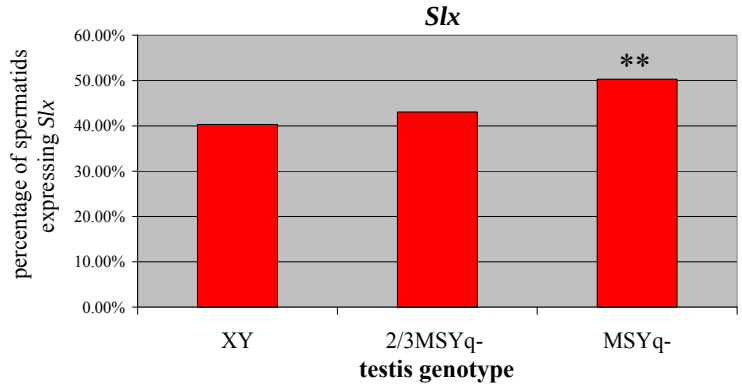

B)

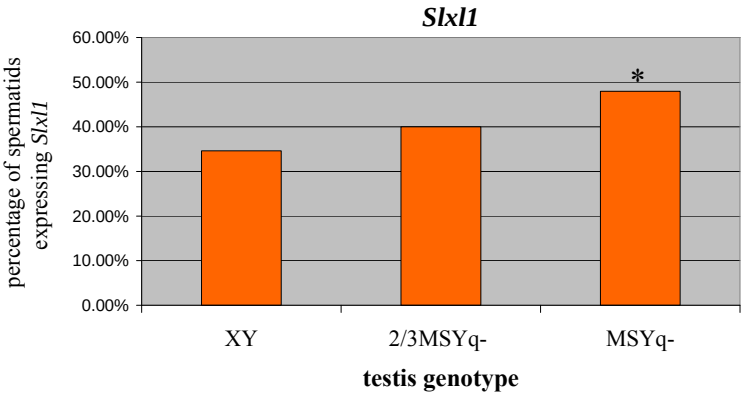

C)

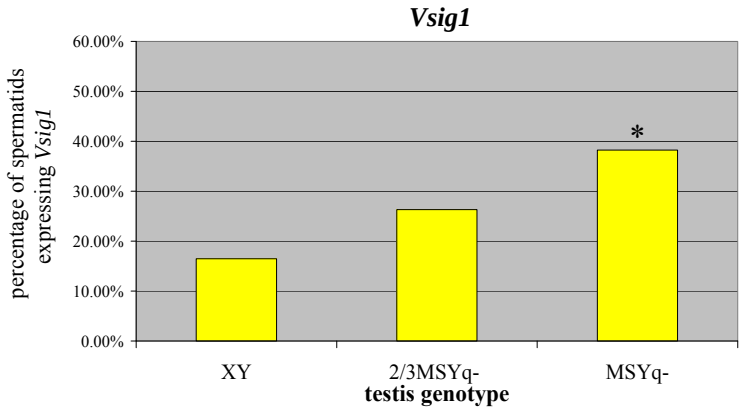

D)

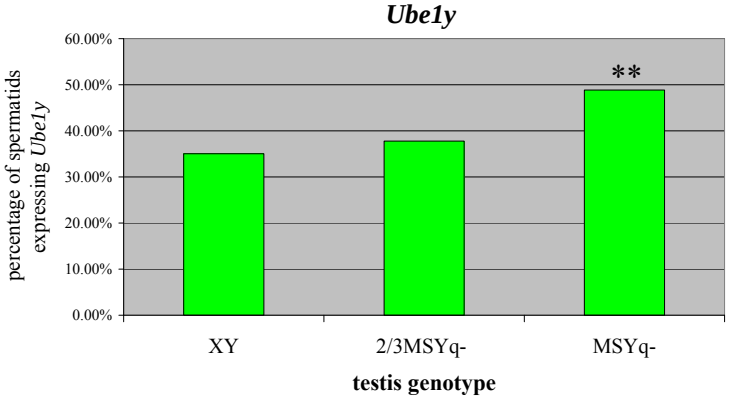

E)

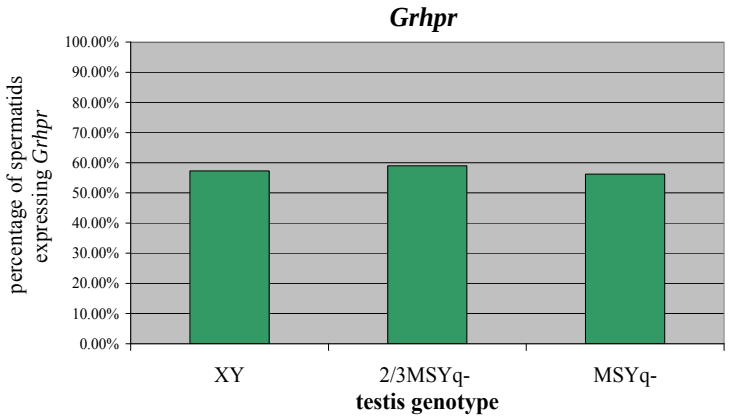
Grhpr
100.00%
90.00%
80.00%
70.00%
60.00%
50.00%
40.00%
30.00%
20.00%
10.00%
0.00%
percentage of spermatids expressing Grhpr
XY
2/3MSYq-
MSYq-
testis genotype

F)

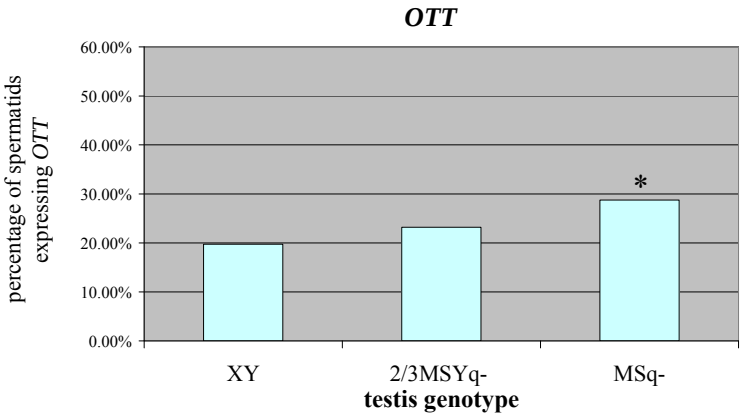
OTT
60.00%
50.00%
40.00%
30.00%
20.00%
10.00%
0.00%
*
percentage of spermatids expressing OTT
XY
2/3MSYq-
MSq-
testis genotype

G)

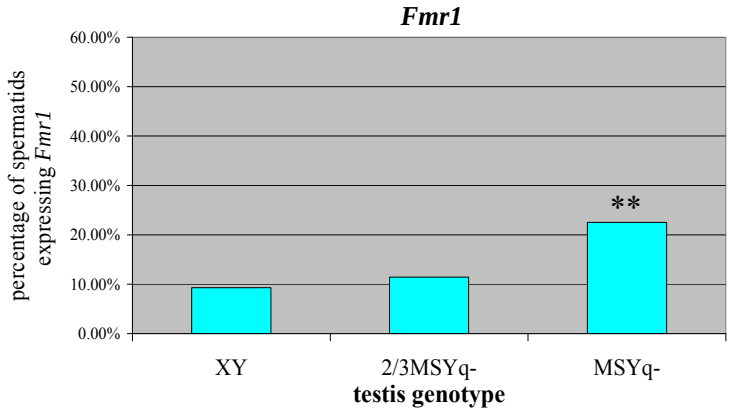
Fmr1
60.00%
50.00%
40.00%
30.00%
20.00%
10.00%
0.00%
**
percentage of spermatids expressing Fmr1
XY
2/3MSYq-
MSYq-
testis genotype

H)

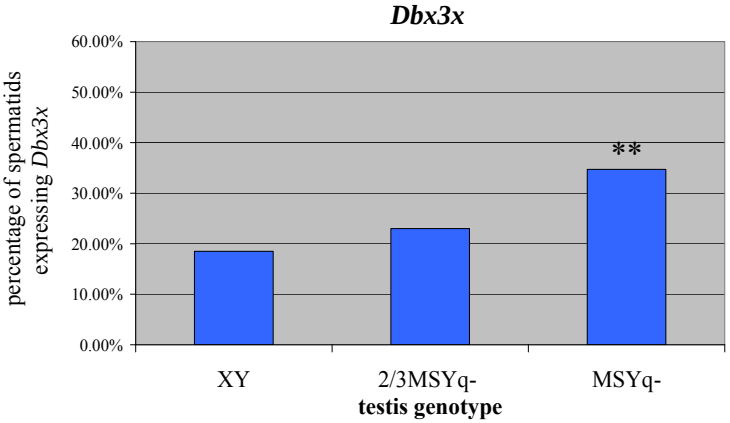
Dbx3x
60.00%
50.00%
40.00%
30.00%
20.00%
10.00%
0.00%
**
percentage of spermatids expressing Dbx3x
XY
2/3MSYq-
MSYq-
testis genotype

I)

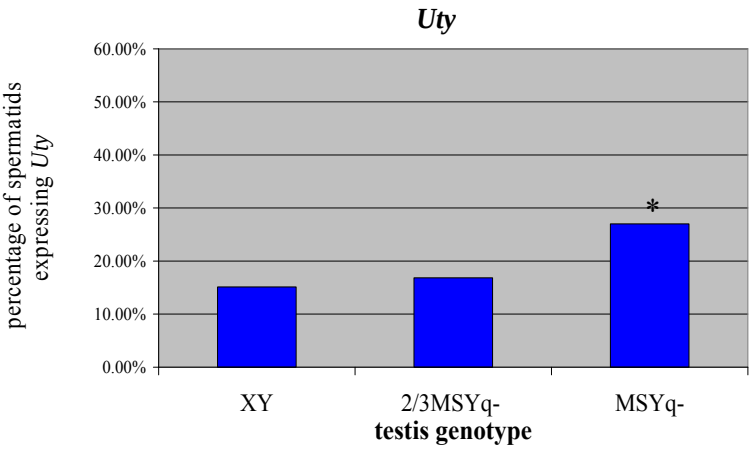
Uty
percentage of spermatids expressing Uty
60.00%
50.00%
40.00%
30.00%
20.00%
10.00%
0.00%
*
XY
2/3MSYq-
MSYq-
testis genotype

J)

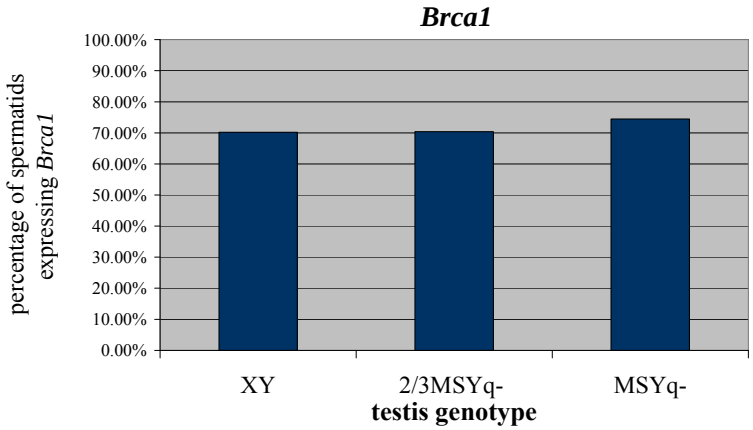
Brca1
percentage of spermatids expressing Brca1
100.00%
90.00%
80.00%
70.00%
60.00%
50.00%
40.00%
30.00%
20.00%
10.00%
0.00%
XY
2/3MSYq-
MSYq-
testis genotype

K)

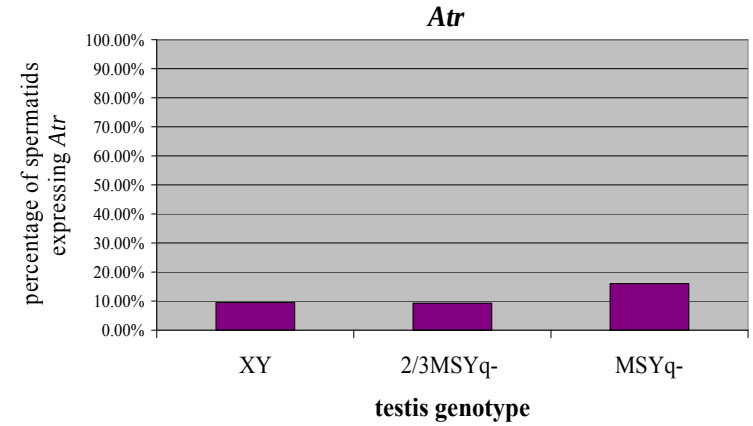
Atr
percentage of spermatids expressing Atr
100.00%
90.00%
80.00%
70.00%
60.00%
50.00%
40.00%
30.00%
20.00%
10.00%
0.00%
XY
2/3MSYq-
MSYq-
testis genotype

L)

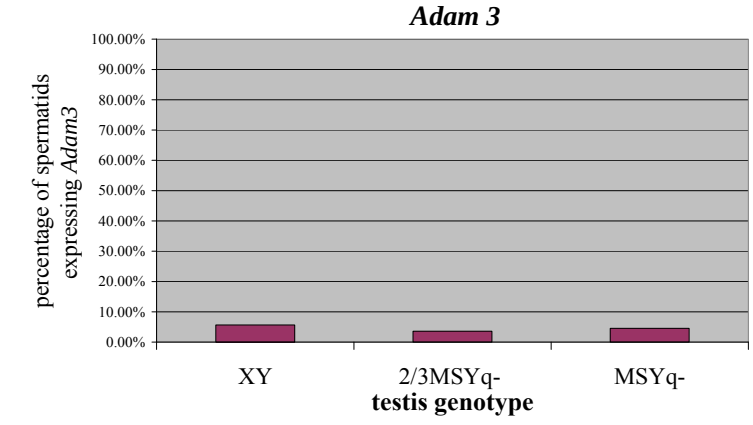
Adam 3
percentage of spermatids expressing Adam3
100.00%
90.00%
80.00%
70.00%
60.00%
50.00%
40.00%
30.00%
20.00%
10.00%
0.00%
XY
2/3MSYq-
MSYq-
testis genotype

M)

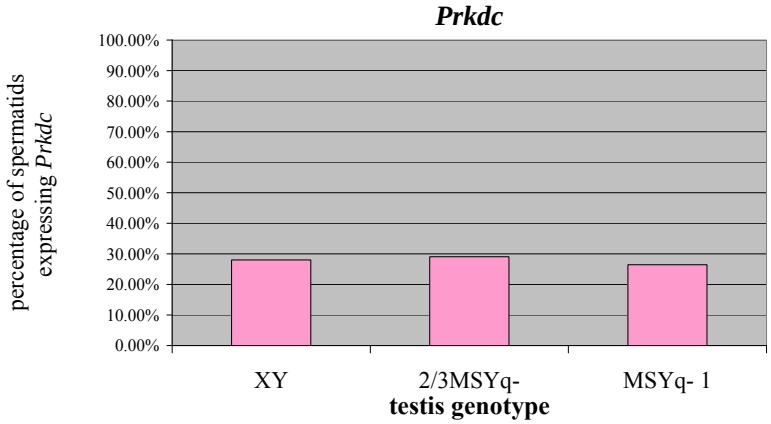
Prkdc
100.00%
90.00%
80.00%
70.00%
60.00%
50.00%
40.00%
30.00%
20.00%
10.00%
0.00%
percentage of spermatids expressing Prkdc
XY
2/3MSYq-
MSYq- 1
testis genotype

Figure 5.1 Gene-specific RNA FISH for *Slx* and *Slxl1*

RNA FISH on round spermatids from XY (top panel), 2/3MSYq- (middle panel) and MSYq- (bottom panel) mice for:

(A) *Slx*
(B) *Slxl1*

The number of RNA signals per spermatid appears to be increased in the two MSYq- models compared to the XY control.

Left panel; round spermatid nucleus stained with DAPI (blue).
Middle panel; RNA FISH signal (red).
Right panel; merge

Figure 5.1

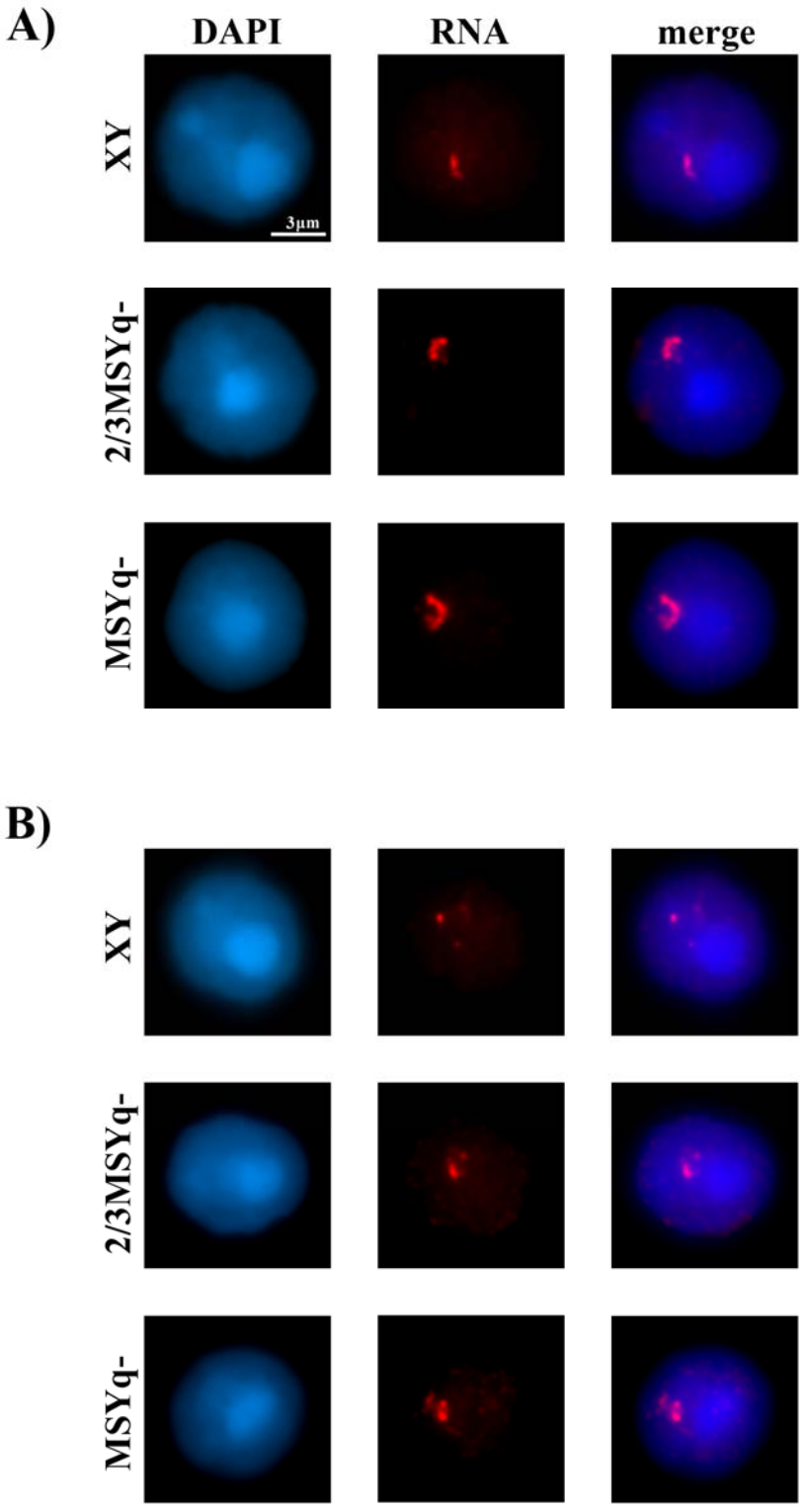

5.2.2 The epigenetic profile of the spermatid sex chromosomes is altered in the MSYq- mice

In spermatids, the sex chromosomes form a facultative heterochromatic structure next to the chromocentre (the centromeric heterochromatin domain) and are enriched for a number of histone post-translational modifications and histone variants associated with both active and inactive chromatin (Baarends et al., 2007; Greaves et al., 2006; Khalil et al., 2004; Namekawa et al., 2006; Turner et al., 2006). These epigenetic marks are thought to play an important role in maintaining the transcriptional repression of X and Y chromosomes during spermiogenesis (Greaves et al; 2006; Namekawa et al., 2006; Turner et al., 2006). It is conceivable that the disruption in PSCR observed in the MSYq deletion models may be accompanied by changes in the conformation and epigenetic profile of the sex chromosomes. To explore this possibility, histone H3 methylation, histone H4 acetylation and the localisation of the heterochromatin-associated protein CBX1 was examined in spermatids from XY and MSYq- mice. The results are shown in Figures 5.2 to 5.6 and summarised in Table 5.4.

To determine if the sex chromosomes in spermatids from MSYq- mice still form a heterochromatic structure, spermatids from XY and MSYq- mice were stained with DAPI. In XY mice, 71.6% (514/718) of round spermatids had a cytologically visible DAPI-dense structure located next to the chromocentre and chromosome painting confirmed that this structure corresponded to either the X or the Y chromosome. In spermatids from MSYq- mice, the sex chromosome chromatin domain was still discernable in 37.3% (265/710) of round spermatids. Chromosome painting revealed that the DAPI-dense sex chromosome domain is only present in X-bearing round spermatids from MSYq- mice, indicating that the $Y^{*x}Sxr^{a}$ and Y^{*x} chromosomes are not detected using DAPI. Taken together these results imply, at least with respect to the X chromosome, that the increased transcription in these spermatids is not associated with de-heterochromatinisation.

$H3_{K9me2}$

Dimethylation of histone H3 at lysine 9 ($H3_{K9me2}$) is a marker of transcriptionally silent chromatin. On surface-spread testicular cells, three patterns of $H3_{K9me2}$ localisation were identified in round spermatids from normal males; sex chromosome and chromocentre staining (Figure 5.2.Ai, upper panel), sex chromosome staining only

(Figure 5.2.Aii, upper panel) and diffuse nuclear staining (Figure 5.2.Aiii, upper panel). These three staining patterns were also observed in round spermatids from MSYq- mutant mice (lower panels in Figure 5.2.Ai, 5.2.Aii and 5.2.Aiii). A fourth staining pattern was observed in some MSYq- spermatids that lacked a visible sex chromosome under DAPI, with $H3_{K9me2}$ restricted to the chromocentre; these are presumptively $Y^{*x}Sxr^{a}$-bearing spermatids. In XY males, $H3_{K9me2}$ was enriched on the cytologically visible X or Y chromosome in 66.6% (211/317) of round spermatids (Figure 5.2.B). $H3_{K9me2}$ localisation to the sex chromosome domain was observed in 27.9% (88/316) of round spermatids from MSYq- mice, and these were confirmed as being X-bearing spermatids. Visually, the level of $H3_{K9me2}$ enrichment on the sex chromosomes in spermatids from XY males was comparable to that on the X chromosome of MSYq- spermatids. There was, however, a statistically significant reduction in the number of round spermatids with $H3_{K9me2}$ chromocentre staining, from 57.1% (181/317) in XY spermatids to 39.6% (125/316) in MSYq- spermatids ($P<0.005$, Chi^2 test).

$H3_{K9me3}$

Trimethylation of $H3_{K9}$ is associated with constitutive heterochromatin and is enriched on the pericentric regions of mouse chromosomes. In round spermatids, $H3_{K9me3}$ has one of two patterns; it either stains the chromocentre only (Figure 5.3.Ai) or is enriched on the sex chromosome and chromocentre (Figure 5.3.Aii). On surface-spread testis cells, localisation of $H3_{K9me3}$ to the X or Y chromosome was seen in 77.3% (157/203) of round spermatids from XY mice (Figure 5.3.B, top panel), and 41.6% (84/202) of round spermatids from MSYq- mice. In MSYq- mice, sex chromosome enrichment of $H3_{K9me3}$ was only observed in X-bearing round spermatids (Figure 5.3.B, bottom panel). Although the chromocentre was brightly stained for $H3_{K9me3}$ in XY and MSYq- spermatids (Figure 5.3.Ai), the intensity of $H3_{K9me3}$ sex chromosome staining was much fainter in MSYq- spermatids than in spermatids from normal males (Figure 5.3.Aii).

The localisation of $H3_{K9me3}$ during spermiogenesis was further studied by immunofluorescence staining of XY and MSYq- testis sections. In stage XII seminiferous tubules from XY males, $H3_{K9me3}$ was observed in the whole nucleus of late zygotene spermatocytes and on the sex chromosomes of dividing MI and MII cells (Figure 5.4.A, upper panel; sex chromosome is indicated by an arrow). In MSYq- cells

undergoing the meiotic divisions, $H3_{K9me3}$ was also enriched on the sex chromosome; in addition, it was enriched on the centromeric heterochromatin (Figure 5.4.A, lower panel, starred). The localisation of $H3_{K9me3}$ remained unchanged in zygotene spermatocytes and elongating spermatids from stage XII tubules.

In stage I tubules from XY mice, faint chromocentre $H3_{K9me3}$ staining was observed in round spermatids, with robust staining of the DAPI-dense sex chromosome (Figure 5.4.B, upper panel). However, in MSYq- round spermatids from stage I tubules, $H3_{K9me3}$ staining of the cytologically distinct sex chromosome is much weaker than that detected in XY spermatids, with staining of the chromocentre (clustered centromeric heterochromatin) being prominent (Figure 5.4.B, lower panel). The weaker sex chromosome staining is similar to the decrease in $H3_{K9me3}$ sex chromosome staining seen in round spermatids prepared by surface spreads. The chromocentre of spermatids from MSYq- tubules at other stages was also more strongly stained with $H3_{K9me3}$ than the chromocentres of XY spermatids; this can be clearly seen by comparing the chromocentre staining to that of the pachytene sex body in stage II-V tubules (Figure 5.4.C).

Together, these data point to a decrease in $H3_{K9me3}$ enrichment on the sex chromosome domain in round spermatids from MSYq- mice compared to XY mice, together with increased enrichment of $H3_{K9me3}$ on the centromeric heterochromatin in M1 cells from MSYq- mice.

CBX1

The heterochromatin-associated protein CBX1 (also called M31 and HP1β) is recruited by methylation of $H3_{K9}$ (Lachner et al., 2001), and has been considered a marker of inactive chromatin. CBX1 is present on the centromeric heterochromatin and sex chromosomes in secondary spermatocytes and spermatids until histones are replaced by transition proteins at spermatid stage 11 (Greaves et al., 2006; Namekawa et al., 2006). On surface spread spermatogenic cells, CBX1 was present on the chromocentre of all round spermatids analysed from XY (n=374) and MSYq- mice (n=377). In XY mice, CBX1 was enriched on the DAPI-dense X or Y chromosome in 82.1% (307/374) of round spermatids (Figure 5.5.B). In round spermatids from MSYq- mice, CBX1 localised to the sex chromosome domain in 49.1% (185/377) of spermatids examined (Figure 5.5.B, lower panel); chromosome painting confirmed that these were the X-

bearing spermatids (100%, 35/35). CBX1 staining was much fainter on the cytologically distinct sex chromosome in MSYq- spermatids than in XY spermatids, although there was no change in the intensity of chromocentre staining (compare upper and lower panels in Figure 5.5.B).

$H4_{K8Ac}$

Acetylation of histone H4 on lysine 8 ($H4_{K8Ac}$) is found in active regions of the genome in somatic cells and is observed on the sex chromosome of round spermatids, where it has been hypothesised to play a role in transcriptional activation of the X (Khalil et al., 2004). In stage I tubules from XY males, $H4_{K8Ac}$ is found in the nuclei of round spermatids, were it is enriched on the cytologically visible sex chromosome chromatin domain (arrowed) but excluded from the chromocentre (Figure 5.6.A, upper panel, arrowed). Staining is also seen in the condensing nuclei of stage 13 elongating spermatids in the same tubule (Figure 5.6.A, upper panel, starred). In contrast, there is little or no enrichment of $H4_{K8Ac}$ on the cytologically visible sex chromosome of stage 1 round spermatids from MSYq- mice (Figure 5.6.A, lower panel, arrowed). In the MSYq- testis, $H4_{K8Ac}$ is still present in stage 13 elongating spermatids, but appears to be polarised towards one end of the nucleus (Figure 5.6.A, lower panel, starred); this may be due to the abnormal head morphology exhibited by these spermatids. The loss of $H4_{K8Ac}$ enrichment on the sex chromosome in MSYq- round spermatids is seen more clearly in tubule stages II-IV (Figure 5.6.B, 5.6.C), although no difference in the intensity of the pachytene sex body staining is observed.

Figure 5.2 Dimethylation of Histone $H3_{K9}$ in round spermatids from XY and MSYq- male mice

Surface spread spermatogenic cells from XY (top row) and MSYq- males (bottom row) were stained with DAPI (blue) and immunostained with $H3_{K9me2}$ (red).

A) Three patterns of $H3_{K9me2}$ localisation were seen in round spermatid nuclei;

i) Enrichment of $H3_{K9me2}$ on the sex chromosome (arrowed) and chromocentre
ii) $H3_{K9me2}$ localisation to the sex chromosome only
iii) Faint, diffuse nuclear $H3_{K9me2}$

B) Chromosome painting on round spermatids with $H3_{K9me2}$ enriched on the sex chromosome. In spermatids from XY males (upper row), $H3_{K9me2}$ is present on the sex chromosome in both X- and Y-bearing round spermatids (n=30) but is only enriched on the X chromosome (bottom row, n=20) in round spermatids from MSYq- males.

Left panel; DAPI
Middle panel; $H3_{K9me2}$ and DAPI
Right panel; Y chromosome (green, top row) or X chromosome (green, bottom row) paint and DAPI

$H3_{K9me2}$ enrichment on the spermatid sex chromosome is unaffected in MSYq- mice but there is a significant reduction in the number of spermatids with $H3_{K9me2}$ localisation to the chromocentre in these mice compared to the XY control.

Figure 5.2

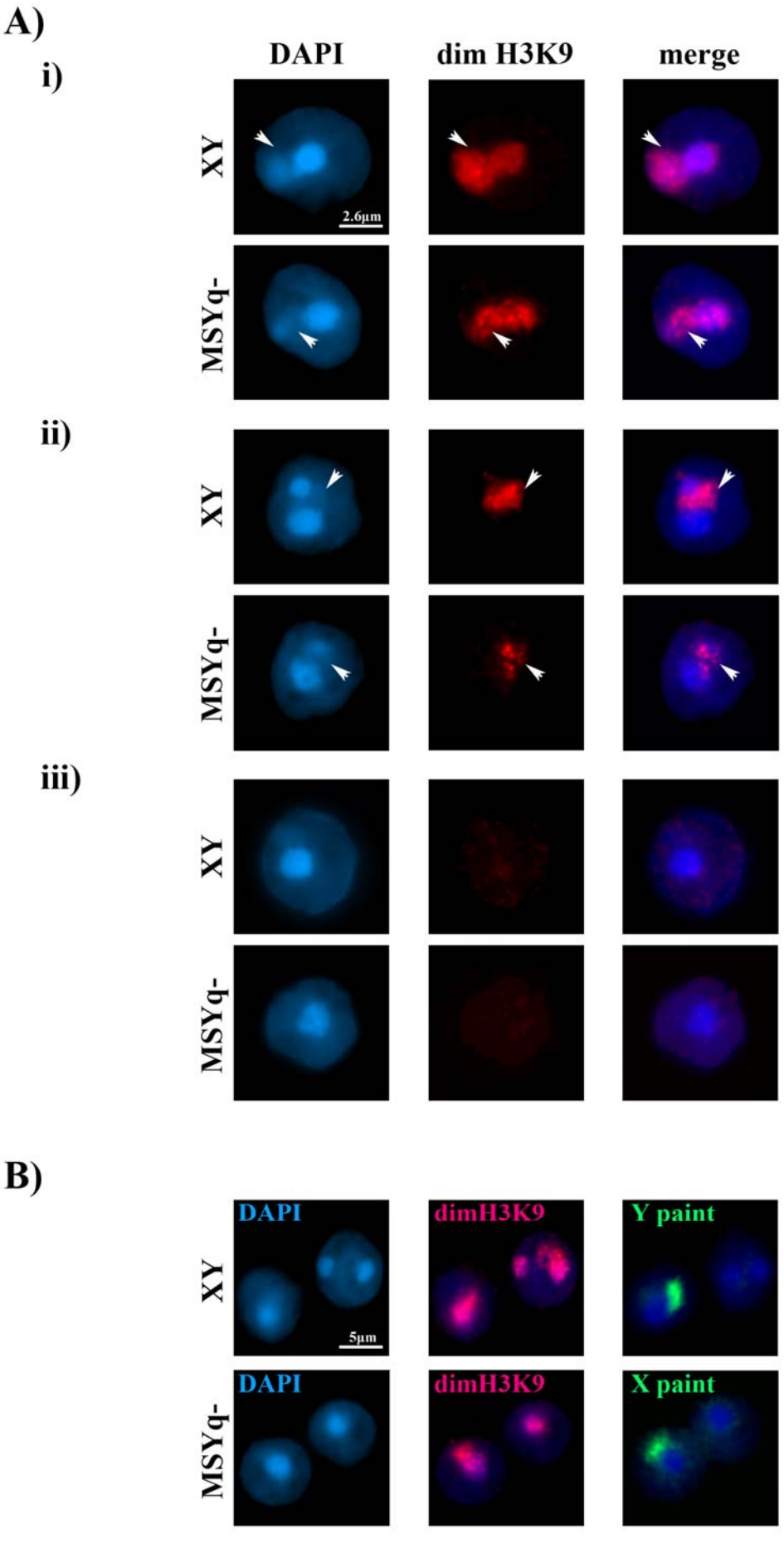
A)
i)
ii)
iii)
DAPI
dim H3K9
merge
XY
MSYq-
2.6µm
B)
DAPI
dimH3K9
Y paint
X paint
5µm

Figure 5.3 Immunostaining of round spermatid nuclei for trimethylated $H3_{K9}$

A) The nuclei are stained with DAPI (blue) and an anti-$H3_{K9me3}$ antibody (red). The percentage of round spermatids with each staining pattern is given in the right hand panel.

   i) Enrichment of $H3_{K9me3}$ on the chromocentre in round spermatids from XY (top row) and MSYq- (bottom row) males.
   ii) Localisation of $H3_{K9me3}$ to the sex chromosome (arrowed) and chromocentre in XY (top row) and MSYq- (bottom row) round spermatids. There is a decrease in $H3_{K9me3}$ enrichment on the sex chromosome of MSYq- spermatids compared to the XY control.

B) Chromosome painting on round spermatids with sex chromosome $H3_{K9me3}$ enrichment. In spermatids from XY males (upper row), $H3_{K9me3}$ is present on the sex chromosome in both X- and Y-bearing round spermatids (n=44) but is only enriched on the X chromosome (bottom row, n=39) in round spermatids from MSYq- males.

   Left panel; DAPI (blue)
   Middle panel; $H3_{K9me3}$ (red) and DAPI (blue)
   Right panel; Y chromosome (green, top row) or X chromosome (green, bottom row) paint and DAPI (blue)

Figure 5.3

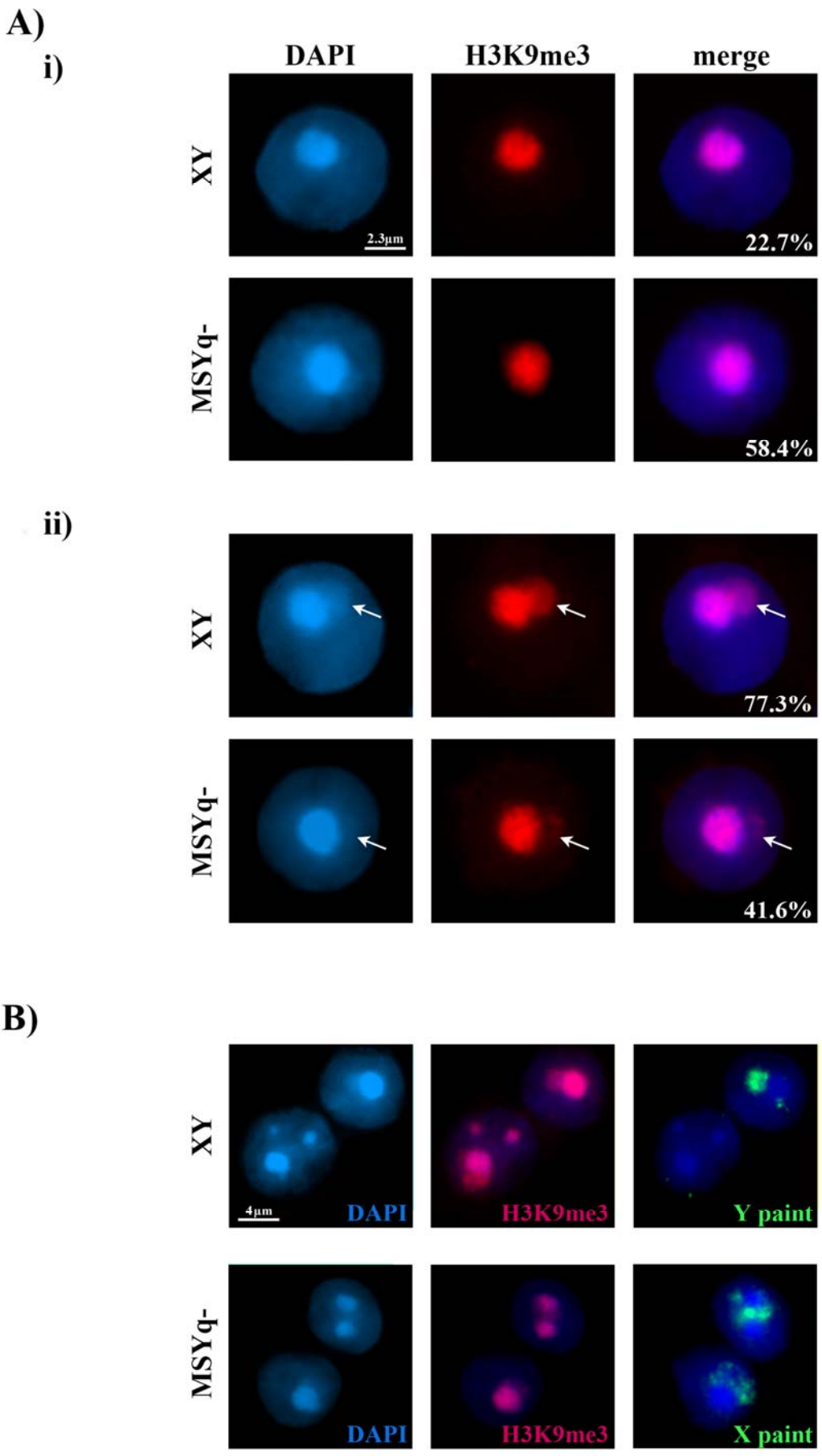
A)
i)
DAPI
H3K9me3
merge
XY
2.3µm
22.7%
MSYq-
58.4%
ii)
XY
77.3%
MSYq-
41.6%
B)
XY
4µm
DAPI
H3K9me3
Y paint
MSYq-
DAPI
H3K9me3
X paint

Figure 5.4 Localisation of $H3_{K9me3}$ in the seminiferous tubules of XY and MSYq- testes

The testis sections are co-stained with $H3_{K9me3}$ (red) and γH2AX (green), and the cell nuclei are stained with DAPI (blue). Tubules were staged according to Russell et al., 1990 (see Figure 1.5), using γH2AX to identify the different stages of meiotic cells.

A) Stage XII tubules from XY (top row) and MSYq- (bottom row) testis sections. $H3_{K9me3}$ localises to the whole nucleus of zygotene spermatocytes and is enriched on the forming sex body (stained with γH2AX). The sex chromosome (arrowed and inset) is enriched in $H3_{K9me3}$ in cells undergoing the meiotic divisions in XY and MSYq- males, but $H3_{K9me3}$ also localises to the centromeric heterochromatin in MSYq- tubules (starred, inset).

B) Stage I seminiferous tubules from XY (top row) and MSYq- (bottom row) males. $H3_{K9me3}$ is enriched on the sex chromosome in XY spermatids (top row inset) and is faint on the chromocentre. However, in MSYq- spermatids, $H3_{K9me3}$ is reduced on the sex chromosome but appears increased on the chromocentre (bottom row inset). There is no difference in $H3_{K9me3}$ localisation in pachytene spermatocytes between the genotypes, and $H3_{K9me3}$ is not present in stage 13 spermatids.

C) Stage II-V tubules from XY (top row) and MSYq- (bottom row) testis sections. $H3_{K9me3}$ continues to be enriched on the sex chromosome in XY spermatids at these stages and only the edge of chromocentre is stained, appearing as a 'halo' (see inset). However, in MSYq- spermatids, $H3_{K9me3}$ localises to the whole chromocentre but is dramatically reduced on the sex chromosome (see inset).

NB. Tubule stages II to V are not distinguishable from each other using DAPI and γH2AX staining, and so are grouped together. No difference in $H3_{K9me3}$ localisation is seen between these stages.

Figure 5.4

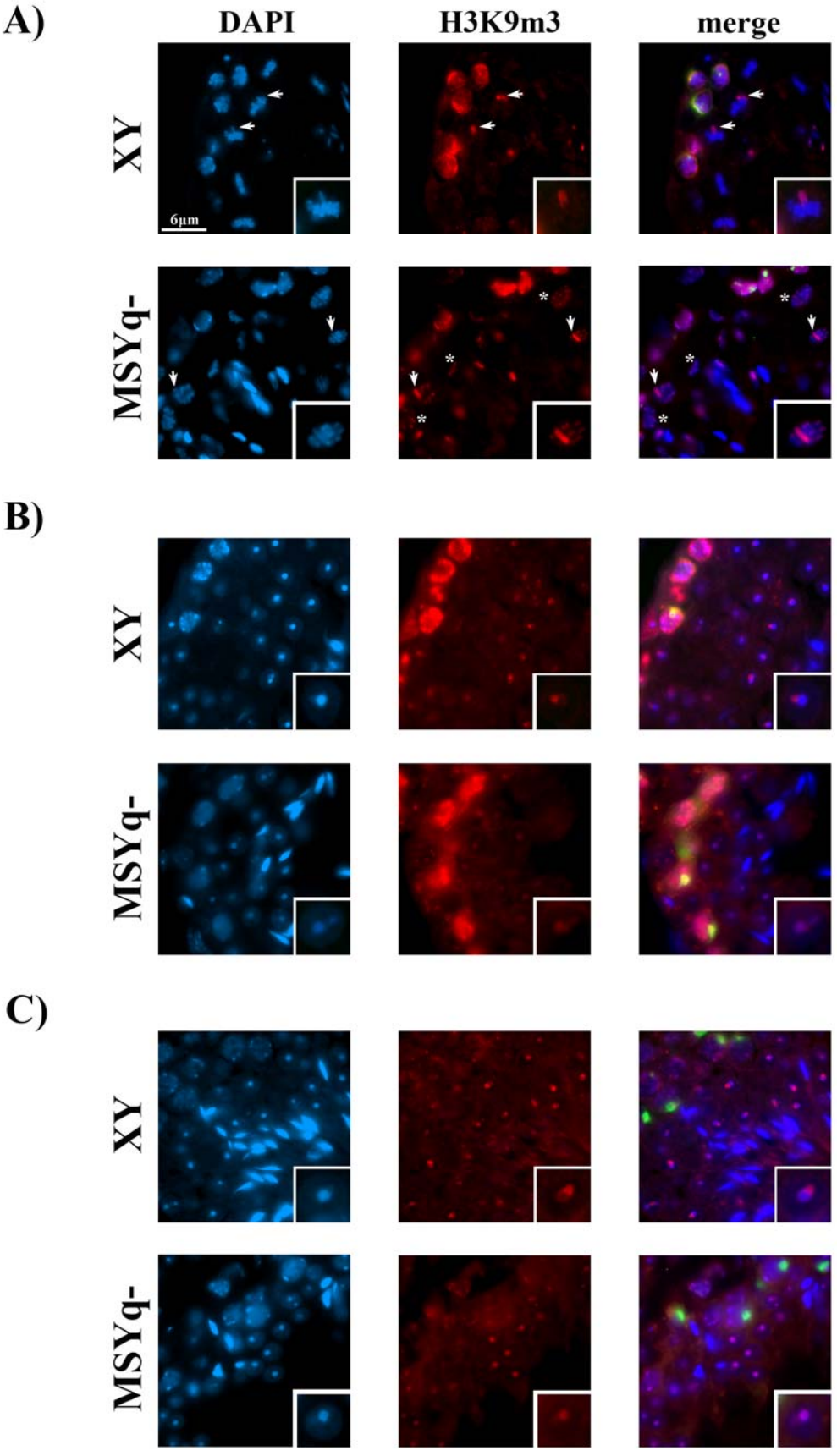

Figure 5.5 Localisation of the heterochromatin-associated protein CBX1 in round spermatids

Spermatid nuclei are stained with DAPI (blue, left panel) and CBX1 (green, middle panel). The percentage of round spermatids exhibiting each staining pattern is given in the right hand panel, where the DAPI and CBX1 signals are merged.

A) Localisation of CBX1 to the chromocentre in spermatids from XY (top row) and MSYq- (bottom row) males. No difference in chromocentre staining is seen between the two genotypes.

B) Enrichment of CBX1 on the sex chromosome and chromocentre of XY (top row) and MSYq- (bottom row) spermatids. The sex chromosome is visible as a DAPI dense structure (arrowed) next to the chromocentre. The level of CBX1 is decreased on the sex chromosome of round spermatids from MSYq- males compared to the XY control.

Figure 5.5

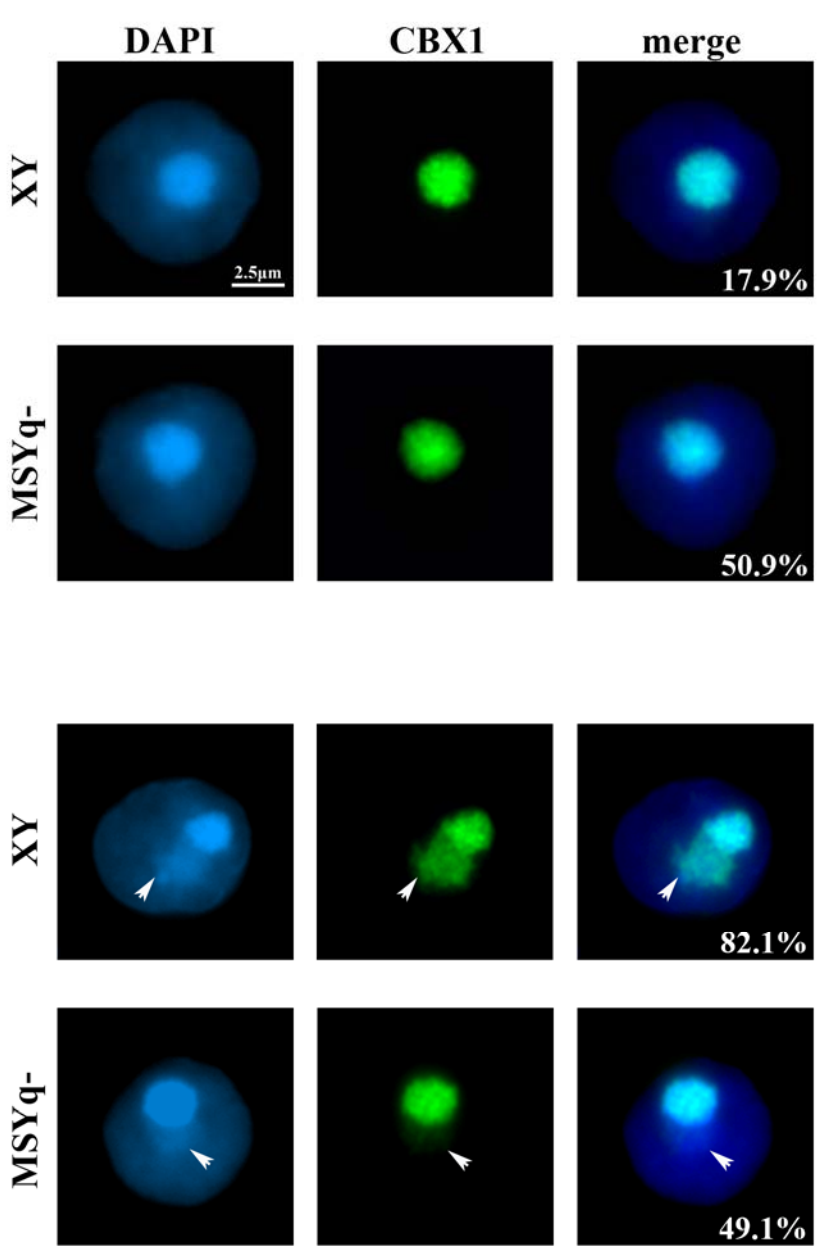

Figure 5.6 Histone $H4_{K8}$ acetylation

$H4_{K8Ac}$ (red) and γH2AX (green) immunostaining of seminiferous tubules from XY and MSYq- testis sections. The cell nuclei are counterstained with DAPI (blue). Tubules were staged according to Russell et al. (1990; see Figure 1.5) based on the γH2AX staining pattern in meiotic cells and the nuclei morphology seen with DAPI.

A) Stage I tubules from XY (top row) and MSYq- (bottom row) males. In stage 1 spermatids from XY males, $H4_{K8Ac}$ is present throughout the nucleus excluding the chromocentre and is enriched on the sex chromosome (arrowed). In stage 1 MSYq- spermatids, $H4_{K8Ac}$ is still present in the nucleus but shows little or no enrichment on the DAPI-dense sex chromosome (arrowed). $H4_{K8Ac}$ is also present in stage 13 spermatids, but appears to be polarised towards one end of the nucleus in MSYq- spermatids.

B) and C) Stage II-V tubules from XY (top row) and MSYq- (bottom row) testis sections. $H4_{K8Ac}$ enrichment on the sex chromosome (arrowed) is increased in stage 2-5 XY spermatids compared to stage 1 spermatids, with $H4_{K8Ac}$ staining being as intense as the pachytene sex body (identified by γH2AX staining). $H4_{K8Ac}$ enrichment on the sex chromosome (arrowed) of stage 2-5 spermatids from MSYq- mice remains dramatically reduced or absent, although pachytene sex body staining appears normal.

Figure 5.6

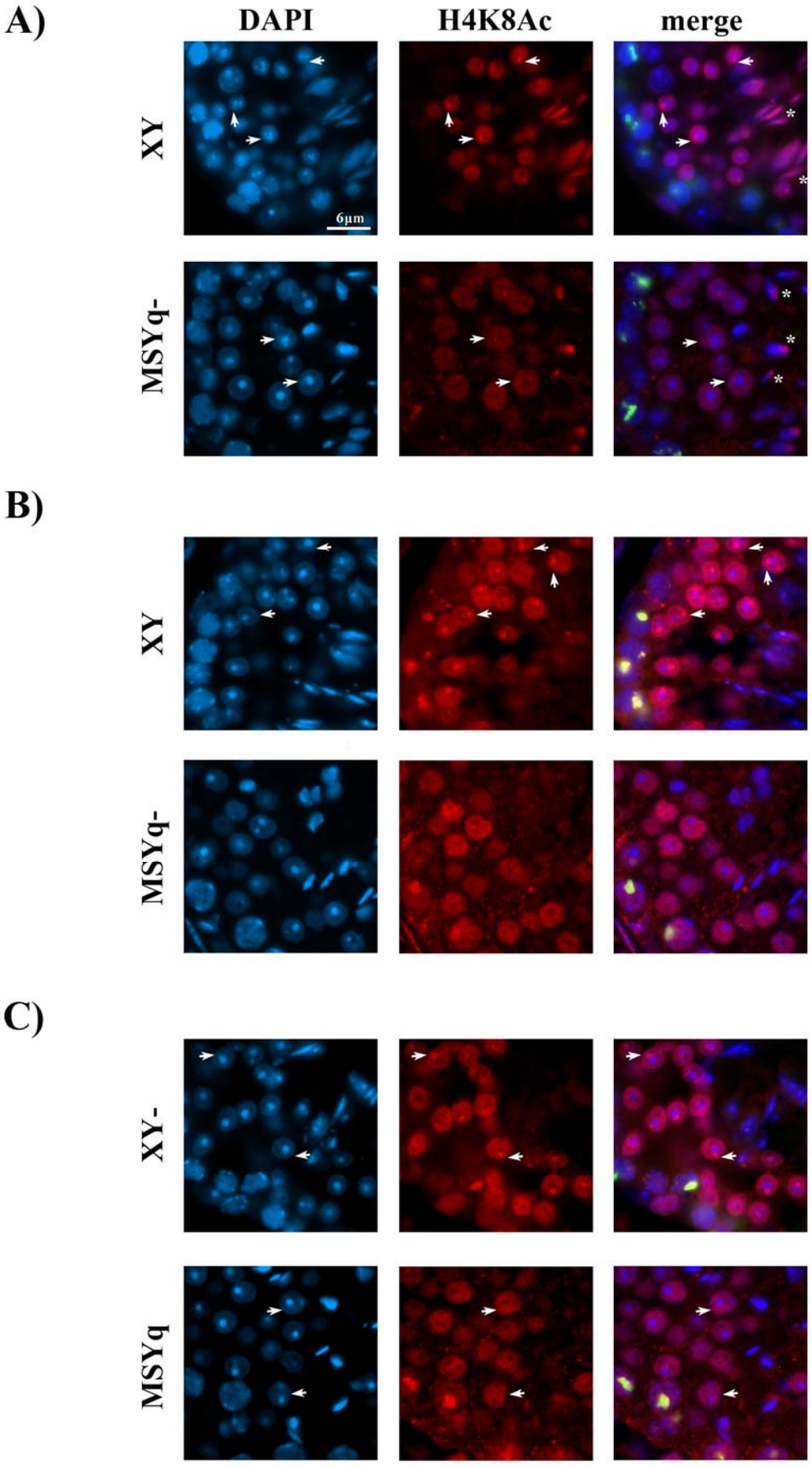

Table 5.4

	spermatid staining pattern	XY	MSYq-	comments
DAPI	**visible sex chromosome**	71.59% (514/718)	37.32% (265/710)	- the Y*^{x}*Sxr*^{a}* chromosome not is visible under DAPI
$H3_{K9me2}$	**sex chromosome**	66.56% (211/317)	27.85% (88/316)	- $H3_{K9me2}$ only seen on X chromosome in MSYq- spermatids
	chromocentre	57.1% (181/317)	39.56% (125/316)	- reduced number of spermatids with $H3_{K9me2}$
	no staining	23.03% (73/317)	51.27% (162/316)	enrichment on chromocentre in MSYq- mice
CBX1	**sex chromosome and chromocentre**	82.09% (307/374)	49.07% (185/377)	- CBX1 reduced on X chromosome in MSYq- spermatids
	chromocentre only	17.91% (67/374)	50.93% (192/377)	
$H3_{K9me3}$	**sex chromosome and chromocentre**	77.34% (157/203)	41.58% (84/202)	- $H3_{K9me3}$ reduced on X chromosome in MSYq- spermatids
	chromocentre only	22.66% (46/203)	58.42% (118/202)	- $H3_{K9me3}$ increased on chromocentre in MSYq- spermatids?

Table 5.4 A summary of the epigenetic marks enriched on the sex chromosome and chromocentre in round spermatids from XY and MSYq- males

For each genotype, testis material from three different individuals was used to make a single cell suspension.

5.2.3 The testis protein levels of up-regulated sex-linked genes are increased in the MSYq deletion models

To determine if the transcriptional up-regulation of sex-linked genes observed in the MSYq deletion mutants leads to a corresponding increase in the encoded proteins, western blot analysis was performed for SLX using testis protein samples from 2/3MSYq-, 9/10MSYq- and MSYq- mice. SLX levels were increased in all three MSYq deletion models (Figure 5.7.A). Protein quantification revealed there is approximately 2.5-fold increase in SLX levels in the 2/3MSYq- testes compared to the XY controls (Figure 5.7.B, 5.7.C), even though there is less than a 1.5 fold up-regulation of *Slx* transcripts (Ellis et al., 2005). Immunostaining of 2/3MSYq-, 9/10MSYq- and MSYq- testis sections revealed no change in the distribution and sub-cellular localisation of SLX, with staining restricted to the cytoplasm of round and early elongating spermatids (Figure 5.8). However, staining of spermatids was much stronger in seminiferous tubules from 2/3MSYq-, 9/10MSYq- and MSYq- mice compared to the XY control (Figure 5.8.A). Thus the increased amount of SLX in the testis of the three MSYq deletion models does not lead to additional ectopic expression of SLX in other spermatogenic cell types, but results in elevated protein levels in the cells that normally express it.

Since PSCR is a downstream consequence of MSUC during pachytene (Turner et al., 2006), any spermatid-expressed gene inserted on the X chromosome should also be up-regulated in the MSYq deletion models. To test this, an X-linked reporter transgene was analysed in these mice. The D4/XEGFP transgenic line has 22-24 copies of a ubiquitous EGFP transgene inserted on the distal part of the mouse X chromosome (Hadjantonakis et al., 2001; Hadjantonakis et al., 1998). This transgene is active in the early stages of spermatogenesis during the mitotic divisions, with the protein localising to the cytoplasm of spermatogonia. The EGFP transgene is inactivated during MSCI and the protein is absent in meiotic cells and round spermatids. Reactivation of the transgene occurs post-meiotically, and the GFP protein is present in the cytoplasm of elongating spermatids, although levels are lower than in spermatogonia (see Figure 5.10.B, top panel). Western blot analysis of XY and 2/3MSYq- males carrying this transgene demonstrated that there is an approximately 2.1-fold rise in whole testis GFP levels in 2/3MSYq- males compared to XY controls (Figure 5.9). Immunofluorescence staining of testis sections from XY and 2/3MSYq- males carrying the transgene

revealed that the pattern of GFP localisation is unaffected in the 2/3MSYq- testis. However, the level of GFP appears to be increased in elongating spermatids from 2/3MSYq- mice, although the spermatogonial GFP levels are the same between the XY and 2/3MSYq- testes (Figure 5.10.A, 5.10.B). This demonstrates that the X-linked EGFP transgene is also affected by the sex chromosome transcriptional de-repression in the MSYq deletion models. Examination of seminiferous tubule squashes from transgenic XY and MSYq- males showed that GFP is cytoplasmic in elongating spermatids from both genotypes, and there is no premature expression of the GFP protein in round spermatids from MSYq- mice (Figure 5.9.C). Together, the western blot and immunofluorescence data imply that the elongating spermatids of transgenic 2/3MSYq- mice have a greater than 2.1 fold increase in GFP levels compared to transgenic XY controls.

Figure 5.7 Quantification of SLX levels in the testis of XY, 2/3MSYq-, 9/10MSYq- and MSYq- mice

A) Western blot analysis of whole testis protein lysates from XY, 2/3MSYq, 9/10MSYq- and MSYq- males. Membranes were probed with two of the anti-XMR/SLX antibodies characterised in Chapter 4, and then reprobed for actin as a loading control.

B) Western blot analysis of whole testis SLX levels in three XY and three 2/3MSYq- males. After probing with the anti-XMR^{69-81} and anti-XMR^{96-106} antibodies, the membranes were reprobed with an antibody against actin.

C) Quantification of SLX levels in the testes of XY and 2/3MSYq- males. The films from B) were scanned and the levels SLX quantified using the Image J computer program, with actin as a loading control. The ratio of SLX to actin was calculated for each lane and the XY sample was given an arbitrary value of 1. A T-test was performed, and the difference in testis SLX levels between XY and 2/3MSYq- males was found to be statistically significant.

* $P = < 0.01$
** $P = < 0.05$

Figure 5.7

A)

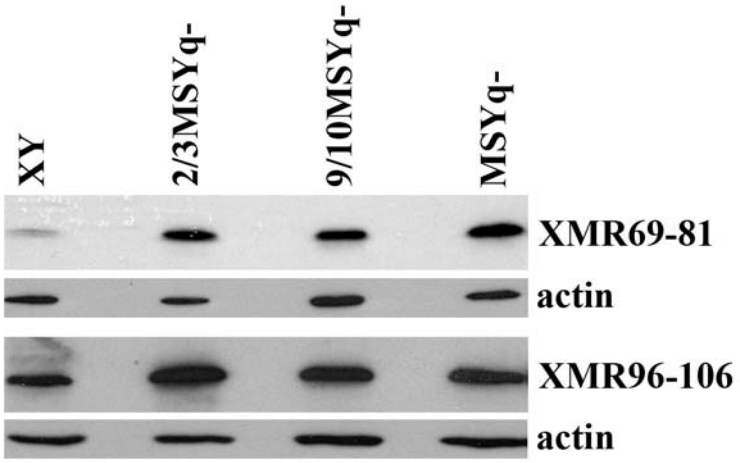

B)

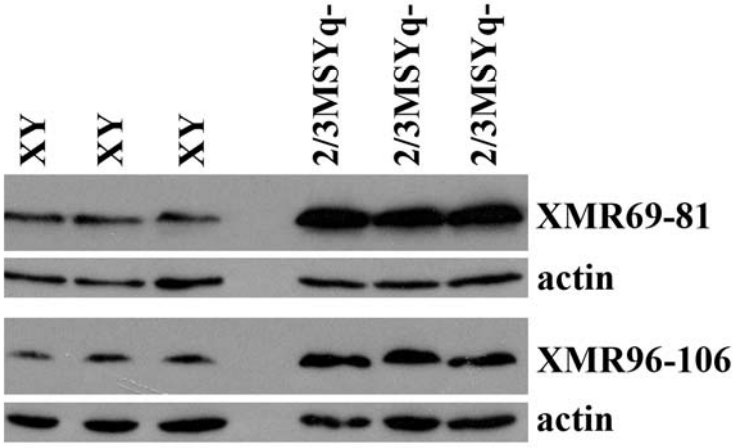

C)

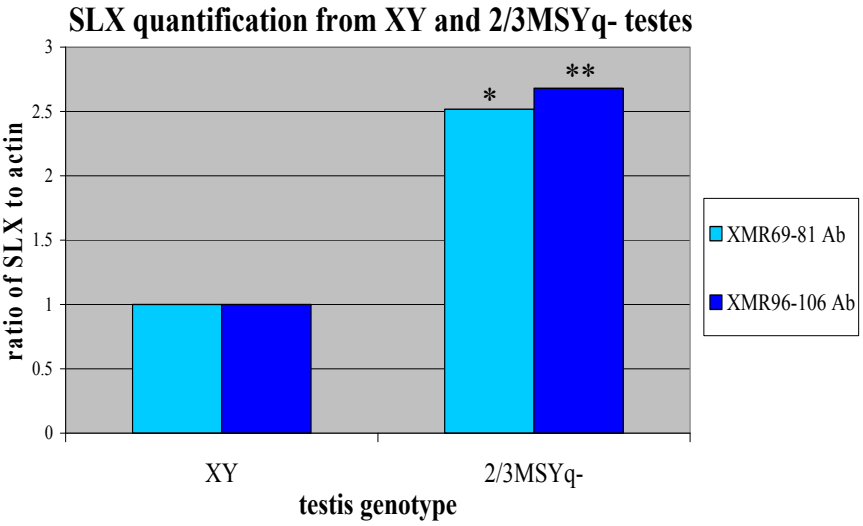

Figure 5.8 SLX localisation in the testis of the three MSYq deletion models

Testis sections were immunostained with anti-XMR/SLX$^{69-81}$ antibody (green) and DAPI (blue).

A) SLX staining of seminiferous tubules from XY (top row), 2/3MSYq- (upper middle row), 9/10MSYq- (lower middle row) and MSYq- (bottom row) testes sections. The expression pattern is identical in all four genotypes, with SLX restricted to round and early elongating spermatids, although staining is stronger in the three MSYq deletion models compared to the XY control.

B) Seminiferous tubules from 2/3MSYq- (top row), 9/10MSYq- (middle row) and MSYq- (bottom row) testes stained for SLX. The subcellular localisation of SLX is unaffected in the three MSYq- models, and shows the same uniform staining of the spermatid cytoplasm as observed in XY spermatids (see Figure 4.9.A).

Figure 5.8

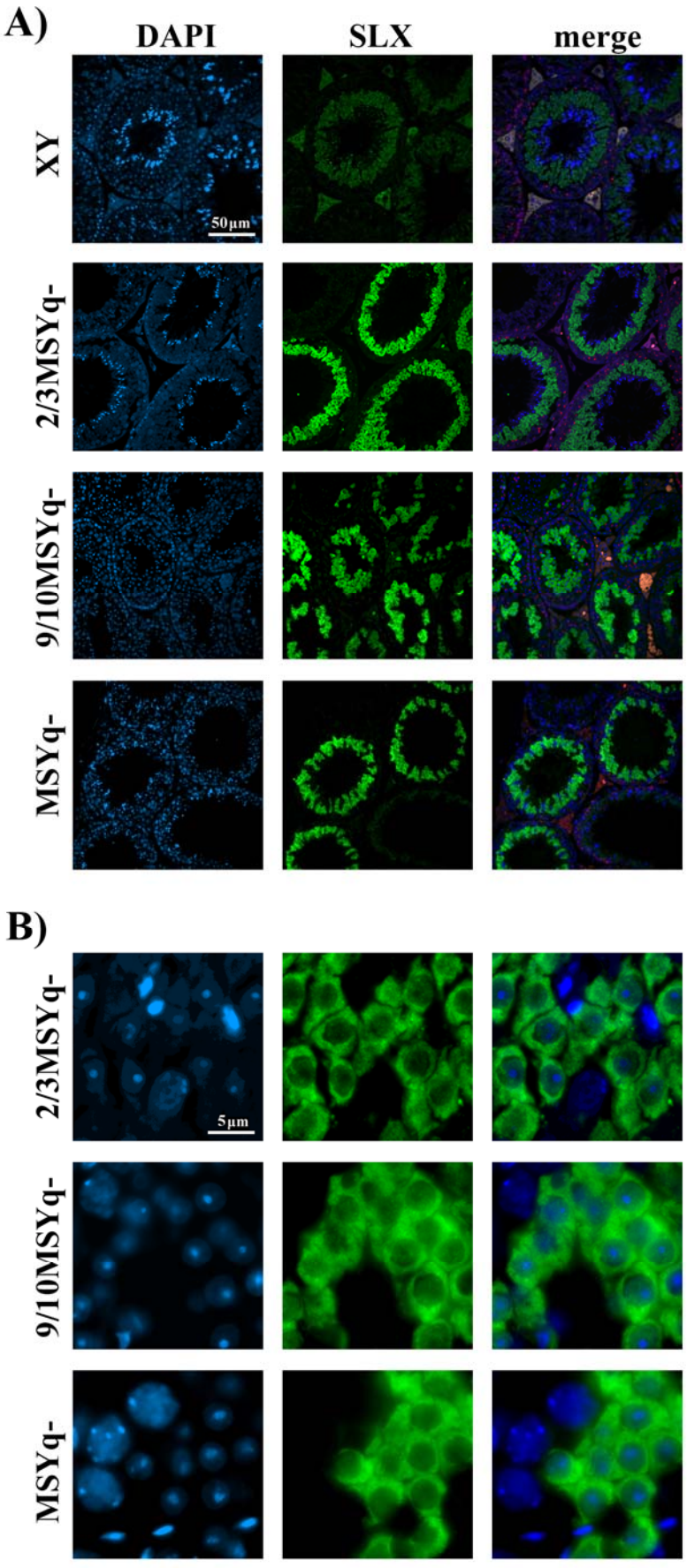
A)
DAPI
SLX
merge
XY
2/3MSYq-
9/10MSYq-
MSYq-
50µm
B)
2/3MSYq-
9/10MSYq-
MSYq-
5µm

Figure 5.9 Quantification of whole testis GFP levels in XY and 2/3MSYq- males carrying the X-linked EGFP transgene

A) Western blot analysis of whole testis protein samples from four transgenic XY mice and four transgenic 2/3MSYq- mice. The membrane was probed with an anti-GFP antibody (top panel) and reprobed with an anti-actin antibody (bottom panel) as a loading control.

B) Quantification of GFP levels from the western blot in A) using ImageJ software. The level of GFP is represented as a ratio to the actin loading control.

C) Mean relative GFP levels in the transgenic XY and 2/3MSYq- testes analysed by western blot in A) and quantified in B). The level of GFP in the XY testes is given an arbitrary value of one. A Student T test was performed and the difference in testis GFP levels between the two genotypes was statistically significant ($P=<0.025$).

Figure 5.9

A)

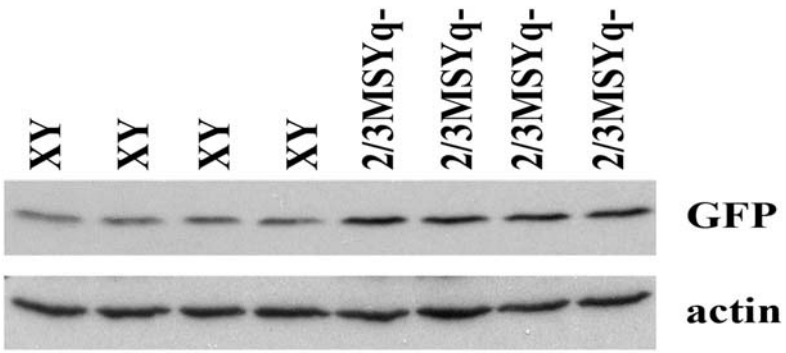

B)

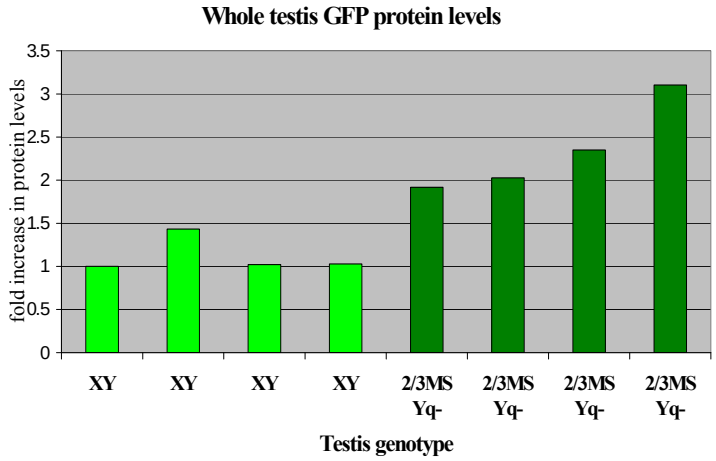

C)

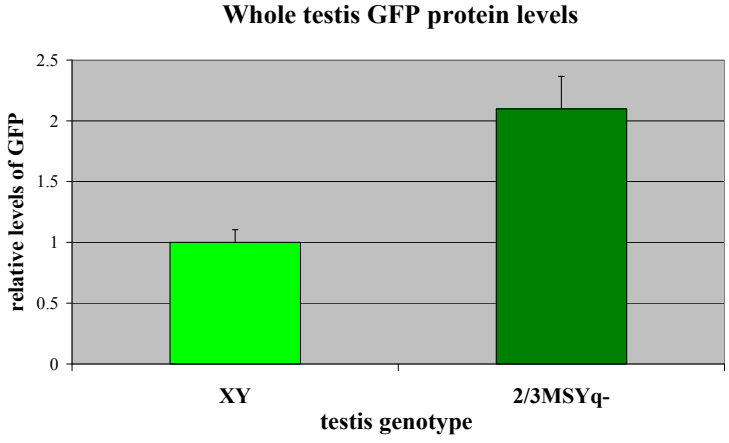

Figure 5.10 GFP localisation in XY, 2/3MSYq- and MSYq- spermatogenic cells carrying an X-linked EGFP reporter transgene

Immunostaining of transgenic XY (top row) and 2/3MSYq- (bottom row) testis sections with an anti-GFP antibody (green) and DAPI (blue) under

A) 20X magnification and

B) 40X magnification.

The GFP reporter gene is active in spermatogonia and leptotene spermatocytes (arrow head) located next to the basal lamina, and the protein is expressed at high levels in the cytoplasm of these cells. The gene is inactivated during MSCI and is reactivated during spermiogenesis. GFP localises to the cytoplasm of elongating and condensing spermatids (starred) in the adluminal compartment of the tubule. In the MSYq- sections, there is an increase in GFP levels in the spermatid cytoplasm, and the Sertoli cell cytoplasm also appears to be GFP positive (arrowed).

C) GFP immunostaining of seminiferous tubule squashes from XY (top row) and MSYq- (bottom row) males carrying the EGFP transgene. In both genotypes, GFP localises to the cytoplasm of condensing spermatids (starred) and spermatogonia.

Figure 5.10

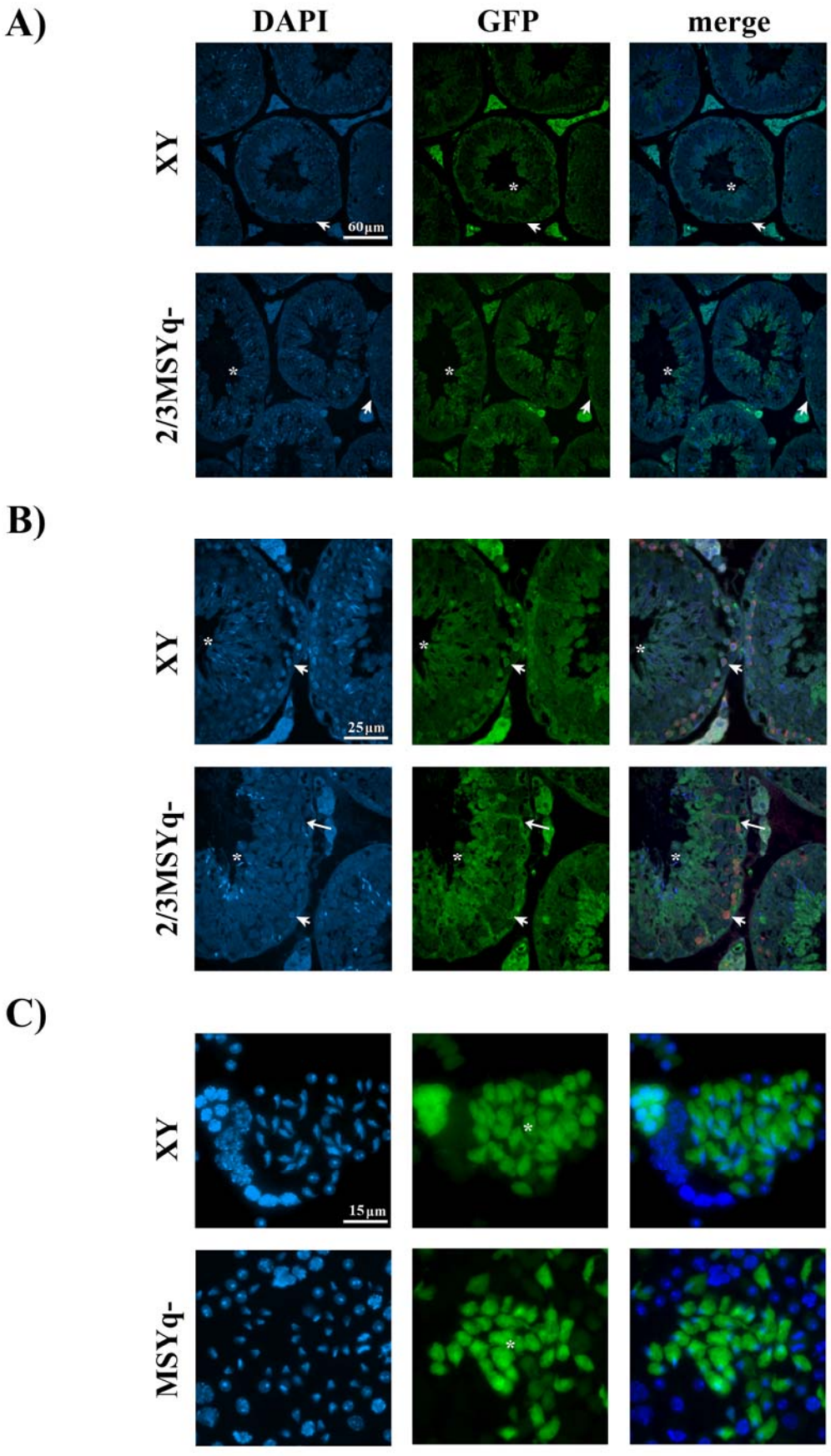

5.3 Discussion

The aim of this chapter was to identify if the up-regulation of a small number of X- and Yp-encoded transcripts in mice with deletions of the MSYq was a chromatin-mediated effect. To summarise, I have used RNA FISH to investigate the method of up-regulation of X and Y transcripts observed in round spermatids from males with deletions of the Y chromosome long arm. My findings show that this is primarily a consequence of increased gene transcription, although an additional post-transcriptional effect can not be ruled out. Furthermore, I have found that the epigenetic status of round spermatids is altered in MSYq- mice compared to the XY control, with a decreased enrichment of CBX1, $H3_{K9me3}$ and $H4_{K8Ac}$ on the sex chromosomes, and reduced $H3_{K9me2}$ on the chromocentre. Western blot analysis and immunocytochemistry has demonstrated that the spermatid protein levels of the up-regulated genes are also increased in the MSYq deletion mutant models, although their localisation pattern is unaffected.

For all eight sex-linked genes assayed by RNA FISH, there was a significant increase in the percentage of round spermatids with an RNA signal in cells from MSYq- mice compared to XY mice. It is unknown if this represents an increase in the proportion of spermatids that transcribe a particular gene in the MSYq- testis compared to the XY testis, or if the percentage of spermatids expressing a gene is unchanged, but there is an increase in the number of round spermatids expressing the gene above the threshold for detection by RNA FISH. Nevertheless, these data suggest that there is an increase in gene transcription that specifically affects spermatid-expressed X- and Y-linked genes independent of gene copy number or expression profile. In the light of this data, it is feasible that all X- and Y-linked genes expressed in spermatids are de-repressed in the MSYq- testis due to a breakdown in the post-meiotic maintenance of sex chromosome repression in these mice.

Previously, only fourteen X- and Y-linked spermatid-expressed genes were identified as up-regulated in the three MSYq deletion models based on microarray analysis (Ellis et al., 2005). This list excludes four genes (*Ddx3x*, *Ott*, *Fmr1* and *Uty*) now found to be up-regulated by RNA FISH. There are two potential reasons why these genes were missed in the initial microarray screen. Firstly, the testis cDNA library used for the microarray analysis was subtracted for transcripts expressed in testicular somatic cells.

Thus, genes that are transcribed in Sertoli cells as well as germ cells (e.g. *Fmr1*, unpublished observation) would have been systematically excluded. Secondly, by using whole testis RNA, the microarray analysis of the three MSYq deletion models was biased towards genes which were either spermatid-specific (e.g. *Satl1*, *Mgclh*) or those expressed at high levels in spermatids (*Ube1y* and *Ube1x*). Genes that are expressed at high levels prior to MSCI, such as *Ddx3x* and *Uty*, were missed in this screen, and even multicopy genes that show a substantial degree of reactivation in spermatids were not identified (e.g. *Ott*; Mueller et al., 2008). This is because these genes are required to have a much higher increase in spermatid transcription for the whole testis transcript levels to rise by at least 1.5-fold, the value chosen to filter data. Thus, inherent biases in interpretation of the data led to a failure in identifying all genes whose spermatid transcript levels are up-regulated in these mice.

To identify all sex-linked genes that are up-regulated in the MSYq deletion models, the microarray analysis could be repeated on purified spermatids using an array with a more extensive gene coverage. This approach was used to examine the effect of MSCI on X chromosome gene transcription in spermatocytes and spermatids from wild-type mice, and led to the identification of 101 X-linked genes that are expressed in spermatids (Namekawa et al., 2006). However, re-examination of the raw microarray values, together with gene-specific RNA FISH, indicates that the number of X-linked genes expressed in spermatids has been underestimated and may be much higher than previously predicted (Mueller et al., 2008). Assuming the defect in post-meiotic silencing in MSYq deletion mice affects the entire X and Y chromosome, this data implies that the de-repression of sex-linked genes may involve hundreds of genes.

A similar transcriptional de-repression of the X chromosome has been reported in spermatids from mice lacking the ubiquitin-conjugating enzyme HR6B; up-regulated genes include *Ube1x*, which also has increased mRNA levels in the MSYq deletion mice (Baarends et al 2007; Ellis et al., 2005). HR6B is expressed at high levels in the testis, especially in spermatids during the period when complex chromatin modifications occur (Koken et al., 1996). *Hr6b* knockout mice are phenotypically normal, but male mice lacking HR6B are sterile and have a pronounced overall regression of spermatogenesis (Roest et al., 1996). Analysis revealed that over 90% of the sperm from these mice are malformed and show a range of morphological abnormalities. At least 70% of the sperm have defective heads, and these are

morphologically very similar to those seen in the 9/10MSYq- and MSYq- mice. *Hr6b* knockout spermatocytes have an increase in the transcriptionally active histone modification $H3_{K4me2}$ on the X and Y chromosomes in diplotene cells, and this persists on the sex chromosome in round spermatids (Baarends et al., 2007). In addition, analysis of the facultative heterochromatin marker $H3_{K9me2}$ revealed that this modification was reduced on the chromocentre of *Hr6b* -/- spermatids (Baarends et al., 2007) and $H3_{K9me2}$ is also reduced on the chromocentre in round spermatids from MSYq- mice. The de-repression of the sex chromosomes, loss of $H3_{K9me2}$ from the chromocentre and the similar sperm head defects observed in the MSYq- and *Hr6b* knockout spermatids suggest that the PSCR defect observed in these mice is similar. Together, these findings imply that the ubiquitin-conjugating enzyme HR6B and a genetic element located on the Y long arm are required for PSCR to occur normally.

Further analysis of the epigenetic profile of the spermatid sex chromosomes revealed that there was a reduction or loss of both active ($H4_{K8Ac}$) and inactive ($H3_{K9me3}$ and CBX1) histone modifications and histone-associated proteins in the MSYq- mice compared to XY mice. Together, the changes in the epigenetic marks on the sex chromosomes in MSYq- spermatids may result in an altered chromatin conformation that allows higher levels of gene transcription. In MSYq- mice, changes in $H3_{K9me3}$ localisation were seen as early as MI, with enrichment of $H3_{K9me3}$ on the centromeric heterochromatin as well as the sex chromosome in the dividing MSYq- cells. Further examination of CBX1 and $H3_{K9me2}$ is needed to determine if the localisation of these proteins are disturbed in cells undergoing the meiotic divisions and secondary spermatocytes from the MSYq- mice. CBX1, $H3_{K9me2}$ and $H3_{K9me3}$ begin to localise to the sex chromosomes between pachytene and diplotene, and this is thought to reflect the transition from MSCI to PSCR (Kim et al., 2007b). It is possible that the de-repression of the sex chromosomes occurs prior to spermiogenesis in the MSYq- mice. It will be necessary to examine the expression of sex-linked genes in late pachytene, diplotene and secondary spermatocytes, to see if there is premature reactivation of genes in the MSYq- mice. However, meiotic cells where the sex chromosomes escape MSCI (e.g. XYY spermatocytes that form a YY bivalent; Turner et al., 2006) are removed during pachytene, so it is possible that any cells with early MSCI/PSCR failure will be eliminated.

Acetylation of histone $H4_{K8}$ and $H4_{K12}$ on the round spermatid sex chromosome has been proposed to assist the replacement of H2A and macroH2A with H2A.Z after MSCI (Greaves et al., 2006). Moreover, H2A.Z enrichment on the sex chromosomes has been suggested to maintain their repression in round spermatids by facilitating compaction of the chromatin (Greaves et al., 2006). It is thus possible that the reduction or loss of $H4_{K8Ac}$ on the sex chromosomes in round spermatids from MSYq- mice is associated with decreased levels of H2A.Z and this may underlie the up-regulation of sex-linked genes observed in spermatids from MSYq deletion mice. Histone H4 acetylation may also play a role in the replacement of histones with transition proteins during the later stages of spermiogenesis (Greaves et al., 2006). The nuclear localisation of $H4_{K8Ac}$ in stage 13 spermatids is altered in spermatids from MSYq- mice compared to XY mice, and this suggests that epigenetic marks present in the nucleus of elongating and condensing spermatids are also affected in MSYq- mice. The localisation of transition protein 2 (TP2) is disturbed in *Hr6b*-/- spermatids (Roest et al., 1996) and in light of the similar changes to the epigenetic profile of *Hr6b*-/- and MSYq- round spermatids, it is conceivable that spermatids from MSYq- mice also have mis-localised TP2. Further analysis of the three MSYq deletion models will be necessary to determine if the replacement of histones with transition proteins and protamines is disrupted in these mice. Such disruptions could affect the compaction of the nucleus in elongating and condensing spermatids, resulting in the grossly abnormal sperm head defects reported in epididymal sperm from 9/10MSYq- and MSYq- mice.

Analysis of *Slx* and an X-linked EGFP reporter gene revealed that the transcriptional up-regulation of X- and Yp-encoded genes leads to increased levels of the corresponding proteins. No difference in the cell type of expression or sub-cellular localisation was seen for either SLX or GFP. Furthermore, the rise in GFP protein levels provides evidence that the up-regulation of sex-linked genes in the MSYq deletion models is independent of gene sequence and is not restricted to genes necessary for spermiogenesis. Assuming that all up-regulated genes show a resultant increase in spermatid protein levels, the spermiogenic defects seen in the three MSYq deletion mutants may be due to the over-expression of one or more X- and Y-encoded proteins, rather than a direct effect of deletion of a MSYq-encoded gene. Ellis et al. (2005) suggested that *Mgclh* and *AK005922* were potential candidates for the sperm head defects in the MSYq deletion models because these genes showed the largest increase in mRNA levels. *Mgclh* is the spermatid-specific X-linked homologue of the

ubiquitously expressed *Mgcl1* gene. *Mgcl1* -/- mice are sterile and have defects in chromatin condensation and acrosome formation (Kimura et al., 2003), and so it is probable that *Mgclh* has a role in sperm head development (Ellis et al., 2005). *AK005922* encodes the histone variant H2AL1, a component of a novel nucleosome-like structure that specifically organises pericentric heterochromatin in condensing spermatids (Govin et al., 2007). H2AL1 and the related H2AL2 protein are first detected in round spermatids, and their levels increase during spermiogenesis as spermatids condense (Govin et al., 2007). Over-expression of H2AL1/2 in round spermatids from the three MSYq deletion mutants may lead to premature packaging of the pericentric heterochromatin into the nucleosome-like structures, which usually does not take place until the spermatids are condensing. This could alter gene transcription from pericentromeric regions as well as disrupt the chromatin conformation, leading to malformed sperm heads.

In 2/3MSYq- males, the rise in testis SLX levels relative to XY males is approximately 1.7-fold higher than the reported increase in *Slx* transcript levels. This suggests that genes which are only slightly up-regulated at the mRNA level may nevertheless show a large increase in the corresponding protein levels in the MSYq deletion mice. As a consequence of this, it is impossible to predict which genes are most likely to show the largest change in protein levels in the three MSYq deletion models. Furthermore, it is possible that genes such as *Fmr1* that are transcribed at low levels and not normally translated in spermatids could be transcribed at sufficiently high levels to be translated in spermatids from the MSYq deletion mice. Therefore, the testicular phenotypes associated with deletions of the mouse MSYq may be the result of a combination of deficiency of MSYq-encoded proteins, over-expression of spermatids-expressed proteins and the presence of sex chromosome-encoded proteins not normally translated in spermatids. If this is the case, identification of the individual genes responsible for the sex ratio distortion and sperm head defects in the MSYq deletion mutants may prove difficult. However, identifying which Y gene deficiency triggers these phenotypes through transgenic or knock-down strategies should be more straightforward, although it will be difficult to determine the mechanism involved.

If the *Hr6b* knockout mice do have the same PSCR defect as the MSYq- mice, then *Hr6b*-/- mice are also expected to have changes in protein levels of X-encoded genes. In addition, although Baarends et al. (2007) only analysed the expression of X-linked

genes, it is probable that the Y-linked genes (including those on the MSYq) are de-repressed in *Hr6b* knockout spermatids too. Studies investigating the expression of X- and Y-encoded proteins should be carried out in *Hr6b* knockout spermatids, and analysis of proteins encoded by the MSYq (e.g. SLY, SSTY1) will be of particular interest. It is possible that one of the genes on the MSYq is required to ensure that shedding of condensing spermatids occurs in stage VIII tubules in normal males. Over-expression of this protein may lead to premature shedding of round and elongating spermatids, observed in the *Hr6b* -/- testes (Roest et al., 1996). Conversely, lack of this protein could be responsible for the delayed shedding of mature sperm reported in the 9/10MSYq- and MSYq- mice (Touré et al., 2004b; P Burgoyne and D Escalier, unpublished data).

In conclusion, this chapter has shown that the up-regulation of X- and Yp-linked transcripts in spermatids from the three MSYq deletion models is the result of increased transcription of these genes, potentially mediated by changes in the epigenetic status of the sex chromosomes in round spermatids. However, an additional post-transcriptional effect can not be discounted and so altered levels of SLX and SLY may still contribute towards the up-regulation of sex-linked genes in the MSYq deletion models. Transgenic analysis of *Slx* and *Sly* is presented in the next chapter.

Chapter 6

Generation and characterisation of *Sly* and *Slx* transgenic mice

Generation and characterisation of *Sly* and *Slx* transgenic mice

6.1 Introduction

Expression analysis of *Sly* and *Slx* (chapters 3 and 4) has shown that these genes are transcribed in post-meiotic germ cells of the testis and encode proteins that localise to the spermatid cytoplasm in a stage-specific manner. However, the function of *Sly* and *Slx* in spermiogenesis remains elusive, although analyses of mice with deletions of the MSYq imply these genes may play a role in sperm maturation and development. *Sly* is reduced or absent in spermatids from the three MSYq deletion models and conversely, these mice also have increased transcription and translation of *Slx* (and other sex-linked genes). This has lead to the prediction that there are regulatory interactions between *Sly* and *Slx*, disturbances of which may contribute to the phenotypes observed in the MSYq deletion models (Ellis et al., 2005; Touré et al., 2005). An interaction between *Sly* and *Slx* may potentially be mediated by double-stranded RNA in a manner analogous to that observed between the X-linked *Ste* gene and its Y-linked homologue *Su(Ste)* in *Drosophila* (Aravin et al., 2001). One way to identify the putative interactions between these two genes is to analyse the transcription and translation of *Slx* when *Sly* expression is abolished and vice-versa. Given the multicopy nature of *Sly* and *Slx*, the most straightforward method to accomplish this is by RNAi-mediated knock-down rather than abrogating their function by conventional gene targeting approaches involving homologous recombination.

The functions of Y-encoded genes have primarily been inferred from analysis of mice carrying naturally occurring deletions, together with the identification of candidate genes mapping to these regions. Defining the genetic basis for the phenotypes associated with various Y chromosome deletions has been held back by the lack of success in producing mice with targeted mutations in specific Y-linked genes. Instead, the approach of transgenic rescue has been used, and the first mouse Y chromosome gene to be successfully introduced as a transgene was the testis-determining gene *Sry* (Koopman et al., 1991). In this study, a 14Kb genomic DNA fragment encoding the *Sry* locus was sufficient to induce testis formation and male development when introduced into an XX female mouse embryo. Since then, transgenes for other single copy and multicopy Y-linked genes have been reintroduced into various deletion

mutants, and this led to the identification of *Eif2s3y* as the Y-encoded spermatogonial proliferation factor (Mazeyrat et al., 2001). Over-expression of *Sly* and *Slx* can be investigated by introducing these genes as transgenes and this may help to illuminate the roles they play in spermiogenesis. *Sly* transgenic mice can also be used to determine whether loss of this Yq gene alone is responsible for the defective spermiogenesis observed in mice with MSYq deletions.

This chapter describes the generation and characterisation of mice carrying a *Sly* or *Slx* transgene. These transgenic mice will be used to analyse the potential interaction between *Sly* and *Slx* and to determine if deregulation of these genes contributes to the defective sperm maturation and function observed in the three MSYq deletion mouse models.

6.2 Results

6.2.1 Generation of *Sly* BAC transgenic lines

To investigate whether deletion of *Sly* is responsible for the X/Y gene up-regulation, sex ratio distortion and sperm head defects seen in MSYq deletion models, *Sly* transgenic mice were made. As the *Sly* promoter sequence has not been characterised, a BAC transgenic approach was used. The sequenced Y chromosomal BAC clone RP24-402P5 contains a copy of the *Sly* gene that has retained an ORF and is thus expected to be transcribed and translated. This BAC also contains 74Kb of DNA upstream of the *Sly* transcription start site and 20Kb downstream of the *Sly* gene, increasing the likelihood that it contains all the promoter and enhancer elements necessary to drive spermatid-specific expression of *Sly*. Nineteen transgenic lines that contained the BAC vector were produced by pronuclear injection of caesium-chloride purified BAC DNA. To identify which of the nineteen BAC lines contained the *Sly* insert, extensive PCR analysis was performed on transgenic females (males have an endogenous copy of the BAC insert and so cannot be used to characterise the transgene). The structure of the RP24-402P5 BAC used to generate transgenics is shown in Figure 6.1 and the positions of the PCR primers used for genotyping are indicated by arrows. Only two of the lines, Ylr 8 and Ylr 12, contained the complete *Sly* gene along with sequences upstream of the transcription start site.

Figure 6.1

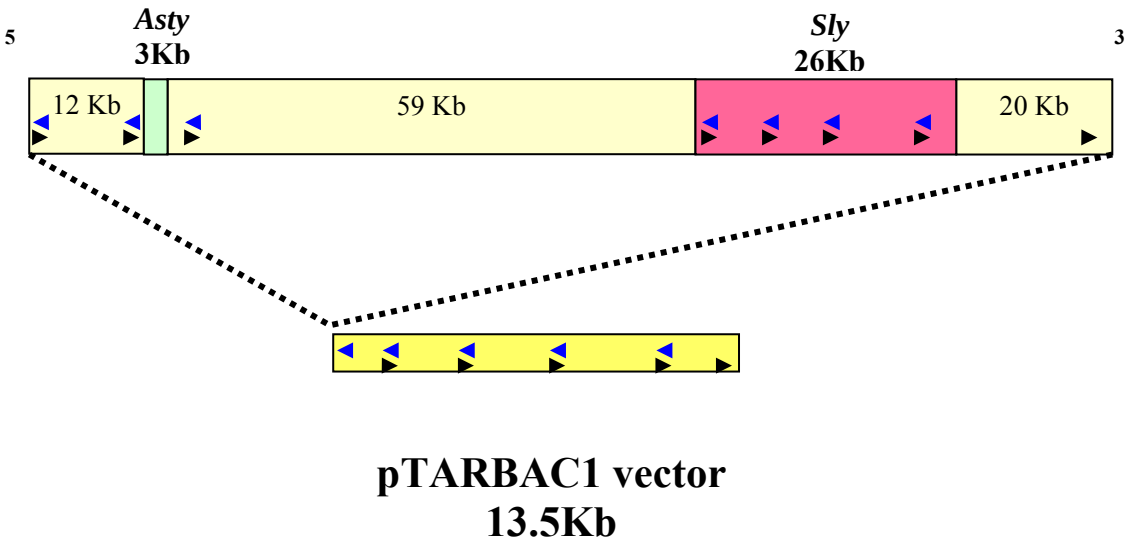

Figure 6.1 A schematic diagram of the *Sly*-containing RP24-402P5 BAC

The RP24-402P5 BAC contains 120Kb of mouse MSYq genomic DNA inserted into a 13.5Kb pTARBAC vector. The genomic insert contains a copy of the *Asty* gene (green) and the *Sly* gene (pink), as well as the surrounding DNA sequences.

Nineteen transgenic founders were made by pronuclear injection of the BAC and female carriers of the transgene were analysed by PCR. The positions of the primers used for genotyping are indicated by the blue and black arrows. Two transgenic lines, Ylr 8 and Ylr 12, contained the complete insert.

6.2.2 Expression analysis of Ylr 8 and Ylr 12 *Sly* BAC transgenic lines

To determine if the *Sly* transgenes were expressed, RT-PCR was performed using *Sly*-specific primers on testis RNA samples from MSYq- mice hemizygous for the Ylr 8 or Ylr 12 transgene. These mice lack all endogenous copies of *Sly* (Touré et al., 2005), and so a band corresponding to the *Sly* transcript will only be present if the transgene is transcribed. The *Sly* specific band was seen in MSYq- Ylr 8 (Figure 6.2.A, lanes 3, 6 and 7) and MSYq- Ylr 12 (Figure 6.2.A, lane 2) transgenic samples, but was not present in the non-transgenic MSYq- controls (Figure 6.2.A, lanes 1, 4 and 5). This confirms that both transgenic lines are transcribing the transgene.

When on a fertile XY or 2/3MSYq- background, the transgenic males from both lines transmit the transgene to female and male offspring, indicating that the *Sly* transgene has integrated on an autosome. To identify which spermatogenic cells express the transgenic *Sly* gene, RNA FISH was performed on testis material from 2/3MSYq- mice hemizygous for either Ylr 8 and Ylr 12 transgene. Expression of *Sly* from the Y chromosome was clearly observed in round spermatids but no transgenic signal could be identified. Potentially, this may be due to masking of the transgenic signal by the high levels of endogenous *Sly* signals and so RNA FISH was repeated on hemizygous transgenic MSYq- mice. For transgenic line Ylr 8, *Sly* RNA FISH signals were detected only in round spermatids, suggesting that the transgene is expressed in a pattern identical to the endogenous *Sly* genes (Figure 6.2.B). These RNA FISH signals were located away from the DAPI dense sex chromosome, consistent with integration of the transgene into an autosome. No *Sly* RNA signals were observed in spermatogenic cells from MSYq- Ylr 12 tg/+ males, although RT-PCR analysis indicated that this transgene was transcribed.

To investigate if the Ylr 8 and Ylr 12 transgene-encoded *Sly* transcripts are translated, western blot analysis of whole testis samples from hemizygous transgenic MSYq- males was performed. As expected, the 40kDa band corresponding to SLY was observed in both the XY and 2/3MSYq- control samples (Figure 6.2.C, lanes 1 and 2). A faint SLY band was present in the Ylr 8 tg/+ MSYq- sample (Figure 6.2.C, lane 3), demonstrating that the *Sly* transgene is translated at low levels within this transgenic line. SLY was not detected in the MSYq- Ylr 12 tg/+ or MSYq- samples (Figure 6.2.C,

lanes 4 and 5). This suggests that the Ylr 12 transgenic line is not translated or that the transgene is translated at levels undetectable by western blot analysis.

Figure 6.2 Expression analyses of the Ylr 8 and Ylr 12 transgenic lines

A) RT-PCR analysis of whole testis cDNA from transgenic and non-transgenic MSYq- mice using primers specific to *Sly* designed by Ellis et al.(2005). Primers that amplify *Hprt* transcripts were used as a loading control. An XY cDNA sample (lane 8) was included as a control for the *Sly* primers.

Sly is not amplified from MSYq- samples (lanes 1, 4, and 5), confirming that these mice lack endogenous *Sly* transcription. A band corresponding to *Sly* was detected in transgenic MSYq- samples carrying the Ylr 8 transgene (lanes 3, 6, and 7) and Ylr 12 transgene (lane 2), indicating that these transgenic lines express the *Sly* transgene.

B) Gene-specific RNA FISH on a surface spread spermatid nucleus from a MSYq- Ylr 8 hemizygous testis lacking all endogenous copies of *Sly*.

Sly-specific RNA FISH (red) signals were only seen in round spermatid nuclei, confirming that the Ylr 8 transgene is expressed in a pattern identical to the endogenous multicopy *Sly* loci. DNA FISH (green) confirmed that the RNA FISH signal originated from the Ylr 8 transgene. The spermatid nucleus is stained with DAPI (blue).

C) Western blot analysis of testis samples from MSYq- males carrying the Ylr 8 and Ylr 12 transgenes. Blots were probed with the SLY-specific antibodies i) SK97 and ii) SK98 characterised in chapter 3.

A band corresponding to SLY (arrowed) was seen in the Ylr 8 hemizygous MSYq- sample as well as the XY and 2/3MSYq- control samples. No SLY is detected in the MSYq- Ylr 12 transgenic sample, or the non-transgenic MSYq- control. This suggests that the Ylr 12 transgenic line does not translate the transgene.

Figure 6.2.

A)

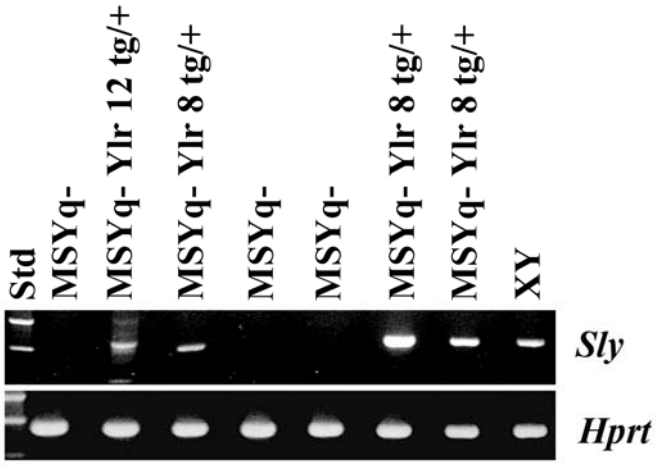

B)

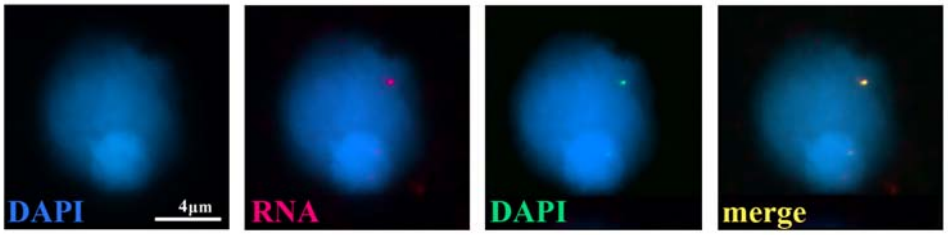

C)

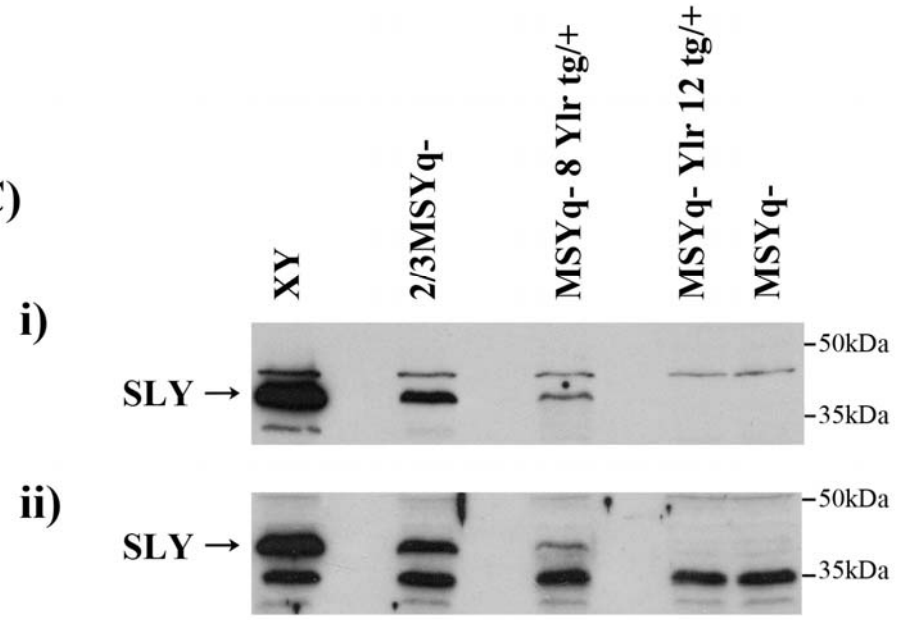

6.2.3 Northern blot analysis of the Ylr 8 transgenic line

To examine if *Sly* was transcribed at high levels from the Ylr 8 transgene, northern blot analysis was carried out on whole testis RNA from 2/3MSYq- males hemizygous for the Ylr 8 transgene with non-transgenic littermates as controls. There was no significant difference in *Sly* transcript levels between transgenic and control samples, indicating that the transgene is expressed at low levels (Figure 6.3.A and Figure 6.4.A). To see if there were any changes in X-linked gene expression in the Ylr 8 transgenic males, the northern blot membrane was re-probed for *Slx*, *AK005922* and *Mgclh*, the three most highly up-regulated X-linked genes in MSYq deletion models (Ellis et al., 2005). The mRNA levels of these genes did not differ significantly between control and transgenic mice (Figures 6.3.B-D and 6.4.B-D).

6.2.4 Analysis of the sperm head abnormalities in 2/3MSYq- mice with or without the Ylr 8 transgene

To explore the possibility that low levels of transgenic *Sly* expression may ameliorate the sperm defects observed in the 2/3MSYq- deletion mice, sperm head analysis was performed in males from the Ylr 8 transgenic line. Sperm smears from the caput 1 and caput 2 of the epididymis of seven transgenic and seven non-transgenic littermates were silver-stained and scored as ‘normal’, ‘slightly abnormal’ and ‘grossly abnormal’ using the chart in Figure 6.5.A. No difference was seen between the two genotypes in the percentage of abnormal sperm (Figure 6.5.B, 6.5.C), implying that the Ylr 8 transgene is unable to rescue the sperm head defects in the 2/3MSYq- mice.

Figure 6.3

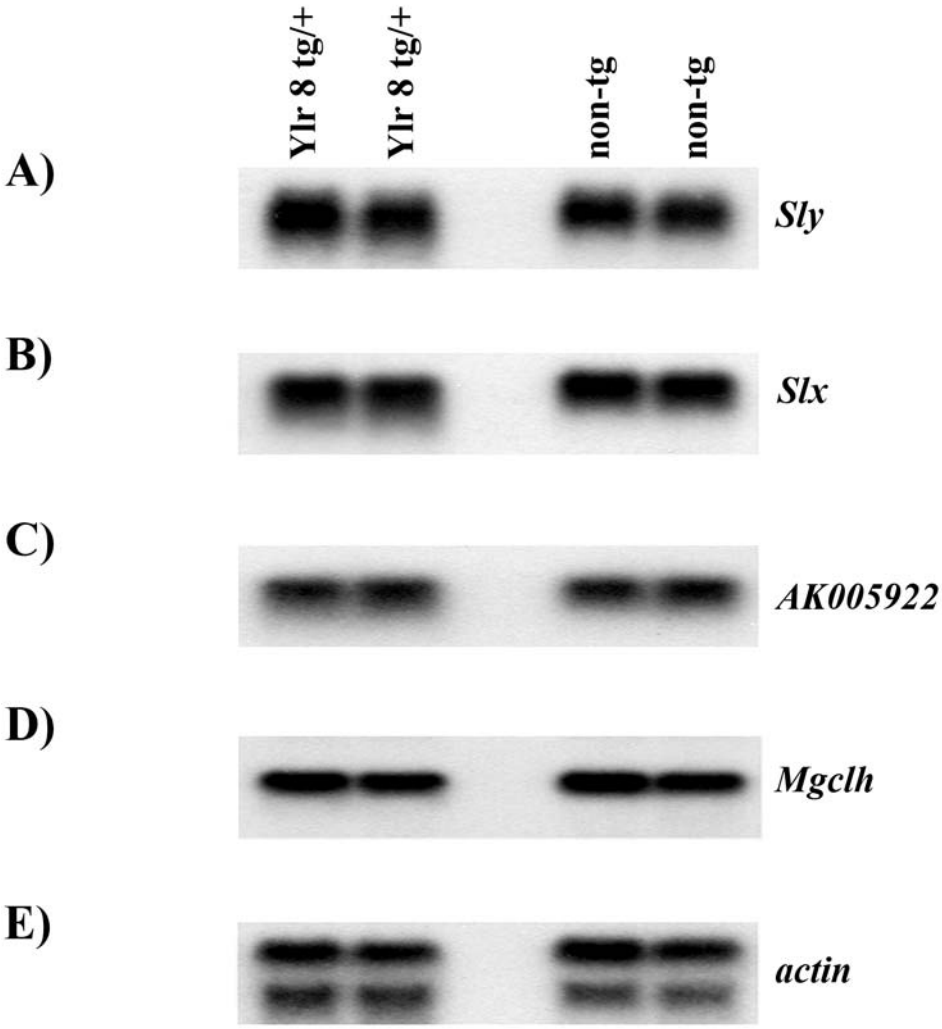

Figure 6.3 Northern blot analysis of 2/3MSYq- males hemizygous for the Ylr 8 transgene

Whole testis RNA was extracted from two transgenic and two non-transgenic 2/3MSYq- Ylr line 8 males and run on a Northern blot. The membrane was incubated with probes to the following genes;
A) *Sly*
B) *Slx*
C) *AK005922* (encodes the H2AL1 protein)
D) *Mgclh*
E) α and β *actin*

There is no significant increase in the *Sly* transcript levels between transgenic and non-transgenic littermates, indicating that the Ylr 8 transgene is transcribed at low levels. No difference is seen between the two genotypes in *Slx*, *AK005922* and *Mgclh* transcript levels, the three X-linked genes that are most highly up-regulated in the MSYq- models based on microarray analysis (Ellis et al., 2005). A probe against α and β *actin* was used as a loading control.

Figure 6.4 Quantification of RNA levels from the northern blot analysis of Ylr line 8

The northern blot membranes from Figure 6.3 were exposed to a phosphoimager screen overnight and the RNA levels of the following genes were quantified using the ImageQuant computer program and normalised against actin.

A) *Sly*
B) *Slx*
C) *AK005922*
D) *Mgclh*

The error bars represent the standard error in transcript levels between individuals of the same genotype.

Figure 6.4

A)

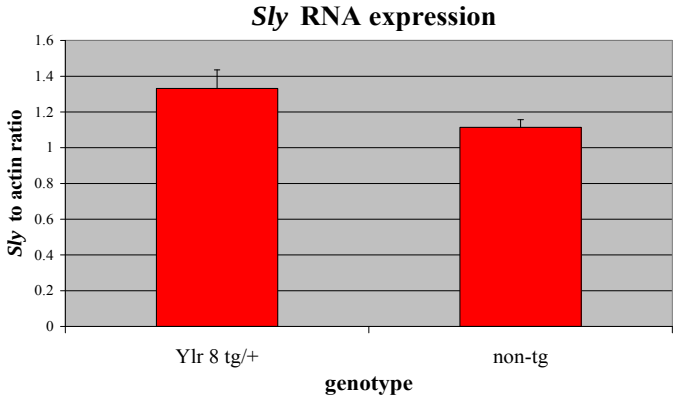

B)

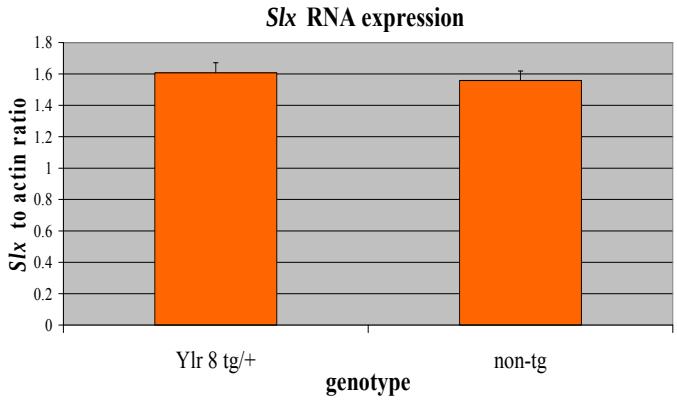

C)

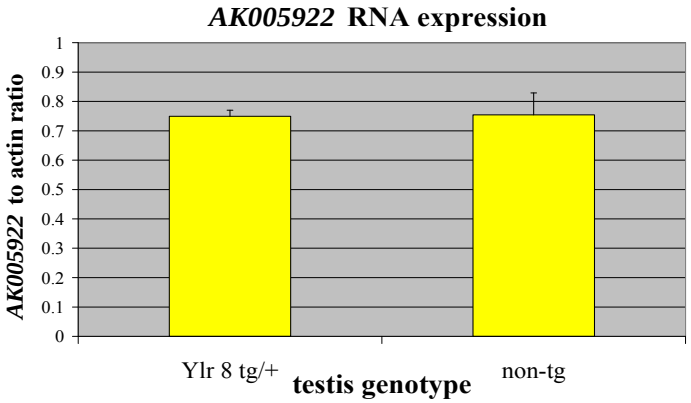

D)

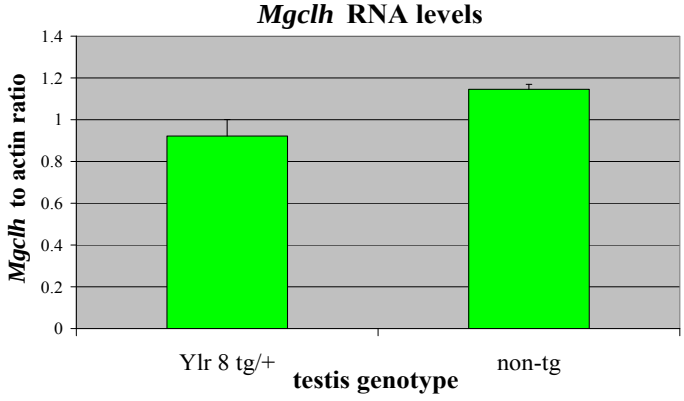

Figure 6.5 Sperm head abnormalities in 2/3MSYq- males with or without the Ylr 8 transgene

Epididymal sperm smears from the caput 1 and caput 2 of seven Ylr 8 hemizygous transgenic males and seven non-transgenic litter mates were silver-stained. The slides were coded and randomised and one hundred sperm from each mouse were examined by Maria Szot and classified as described by Mahadevaiah et al. (1998).

A) Diagram of the standard categories used in classifying abnormal sperm heads.

B) Graphical representation of the frequency of normal, slightly abnormal and grossly abnormal sperm from the caput 1 of transgenic and non-transgene males

C) Graphical representation of the sperm head abnormality profiles of sperm from the caput 2 of each genotype.

The error bars in B) and C) represent the standard error between males within each genotype.

Figure 6.5

A)

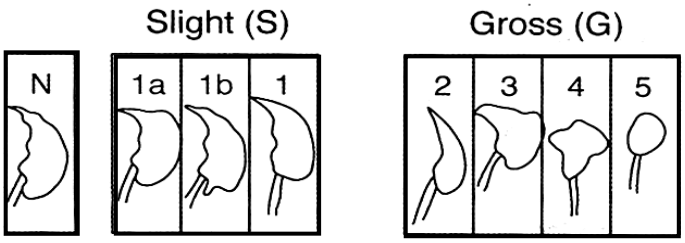

B)

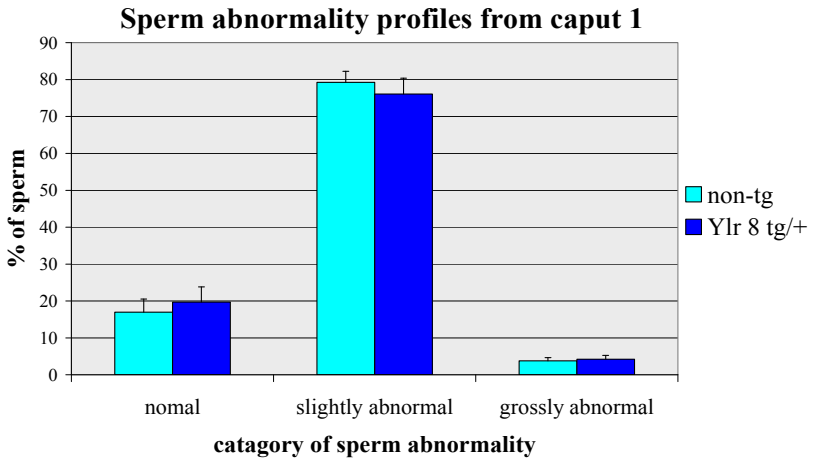

C)

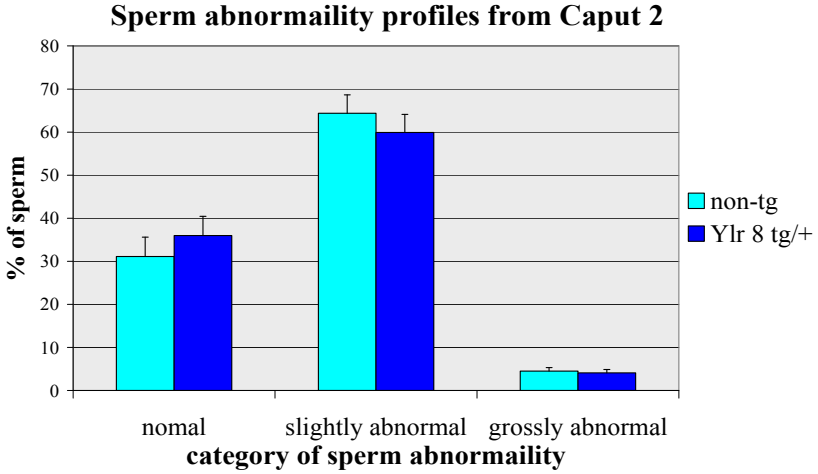

6.2.5 Generation of mP1-*Sly* transgenic mice

The results above indicate that the Ylr 8 *Sly*-containing BAC transgenic line failed to reduce the frequency of sperm head defects seen in the three MSYq deletion models. However, this may be due to the low expression level of the transgene rather than the inability of *Sly* to rescue this phenotype. In an attempt to make *Sly* transgenic mice that transcribe and translate the transgene at high levels, the mouse protamine 1 (mP1) promoter was used. This promoter is known to drive transgene expression in round spermatids (Peschon et al., 1987) and has previously been used to drive transcription of the multicopy *Rbmy* (Szot et al., 2003) and *Ssty1* (Touré et al., 2004) Y-linked genes. There are several *Sly* mRNA sequences that have different 5'UTR and 3'UTR sequences and it is unknown which of these transcripts are translated. The majority of *Sly* transcripts have the same ORF, and so this was cloned into a construct containing the mP1 promoter and an SV40 polyA sequence to ensure efficient polyadenylation of the transcript.

Pronuclear injection of the mP1-*Sly* construct produced two transgenic founders, *Sly* 13 and *Sly* 14, both of which transmit the transgene to male and female offspring. PCR genotyping revealed that transgenic lines *Sly* 13 and *Sly* 14 contained the complete *Sly*-SV40 polyA fusion gene, and so are expected to be transcribed. Preliminary western blot analysis was carried out on transgenic and non-transgenic XY testis samples from *Sly* line 13. There was a slight increase in the level of SLY in testis of mP1-*Sly* tg/+ males compared to non-transgenic littermates (Figure 6.6), suggesting that the transgene may be translated. Further transcriptional and translational analysis will be carried out to confirm this, and these transgenic mice are currently being bred onto the 2/3MSYq- background.

Figure 6.6 Analysis of whole testis SLY levels in mP1-*Sly* line 13

A) Western blot analysis of whole testis lysates from XY male littermates with or without the mP1-*Sly* transgene. Membranes were incubated with the SLY-specific SK97 (upper panel) and SK98 (lower panel) antibodies before being re-probed with an anti-actin antibody as a loading control.

B) Graphical representation of SLY levels in the four samples used for western blot analysis. The films used in A) were scanned and the protein band quantified using ImageJ software. SLY levels are given as a ratio to the actin loading control.

C) Mean SLY levels in transgenic and non-transgenic XY testes based on the western blot in A). The error bars represent the standard error between males of the same genotype. There is an increase in SLY levels in males carrying the mP1-*Sly* transgene compared to non-transgenic controls, and this is statistically significant ($P=<0.05$; Student T test).

Figure 6.6

A)

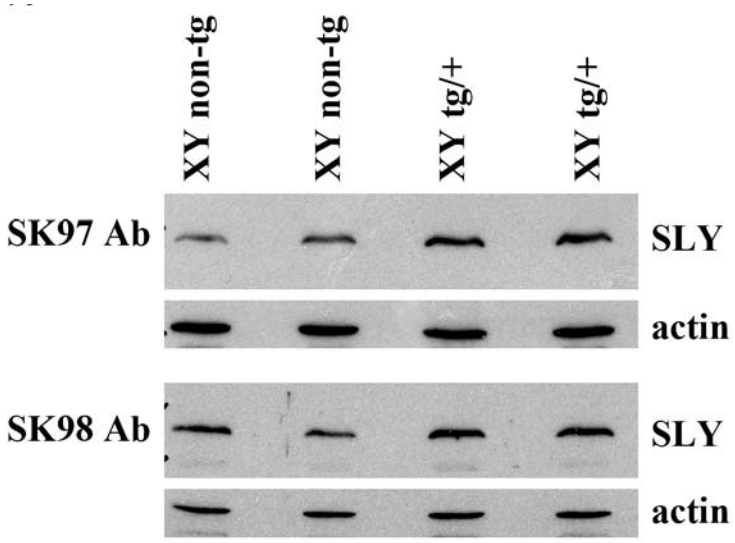

B)

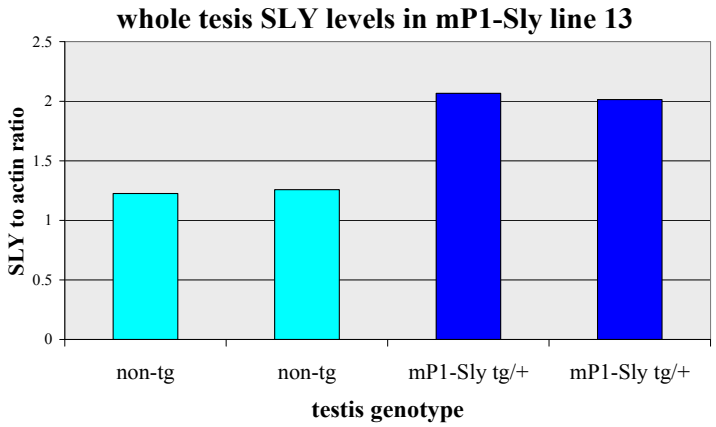

C)

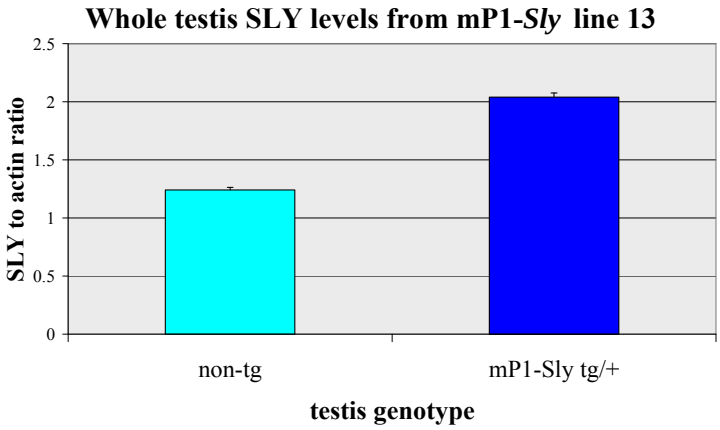

6.2.6 Generation and characterisation of mP1-*Slx* transgenic lines

To investigate if over-expression of *Slx* contributes to any of the phenotypes observed in the three MSYq deletion models, transgenic mice were made. The *Sly* transgenic data presented above indicates that the high levels of transgene expression required for SLX over-expression studies may not be obtained using the BAC transgenic approach. To generate high levels of *Slx* transgene expression, transgenic mice were produced by driving the *Slx* ORF under the mP1. Ten transgenic founders (mP1-*Slx* lines 3 to 12) were produced by pronuclear injection, and PCR analysis confirmed that all ten founders contained the entire *Slx*-SV40 polyA fusion gene. Nine of the founders transmitted the transgene to their male and female offspring.

To ascertain whether the mP1-*Slx* transgene was transcribed, RT-PCR analysis was performed for six of the transgenic lines on whole testis RNA samples from XY hemizygous transgenic males together with non-transgenic littermates. The PCR primers used were designed to be specific to the transcript produced by the transgene and amplified a band of approximately 1Kb. The *Slx*-SV40 polyA RT-PCR product was detected in all six transgenic lines (Figures 6.7.A to 6.12.A), indicating that these lines transcribe the transgene. No band was observed in RNA samples from non-transgenic littermates, verifying that the PCR primers are unable to amplify endogenous *Slx* transcripts.

To establish if the mP1-*Slx* encoded transcripts are translated in the testis of transgenic males, western blot analyses were performed for all six transcribing lines. No difference in whole testis SLX levels was seen between transgenic and non-transgenic males for any of the mP1-*Slx* transgenic lines (Figures 6.7.B, C to 6.12.B, C).

Figure 6.7 Expression analysis of mP1-*Slx* line 4

A) RT-PCR analysis on whole testis RNA from transgenic and non-transgenic males using primers specific to the mP1-*Slx* transgene. A band representing the *Slx*-SV40 polyA fusion transcript is present in samples carry the mP1-*Slx* transgene, demonstrating that this transgene is expressed. No band is seen in –RT samples, indicating that there is no DNA contamination of these samples.

B) Western blot analysis of whole testis SLX levels in XY males with or without the mP1-*Slx* transgene. Membranes were probed with two of the anti-SLX antibodies (anti-XMR$^{69\text{-}81}$ and anti-XMR$^{96\text{-}106}$) characterised in chapter 4 and then re-probed for actin as a loading control.

C) Quantification of SLX levels in the testis of mP1-*Slx* line 4 males hemizygous for the transgene with non-transgenic littermates as a control. The western blots from B) were scanned and the level of SLX was quantified as a ratio to actin using the ImageJ computer program. Error bars represent the standard deviation in SLX levels between individuals of the same genotype (n=2).

Figure 6.7

A)

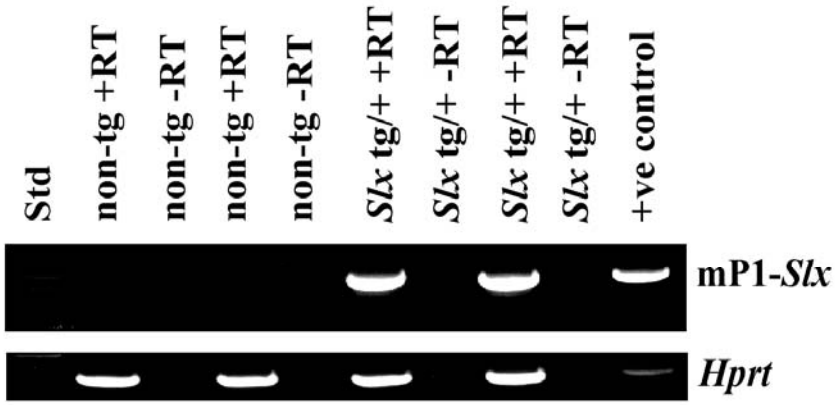

B)

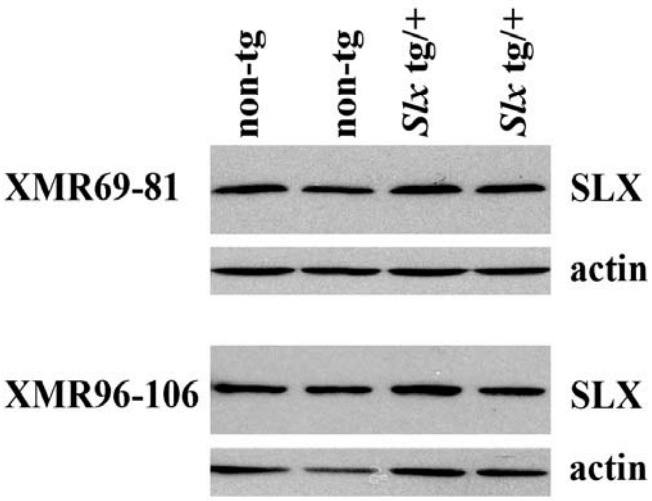

C)

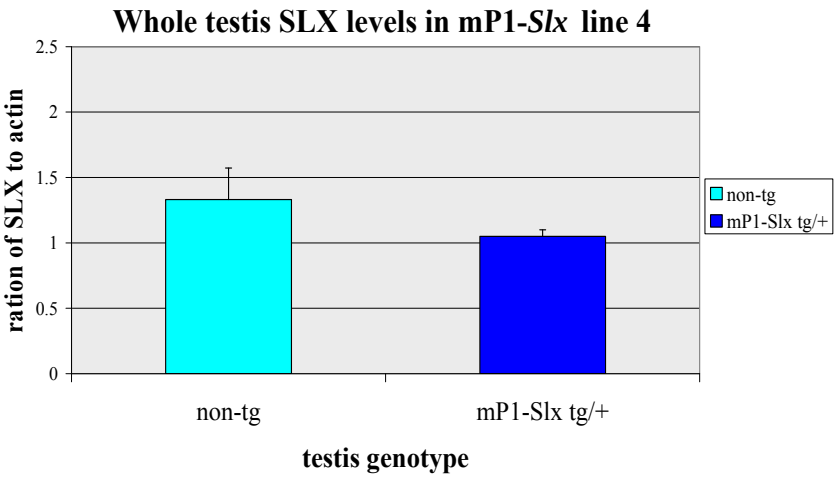

Figure 6.8 RT-PCR and western blot analysis of mP1-*Slx* line 5

A) RT-PCR analysis using primers that specifically amplify the *Slx*-SV40 polyA fusion transcript encoded by the mP1-*Slx* transgene. A 1Kb band corresponding to this transcript is present in samples from hemizygous transgenic males, indicating that the mP1-*Slx* transgene is transcribed.

B) Western blot analysis of whole testis SLX levels in transgenic and non-transgenic mice. After being incubated with the anti-SLX antibodies, membranes were re-probed with an antibody against actin as a loading control.

C) Quantification of SLX levels relative to actin in XY males with or without the mP1-*Slx* transgene based on the western blot films in B). Error bars represent the standard error in SLX levels between males of the same genotype.

Figure 6.8

A)

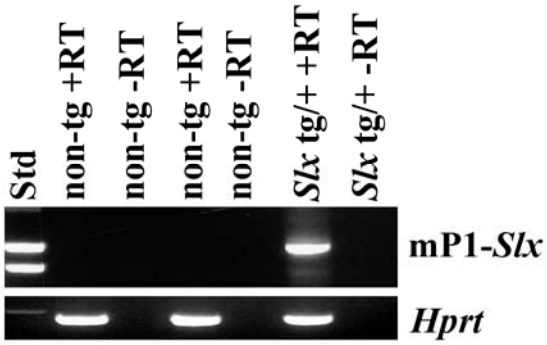

B)

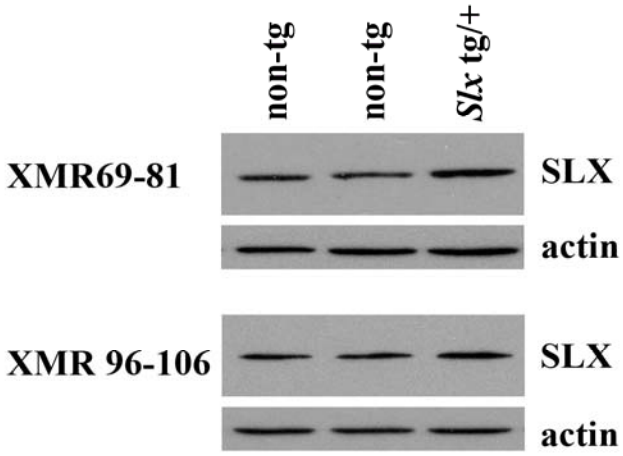

C)

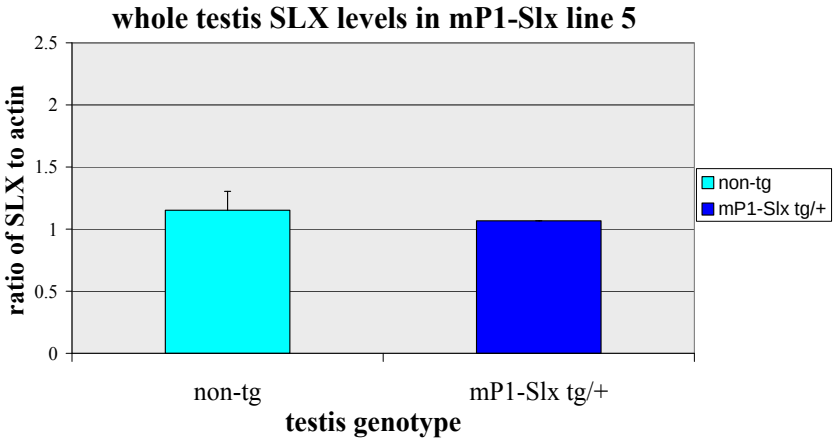

Figure 6.9 Expression analysis of mP1-*Slx* line 7

A) RT-PCR analysis of XY testis cDNA samples from males with and without the mP1-*Slx* transgene using primers that specifically amplify the transcript encoded by the transgene.

B) Western blot analysis of testis SLX levels in transgenic and non-transgenic males from mP1-*Slx* line 7

C) Quantification of testis SLX levels in males carrying the mP1-*Slx* transgene using non-transgenic littermates as a control. Error bars represent the standard error in SLX levels between males of the same genotype.

Figure 6.9

A)

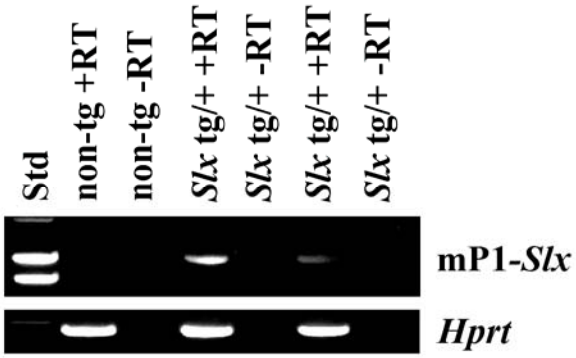

B)

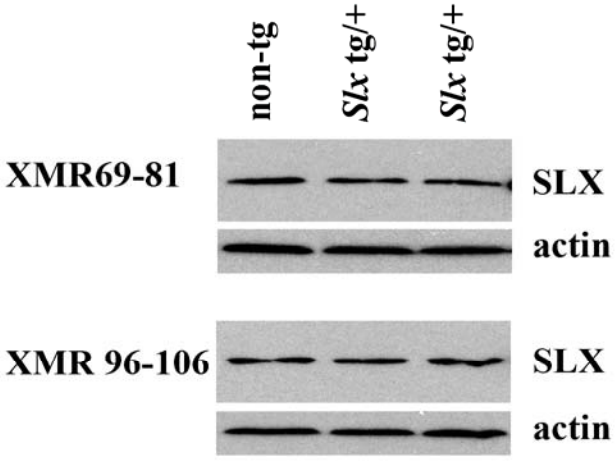

C)

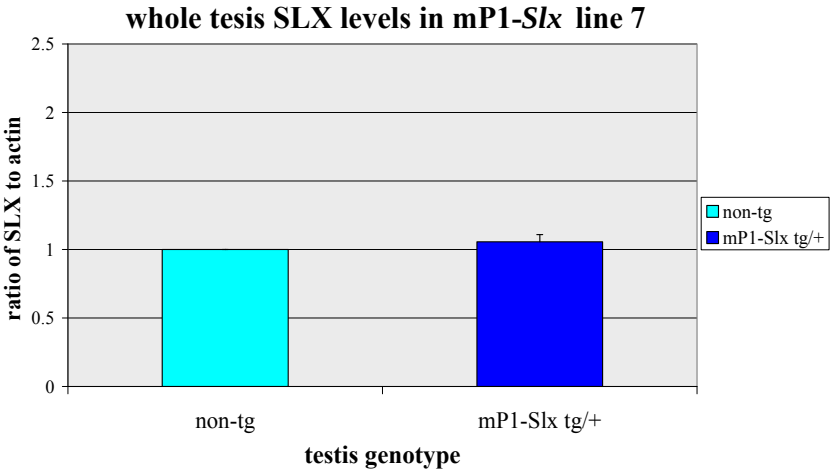

Figure 6.10 RT-PCR and western blot analysis of mP1-*Slx* line 8

A) RT-PCR analysis on whole testis RNA from transgenic and non-transgenic males using primers specific to the mP1-*Slx* transgene. A band representing the *Slx*-SV40 polyA fusion transcript is present in samples carry the mP1-*Slx* transgene, demonstrating that this transgene is expressed. No band is seen in –RT samples, indicating that there is no DNA contamination of these samples

B) Western blot analysis of whole testis SLX levels in XY males with or without the mP1-*Slx* transgene. Membranes were probed with two of the anti-SLX antibodies (anti-XMR$^{69\text{-}81}$ and anti-XMR$^{96\text{-}106}$) characterised in chapter 4 and then re-probed for actin as a loading control.

C) Quantification of SLX levels in the testis of mP1-*Slx* line 4 males hemizygous for the transgene with non-transgenic littermates as a control. The western blots from B) were scanned and the level of SLX was quantified as a ratio to actin using the ImageJ computer program. Error bars represent the standard deviation in SLX levels between individuals of the same genotype.

Figure 6.10

A)

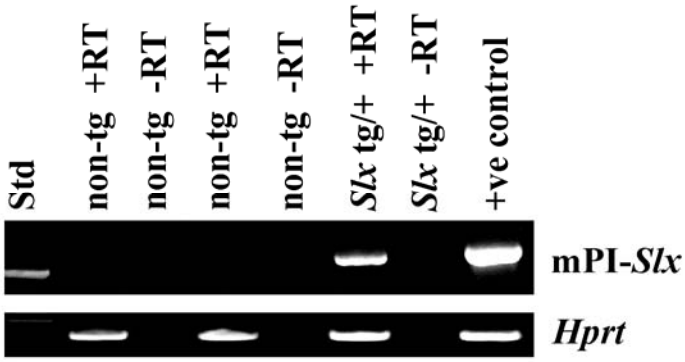

B)

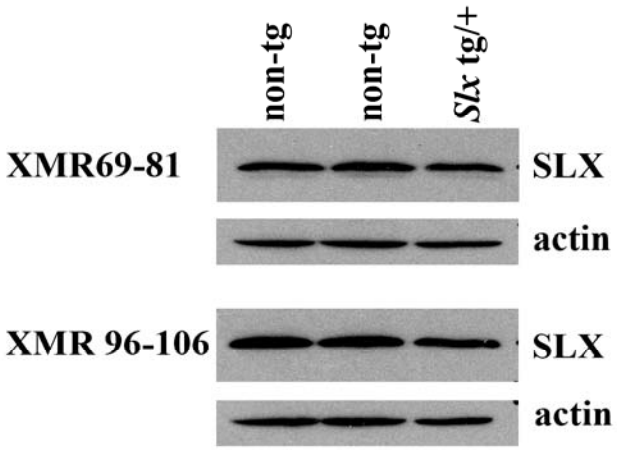

D)

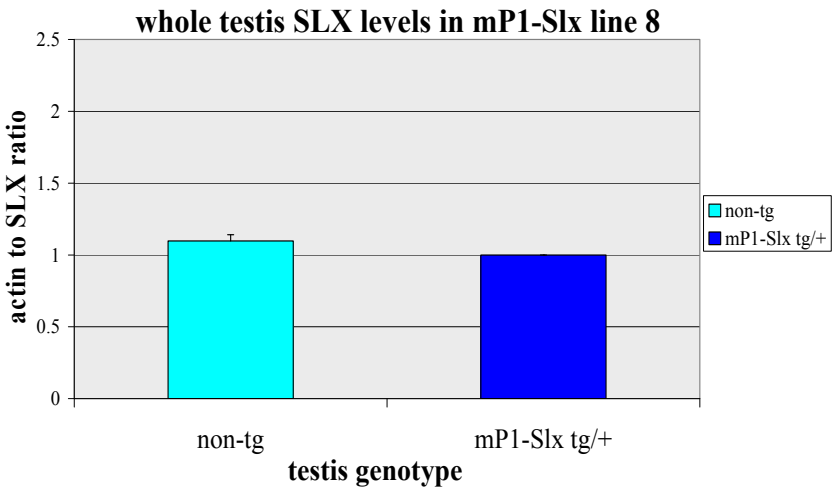

Figure 6.11 Expression analysis of mP1-*Slx* line 10

A) RT-PCR analysis using primers that specifically amplify the *Slx*-SV40 polyA fusion transcript encoded by the mP1-*Slx* transgene. A 1Kb band corresponding to this transcript is present in samples from hemizygous transgenic males, indicating that the mP1-*Slx* transgene is transcribed.

B) Western blot analysis of whole testis SLX levels in transgenic and non-transgenic mice. After being incubated with the anti-SLX antibodies, membranes were re-probed for actin as a loading control.

C) Quantification of SLX levels relative to actin in XY males with or without the mP1-*Slx* transgene based on the western blot films in B). Error bars represent the standard error in SLX levels between males of the same genotype.

Figure 6.11

A)

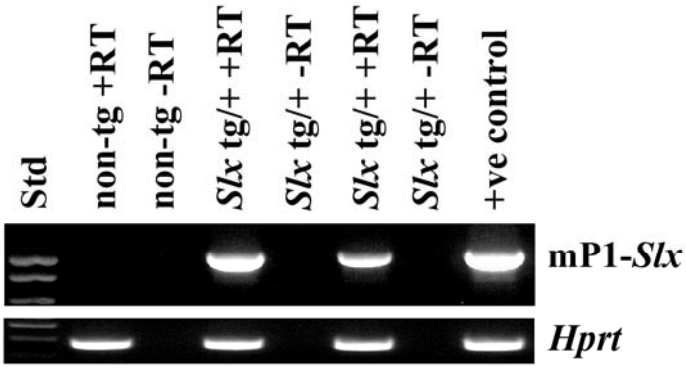

B)

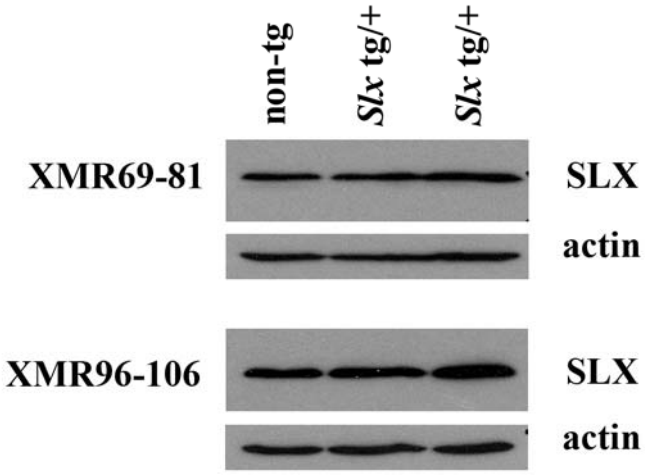

C)

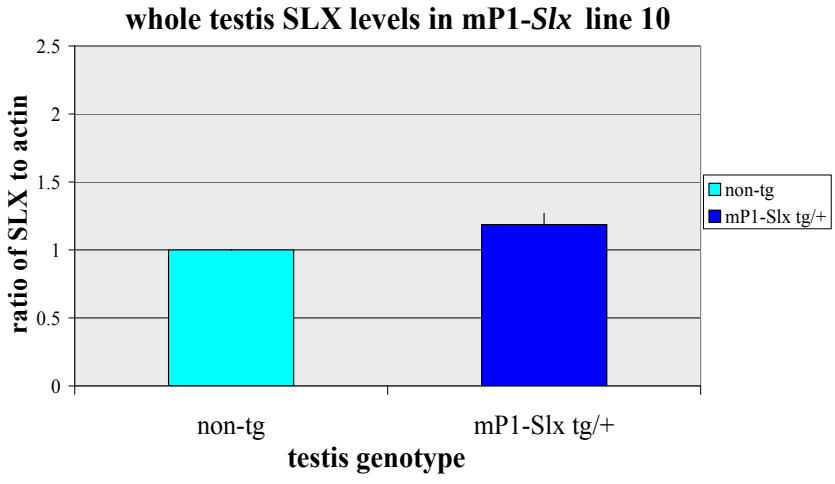

Figure 6.12 RT-PCR and western blot analysis of mP1-*Slx* line 11

A) RT-PCR analysis of XY testis cDNA samples from males with and without the mP1-*Slx* transgene using primers that specifically amplify the transcript encoded by the transgene.

B) Western blot analysis of testis SLX levels in transgenic and non-transgenic males from mP1-*Slx* line 7

C) Quantification of testis SLX levels in males carrying the mP1-*Slx* transgene using non-transgenic littermates as a control. Error bars represent the standard error in SLX levels between males of the same genotype.

Figure 6.12

A)

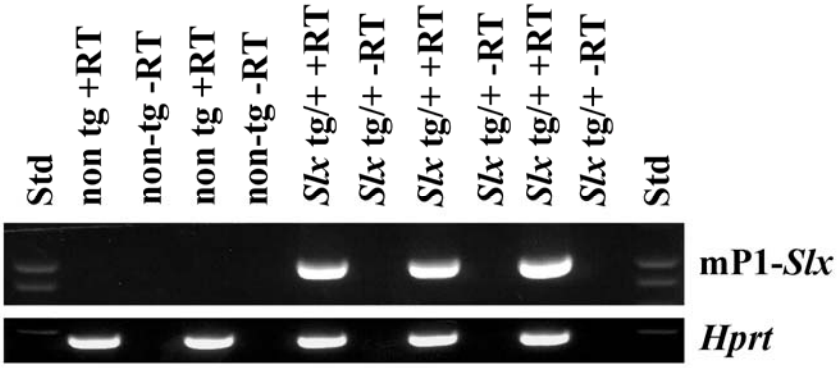

B)

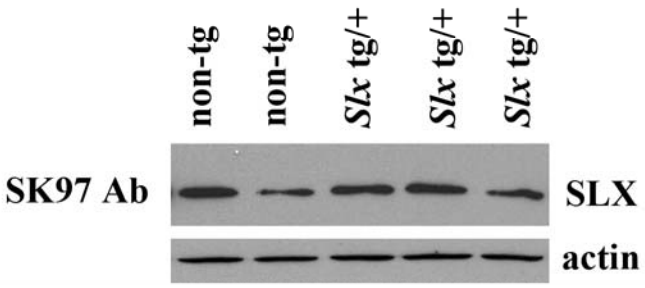

C)

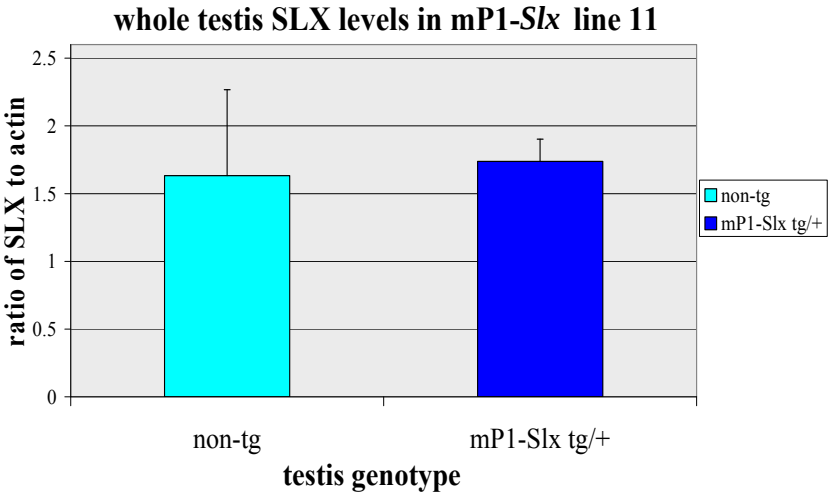

6.2.7 Generation of mP1-*Slx* cDNA transgenic mice

The western blot data presented above for the mP1-*Slx* transgenic lines suggest that although the mP1-*Slx* transgene is transcribed, it is not translated. This transgene contains the *Slx* ORF and so it is possible that sequences within the 5'UTR and 3'UTR of *Slx* are required for efficient translation in spermatids. I thus decided to make transgenic mice using the *Slx* cDNA sequence that includes these untranslated regions. However, there are several *Slx* transcript variants that all encode the same ORF but have different 5'UTR and 3'UTR sequences and it is unknown if all of these alternative transcripts are translated. I elected to use the official *Slx* transcript (accession number NM_009529), which contains the longest 3'UTR and 5'UTR and this was cloned into a construct containing the mP1 promoter and an SV40 poly A sequence. This plasmid was used for pronuclear injection and produced four transgenic founders. PCR analysis demonstrated that all four founders contain the full length transgenic *Slx* cDNA-SV40 polyA fusion sequence, although they appear to have different copy numbers of the transgene. These mice are currently being bred and transgenic offspring will be analysed.

6.3 Discussion

In this chapter, I have described the generation and characterisation of *Sly* and *Slx* transgenic mice. *Sly* transgenic mice were originally made by pronuclear injection using a Y chromosome BAC that contains a copy of this gene. Two transmitting transgenic founders with the complete *Sly* gene were produced. RT-PCR data revealed that the transgene is transcribed in both transgenic lines, although only one line produces low levels of transgenic SLY protein. No amelioration of the sperm head defects were observed in 2/3MSYq- mice carrying the BAC transgene, possibly due to low levels of transgene expression. Next, a construct was produced containing the *Sly* ORF driven by the spermatid-specific mouse protamine 1 (mP1) promoter and used to make two transgenic lines. Preliminary western blot analysis for one of the mP1-*Sly* lines suggests that the transgene is transcribed and translated. The mP1 promoter was also used to generate transgenic mice containing the *Slx* ORF, but although the six mP1-*Slx* lines analysed transcribed the transgene, no increase in testis SLX levels were seen. New *Slx* transgenics were made using the full length official *Slx* cDNA sequence driven by the mP1 promoter and these lines are currently being bred.

Northern blot analysis of *Sly*-containing BAC transgenic Ylr 8 line showed that the level of *Sly* mRNA in the testes of hemizygous transgenic males did not differ significantly from non-transgenic littermates. This suggests that the *Sly* transgene is expressed at very low levels. It is possible that the transgene is present in only one or two copies and is therefore unable to drive expression of *Sly* equal to endogenous levels. However, this explanation does not coincide with recent observations by Mueller et al. (2008). They reported that the degree of post-meiotic repression of X-linked genes is dependent on the gene copy number, and suggested that X-linked gene amplification may have evolved to compensate for post-meiotic repression of the sex chromosomes. This idea could also explain the highly amplified nature of MSYq-linked genes, all of which are expressed specifically in spermatids. Assuming this theory is correct, once an X- or Y-linked gene is located on an autosome away from the repressive chromatin environment affecting the sex chromosomes, it is predicted to be expressed at high levels. Thus a single copy of the *Sly* containing Ylr 8 transgene would be expected to be sufficient to drive high levels of *Sly* transcription now that the gene has been removed from the Y chromosome. This is not the case for the Ylr 8 transgenic line.

One explanation for the low level of transgenic *Sly* expression in the Ylr 8 line is that the transgene may present in multiple copies as a concatameric array. In transgenic plants, *Drosophila melanogaster* and mammals, it has been reported that as the copy number of a transgene increases, there is a decline in the expression of the transgene, a phenomenon known as repeat-induced gene silencing. DNA methylation and chromatin compaction of a transgenic locus is enhanced as the transgene copy number increases, resulting in heterochromatinisation (Garrick et al., 1998). Thus, although the *Sly* transgene is located away from the repressive effects of the Y chromosomes in the Ylr 8 line, it may still be suppressed, resulting in low expression of the transgene. An alternative explanation is that the *Sly* locus contained within the RP24-402P5 BAC used to make transgenics lacks some of the enhancer elements needed to drive high levels of expression. It is also plausible that the endogenous copies of *Sly* are all transcribed at different levels, possibly due to differences within their promoter sequences. The *Sly* copy used to make transgenics may normally be expressed at low levels in the testis as a result of an inefficient promoter. Therefore, autosomal integration of this *Sly* locus may have no effect on the level of transcription of this gene.

To determine if *Sly* is able to complement one or more of the MSYq deletion phenotypes, it is necessary for normal levels of SLY to be restored in these mice. As *Sly* is present in approximately 65 copies, low copy number BAC transgenic lines may never be able to express the transgene at sufficiently high levels. The mouse protamine 1 (mP1) promoter drives transgene expression specifically in round spermatids (Peschon et al., 1987). This promoter has been used to make transgenic mice expressing near-endogenous levels of *Rbmy*, a gene on the mouse Y chromosome short arm present in approximately fifty copies (Szot et al., 2003). Two mP1-*Sly* transgenic mice lines were generated, and preliminary results indicate that one of these lines may be transcribing and translating the transgene. Both transgenic lines are currently being bred onto the 2/3MSYq- background and will be analysed to see if the transgene is transcribed and translated. If this is found to be the case, and the SLY protein levels reach those observed in an XY testis, it will be very interesting to see if 9/10MSYq- and MSYq- mice carrying the transgene are fertile or if the offspring sex ratio distortion is corrected in transgenic 2/3MSYq- mice. The sperm from transgenic mice will be examined in detail to determine if the *Sly* transgene is able to rescue the sperm

head defects observed in the three MSYq deletion models. Analysis of the X and Y-linked gene transcription in round spermatids from MSYq- mice with and without the mP1-*Sly* transgene will reveal if *Sly* plays a role in the PSCR defects seen in the MSYq- mice. These transgenic mice could also be used for over-expression studies and to identify any regulatory interaction between *Sly* and *Slx*.

In the previous chapter, it was shown that SLX levels are significantly increased in spermatids from mice with deletions of the MSYq. It is therefore plausible that over-expression of SLX contributes to one or more of the phenotypes seen in these mice including offspring sex ratio distortion, defective PSCR and increased numbers of abnormal sperm. To investigate this possibility, mP1-*Slx* transgenic mice were made and all six transgenic lines analysed were transcribed. However, none of the lines had an increase in testis SLX levels in mice carrying the mP1-*Slx* transgene compared to non-transgenic littermates by western blot analysis. This could be due to low levels of mP1-*Slx* transgene expression transgene and northern blot analysis could be employed to verify this idea. However, the mP1 promoter is a strong promoter and so is expected to drive high levels of transgene expression. While it is possible that the DNA surrounding the transgenic locus represses transcription of the mP1-*Slx* transgene, it is unlikely that the transgene has integrated into repressive regions of the genome in all six transgenic lines. Furthermore, the copy number of the transgene is expected to differ between each line and this should result in variation in the level of transgene expression.

The lack of SLX up-regulation in mP1-*Slx* transgenic mice could be accounted for if the *Slx*-SV40 polyA fusion transcript encoded by this transgene is not translated. The mP1-*Slx* transgene only contains the *Slx* ORF and so does not contain the 3' and 5' untranslated regions found in the full length *Slx* transcript.. The untranslated regions of many mRNAs, including the mouse protamine 1 transcript, are important for temporal control of protein translation (Braun, 1990; Braun et al., 1989). The 3'UTR and 5'UTR may contain binding sites for regulatory proteins and miRNAs (reviewed by Derrigo et al., 2000), and are known to influence sub-cellular protein localisation (Braun et al., 1989). The untranslated sequences in the *Slx* mRNA could therefore contain elements that are essential for translation, and so new mP1-*Slx* cDNA transgenics were made using the mP1 promoter to drive transcription of the full length *Slx* cDNA sequence rather than the ORF. These lines are currently breeding and will hopefully transcribe

and translate the *Slx* cDNA transgene. However, the expression levels of these new mP1-*Slx* cDNA transgenic lines may be insufficient to illuminate the effect that SLX over-expression has on spermiogenesis. In light of the multicopy nature of *Slx*, RNAi-mediated knockdown may be the best approach to elucidate the specific function of this gene in spermatid development and function.

In conclusion, examination of mice transgenic for either *Sly* or *Slx* has so far failed to uncover the role of these genes in mouse spermiogenesis. New transgenic lines have been made using constructs that are expected to drive expression of the transgenes at levels equal to those observed for the endogenous *Sly* and *Slx* genes. The mP1-*Sly* and mP1-*Slx* cDNA transgenic lines may prove invaluable in ascertaining the function of these genes during sperm develop and identifying whether they contribute to the phenotypes observed in the three MSYq deletion mouse models.

Chapter 7

General discussion and future directions

General discussion and future directions

Analysis of germ cells in an XO/XYY mosaic mouse provided the first indication that the mouse Y chromosome has a role in spermatogenesis (Evans et al., 1969). Deletions of the MSYq are associated with an increased incidence of sperm head defects, abnormal sperm motility, offspring sex ratio distortion and reduced or absent fertilising ability (Burgoyne et al., 1992; Conway et al., 1994; Grzmil et al., 2007; Styrna et al., 2002; Styrna et al., 1991a; Styrna et al., 2003; Styrna et al., 1991b; Styrna and Krzanowska, 1995; Touré et al., 2004b; Xian et al., 1992). Furthermore, the MSYq appears to regulate the expression of a small number of X- and Yp-linked genes during spermiogenesis; these genes are up-regulated in spermatids from mice with MSYq deletions in proportion to the deletion size (Ellis et al., 2005). The correlation between the extent of the MSYq deletion and the severity of the testicular phenotypes exhibited by mice with these deletions led Burgoyne et al. (1992) to suggest that a multicopy 'spermiogenesis factor' on the MSYq may be responsible. However, the identity of this factor is currently unknown.

Touré et al. (2005) and Ellis et al. (2005) proposed that one promising candidate for the 'spermiogenesis factor' is *Sly*, a newly identified multicopy Yq-encoded gene. The putative SLY protein shares a substantial degree of homology to the XLR superfamily of nuclear proteins, all of which contain a conserved COR1 domain implicated in chromatin binding (Bergsagel et al., 1994; Calenda et al., 1994; Ellis et al., 2005; Lammers et al., 1994; Touré et al., 2005). Ellis and colleagues (Ellis et al., 2005) proposed that the putative SLY plays a key function in sperm development by binding to the sex chromosomes in spermatids, potentially regulating their gene expression and chromatin conformation. Based on this hypothesis, it was suggested that the increased prevalence of abnormal spermatozoa and offspring sex ratio distortion in the MSYq deletion models may be a consequence of *Sly* deficiency triggering the up-regulation of sex-linked genes involved in sperm head development and meiotic drive. The primary objective of the studies carried out in this thesis was to explore the role of *Sly* and its X-linked homologue (*Xmr*/*Slx*) in spermatogenesis, and to determine to what extent these genes contribute to the phenotypes associated with MSYq deletions.

7.1 *Sly* encodes a spermatid cytoplasmic protein and is implicated in acrosome development and function

In agreement with previous studies (Ellis et al., 2005; Touré et al., 2005), analysis of nascent *Sly* transcripts confirmed that this gene is transcribed exclusively in the testis during spermiogenesis in virtually all Y-bearing round spermatids. The expression and function of the SLY protein was also characterised in detail in chapter 3. Inconsistent with the predicted chromatin-associated role of this protein (Ellis et al., 2005; Touré et al., 2005), SLY localised to the spermatid cytoplasm, potentially due to a mutation of the NLS motif present in the related XLR and SYCP3 proteins. These results indicate that SLY is unlikely to directly regulate the chromatin conformation and gene expression of the X and Y chromosomes in spermatids as hypothesised (Ellis et al., 2005), although this cannot be completely ruled out based on the present data. To gain insight into the function of SLY in spermiogenesis, a yeast-two-hybrid screen was performed and this identified several potential interacting proteins, including the acrosomal protein DKKL1, the histone acetyltransferase TIP60 and the chromatoid body protein RanBMP (Kohn et al., 2005; McAllister et al., 2002; Shibata et al., 2004).

Co-immunoprecipitation confirmed the interaction between SLY and DKKL1, advocating a role for SLY in development or function of the acrosome. The acrosome is a cap-like structure that forms over the head of the sperm and contains enzymes such as acrosin, a trypsin-like protease, that are essential for digesting the zona pellucida at fertilisation (reviewed by Geraci and Giudice, 2006). Although the acrosome has not been examined in spermatids from our 2/3MYSq-, 9/10MSYq- and MSYq- models, numerous acrosomal defects have been reported in sperm from B10.BR-Y^{del} mice that lack approximately two-thirds of the MSYq (Siruntawineti et al., 2002; Styrna et al., 1991a; Styrna et al., 2003). The Y^{del} mice have an increase in the percentage of sperm with abnormal heads, the most common defect being a flattening of the sperm head not observed in normal mice; this flattening has been ascribed to the abnormal formation of the acrosome during spermiogenesis. Electron microscopy revealed that the acrosomal vesicle in some round spermatids from Y^{del} mice does not contain pro-acrosomal granules, although the acrosomal cap forms normally (Styrna et al., 1991a). The shape of the acrosomal vesicle is also distorted in some spermatids, leading to an invagination into the nucleus (Styrna et al., 2003). Small, round vesicles form in the

acrosome of Y^{del} elongating spermatids beginning at tubule stage IX, and these are retained in condensing spermatids undergoing spermiation (Siruntawineti et al., 2002). In addition, the proportion of spermatids with vesicles is similar to the frequency of sperm with flat heads, leading to the suggestion that these vesicles are responsible for the flattened acrosome in Y^{del} mice (Siruntawineti et al., 2002). Analysis of epididymal sperm demonstrated that Y^{del} mice have an increased incidence of sperm with damaged or absent acrosomes and a decrease in the proportion of live sperm (Styrna et al., 2003; Styrna and Krzanowska, 1995). Furthermore, sperm from Y^{del} mice have decreased levels and activity of acrosin (Styrna et al., 1991a). This is thought to contribute to the reduced *in vitro* fertilising ability of Y^{del} mice (Xian et al., 1992).

The aberrant acrosome formation and content observed in the Y^{del} sperm led Styrna and colleagues (Styrna et al., 1991a; Styrna et al., 1991b) to conclude that a MSYq-linked factor is involved in controlling acrosomal development by co-ordinating the various synthetic and morphological processes involved. Examination of the acrosome in 2/3MSYq-, 9/10MSYq- and MSYq- spermatids is expected to substantiate the conclusion that a MSYq gene is necessary for normal acrosome formation. The interaction between SLY and DKKL1 is a compelling piece of evidence for *Sly* being the acrosomal factor, and this could be confirmed by expressing endogenous levels of *Sly* from a transgene in the MSYq deletion models. It has been hypothesised that DKKL1 plays a role in facilitating acrosome formation, preventing premature spermiation or guiding the mature sperm to the oocyte (Kohn et al., 2005), and defects in these processes have been reported in the MSYq deletion models (Siruntawineti et al., 2002; Styrna et al., 2002; Styrna et al., 1991a; Styrna et al., 2003; Styrna et al., 1991b; Styrna and Krzanowska, 1995; Touré et al., 2004b; Ward et al., 2006; Xian et al., 1992). One area of future research will be to investigate if the localisation and activity of DKKL1 and other acrosomal proteins are altered in the three MSYq deletion models, in order to establish the underlying cause of the acrosomal defects associated with deletion of the MSYq.

Besides its prospective role in the acrosome, SLY may be involved in other spermiogenic processes. Although cytoplasmic, SLY could indirectly repress transcription of the X- and Yp-encoded genes during spermiogenesis through its potential interaction with the histone acetyltransferase TIP60; this is discussed in more detail below in section 7.6.

7.2 *Slx* is transcribed in spermatids and encodes a cytoplasmic protein

The results of chapter 3 imply that SLY is not a chromatin-associated nuclear protein, and so it is improbable that SLY directly regulates the chromatin conformation and transcription of the sex chromosomes during spermiogenesis as previously hypothesised (Ellis et al., 2005). However, another candidate gene for the up-regulation of X- and Y-encoded genes in the three MSYq deletion models is *Slx* (previously *Xmr*), the multicopy X-linked homologue of *Sly*. *Slx* was reported to encode a testis-specific nuclear protein that localises to the transcriptionally silent sex body domain in pachytene spermatocytes (Calenda et al., 1994; Escalier and Garchon 2005; Escalier and Garchon 2000). Further analysis of *Slx* suggested that this gene is also transcribed in round and early elongating spermatids (Ellis et al., 2005). In chapter 4, I re-examined the transcription and translation of *Slx* during spermatogenesis to ascertain if the protein encoded by this gene is involved in regulating sex-linked gene expression during spermiogenesis.

My findings, as well as data from published microarray studies, substantiated reports from Ellis et al. (2005) that *Slx* is transcribed predominantly in spermatids with little or no evidence of transcription during meiosis. Consistent with the transcriptional data, protein analysis using three antibodies designed specifically to SLX revealed that this protein is undetectable in meiotic cells. Instead, SLX is expressed in spermatids from stages 2 to 11, where it localises to the cytoplasmic compartment. To explain the contradictory SLX expression patterns reported in previous studies by the Garchon group (Calenda et al., 1994; Escalier and Garchon, 2005; Escalier and Garchon, 2000) and those described in chapter 4, I demonstrated that the anti-XLR antibody used in the earlier studies is unable to detect SLX. The identity of the sex-body protein recognised by the anti-XLR antibody is currently unknown, although XLR is a very good candidate based on its expression pattern in oocytes during female meiosis (Escalier et al., 2002) and my findings that the gene encoding this protein is transcribed in the testis.

The cytoplasmic localisation of SLX can be explained by loss of the NLS motif present in XLR due to changes in the intron/exon boundaries between *Slx* and *Xlr* (Ellis et al., 2007). Nevertheless, my analysis of *S. cerevisiae* transformed with a *Slx*-containing plasmid reveals that the protein encoded by *Slx* has transcriptional activator

activity when present in the nucleus. This raises the possibility that SLX is involved in controlling gene activity during spermiogenesis, although this idea is not supported by the results of chapter 4. It is feasible that SLX is present in the spermatid nucleus at a level undetectable by conventional techniques. Alternatively, SLX may re-localise to the nucleus in response to a specific physiological stimuli such as heat shock. In either case, SLX localisation to the nucleus would require chaperone proteins to transport it into the nucleus due to loss of the NLS. In addition, if SLX is involved in transcriptional regulation, it is expected to form complexes with other chromatin-associated proteins such as transcription factors and chromatin modifiers. Unfortunately, identification of SLX interacting proteins was not possible by a yeast two-hybrid-screen, and the role of SLX in spermiogenesis is unknown at present. Examination of mice that are deficient for, or over-express *Slx* will help to uncover the function of SLX; future studies should concentrate on analysing the downstream transcriptional changes in these mice, paying particular attention to the transcription of genes located on the sex chromosomes.

7.3. PSCR and the epigenetic profile of the sex chromosomes are disturbed in round spermatids from the MSYq deletion models

Ellis and colleagues (Ellis et al., 2005) presumed that the increased mRNA levels of specific sex-linked genes in MSYq deletion models was a consequence of increased transcription of these genes, possibly due to defects in PSCR. However, less than 1% of the genes encoded by the X and Y chromosomes were reported to be differentially expressed in the three MSYq deletion models. This suggests that the up-regulation is restricted to a small group of predominantly spermatid-expressed genes. In chapter 5, RNA FISH was used to examine if the up-regulated mRNA levels of these X- and Yp-encoded genes resulted from increased gene transcription. For all spermatid-expressed X- and Yp-encoded genes assayed, the percentage of round spermatids transcribing the gene (evidenced by an RNA FISH signal) was significantly increased in MSYq- males compared to XY controls. This up-regulation was independent of gene copy number, expression pattern, and sub-chromosomal location, but was restricted to sex-linked genes in agreement with previous data (Ellis et al., 2005). Together, the RNA FISH studies imply that the increased sex-linked transcript levels in the three MSYq deletion

models is a consequence of a universal reduction in spermatid sex chromosome repression that affects all spermatid-expressed sex-linked genes. However, an additional post-transcriptional effect cannot be dismissed. Analysis of *Slx* and an X-linked reporter gene revealed that up-regulation of these genes is associated with increased protein levels, and thus over-expression of X- and Yp-encoded proteins may contribute to or be the cause of the defective sperm heads exhibited by the MSYq deletion models.

The epigenetic profile of round spermatids from MSYq- males were also investigated in chapter 5, and a number of changes were observed. These include reduced enrichment of the heterochromatin-associated histone modification $H3_{K9me3}$ and heterochromatin protein CBX1 on the sex chromosome chromatin domain, and decreased levels of the 'active' histone modification $H4_{K8Ac}$ on the sex chromosome. Alterations to the histone code may occur prior to spermiogenesis, as indicated by the unusual enrichment of $H3_{K9me3}$ on the pericentric heterochromatin of MI cells in the MSYq- testis. Thus, future research should concentrate on determining exactly when the transcriptional up-regulation and changes to the epigenetic character of the sex chromosomes first occur in the testes of MSYq- mice. In addition, the replacement of histones with transition proteins and protamines should also be analysed in MSYq- spermatids, to examine whether defects in chromatin condensation may be responsible for the grossly abnormal morphology of 9/10MSYq- and MSYq- sperm.

A similar up-regulation X-encoded transcripts has been reported in spermatids from mice lacking the ubiquitin-conjugating enzyme HR6B (Baarends et al., 2007). One of the affected genes is *Ube1x*, and this gene is also up-regulated in the MSYq- testis (Ellis et al., 2005). Baarends et al. (2007) suggested that the increased transcription of X-linked genes in *Hr6b*-/- spermatids is a consequence of defective PSCR, although it is not known if Y-encoded genes are also up-regulated. The heterochromatin-associated histone modification $H3_{K9me2}$ is absent on the chromocentre of *Hr6b*-/- spermatids (Baarends et al., 2007); this modification is also absent on the chromocentre in a significantly higher proportion of MSYq- spermatids than XY spermatids. Furthermore, the two models are alike in that the enrichment of $H3_{K9me2}$ on the sex chromosome is unaffected (Baarends et al., 2007). The phenotypes of MSYq- and *Hr6b*-/- spermatids are very similar with respect to X-linked gene transcription and altered epigenetic marks on sex chromosomes, and suggest that PSCR is also defective

in spermatids from MSYq- mice.

The cause-effect relationship between the altered sex chromosome histone code and the reduced efficiency of PSCR in *Hr6b*-/- spermatids and MSYq- spermatids has not yet been explored. The increased sex-linked gene transcription in the MSYq- spermatids may be the result of altered sex chromosome chromatin conformation caused by changes in their epigenetic profile; this could allow the transcriptional machinery increased chromatin access. For example, over-expression of the *S. pombe* Epe1 protein reduces the levels of $H3_{K9me2}$ at heterochromatic domains, increasing transcription from these regions (Zofall and Grewal, 2006). Alternatively, increased transcription of the sex chromosomes during spermiogenesis may lead to the replacement of facultative heterochromatin markers such as $H3_{K9me3}$ with 'active' modifications and proteins. Nevertheless, the correlation between defective PSCR and changes in the epigenetic profile of the sex chromosomes in MSYq- spermatids suggest an unidentified MSYq-linked factor is required for establishment and maintenance of PSCR in normal spermatids. Moreover, the similarities between the altered PSCR, epigenetic profile and sperm-head phenotypes of spermatids deficient for HR6B and those with MSYq deletions, indicate that *Hr6b* and the putative MSYq encoded factor may be components of the same genetic pathway involved in controlling PSCR. Hypotheses that could explain the underlying molecular basis of PSCR and the role played by a Y-linked 'PSCR' factor are presented in section 7.6.

7.4 Identifying the function of *Sly* and *Slx* in spermiogenesis by transgenic analysis

The experiments described in chapters 3-5 failed to identify the role of *Sly* and *Slx* in spermiogenesis, although deletion analysis and a yeast-two-hybrid screen suggest that *Sly* may be involved in acrosome formation and/or function. In an attempt to determine if *Sly* deficiency is the underlying genetic cause of the testicular phenotypes associated with MSYq deletions, this gene was re-introduced into the 2/3MSYq- and MSYq- backgrounds. No amelioration of the sperm head abnormalities or defective PSCR was observed in males carrying an *Sly* BAC transgene compared to non-transgenic controls. However, this may be due to very low levels of transgene expression rather

than failure of *Sly* to rescue these phenotypes. In order to achieve near-endogenous levels of *Sly* expression, new *Sly* transgenic lines were created using the spermatid-specific mouse protamine 1 (mP1) promoter. Preliminary data suggests that at least one of the mP1-*Sly* transgenic lines is expressing the transgene at high levels. Should this be the case, this line will prove invaluable for confirming the potential role of *Sly* as a regulator of acrosome formation, as discussed above. The mP1-*Sly* transgenic mice will also be useful in determining whether *Sly* deficiency is a factor in other MSYq deletion phenotypes such as sex-ratio distortion. In addition, by allowing the effect of *Sly* over-expression on *Slx* transcription and translation to be investigated *in vivo*, mP1-*Sly* transgenic mice may expose the alleged regulatory relationship between *Sly* and *Slx* predicted by Ellis et al. (2005).

Deletion of the MSYq is associated with over-expression of SLX and this may contribute to one or more testicular phenotypes reported in the three MSYq deletion models. Chapter 6 also described the production and expression of mP1-*Slx* transgenic lines which were made to investigate this possibility. Although all mP1-*Slx* transgenic lines analysed were transcribed, there was no obvious difference in testis SLX levels between transgenic and non-transgenic mice, suggesting that the transgene is not translated or is translated at undetectable levels. New *Slx* transgenic lines were made that contained the 3' and 5' untranslated regions that may be required for efficient translation, and these mP1-*Slx* cDNA mice are currently being bred. If the mP1-*Slx* cDNA transgenic lines are not expressed at high levels, RNAi-mediated knock down of *Slx* may be the only way to elucidate the role of this gene during spermiogenesis in normal and MSYq deletion mice.

7.5 Does the MSYq encode a suppressor of meiotic drive?

A meiotic driver is a genetic element (an allele, gene or chromosome variant) that increases its own transmission to the next generation at the expense of gametes that do not carry the element. Meiotic driver systems have been described in a wide variety of organisms including fungi, insects, plants and mammals (reviewed by Lyttle, 1991), and are located on autosomes (e.g. the *t*-complex in mice; Lyon, 2000) and sex chromosomes (e.g. the *Dox* gene in *D. simulans*; Tao et al., 2007a). Mathematical

models suggest that the sex chromosomes are more likely to evolve and maintain meiotic drivers than autosomes (Hurst and Pomiankowski, 1991). This is because the sex chromosomes are genetically isolated from each other and so mutations biasing the sex ratio (sex ratio distorters or SRDs) can accumulate on these chromosomes as long as the biased transmission of the mutations outweighs their deleterious effects on fitness. X-linked meiotic drive has been reported in at least twelve species of *Drosophila* (Montchamp-Moreau, 2006) and appears to be more frequent than Y-linked meiotic drive, although this has been reported in the fruitfly *C. capitata* and the mosquito *A. aegypti* (Owusu-Daaku et al., 2007; Shahjahan et al., 2006).

As well as causing a deviation in the sex ratio, known SRDs reduce the overall male reproductive fitness because they reduce the number of functional sperm. Accordingly, there is strong selection for sex-linked or autosomal genes that suppress the deleterious effects of the distorter (Carvalho et al., 1997; Hamilton, 1967; Hurst, 1992; Montchamp-Moreau, 2006). However, if the suppressor gene acts in a dose-dependent fashion, then duplication of the driver element will alter sex ratio again causing an increased selective pressure for duplication of the suppressor gene. This may lead to a massive amplification of both elements and represents a dynamic intragenomic conflict or genetic 'arms race' between the distorter and suppressor (Hurst, 1992; Hurst, 1996). The effects of the sex ratio meiotic drive system are transient on an evolutionary time scale due to the rapid spread of suppressors within a population, and thus biased sex ratios are rarely observed in naturally occurring populations (Montchamp-Moreau, 2006; Tao et al., 2007b). However, new sex ratio distorters may evolve that are unaffected by existing suppressor elements, allowing sex ratio meiotic drive to continue *ad infinitum*. Such intragenomic conflict can change the architecture of the sex chromosomes to such a degree that geographically restricted populations may become reproductively isolated leading to speciation; this could account for the accelerated rate of evolution among meiotic and post-meiotic genes. The silencing of the mammalian sex chromosomes in the male germ line by MSCI and PSCR has been proposed to act as a genomic defence mechanism against sex ratio distorters by silencing these genes during and after meiosis, thus maintaining a normal sex ratio (Ellis et al., 2005; Montchamp-Moreau, 2006; Tao et al., 2007b; Turner et al., 2006).

The sex ratio distortion in offspring of 2/3MSYq- males is thought to be a consequence of a disruption in the equilibrium between an X-linked meiotic driver and a suppressor

gene located on the Yq. Several observations support this hypothesis, and these are described below. Firstly, there is markedly reduced transmission of the 2/3MSYq- chromosome in mice that produce Y and 2/3MSYq- gametes, despite abundant sperm containing the 2/3MSYq- chromosome being present in the epididymis (Burgoyne, 1998b). This implies that the 2/3MSYq- bearing sperm are out-competed by Y-bearing sperm, and this may be a consequence of meiotic drive; sperm competition studies in *Drosophila* have demonstrated that males with a driving X chromosome are at a disadvantage relative to males without a driving X chromosome (Taylor and Jaenike, 2002). Secondly, epididymal fluid from B10.BR control males is believed to contain a substance that has an inhibitory effect on the fertilising ability of sperm from B10.BR-Y^{del} males, which have a deletion of the MSYq (Xian et al., 1992). This is reminiscent of a study into the meiotic drive system of the stalk-eyed fly, *Cyrtodiopsis whitei*, which found that sperm from meiotic drive males may be incapacitated by seminal fluid from non-drive males (Fry and Wilkinson, 2004). Furthermore, the hybrid breakdown in male offspring of *M. m. domesticus* x *M. m. molossinus* intraspecific crosses is the result of incompatibility between X-linked gene(s) with autosomal and/or Y-linked gene(s); Haldane's rule (Haldane, 1922) suggests that the sterility of the heterogametic sex in the F1 generation of an interspecies cross may be caused by unbalancing of divergent meiotic drivers and suppressors. Together with the highly amplified nature of some spermatid-expressed X- and Yq-linked genes, these data suggest that there may be ongoing intragenomic conflict between the murine X and Y chromosomes which is revealed in mice with Yq deletions.

Two genetically characterised sex ratio meiotic drive systems are the *Dox*/*Nmy* distorter/suppressor complex in *D. simulans* (Tao et al., 2007a; Tao et al., 2007b) and the *Stellate*/*Supressor of Stellate* (*Ste*/*Su(Ste)*) system in *D. melanogaster* (Hurst, 1992; Hurst, 1996). Unbalancing of the *Dox* and *Ste* X-linked distorter genes from their suppressor results in a shortage of, or reduced fertilising ability of Y-bearing sperm by an unknown mechanism (Aravin et al., 2001; Tao et al., 2007a). In both cases, the suppressor gene has evolved by retrotransposition of the X-linked distorter gene (Balakireva et al., 1992; Tao et al., 2007b) and suppression appears to be mediated by a classical post-transcriptional RNAi mechanism. This has been convincingly demonstrated for *Ste*/*Su(Ste)*, where suppression requires components of the RNAi pathway including *aubergine,* and *spindle-E,* and involves the production of rasiRNAs (Aravin et al., 2004; Aravin et al., 2001; Nishida et al., 2007; Stapleton et al., 2001).

How X-linked meiotic drivers preferentially disrupt the development or function of Y-bearing sperm is currently unknown, although one possibility is that Y-bearing sperm are intrinsically more susceptible to the effects of the driver. For example, the sex ratio distortion in male flies carrying the *Dox* driver is attributed to defects in nuclear condensation in Y-bearing sperm. In this species, the Y chromosome is heterochromatic and larger than the X chromosome, so sperm containing the Y chromosome are more severely affected by problems with heterochromatin condensation compared to X-bearing sperm (Tao et al., 2007a). Alternatively, there could be unequal sharing of the meiotic driver or downstream products between X- and Y-bearing sperm, leading to defective maturation of Y-bearing spermatids.

Assuming a similar RNAi mediated mechanism is responsible for the putative X-linked meiotic drive system in mice, there are three multicopy MSYq-encoded candidate suppressor genes (*Ssty*, *Asty* and *Sly*) that arose by retrotransposition of their X-linked homologue. In addition, the multicopy *Orly* gene contains sequences derived from *Ssty*, *Asty* and *Sly* and so also shares homology with their X-linked progenitors (Ellis et al., 2007; Touré et al., 2005; Tour é et al., 2004). However, *Ssty* and *Sly* have retained their ORFs and encode for functional proteins unlike the *Nmy* and *Su(Ste)* suppressor genes in *Drosophila*. This suggests that any suppression of X-linked drivers by *Ssty* and *Sly* may be mediated at protein rather than RNA level, possibly by competition between the distorter and suppressor for interacting proteins. In contrast, any conflict between *Asty* and its X-encoded homologue *Astx* would almost certainly be mediated by an RNAi mechanism; *Asty* has lost the ORF found in *Astx*, although these genes share 92-94% nucleotide identity over introns and exons. The highly amplified copy number of *Asty* suggests that this gene has been selected for, despite not coding for a protein, indicating that *Asty* may act at the RNA level.

The underlying cause of the female-biased sex ratio observed in the offspring of 2/3MSYq- males may not represent the uncovering of an intragenomic conflict between an X-linked distorter element and a Yq-linked suppressor *per se*. Instead, the transcription of an X-linked distorter gene may be indirectly up-regulated in spermatids from the MSYq deletion models as a consequence of defective PSCR. Unless the suppressor of the X-linked meiotic driver is also sex-linked and thus up-regulated, the equilibrium between the driver and suppressor is disturbed. Mild over-expression of an X-linked distorter is expected to lead to sex ratio distortion as

observed in 2/3MSYq- mice if the distorter is usually suppressed in a dosage-dependent manner. Furthermore, gross over-expression of the X-linked distorter may be the cause of sterility in the 9/10MSYq- and MSYq- mice, as unrepressed drivers (e.g. *Stellate* in *D. melanogaster*) can lead to sterility rather than drive.

The *D. simulans* X chromosome is known to contain several distorter genes that act together to produce meiotic drive (reviewed by Montchamp-Moreau, 2006), and this could also be the case with the mouse X chromosome. Multiple X-linked distorter genes are expected to be targeted for suppression by a variety of autosomal and Y-linked elements. Polymorphisms in the expression levels of X-linked distorters, and their Y-linked and autosomally-encoded suppressor genes may underlie the variation in the proportion of sperm abnormalities, the shape of the sperm head and the offspring sex ratio in different laboratory mice strains. Several testis-transcribed genes are differentially expressed between different mice species and subspecies including X-linked *Slx* gene (Voolstra et al., 2007; R Scarvetta and D Tautz, personal communication). Furthermore, mice carrying the Y^{RIII} chromosome differ in the proportion of abnormal sperm and offspring sex ratio depending on the genetic background, with both phenotypes more severely affected on inbred backgrounds (Conway et al., 1994). This implies that Y-linked elements interact with X-linked and autosomal genes whose expression varies between mice strains, and these operate together to control sperm head development and the sex ratio.

7. 6 Does the Y chromosome have a role in regulating PSCR?

The heterochromatic structure and transcriptional repression of the sex chromosomes in spermatids is a downstream consequence of MSCI (Turner et al., 2006). In addition, PSCR is not specific to the sex chromosomes; unpaired autosomal regions subject to MSUC in spermatocytes continue to be repressed in spermatids and become enriched in histone modifications associated with inactive chromatin (Turner et al., 2006). The transition from MSCI to PSCR has not been clearly defined, and may represent a continual process. However, although the molecular basis for MSCI is known and involves BRCA1, ATR and γH2AX (reviewed by Turner, 2007), these proteins are not maintained on the sex chromosomes in spermatids and the mechanism underlying

PSCR is currently unknown. The defective transcriptional repression and disturbed epigenetic profiles of the spermatid sex chromosomes in the MSYq- mice suggest that one or more genetic factors on the MSYq are required for normal PSCR to occur. Identifying the putative MSYq-encoded 'PSCR factor' will be an exciting area of future research that will help to elucidate the molecular basis for PSCR and may have wider implications for epigenetic gene regulation and sex chromosome evolution.

There are several ways in which a gene on the MSYq could regulate PSCR. Firstly this factor may act at the protein level and two candidate genes are *Ssty1* and *Sly*, both of which are known to encode spermatid proteins. *Ssty1* is a member of the *Spin/Ssty* gene family and encodes a protein that shares homology with SPIN, a protein that localises to the metaphase spindle in mouse oocytes (Oh et al., 1998; Touré et al., 2004a). However, the function and mode of action of SSTY1 and SPIN have not been identified, nor has the cellular localisation of SSTY1 (Oh et al., 1998; Touré et al., 2004a). It is conceivable that SSTY1 is a nuclear protein involved in controlling sex chromosome gene expression during spermiogenesis, although structural prediction programs have not identified any chromatin or DNA binding domains within the SSTY protein (Touré et al., 2004a).

Expression analysis of SLY indicates that this protein is cytoplasmic and thus unlikely to directly regulate sex chromosome gene expression and epigenetic modifications in spermatids. However, one of the proteins found to interact with SLY in a yeast-two-hybrid screen is the tumour suppressor histone acetyltransferase TIP60 (Gorrini et al., 2007). The TIP60 complex is involved in chromatin remodelling including dephosphorylation of nucleosomal γH2AX (Jha et al., 2008), exchange of phosphorylated H2AV for unmodified H2AV in regions of DNA damage (Kusch et al., 2004; reviewed by Morrison and Shen, 2005), and chromatin incorporation of the histone variant H2AZ (Auger et al., 2008). TIP60 can interact with a variety of transcription factors and chromatin remodelling complexes to regulate gene transcription by repressing or stimulating activity of specific promoters (Ai et al., 2007; DeRan et al., 2008; Liu et al., 2007a). TIP60 can also affect transcription through altering the local chromatin conformation and the TIP60 complex has been shown to promote the generation of silent heterochromatin in *Drosophila* (Qi et al., 2006). In addition, several proteins are acetylated by TIP60 leading to activation (e.g. ATM; Sun et al., 2007) or suppression (e.g. Notch IC; Kim et al., 2007a) of target

proteins. SLY may bind to TIP60 in the cytoplasm, although antibody staining suggests that the majority of TIP60 is found in the nucleus (see Figure 3.8.D). In MSYq- spermatids, absence of SLY could alter the activity or cellular localisation of TIP60, potentially explaining the defective PSCR and reduction/loss of histone $H4_{K8}$ acetylation on the sex chromosomes.

Rather than act at the protein level, the MSYq may encode a non-coding RNA (ncRNA) that can regulate PSCR and the histone modifications associated with the spermatid sex chromosomes. Non-coding RNAs that coat the X chromosome have been described in mammals (e.g. the *Xist* RNA that mediates female X inactivation; reviewed by Masui and Heard, 2006) and *Drosophila* (the *roX* transcripts involved in male dosage compensation; reviewed by Deng and Meller, 2006). These ncRNAs alter the chromatin conformation and gene expression of the X chromosome to cause chromosome wide transcriptional silencing or transcriptional up-regulation respectively. It is thus feasible that a ncRNA could localise to the sex chromosome in spermatids and mediate PSCR in a manner analogous to the *Xist* RNA in imprinted and random X-inactivation. This non-coding RNA may be derived from the MSYq, or an MSYq-encoded genetic element could regulate the localisation of the ncRNA to the X and Y chromosomes in spermatids. Nevertheless, in both scenarios, the consequence of MSYq deletions would be loss of this non-coding transcript from the sex chromosomes, leading to the defective PSCR and altered histone marks observed in the MSYq deletion models.

The *Xist* transcript is a multifunctional RNA that coats the X chromosome in *cis* to induce the dynamic genomic reorganisation and transcriptional inactivation of over one thousand X-linked genes (Brown et al., 1992; Clemson et al., 1996; Masui and Heard, 2006). After the future inactive X (X_i) chromosome is coated with *Xist*, RNA PolII and its associated transcription factors are rapidly excluded from the X_i, although this is not sufficient to induce gene silencing (Chaumeil et al., 2006). This is followed by loss of active euchromatic histone marks such as $H3_{K9}$ and H4 acetylation and $H3_{K4}$ methylation (Boggs et al., 1996; Chaumeil et al., 2006; Chaumeil et al., 2002; Jeppesen and Turner, 1993; Keohane et al., 1996). The X_i then becomes enriched with markers of facultative heterochromatin such as $H3_{K9me2}$ (Boggs et al., 2002; Heard et al., 2001; Mermoud et al., 2002; Peters et al., 2002), $H3_{K27me3}$ (Plath et al., 2003; Rougeulle et al., 2004; Silva et al., 2003) and macroH2A. These epigenetic marks

allow stable inheritance of the inactive state during cellular division and differentiation, although they are not sufficient for the silencing function of *Xist* (Masui and Heard, 2006). Several polycomb group proteins accumulate on the X_i after it is coated by *Xist* RNA and studies of mice with mutations of different polycomb group proteins suggest these proteins may be involved in the maintenance of X inactivation (de Napoles et al., 2004; Mak et al., 2002; Plath et al., 2004; Silva et al., 2003). Many of the epigenetic marks associated with the sex chromosome chromatin domain in spermatids are similar to those on the X_i in female somatic cells, including $H3_{K9me2}$, $H3_{K27me3}$, $H2A_{K119}$ ubiquitination and macroH2A (Baarends et al., 2007; Greaves et al., 2006; Namekawa et al., 2006; Turner et al., 2006). Thus, although MSCI and PSCR are independent of *Xist* (Turner et al., 2002; J Lee unpublished data), PSCR may utilise the same downstream protein machinery as female X inactivation to trigger facultative heterochromatin formation and transcriptional repression, including Polycomb chromatin remodeling complexes.

It has been suggested that the spread of silencing along the Xi is mediated by 'spreading stations' such as L1 elements (Lyon, 1998; Lyon, 2006); these stations could also be involved in PSCR. The differences in gene reactivation following MSCI may potentially be explained if the efficiency of gene repression correlates with the distance of a gene from a 'spreading centre', with genes further away being transcribed in a higher proportion of spermatids. For single copy X-linked genes, it will be interesting to see if there is a link between escape from somatic X-inactivation and the level of expression in spermatids. Four genes known to show low or no reactivation in post-meiotic germ cells are *Zfx*, *Fmr1*, *Xiap* and *Scml2* (Mueller et al., 2008), and these are all subject to somatic X inactivation. Further research is needed to establish if genes that escape X inactivation (e.g. *Jarid1c* and *Eif2s3x*) also evade PSCR.

Non-coding RNAs can also actively regulate eukaryotic mRNA transcription by interacting with and affecting the function of the transcriptional machinery by a wide variety of different mechanisms (reviewed by Goodrich and Kugel, 2006). Non-coding RNAs act in *trans* by targeting transcriptional activators or repressors, general transcription factors, and even RNA PolII. In mammals, ncRNAs have been described that control gene expression by; (1) acting as transcriptional co-activators (e.g. the SRA RNA; Lanz et al., 1999; Lanz et al., 2002), (2) regulating the oligomerisation and activity of transcriptional activators (e.g. the human HSR1 ncRNA; Shamovsky et al.,

2006), (3) controlling the intracellualar localisation of an activator (e.g. NRON ncRNA; Willingham et al., 2005) and (4) changing the properties of a transcriptional repressor (e.g. the NRSE 20bp dsRNA; Kuwabara et al., 2004). Accordingly, ncRNAs originating from the MSYq could regulate PSCR by similar mechanisms. A transcript originating from the SINE family of retrotransopons has been reported to bind to the RNA POLII and repress transcription from specific genes (Allen et al., 2004; Espinoza et al., 2004), and so ncRNAs could originate from repetitive transposable elements on the MSYq, as well as the multi-copy *Ssty*, *Sly*, *Asty* and *Orly* genes.

The de-repression of the sex chromosomes and their altered histone code in spermatids from the MSYq deletion models may not be due to deletion of a particular genetic element encoded by this chromosome region. Instead, the MSYq mediated effect on PSCR could be due to the heterochromatic nature of this chromosome. Several transcription factors have been described that concentrate at heterochromatic regions of the genome, potentially negatively regulating the activity of these factors (Brown et al., 1997; Cobb et al., 2000; Francastel et al., 2001; Jolly et al., 2002; Liu et al., 2007b; Piwien Pilipuk et al., 2003; Platero et al., 1998; Shestakova et al., 2004; Tang and Lane, 1999). For example, the C/EBPα transcription factor binds to the transcriptionally inactive mouse major α-satellite repeat in the pericentrimeric heterochromatin, reducing its transcriptional activity. When C/EBPα is prevented from binding to α-satellite repeats, the concentration of this protein in non-heterochromatic regions of the nucleus is increased. This produces an elevation in the binding of C/EBPα to promotor regions, leading to increased transcription of target genes (Liu et al., 2007b). In light of these studies, it is tempting to hypothesize that the heterochromatic MSYq may sequester proteins such as transcription factors or chromatin regulators required for transcription of genes located within heterochromatin. Deletion of the MSYq would increase the availability of these limiting proteins at other heterochromatic regions (e.g. the X and Yp chromosomes), consequently causing increased transcription of genes within these areas. This could also explain why the altered localisation of $H3_{K9me3}$ in the MSYq- testis appears to precede spermiogenesis despite transcription of MSYq-encoded genes being restricted to spermatids.

7.7. Summary

In conclusion, in this thesis I have characterised the expression and function of the multi-copy *Sly* gene during spermiogenesis. My data indicates that SLY is the MSYq-encoded 'acrosomal factor' suggested by others to be responsible for controlling the formation and protein content of the acrosome during spermiogenesis (Styrna et al., 1991a; Styrna et al., 1991b). I have also re-analysed the expression of the related multicopy X-linked gene *Slx* (previously *Xmr*) and convincingly demonstrate that the protein encoded by this gene predominantly or specifically localises to the cytoplasm of spermatids (Reynard et al., 2007), rather than the sex body of spermatocytes as previously reported (Calenda et al., 1994; Escalier and Garchon, 2005; Escalier and Garchon, 2000). Furthermore, I have examined the up-regulation of X- and Yp-linked genes in the MSYq deletion models in detail. My findings suggest that there is a defect in PSCR in spermatids from these mice, which leads to a chromosome-wide increase in transcription of spermatid-expressed genes. Associated with this, there is a reduction in the enrichment of repressive histone marks on the sex chromosome chromatin domain in round spermatids from MSYq- mice compared to XY controls. Protein analysis revealed that the up-regulated spermatid-expressed genes also have increased protein levels, although the cellular expression pattern is unchanged. Together, these data strongly imply that the MSYq is required for normal repression of post-meiotically expressed sex-linked genes, and that the testis phenotypes exhibited by the MSYq deletion models may result from a combination of MSYq-encoded gene deficiency and over-expression of other X- and Yp-linked transcripts in spermatids. The various functions of the MSYq during spermiogenesis may be elucidated in the future by examination of mice transgenic for *Sly* and *Slx*, together with more detailed analysis of sperm development in the three MSYq deletion models.

Acknowledgements

I wish to thank my supervisor, Paul Burgoyne, for accepting me into his lab and for allowing me free range with my project. I am indebted to James Turner for the unceasing guidance and encouragement he has given me during the course of my PhD, the critical reading of this thesis, and all the in depth discussions we have had over the last three years. A special thanks goes to past and present members of the Burgoyne lab, especially Shanti for the support and friendship she has given me.

I thank all members of the Lovell-Badge and Turner labs for technical help, and suggestions during lab meeting, particularly Charlie Scott for teaching me how to use the cryostat (and for shopping trips to Brent Cross), Ryo Sekido for numerous constructs and antibodies, and Denise Goldberg-Johnson for critical reading of my introduction and discussion.

I would also like to express my gratitude to Rick Cote, John Lough, Prim Singh and Christer Hoog for their generous gifts of antibodies, Monika Ward for providing testis material, members of the Cha lab for allowing me to use their bench space and reagents, Tony Johnson for help with yeast techniques, Steve Sedgewick for the critical reading of my yeast-two-hybrid results, James Cauwood for rapid reading of the materials and methods chapter, Wendy Hatton for testis sections, Pete Laskey for assistance with co-immunoprecipitation, and everyone in Duncan Blue for looking after my mice, especially Andrew.

A huge thank you goes to the Fawcett girls (and boys), principally Em, Nic, Piers, and Jamie for their constant friendship, optimism and faith during last three years. Finally, I would like to say a very special thank you to my family for their continous love and support.

This work was supported by an MRC studentship.

Appendices and Bibliography

Appendix 1

pGBKT7 DNA Binding Domain plasmid (Clontech)

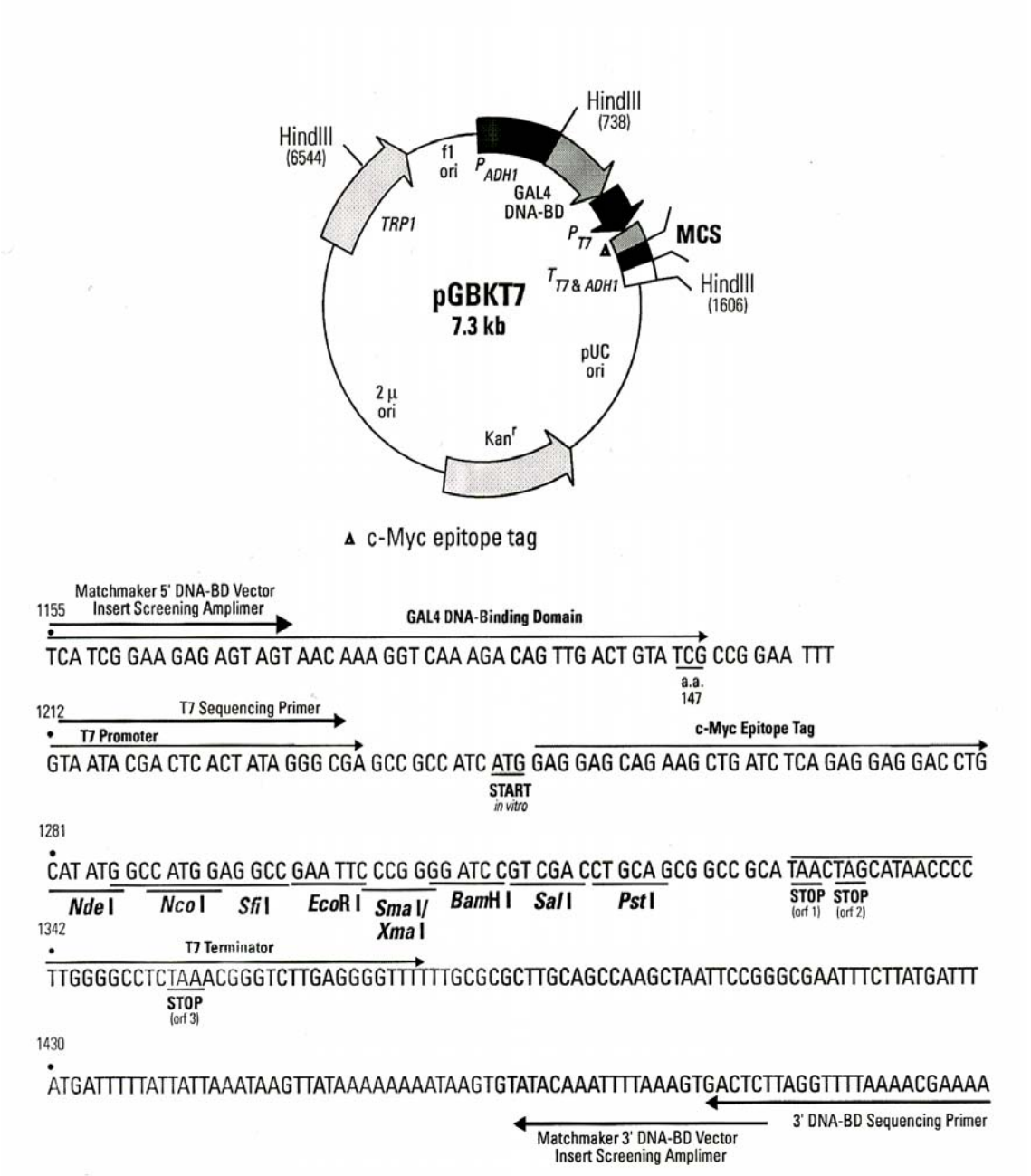

Restriction Map and Multiple Cloning Site (MCS) of pGBKT7. Unique restriction sites are in bold.

Appendix 2

pCMV/SV-Flag 1 vector (Y.Kamachi)

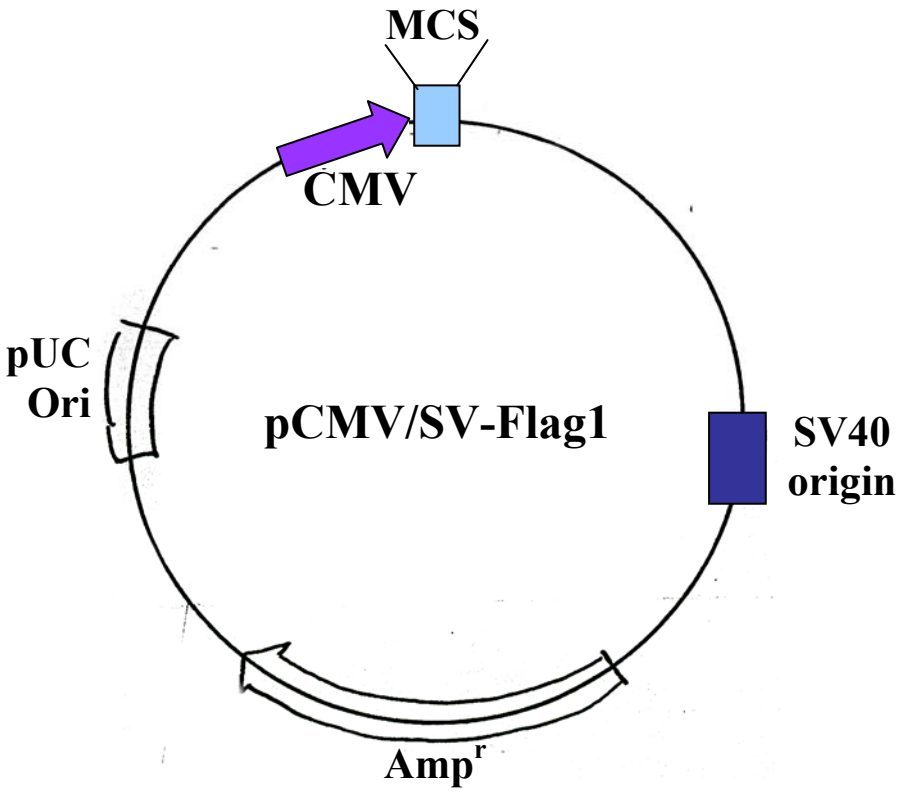

Multiple Cloning site sequence

HindIII
AAGCTTCCACC ATG GAC TAC AAG GAC GAC GAT GAC AAG

BamHI **EcoRI** **SacI** **SalI** **HindIII** **NotI/EagI**
GGA TCC GAA TTC GAG CTC CGT CGA CAA GCT TGC GGC CGC

XhoI **XbaI** **ApaI**
ACT CGA GCA TGC ATC TAG AGG GCC CTA

Restriction endonuclease sites are underlined, with the enzyme that recognises the sequence listed above the site in bold. The FLAG sequence is highlighted in yellow. The FLAG amino acid sequence is below;

MDYKDDDDKGSEFELRRQACGRTRACI

Appendix 3

pACT2 Activation domain plasmid (Clontech)

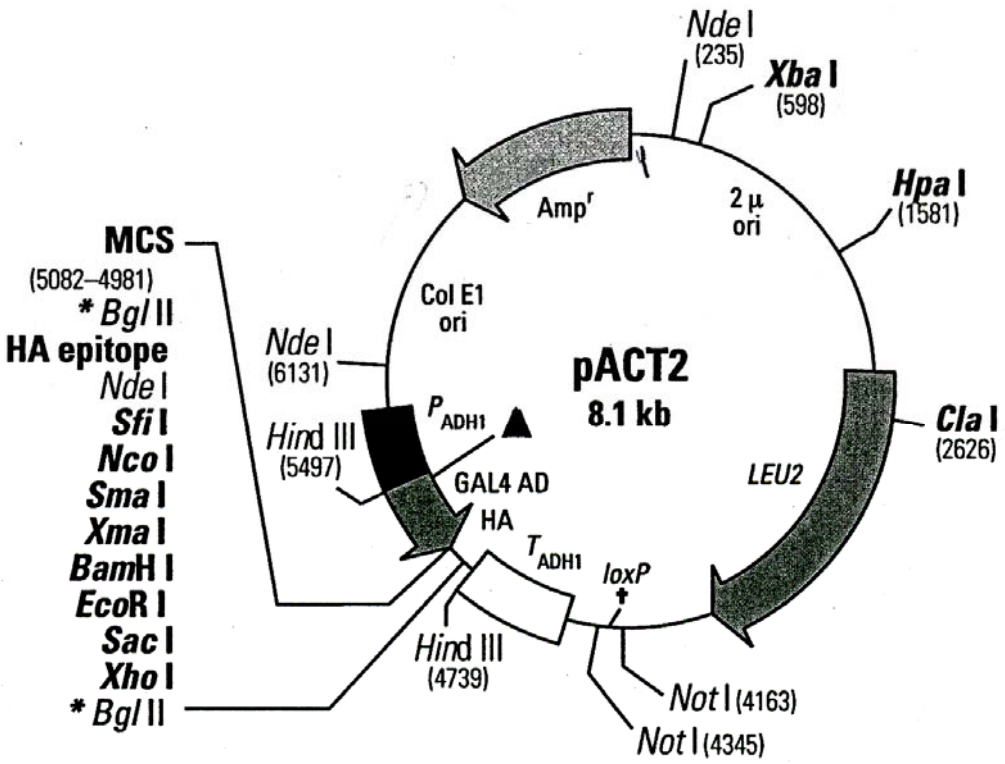

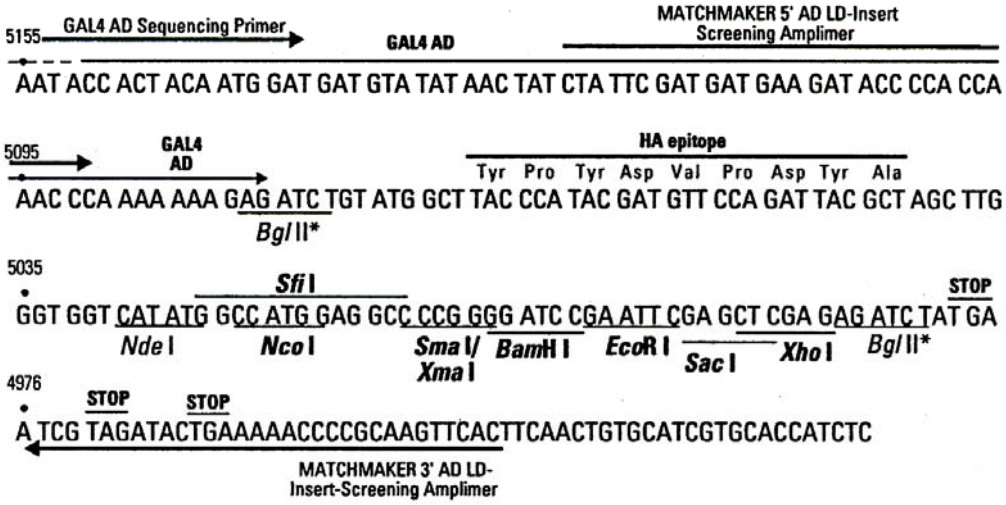

Restriction Map and Multiple Cloning Site (MCS) of pACT2 AD.

Appendix 4

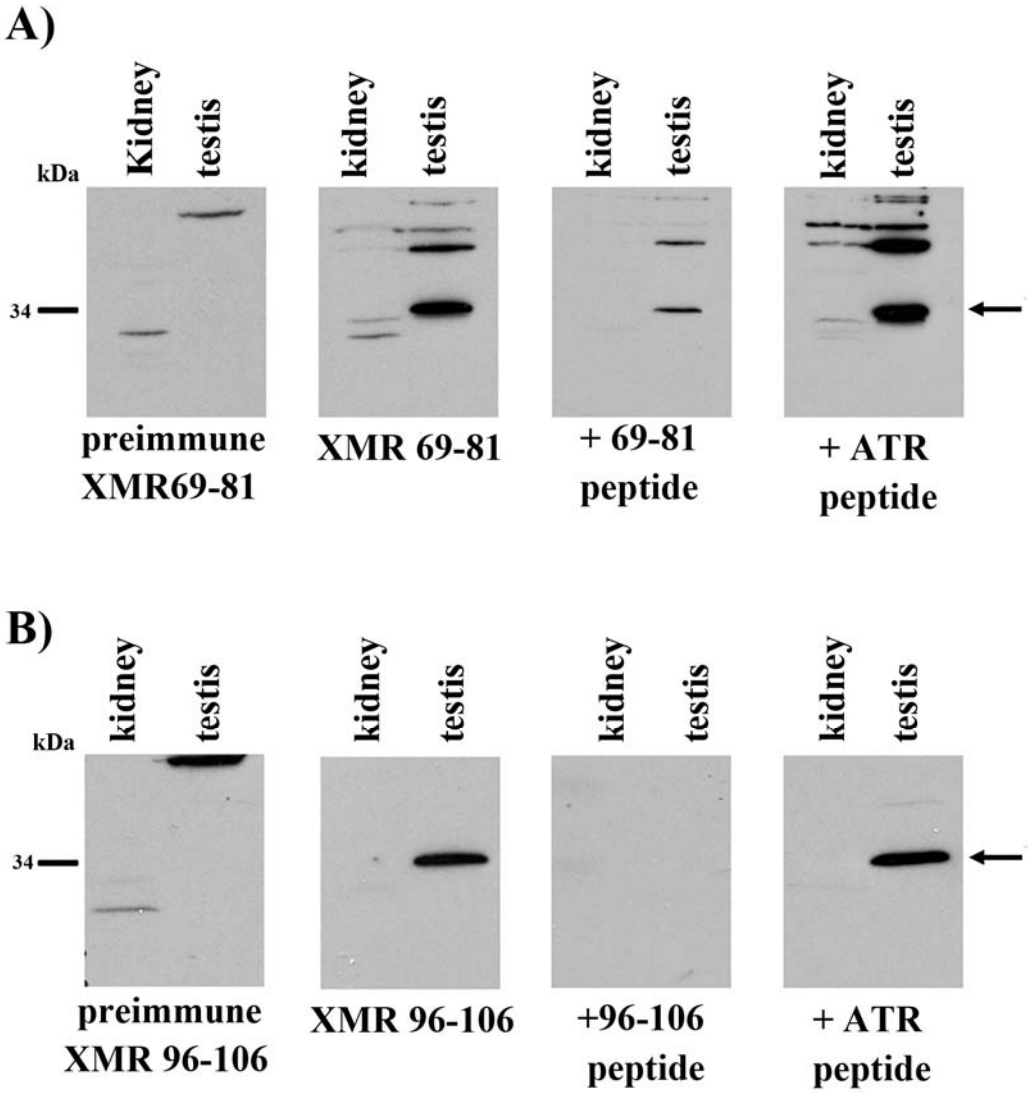

Appendix 4 Characterisation of the anti-XMR$^{69-81}$ and anti-XMR$^{96-106}$ antibodies

A) Western blot analysis of kidney and testis protein lysates from an adult male mouse. Membranes were either probed with the pre-immune serum for the anti-XMR$^{69-81}$ antibody (far left), purified anti-XMR$^{69-81}$ antibody (left), the anti-XMR$^{69-81}$ antibody after preimcubation with the peptide to which it was raised for 4hrs (right), and purified anti-XMR$^{69-81}$ antibody after preabsorbtion with the non-specific ATR peptide (far right).

B) Analysis of kidney and testis protein lysates after incubating with the pre-immune serum for the anti-XMR$^{96-106}$ antibody (far left), the purified anti-XMR$^{96-106}$ antibody (left), the anti-XMR$^{96-106}$ antibody after 4hrs of pre-absorbtion with the peptide to which it was raised (right) and the purified anti-XMR$^{96-106}$ antibody after preincubation with the non-specific ATR peptide for 4hrs (far right).

Both anti-XMR antibodies detect a testis-specifc 34kDa band (arrowed) that is not detected by the respective pre-immune serums. Detection of the 34kDa band is reduced or absent after preincubation with the peptide to which they were raised but not when the anti-XMR antibodies are pre-incubated with a non-specific peptide.

Bibliography

Agulnik, A. I., Longepied, G., Ty, M. T., Bishop, C. E., and Mitchell, M. (1999). Mouse H-Y encoding *Smcy* gene and its X chromosomal homologue *Smcx*. Mamm Genome *10*, 926-929.

Agulnik, A. I., Mitchell, M. J., Lerner, J. L., Woods, D. R., and Bishop, C. E. (1994a). A mouse Y chromosome gene encoded by a region essential for spermatogenesis and expression of male-specific minor histocompatibility antigens. Hum Mol Gen *3*, 873-878.

Agulnik, A. I., Mitchell, M. J., Mattei, M.-G., Borsani, G., Avner, P. A., and Lerner, J. L. (1994b). A novel X gene with a widely transcribed Y-linked homologue escapes X-inactivation in mouse and human. Hum Mol Gen *3*, 879-884.

Ai, W., Zheng, H., Yang, X., Liu, Y., and Wang, T. C. (2007). Tip60 functions as a potential corepressor of KLF4 in regulation of HDC promoter activity. Nucleic Acids Res *35*, 6137-6149.

Alfonso, P. J., and Kistler, W. S. (1993). Immunohistochemical localization of spermatid nuclear transition protein 2 in the testes of rats and mice. Biol Reprod *48*, 522-529.

Allen, T. A., Von Kaenel, S., Goodrich, J. A., and Kugel, J. F. (2004). The SINE-encoded mouse B2 RNA represses mRNA transcription in response to heat shock. Nat Struct Mol Biol *11*, 816-821.

Allenet, B., Escalier, D., and Garchon, H. J. (1995). A putative human equivalent of the murine Xlr (X-linked, lymphocyte-regulated) protein. Mamm Genome *6*, 640-644.

Alvarez, J. D., Yasui, D. H., Niida, H., Joh, T., Loh, D. Y., and Kohwi-Shigematsu, T. (2000). The MAR-binding protein SATB1 orchestrates temporal and spatial expression of multiple genes during T-cell development. Genes Dev *14*, 521-535.

Aravin, A. A., Klenov, M. S., Vagin, V. V., Bantignies, F., Cavalli, G., and Gvozdev, V. A. (2004). Dissection of a natural RNA silencing process in the Drosophila melanogaster germ line. Mol Cell Biol *24*, 6742-6750.

Aravin, A. A., Naumova, N. M., Tulin, A. V., Vagin, V. V., Rozovsky, Y. M., and
Gvozdev, V. A. (2001). Double-stranded RNA-mediated silencing of genomic tandem repeats and transposable elements in the D. melanogaster germline. Curr Biol *11*, 1017-1027.

Auger, A., Galarneau, L., Altaf, M., Nourani, A., Doyon, Y., Utley, R. T., Cronier, D., Allard, S., and Cote, J. (2008). Eaf1 is the platform for NuA4 molecular assembly that evolutionarily links chromatin acetylation to ATP-dependent exchange of histone H2A variants. Mol Cell Biol *28*, 2257-2270.

Avner, P., Bishop, C. E., Amar, L., Cabrou, J., Hatat, D., Arnaud, D., and Mattei, M. G. (1987). Mapping of mouse X chromosome : possible symmetry in the location of a family of sequences on the mouse X and Y chromosomes. Development *101 (Suppl.)*, 107-116.

Ayoub, N., Noma, K., Isaac, S., Kahan, T., Grewal, S. I., and Cohen, A. (2003). A novel jmjC domain protein modulates heterochromatization in fission yeast. Mol Cell Biol *23*, 4356-4370.

Baarends, W. M., Hoogerbrugge, J. W., Roest, H. P., Ooms, M., Vreeburg, J., Hoeijmakers, J. H. J., and Grootegoed, J. A. (1999). Histone ubiquitination and chromatin remodeling in mouse spermatogenesis. Dev Biol *207*, 322-333.

Baarends, W. M., Wassenaar, E., Hoogerbrugge, J. W., Schoenmakers, S., Sun, Z. W., and Grootegoed, J. A. (2007). Increased phosphorylation and dimethylation of XY body histones in the Hr6b-knockout mouse is associated with derepression of the X chromosome. J Cell Sci *120*, 1841-1851.

Baarends, W. M., Wassenaar, E., van der Laan, R., Hoogerbrugge, J., Sleddens-Linkels, E., Hoeijmakers, J. H., de Boer, P., and Grootegoed, J. A. (2005). Silencing of unpaired chromatin and histone H2A ubiquitination in mammalian meiosis. Mol Cell Biol *25*, 1041-1053.

Baker, D. J., Jeganathan, K. B., Cameron, J. D., Thompson, M., Juneja, S., Kopecka, A., Kumar, R., Jenkins, R. B., de Groen, P. C., Roche, P., and van Deursen, J. M. (2004). BubR1 insufficiency causes early onset of aging-associated phenotypes and infertility in mice. Nat Genet *36*, 744-749.

Balakireva, M. D., Shevelyov, Y., Nurminsky, D. I., Livak, K. J., and Gvozdev, V. A. (1992). Structural organization and diversification of Y-linked sequences comprising Su(Ste) genes in Drosophila melanogaster. Nucleic Acids Res *20*, 3731-3736.

Banks, K. G., Johnson, K. A., Lerner, C. P., Mahaffey, C. L., Bronson, R. T., and Simpson, E. M. (2003). Retroposon compensatory mechanism hypothesis not supported: Zfa knockout mice are fertile. Genomics *82*, 254-260.

Baron, B., Metezeau, P., Hatat, D., Roberts, C., Goldberg, M. E., and Bishop, C. E. (1986). Cloning of cDNA libraries from Y chromosomes purified by flow cytometry. Somatic Cell and Molecular Genetics *12*, 289-295.

Baudat, F., and de Massy, B. (2007). Regulating double-stranded DNA break repair towards crossover or non-crossover during mammalian meiosis. Chromosome Res *15*, 565-577.

Belloni, M., Tritto, P., Bozzetti, M. P., Palumbo, G., and Robbins, L. G. (2002). Does Stellate cause meiotic drive in Drosophila melanogaster? Genetics *161*, 1551-1559.
Bellve, A. R. (1993). Purification, culture, and fractionation of spermatogenic cells. Methods Enzymol *225*, 84-113.

Bellvé, A. R., Millette, C. F., Bhatnagar, Y. M., and O'Brien, D. A. (1977). Dissociation of the mouse testis and characterization of isolated spermatogenic cells. J Histochem Cytochem *25*, 480-494.

Bergsagel, P. L., Timblin, C. R., Kozak, C. A., and Kuehl, W. M. (1994). Sequence and expression of murine cDNAs encoding Xlr3a and Xlr3b, defining a new X-linked lymphocyte-regulated Xlr gene subfamily. Gene *150*, 345-350.

Bergstrom, D. E., Grieco, D. A., Sonti, M. M., Fawcett, J. J., Bell-Prince, C., Cram, L. C., Narayanswami, S., and Simpson, E. M. (1998). The mouse Y chromosome: enrichment, sizing, and cloning by bivariate flow cytometry. Genomics *48*, 304-313.

Bergstrom, D. E., Yan, H., Sonti, M. M., Narayanswami, S., Bayleran, J. K., and Simpson, E. M. (1997). An expanded collection of mouse Y chromosome RDA clones. Mamm Genome *8*, 510-512.

Betran, E., Emerson, J. J., Kaessmann, H., and Long, M. (2004). Sex chromosomes and male functions: where do new genes go? Cell Cycle *3*, 873-875.

Bishop, C. E., Boursot, P., Baron, B., Bonhomme, F., and Hatat, D. (1985). Most classical *Mus musculus domesticus* laboratory mouse strains carry a *Mus musculus musculus* Y chromosome. Nature *315*, 70-72.

Bishop, C. E., and Hatat, D. (1987). Molecular cloning and sequence analysis of a mouse Y chromosome RNA transcript expressed in the testis. Nucleic Acids Res *15*, 2959-2969.

Boggs, B. A., Cheung, P., Heard, E., Spector, D. L., Chinault, A. C., and Allis, C. D. (2002). Differentially methylated forms of histone H3 show unique association patterns with inactive human X chromosomes. Nat Genet *30*, 73-76.

Boggs, B. A., Connors, B., Sobel, R. E., Chinault, A. C., and Allis, C. D. (1996). Reduced levels of histone H3 acetylation on the inactive X chromosome in human females. Chromosoma *105*, 303-309.

Bolcun-Filas, E., Costa, Y., Speed, R., Taggart, M., Benavente, R., De Rooij, D. G., and Cooke, H. J. (2007). SYCE2 is required for synaptonemal complex assembly, double strand break repair, and homologous recombination. J Cell Biol *176*, 741-747.

Bradley, J., Baltus, A., Skaletsky, H., Royce-Tolland, M., Dewar, K., and Page, D. C. (2004). An X-to-autosome retrogene is required for spermatogenesis in mice. Nat Genet *36*, 872-876.

Braun, R. E. (1990). Temporal translational regulation of the protamine 1 gene during mouse spermatogenesis. Enzyme *44*, 120-128.

Braun, R. E., Peschon, J. J., Behringer, R. R., Brinster, R. L., and Palmiter, R. D. (1989). Protamine 3'-untranslated sequences regulate temporal translational control and subcellular localization of growth hormone in spermatids of transgenic mice. Genes Dev *3*, 793-802.

Brower, J. V., Rodic, N., Seki, T., Jorgensen, M., Fliess, N., Yachnis, A. T., McCarrey, J. R., Oh, S. P., and Terada, N. (2007). Evolutionarily conserved mammalian adenine nucleotide translocase 4 is essential for spermatogenesis. J Biol Chem *282*, 29658-29666.

Brown, C. J., Hendrich, B. D., Rupert, J. L., LafreniŠre, R. G., Xing, Y., Lawrence, J., and Willard, H. F. (1992). The human *XIST* gene: Analysis of a 17kb inactive X-specific RNA that contains conserved repeats and is highly localised within the nucleus. Cell *71*, 527-542.

Brown, G. M., Furlong, R. A., Sargent, C. A., Erickson, R. P., Longepied, G., Mitchell, M., Jones, M. H., Hargreave, T. B., Cooke, H. J., and Affara, N. A. (1998). Characterisation of the coding sequence and fine mapping of the human *DFFRY* gene and comparative expression analysis and mapping to the *Sxrb* interval of the mouse Y chromosome of the *Dffry* gene. Hum Mol Gen *7*, 97-108.

Brown, K. E., Guest, S. S., Smale, S. T., Hahm, K., Merkenschlager, M., and Fisher, A. G. (1997). Association of transcriptionally silent genes with Ikaros complexes at centromeric heterochromatin. Cell *91*, 845-854.

Burgoyne, P. S. (1982). Genetic homology and crossing over in the X and Y chromosomes of mammals. Hum Genet *61*, 85-90.

Burgoyne, P. S. (1987). The role of the mammalian Y chromosome in spermatogenesis. Development *101*, 133-141.

Burgoyne, P. S. (1993a). Deletion mapping the functions of the mouse Y chromosome. In Sex Chromosomes and Sex-Determining Genes, K. C. Reed, and J. A. M. Graves, eds. (Chur, Switzerland, Harwood Academic Publishers), pp. 353-368.

Burgoyne, P. S. (1993b). A Y-chromosomal effect on blastocyst cell number in mice. Development *117*, 341-345.

Burgoyne, P. S. (1998a). The mammalian Y chromosome: a new perspective. Bioessays *20*, 363-366.

Burgoyne, P. S. (1998b). The role of Y-encoded genes in mammalian spermatogenesis. Seminars in Cell & Developmental Biology *9*, 423-432.

Burgoyne, P. S., and Evans, E. P. (2000). A high frequency of XO offspring from X*Paf*Y* male mice: evidence that the *Paf* mutation involves an inversion spanning the X PAR boundary. Cytogen Cell Genet *91*, 57-61.

Burgoyne, P. S., Levy, E. R., and McLaren, A. (1986). Spermatogenic failure in male mice lacking H-Y antigen. Nature *320*, 170-172.

Burgoyne, P. S., Mahadevaiah, S. K., Perry, J., Palmer, S. J., and Ashworth, A. (1998). The Y* rearrangement in mice: new insights into a perplexing PAR. Cytogen Cell Genet *80*, 37-40.

Burgoyne, P. S., Mahadevaiah, S. K., Sutcliffe, M. J., and Palmer, S. J. (1992). Fertility in mice requires X-Y pairing and a Y-chromosomal "spermiogenesis" gene mapping to the long arm. Cell *71*, 391-398.

Burgoyne, P. S., and Mitchell, M. J. (2007). The roles of mouse Y chromosome genes in spermatogenesis. In Y Chromosome and Male Germ Cell Biology, Y.-F. C. Lau, and W. Y. Chan, eds. (Hackensack,NJ, World Scientific Publishers), pp. 27-45.

Burgoyne, P. S., and Palmer, S. J. (1991). The genetics of XY sex reversal in the mouse and other animals. Seminars in Developmental Biology *2*, 277-284.

Burt, A., and Trivers, R (2006). Genes in conflict.The biology of selfish genetic elements. Belknap press of Harvard University Press.

Calenda, A., Allenet, B., Escalier, D., Bach, J.-F., and Garchon, H.-J. (1994). The meiosis-specific Xmr gene product is homologous to the lymphocyte Xlr protein and is a component of the XY body. EMBO J *13*, 100-109.

Capel, B., Rasberry, C., Dyson, J., Bishop, C. E., Simpson, E., Vivian, N., Lovell-Badge, R., Rastan, S., and Cattanach, B. M. (1993). Deletion of Y chromosome sequences located outside the testis determining region can cause XY female sex reversal. Nat Genet *5*, 301-307.

Carpenter, A. T. C. (1987). Gene conversion, recombination nodules, and the initiation of meiotic synapsis. Bioessays *6*, 232-236.

Carvalho, A. B., Vaz, S. C., and Klaczko, L. B. (1997). Polymorphism for Y-linked suppressors of sex-ratio in two natural populations of Drosophila mediopunctata. Genetics *146*, 891-902.

Cattanach, B. M. (1987). Sex-reversed mice and sex determination. Ann NY Acad Sci *513*, 27-29.

Cattanach, B. M., Pollard, C. E., and Hawkes, S. G. (1971). Sex reversed mice : XX and XO males. Cytogenetics *10*, 318-337.

Cavicchia, J. C., and Dym, M. (1977). Relative volume of Sertoli Cells in monkey seminiferous epithelium: a stereological analysis. Am J Anat *150(3)*, 501-507.

Charlesworth, B. (1991). The Evolution of Sex Chromosomes. Science *251*, 1030-1033.

Chaumeil, J., Le Baccon, P., Wutz, A., and Heard, E. (2006). A novel role for Xist RNA in the formation of a repressive nuclear compartment into which genes are recruited when silenced. Genes Dev *20*, 2223-2237.

Chaumeil, J., Okamoto, I., Guggiari, M., and Heard, E. (2002). Integrated kinetics of X chromosome inactivation in differentiating embryonic stem cells. Cytogenet Genome Res *99*, 75-84.

Chiquoine, A. D. (1954). The identification, origin and migration of the primordial germ cells in the mouse embryo. The Anatomical Record *118*, 135-146.

Churikov, D., Siino, J., Svetlova, M., Zhang, K., Gineitis, A., Morton Bradbury, E., and Zalensky, A. (2004). Novel human testis-specific histone H2B encoded by the interrupted gene on the X chromosome. Genomics *84*, 745-756.

Clemson, C. M., McNeil, J. A., Willard, H. F., and Lawrence, J. B. (1996). XIST RNA paints the inactive X chromosome at interphase: evidence for a novel RNA involved in nuclear/chromosome structure. J Cell Biol *132*, 259-275.

Clermont, Y., and Perey, B. (1957). The stages of the cycle of the seminiferous epithelium of the rat: practical definitions in PA-Schiff-hematoxylin and hematoxylin-eosin stained sections. Rev Can Biol *16*, 451-462.

Clotman, F., De Backer, O., De Plaen, E., Boon, T., and Picard, J. (2000). Cell- and stage-specific expression of mage genes during mouse spermatogenesis. Mamm Genome *11*, 696-699.

Cobb, B. S., Morales-Alcelay, S., Kleiger, G., Brown, K. E., Fisher, A. G., and Smale, S. T. (2000). Targeting of Ikaros to pericentromeric heterochromatin by direct DNA binding. Genes Dev *14*, 2146-2160.

Conway, S. J., Mahadevaiah, S. K., Darling, S. M., Capel, B., Rattigan, Á. M., and Burgoyne, P. S. (1994). Y353/B: a candidate multiple-copy spermiogenesis gene on the mouse Y chromosome. Mamm Genome *5*, 203-210.

Davies, W., Isles, A., Smith, R., Karunadasa, D., Burrmann, D., Humby, T., Ojarikre, O., Biggin, C., Skuse, D., Burgoyne, P., and Wilkinson, L. (2005). Xlr3b is a new imprinted candidate for X-linked

parent-of-origin effects on cognitive function in mice. Nat Genet *37*, 625-629.

de Napoles, M., Mermoud, J. E., Wakao, R., Tang, Y. A., Endoh, M., Appanah, R., Nesterova, T. B., Silva, J., Otte, A. P., Vidal, M., *et al.* (2004). Polycomb group proteins Ring1A/B link ubiquitylation of histone H2A to heritable gene silencing and X inactivation. Dev Cell *7*, 663-676.

de Vries, F. A., de Boer, E., van den Bosch, M., Baarends, W. M., Ooms, M., Yuan, L., Liu, J. G., van Zeeland, A. A., Heyting, C., and Pastink, A. (2005). Mouse Sycp1 functions in synaptonemal complex assembly, meiotic recombination, and XY body formation. Genes Dev *19*, 1376-1389.

de Vries, S. S., Baart, E. B., Dekker, M., Siezen, A., de Rooij, D. G., de Boer, P., and te Riele, H. (1999). Mouse MutS-like protein MSH5 is required for proper chromosome synapsis in male and female meiosis. Genes Dev *13*, 523-531.

Delbridge, M. L., and Graves, J. A. (1999). Mammalian Y chromosome evolution and the male-specific functions of Y chromosome-borne genes. Rev Reprod *4*, 101-109.

Delbridge, M. L., Lingenfelter, P. A., Disteche, C. M., and Graves, J. A. (1999). The candidate spermatogenesis gene RBMY has a homologue on the human X chromosome. Nat Genet *22*, 223-224.

Deng, X., and Meller, V. H. (2006). Non-coding RNA in fly dosage compensation. Trends Biochem Sci *31*, 526-532.

DeRan, M., Pulvino, M., Greene, E., Su, C., and Zhao, J. (2008). Transcriptional activation of histone genes requires NPAT-dependent recruitment of TRRAP-Tip60 complex to histone promoters during the G1/S phase transition. Mol Cell Biol *28*, 435-447.

Derrigo, M., Cestelli, A., Savettieri, G., and Di Liegro, I. (2000). RNA-protein interactions in the control of stability and localization of messenger RNA. Int J Mol Med *5*, 111-123.

Dickinson, L. A., Joh, T., Kohwi, Y., and Kohwi-Shigematsu, T. (1992). A tissue-specific MAR/SAR DNA-binding protein with unusual binding site recognition. Cell *70*, 631-645.

Ditton, H. J., Zimmer, J., Kamp, C., Rajpert-De Meyts, E., and Vogt, P. H. (2004). The AZFa gene DBY (DDX3Y) is widely transcribed but the protein is limited to the male germ cells by translation control. Hum Mol Genet *13*, 2333-2341.

Dobson, M. J., Pearlman, R. E., Karaiskakis, A., Spyropoulos, B., and Moens, P. B. (1994). Synaptonemal complex proteins: occurrence, epitope mapping and chromosome disjunction. J Cell Sci *107 (Pt 10)*, 2749-2760.

Eddy, E. M. (2002). Male germ cell gene expression. Recent Prog Horm Res *57*, 103-128.

Eddy, E. M., Toshimori, K., and O'Brien, D. A. (2003). Fibrous sheath of mammalian spermatozoa. Microsc Res Tech *61*, 103-115.

Edelmann, W., Cohen, P. E., Kneitz, B., Winand, N., Lia, M., Heyer, J., Kolodner, R., Pollard, J. W., and Kucherlapati, R. (1999). Mammalian MutS homologue 5 is required for chromosome pairing in meiosis. Nat Genet *21*, 123-127.

Ehrmann, I. E., Ellis, P. S., Mazeyrat, S., Duthie, S., Brockdorff, N., Mattei, M. G., Gavin, M. A., Affara, N. A., Brown, G. M., Simpson, E., *et al.* (1998). Characterization of genes encoding translation initiation factor eIF-2gamma in mouse and human: sex chromosome localisation, escape from X-inactivation and evolution. Hum Mol Gen *7*, 1725-1737.

Eicher, E. M., Hale, D. W., Hunt, P. A., Lee, B. K., Tucker, P. K., King, T. R., Eppig, J. T., and Washburn, L. L. (1991). The mouse Y* chromosome involves a complex rearrangement, including interstitial positioning of the pseudoautosomal region. Cytogen Cell Genet *57*, 221-230.

Eicher, E. M., Hutchison, K. W., Philips, S. J., Tucker, P. K., and Lee, B. (1989). A repeated segment on the mouse Y chromosome is composed of retroviral related Y enriched and Y specific sequences. Genetics *122*, 181-192.

Eicher, E. M., Phillips, S. J., and Washburn, L. L. (1983). The use of molecular probes and chromosomal rearrangements to partition the mouse Y chromosome into functional regions. In Recombinant DNA and Medical Genetics, A. Messer, and I. H. Porter, eds. (New York, Academic Press), pp. 57-71.

Eicher, E. M., and Washburn, L. L. (1978). Assignment of genes to regions of mouse chromosomes. Proc Natl Acad Sci U S A *75*, 946-950.

Eicher, E. M., and Washburn, L. L. (1986). Genetic control of primary sex determination in mice. Annu Rev Genet *20*, 327-360.

Elliott, D. J., and Cooke, H. J. (1997). The molecular genetics of male infertility. Bioessays *19*, 801-809.

Ellis, P. J., Ferguson, L., Clemente, E. J., and Affara, N. A. (2007). Bidirectional transcription of a novel chimeric gene mapping to mouse chromosome Yq. BMC Evol Biol *7*, 171.

Ellis, P. J., Furlong, R. A., Wilson, A., Morris, S., Carter, D., Oliver, G., Print, C., Burgoyne, P. S., Loveland, K. L., and Affara, N. A. (2004). Modulation of the mouse testis transcriptome during postnatal development and in selected models of male infertility. Mol Hum Reprod *10*, 271-281.

Ellis, P. J. I., Clemente, E. J., Ball, P., Touré, A., Ferguson, L., Turner, J. M. A., Loveland, K. L., Affara, N. A., and Burgoyne, P. S. (2005). Deletions on mouse Yq lead to upregulation of multiple X- and Y-linked transcripts in spermatids. Hum Mol Gen *14*, 2705-2715.

Emerson, J. J., Kaessmann, H., Betran, E., and Long, M. (2004). Extensive gene traffic on the mammalian X chromosome. Science *303*, 537-540.

Escalier, D., Allenet, B., Badrichani, A., and Garchon, H. J. (1999). High level expression of the Xlr nuclear protein in immature thymocytes and colocalization with the matrix-associated region-binding SATB1 protein. J Immunol *162*, 292-298.

Escalier, D., Eloy, L., and Garchon, H. J. (2002). Sex-specific gene expression during meiotic prophase I: Xlr (X linked, lymphocyte regulated), not its male homologue Xmr (Xlr related, meiosis regulated), is expressed in mouse oocytes. Biol Reprod *67*, 1646-1652.

Escalier, D., and Garchon, H. J. (2005). XMR, a dual location protein in the XY pair and in its associated nucleolus in mouse spermatocytes. Mol Reprod Dev *72*, 105-112.

Escalier, D., and Garchon, H.-J. (2000). XMR is associated with the asynapsed segments of sex chromosomes in the XY body of mouse primary spermatocytes. Chromosoma *109*, 259-265.

Espinoza, C. A., Allen, T. A., Hieb, A. R., Kugel, J. F., and Goodrich, J. A. (2004). B2 RNA binds directly to RNA polymerase II to repress transcript synthesis. Nat Struct Mol Biol *11*, 822-829.

Evans, E. P., Ford, C. E., and Searle, A. G. (1969). A 39,X/41,XYY mosaic mouse. Cytogenetics *8*, 87-96.

Fennelly, J., Harper, K., Laval, S., Wright, E., and Plumb, M. (1996). Co-amplification to tail-to-tail copies of MuRVY and IAPE retroviral genomes on the Mus musculus Y chromosome. Mamm Genome *7*, 31-36.

Fernandez-Capetillo, O., Mahadevaiah, S. K., Celeste, A., Romanienko, P. J., Camerini-Otero, R. D., Bonner, W. M., Manova, K., Burgoyne, P., and Nussenzweig, A. (2003). H2AX is required for chromatin remodeling and inactivation of sex chromosomes in male mouse meiosis. Dev Cell *4*, 497-508.

Fisher, R. A. (1931). The evolution of dominance. Biol Rev *6*, 345-368.

Foote, S., Vollrath, D., Hilton, A., and Page, D. C. (1992). The human Y chromosome: Overlapping DNA clones spanning the euchromatic region. Science *258*, 60-66.

Foster, J. W., and Graves, J. A. M. (1994). An *SRY*-related sequence on the marsupial X chromosome: implications for the evolution of the mammalian testis-determining gene. Proc Natl Acad Sci USA *91*, 1927-1931.

Francastel, C., Magis, W., and Groudine, M. (2001). Nuclear relocation of a transactivator subunit precedes target gene activation. Proc Natl Acad Sci U S A *98*, 12120-12125.

Fry, C. L., and Wilkinson, G. S. (2004). Sperm survival in female stalk-eyed flies depends on seminal fluid and meiotic drive. Evolution Int J Org Evolution *58*, 1622-1626.

Ganesan, S., Richardson, A. L., Wang, Z. C., Iglehart, J. D., Miron, A., Feunteun, J., Silver, D., and Livingston, D. M. (2005). Abnormalities of the inactive X chromosome are a common feature of BRCA1 mutant and sporadic basal-like breast cancer. Cold Spring Harb Symp Quant Biol *70*, 93-97.

Ganesan, S., Silver, D. P., Greenberg, R. A., Avni, D., Drapkin, R., Miron, A., Mok, S. C., Randrianarison, V., Brodie, S., Salstrom, J., *et al.* (2002). BRCA1 supports XIST RNA concentration on the inactive X chromosome. Cell *111*, 393-405.

Garchon, H. J., and Davis, M. M. (1989). The XLR gene product defines a novel set of proteins stabilized in the nucleus by zinc ions. J Cell Biol *108*, 779-787.

Garchon, H. J., Loh, E., Ho, W. Y., Amar, L., Avner, P., and Davies, M. M. (1989). The XLR sequence family: dispersion on the X and Y chromosomes of a large set of closely related sequences most of which are pseudogenes. Nucleic Acids Res *17*, 9871-9888.

Gardiner-Garden, M., Ballesteros, M., Gordon, M., and Tam, P. P. (1998). Histone- and protamine-DNA association: conservation of different patterns within the beta-globin domain in human sperm. Mol Cell Biol *18*, 3350-3356.

Garrick, D., Fiering, S., Martin, D. I., and Whitelaw, E. (1998). Repeat-induced gene silencing in mammals. Nat Genet *18*, 56-59.

Gill, G., and Ptashne, M. (1987). Mutants of GAL4 protein altered in an activation function. Cell *51*, 121-126.

Gineitis, A. A., Zalenskaya, I. A., Yau, P. M., Bradbury, E. M., and Zalensky, A. O. (2000). Human sperm telomere-binding complex involves histone H2B and secures telomere membrane attachment. J Cell Biol *151*, 1591-1598.

Goodrich, J. A., and Kugel, J. F. (2006). Non-coding-RNA regulators of RNA polymerase II transcription. Nat Rev Mol Cell Biol *7*, 612-616.

Gorrini, C., Squatrito, M., Luise, C., Syed, N., Perna, D., Wark, L., Martinato, F., Sardella, D., Verrecchia, A., Bennett, S., *et al.* (2007). Tip60 is a haplo-insufficient tumour suppressor required for an oncogene-induced DNA damage response. Nature *448*, 1063-1067.

Govin, J., Escoffier, E., Rousseaux, S., Kuhn, L., Ferro, M., Thevenon, J., Catena, R., Davidson, I., Garin, J., Khochbin, S., and Caron, C. (2007). Pericentric heterochromatin reprogramming by new histone variants during mouse spermiogenesis. J Cell Biol *176*, 283-294.

Graves, J. A. (1995). The evolution of mammalian sex chromosomes and the origin of sex determining genes. Philos Trans R Soc Lond B Biol Sci *350*, 305-311; discussion 311-302.

Graves, J. A. (1998). Evolution of the mammalian Y chromosome and sex-determining genes. J Exp Zool *281*, 472-481.

Graves, J. A. (2006). Sex chromosome specialization and degeneration in mammals. Cell *124*, 901-914.

Graves, J. A., Gecz, J., and Hameister, H. (2002). Evolution of the human X--a smart and sexy chromosome that controls speciation and development. Cytogenet Genome Res *99*, 141-145.

Greaves, I. K., Rangasamy, D., Devoy, M., Marshall Graves, J. A., and Tremethick, D. J. (2006). The X and Y chromosomes assemble into H2A.Z, containing facultative heterochromatin, following meiosis. Mol Cell Biol *26*, 5394-5405.

Gregory, S. G., Sekhon, M., Schein, J., Zhao, S., Osoegawa, K., Scott, C. E., Evans, R. S., Burridge, P. W., Cox, T. V., Fox, C. A., *et al.* (2002). A physical map of the mouse genome. Nature *418*, 743-750.

Griswold, M. D. (1998). The central role of Sertoli cells in spermatogenesis. Semin Cell Dev Biol *9*, 411-416.

Grzmil, P., Golas, A., Muller, C., and Styrna, J. (2007). The influence of the deletion on the long arm of the Y chromosome on sperm motility in mice. Theriogenology *67*, 760-766.

Guraya (1980). Recent progress in the morphology, biochemistry and physiology of developing and maturing mammalian testis. Int Rev Cytol *62*, 187-309.

Guraya, S. S. (1987). Biology of spermatogenesis and spermatozoa in mammals (Berlin, Springer Verlag).

Gvozdev, V. A., Kogan, G. L., and Usakin, L. A. (2005). The Y chromosome as a target for acquired and amplified genetic material in evolution. Bioessays *27*, 1256-1262.

Hadjantonakis, A.-K., Cox, L. L., Tam, P. P. L., and Nagy, A. (2001). An X-linked GFP transgene reveals unexpected paternal X-chromosome activity in trophoblast giant cells of the mouse placenta. Genesis *29*, 133-140.

Hadjantonakis, A. K., Gertsenstein, M., Ikawa, M., Okabe, M., and Nagy, A. (1998). Non-invasive sexing of preimplantation stage mammalian embryos. Nat Genet *19*, 220-222.

Hamilton, W. D. (1967). Extraordinary sex ratios. A sex-ratio theory for sex linkage and inbreeding has new implications in cytogenetics and entomology. Science *156*, 477-488.

Handel, M. A. (2004). The XY body: a specialized meiotic chromatin domain. Exp Cell Res *296*, 57-63.

Harbers, K., Franke, U., Soriano, P., Jaenisch, R., and Müller, U. (1990). Structure and chromosomal mapping of a highly polymorphic repetitive DNA sequence from the pseudoautosomal region of the mouse sex chromosomes. Cytogen Cell Genet *53*, 129-133.

Harbers, K., Soriano, P., Müller, U., and Jaenisch, R. (1986). High frequency of unequal recombination in pseudoautosomal region shown by proviral insertion in transgenic mouse. Nature *324*, 682-686.

Hazzouri, M., Pivot-Pajot, C., Faure, A. K., Usson, Y., Pelletier, R., Sele, B., Khochbin, S., and Rousseaux, S. (2000). Regulated hyperacetylation of core histones during mouse spermatogenesis: involvement of histone deacetylases. Eur J Cell Biol *79*, 950-960.

Heard, E., Rougeulle, C., Arnaud, D., Avner, P., Allis, C. D., and Spector, D. L. (2001). Methylation of histone H3 at Lys-9 is an early mark on the X chromosome during X inactivation. Cell *107*, 727-738.

Hendriksen, P. J. M., Hoogerbrugge, J. W., Themmen, A. P. N., Koken, M. H. M., Hoeijmakers, J. H. J., Oostra, B. A., van der Lende, T., and Grootegoed, J. A. (1995).
Postmeiotic transcription of X and Y chromosomal genes during spermatogenesis in the mouse. Dev Biol *170*, 730-733.

Hicks, G. R., and Raikhel, N. V. (1995). Protein import into the nucleus: an integrated view. Annu Rev Cell Dev Biol *11*, 155-188.

Hicks, G. R., Smith, H. M., Shieh, M., and Raikhel, N. V. (1995). Three classes of nuclear import signals bind to plant nuclei. Plant Physiol *107*, 1055-1058.

Hilscher, B. (1981). Spermatogoniogenesis, an interacting proliferation process between stem cell spermatogonia and differentiating spermatogonia. Fortschritte der Andrologie *7*, 46-57.

Hoyer-Fender, S., Costanzi, C., and Pehrson, J. R. (2000). Histone macroH2A1.2 is concentrated in the XY-body by the early pachytene stage of spermatogenesis. Exp Cell Res *258*, 254-260.

Hurst, L. D. (1992). Is *Stellate* a relict meiotic driver? Genetics *130*, 229-230.

Hurst, L. D. (1996). Further evidence consistent with *Stellate*'s involvement in meiotic drive. Genetics *142*, 641-643.

Hurst, L. D., and Pomiankowski, A. (1991). Causes of sex ratio bias may account for unisexual sterility in hybrids:a new explanation of Haldane's rule and related phenomena. Genetics *128*, 841-858.

Hurst, L. D., and Randerson, J. P. (1999). An eXceptional chromosome. Trends in Genetics *15*, 383-385.

Itoh, Y., Hori, T., Saitoh, H., and Mizuno, S. (2001). Chicken spindlin genes on W and Z chromosomes: transcriptional expression of both genes and dynamic behavior of spindlin in interphase and mitotic cells. Chromosome Res *9*, 283-299.

Iwase, M., Satta, Y., Hirai, Y., Hirai, H., Imai, H., and Takahata, N. (2003). The amelogenin loci span an ancient pseudoautosomal boundary in diverse mammalian species. Proc Natl Acad Sci U S A *100*, 5258-5263.

Jeppesen, P., and Turner, B. M. (1993). The inactive X chromosome in female mammals is distinguished by a lack of histone H4 acetylation, a cytogenetic marker for gene expression. Cell *74*, 281-289.

Jha, S., Shibata, E., and Dutta, A. (2008). Human Rvb1/Tip49 is required for the histone acetyltransferase activity of Tip60/NuA4 and for the downregulation of phosphorylation on H2AX after DNA damage. Mol Cell Biol *28*, 2690-2700.

Jolly, C., Konecny, L., Grady, D. L., Kutskova, Y. A., Cotto, J. J., Morimoto, R. I., and Vourc'h, C. (2002). In vivo binding of active heat shock transcription factor 1 to human chromosome 9 heterochromatin during stress. J Cell Biol *156*, 775-781.
Jones, K. W., and Singh, L. (1981). Conserved repeated DNA sequences in vertebrate sex chromosomes. Hum Genet *58*, 46-53.

Kalantry, S., and Magnuson, T. (2006). The Polycomb group protein EED is dispensable for the initiation of random X-chromosome inactivation. PLoS Genet *2*, e66.

Kamachi, Y., Cheah, K. S., and Kondoh, H. (1999). Mechanism of regulatory target selection by the SOX high-mobility-group domain proteins as revealed by comparison of SOX1/2/3 and SOX9. Mol Cell Biol *19*, 107-120.

Kaneko, K. J., and DePamphilis, M. L. (2000). Soggy, a spermatocyte-specific gene, lies 3.8 kb upstream of and antipodal to TEAD-2, a transcription factor expressed at the beginning of mouse development. Nucleic Acids Res *28*, 3982-3990.

Keohane, A. M., O'Neill L, P., Belyaev, N. D., Lavender, J. S., and Turner, B. M. (1996). X-Inactivation and histone H4 acetylation in embryonic stem cells. Dev Biol *180*, 618-630.

Khalil, A. M., Boyar, F. Z., and Driscoll, D. J. (2004). Dynamic histone modifications mark sex chromosome inactivation and reactivation during mammalian spermatogenesis. Proc Natl Acad Sci U S A *101*, 16583-16587.

Khalil, A. M., and Driscoll, D. J. (2006). Histone H3 lysine 4 dimethylation is enriched on the inactive sex chromosomes in male meiosis but absent on the inactive X in female somatic cells. Cytogenet Genome Res *112*, 11-15.

Khil, P. P., Smirnova, N. A., Romanienko, P. J., and Camerini-Otero, R. D. (2004). The mouse X chromosome is enriched for sex-biased genes not subject to selection by meiotic sex chromosome inactivation. Nat Genet *36*, 642-646.

Kim, K. S., Cha, M. C., and Gerton, G. L. (2001). Mouse sperm protein sp56 is a component of the acrosomal matrix. Biol Reprod *64*, 36-43.

Kim, K. S., and Gerton, G. L. (2003). Differential release of soluble and matrix components: evidence for intermediate states of secretion during spontaneous acrosomal exocytosis in mouse sperm. Dev Biol *264*, 141-152.

Kim, M. Y., Ann, E. J., Kim, J. Y., Mo, J. S., Park, J. H., Kim, S. Y., Seo, M. S., and Park, H. S. (2007a). Tip60 histone acetyltransferase acts as a negative regulator of Notch1 signaling by means of acetylation. Mol Cell Biol *27*, 6506-6519.

Kim, S., Namekawa, S. H., Niswander, L. M., Ward, J. O., Lee, J. T., Bardwell, V. J., and Zarkower, D. (2007b). A mammal-specific Doublesex homolog associates with male sex chromatin and is required for male meiosis. PLoS Genet *3*, e62.

Kimura, T., Ito, C., Watanabe, S., Takahashi, T., Ikawa, M., Yomogida, K., Fujita, Y., Ikeuchi, M., Asada, N., Matsumiya, K.*, et al.* (2003). Mouse germ cell-less as an essential component for nuclear integrity. Mol Cell Biol *23*, 1304-1315.

Kleene, K. C. (2003). Patterns, mechanisms, and functions of translation regulation in mammalian spermatogenic cells. Cytogenet Genome Res *103*, 217-224.

Kleiman, S. E., Yogev, L., Gal-Yam, E. N., Hauser, R., Gamzu, R., Botchan, A., Paz, G., Yavetz, H., Maymon, B. B., Schreiber, L.*, et al.* (2003). Reduced human germ cell-less (HGCL) expression in azoospermic men with severe germinal cell impairment. J Androl *24*, 670-675.

Kohn, M. J., Kaneko, K. J., and DePamphilis, M. L. (2005). DkkL1 (Soggy), a Dickkopf family member, localizes to the acrosome during mammalian spermatogenesis. Mol Reprod Dev *71*, 516-522.

Koken, M. H., Hoogerbrugge, J. W., Jasper-Dekker, I., de Wit, J., Willemsen, R., Roest, H. P., Grootegoed, J. A., and Hoeijmakers, J. H. (1996). Expression of the ubiquitin-conjugating DNA repair enzymes HHR6A and B suggests a role in spermatogenesis and chromatin modification. Dev Biol *173*, 119-132.

Koopman, P., Gubbay, J., Vivian, N., Goodfellow, P., and Lovell-Badge, R. (1991). Male development of chromosomally female mice transgenic for *Sry*. Nature *351*, 117-121.

Kotaja, N., and Sassone-Corsi, P. (2007). The chromatoid body: a germ-cell-specific RNA-processing centre. Nat Rev Mol Cell Biol *8*, 85-90.

Krzanowska, H. (1966). Inheritance of reduced male fertility, connected with abnormal spermatozoa, in mice. Acta Biologica Cracoviensia *9*, 61-70.

Krzanowska, H. (1969). Factor responsible for spermatozoan head abnormality located on the Y chromosome in mouse. Genetical Research, Cambridge *13*, 17-24.

Krzanowska, H. (1971). Influence of Y chromosome on fertility in mice. In Proceedings of the International Symposium on the Genetics of the Spermatozoan, R. A. Beatty, and S. Gluecksohn-Waelsch, eds., pp. 370-386.

Krzanowska, H. (1976). Inheritance of sperm head abnormality types in mice: The role of the Y chromosome. Genetical Research, Cambridge *28*, 189-198.

Krzanowska, H. (1986). Interstrain competition amongst mouse spermatozoa inseminated in various proportions, as affected by the genotype of the Y chromosome. J Reprod Fertil *77*, 265-270.

Kusch, T., Florens, L., Macdonald, W. H., Swanson, S. K., Glaser, R. L., Yates, J. R., 3rd, Abmayr, S. M., Washburn, M. P., and Workman, J. L. (2004). Acetylation by Tip60 is required for selective histone variant exchange at DNA lesions. Science *306*, 2084-2087.

Kuwabara, T., Hsieh, J., Nakashima, K., Taira, K., and Gage, F. H. (2004). A small modulatory dsRNA specifies the fate of adult neural stem cells. Cell *116*, 779-793.

Lachner, M., O'Carroll, D., Rea, S., Mechtler, K., and Jenuwein, T. (2001). Methylation of histone H3 lysine 9 creates a binding site for HP1 proteins. Nature *410*, 116-120.

Lahn, B. T., and Page, D. C. (1997). Functional coherence of the human Y chromosome. Science *278*, 675-680.

Lahn, B. T., and Page, D. C. (1999). Four evolutionary strata on the human X chromosome. Science *286*, 964-967.

Lahn, B. T., Pearson, N. M., and Jegalian, K. (2001). The human Y chromosome, in the light of evolution. Nat Rev Genet *2*, 207-216.

Lamar, E. E., and Palmer, E. (1984). Y encoded species specific DNA in mice: evidence that the Y chromosome exists in two polymorphic forms in inbred strains. Cell *37*, 171-177.

Lammers, J. H. M., Offenberg, H. H., Van Aalderen, M., Vink, A. C. G., Dietrich, A. J. J., and Heyting, C. (1994). The gene encoding a major component of synaptonemal complexes of rat is related to X-linked lymphocyte-regulated genes. Mol Cell Biol *14*, 1137-1146.

Lanz, R. B., McKenna, N. J., Onate, S. A., Albrecht, U., Wong, J., Tsai, S. Y., Tsai, M. J., and O'Malley, B. W. (1999). A steroid receptor coactivator, SRA, functions as an RNA and is present in an SRC-1 complex. Cell *97*, 17-27.

Lanz, R. B., Razani, B., Goldberg, A. D., and O'Malley, B. W. (2002). Distinct RNA motifs are important for coactivation of steroid hormone receptors by steroid receptor RNA activator (SRA). Proc Natl Acad Sci U S A *99*, 16081-16086.

Laval, S. H., Glenister, P. H., Rasberry, C., Thornton, C. E., Mahadevaiah, S. K., Cooke, H. J., Burgoyne, P. S., and Cattanach, B. M. (1995). Y chromosome short arm-*Sxr* recombination in X*Sxr*/Y males causes deletion of *Rbm* and XY female sex reversal. Proc Natl Acad Sci USA *92*, 10403-10407.

Lemos, B., Araripe, L. O., and Hartl, D. L. (2008). Polymorphic Y chromosomes harbor cryptic variation with manifold functional consequences. Science *319*, 91-93.

Lercher, M. J., Urrutia, A. O., and Hurst, L. D. (2003). Evidence that the human X chromosome is enriched for male-specific but not female-specific genes. Mol Biol Evol *20*, 1113-1116.

Li, J., Hooker, G. W., and Roeder, G. S. (2006). Saccharomyces cerevisiae Mer2, Mei4 and Rec114 form a complex required for meiotic double-strand break formation. Genetics *173*, 1969-1981.

Liu, Q., Zerbinatti, C. V., Zhang, J., Hoe, H. S., Wang, B., Cole, S. L., Herz, J., Muglia, L., and Bu, G. (2007a). Amyloid precursor protein regulates brain apolipoprotein E and cholesterol metabolism through lipoprotein receptor LRP1. Neuron *56*, 66-78.

Liu, X., Wu, B., Szary, J., Kofoed, E. M., and Schaufele, F. (2007b). Functional sequestration of transcription factor activity by repetitive DNA. J Biol Chem *282*, 20868-20876.

Lu, B. Y., Emtage, P. C., Duyf, B. J., Hilliker, A. J., and Eissenberg, J. C. (2000). Heterochromatin protein 1 is required for the normal expression of two heterochromatin genes in Drosophila. Genetics *155*, 699-708.

Lyon, M. F. (1998). X-chromosome inactivation: a repeat hypothesis. Cytogenet Cell Genet *80*, 133-137.

Lyon, M. F. (2000). An answer to a complex problem: cloning the mouse t-complex responder. Mamm Genome *11*, 817-819.

Lyon, M. F. (2006). Do LINEs Have a Role in X-Chromosome Inactivation? J Biomed Biotechnol *2006*, 59746.

Lyttle, T. W. (1991). Segregation distorters. Annu Rev Genet *25*, 511-557.

Ma, J., and Ptashne, M. (1987). A new class of yeast transcriptional activators. Cell *51*, 113-119.

Maekawa, M., Ito, C., Toyama, Y., Suzuki-Toyota, F., Kimura, T., Nakano, T., and Toshimori, K. (2004). Stage-specific expression of mouse germ cell-less-1 (mGCL-1), and multiple deformations during mgcl-1 deficient spermatogenesis leading to reduced fertility. Arch Histol Cytol *67*, 335-347.

Maekawa, M., Kamimura, K., and Nagano, T. (1996). Peritubular myoid cells in the testis: their structure and function. Arch Histol Cytol *59*, 1-13.

Mahadevaiah, S. K., Odorisio, T., Elliott, D. J., Rattigan, A., Szot, M., Laval, S. H., Washburn, L. L., McCarrey, J. R., Cattanach, B. M., Lovell-Badge, R., and Burgoyne, P. S. (1998). Mouse homologues of the human *AZF* candidate gene *RBM* are expressed in spermatogonia and spermatids, and map to a Y deletion interval associated with a high incidence of sperm abnormalities. Hum Mol Gen *7*, 715-727.

Mahadevaiah, S. K., Turner, J. M. A., Baudat, F., Rogakou, E. P., de Boer, P., Blanco-Rodriguez, J., Jasin, M., Keeney, S., Bonner, W. M., and Burgoyne, P. S. (2001). Recombinational DNA double-strand breaks in mice precede synapsis. Nat Genet *27*, 271-276.

Mak, W., Baxter, J., Silva, J., Newall, A. E., Otte, A. P., and Brockdorff, N. (2002).
Mitotically stable association of polycomb group proteins eed and enx1 with the inactive x chromosome in trophoblast stem cells. Curr Biol *12*, 1016-1020.

Maniatis, T., Fritsch, E. F., and Sambrook, J. (1982). Molecular Cloning (New York, Cold Spring Harbour).

Marais, G., and Galtier, N. (2003). Sex chromosomes: how X-Y recombination stops. Curr Biol *13*, R641-643.

Mardon, G., and Page, D. C. (1989). The sex-determining region of the mouse Y chromosome encodes a protein with a highly acidic domain and 13 zinc fingers. Cell *56*, 765-770.

Masui, O., and Heard, E. (2006). RNA and protein actors in X-chromosome inactivation. Cold Spring Harb Symp Quant Biol *71*, 419-428.

Mazeyrat, S., Saut, N., Grigoriev, V., Mahadevaiah, S. K. M., Ojarikre, O. A., Rattigan, A., Bishop, C., Eicher, E. M., Mitchell, M. J., and Burgoyne, P. S. (2001). A Y-encoded subunit of the translation initiation factor Eif2 is essential for mouse spermatogenesis. Nat Genet *29*, 49-53.

McAllister, D., Merlo, X., and Lough, J. (2002). Characterization and expression of the mouse tat interactive protein 60 kD (TIP60) gene. Gene *289*, 169-176.

McKee, B. D., and Handel, M. A. (1993). Sex chromosomes, recombination, and chromatin conformation. Chromosoma (Berlin) *102*, 71-80.

McLaren, A. (2001). Mammalian germ cells: birth, sex, and immortality. Cell Struct Funct *26*, 119-122.

McLaren, A. (2003). Primordial germ cells in the mouse. Dev Biol *262*, 1-15.

McLaren, A., Simpson, E., Tomonari, K., Chandler, P., and Hogg, H. (1984). Male sexual differentiation in mice lacking H-Y antigen. Nature *312*, 552-555.

Melton, D. W., Konecki, D. S., Brennand, J., and Caskey, C. T. (1984). Structure, expression, and mutation of the hypoxanthine phophoribosyl transferase gene. Proc Natl Acad Sci USA *81*, 2147-2151.

Mendis-Handagama, S. M. (1997). Luteinizing hormone on Leydig cell structure and function. Histol Histopathol *12*, 869-882.

Mermoud, J. E., Popova, B., Peters, A. H., Jenuwein, T., and Brockdorff, N. (2002). Histone H3 lysine 9 methylation occurs rapidly at the onset of random X chromosome inactivation. Curr Biol *12*, 247-251.

Minty, A. J., Caravatti, M., Robert, B., Cohen, A., Daubas, P., Weydert, A., Gros, F., and Buckingham, M. E. (1981). Mouse actin mRNAs. Construction and characterization of a recombinant plasmid

molecule containing a complementary DNA transcript of mouse alpha-actin mRNA. J Biol Chem *256*, 1008-1014.

Mitchell, M., Woods, D. R., Wilcox, S. A., Graves, J. A. M., and Bishop, C. E. (1992). Marsupial Y chromosome encodes a homologue of the mouse Y-linked candidate spermatogenesis gene *Ube1y*. Nature *359*, 528-531.

Miyamoto, T., Hasuike, S., Yogev, L., Maduro, M. R., Ishikawa, M., Westphal, H., and Lamb, D. J. (2003). Azoospermia in patients heterozygous for a mutation in SYCP3. Lancet *362*, 1714-1719.

Montchamp-Moreau, C. (2006). Sex-ratio meiotic drive in Drosophila simulans: cellular mechanism, candidate genes and evolution. Biochem Soc Trans *34*, 562-565.

Moriwaki, K., Suh, D.-S., and Styrna, J. (1988). Genetic factors effecting sperm morphology in the mouse. Mouse News Letter *82*, 138.

Morrison, A. J., and Shen, X. (2005). DNA repair in the context of chromatin. Cell Cycle *4*, 568-571.

Mueller, J. I., Mahadevaiah, S. K., Park, P. J., Warburton, P. E., Page, D. C., and Turner, J. M. A. (2008). The mouse X chromosome is enriched for multicopy testis genes showing postmeiotic expression. Nat. Genetics. Advance online publication.

Muller, H. J. (1914). A Factor for the Fourth Chromosome of Drosophila. Science *39*, 906.

Murphy, W. J., Eizirik, E., Johnson, W. E., Zhang, Y. P., Ryder, O. A., and O'Brien, S. J. (2001). Molecular phylogenetics and the origins of placental mammals. Nature *409*, 614-618.

Najmabadi, H., Chai, N., Kapali, A., Subbarao, M. N., Bhasin, D., Woodhouse, E., Yen, P., and Bhasin, S. (1996). Genomic structure of a Y-specific ribonucleic acid binding motif-containing gene: a putative candidate for a subset of male infertility. J Clin Endo Metab *81*, 2159-2164.

Nallaseth, F. S., and Dewey, M. J. (1986). Moderately repeated mouse Y chromosomal sequence families present distinct types of organization and evolutionary change. Nucleic Acids Res *14*, 5295-5307.

Namekawa, S. H., Park, P. J., Zhang, L. F., Shima, J. E., McCarrey, J. R., Griswold, M. D., and Lee, J. T. (2006). Postmeiotic sex chromatin in the male germline of mice. Curr Biol *16*, 660-667.

Namekawa, S. H., VandeBerg, J. L., McCarrey, J. R., and Lee, J. T. (2007). Sex chromosome silencing in the marsupial male germ line. Proc Natl Acad Sci U S A *104*, 9730-9735.

Navin, A., Prekeris, R., Lisitsyn, N. A., Sonti, M. M., Grieco, D. A., Narayanswami, S., Lander, E. S., and Simpson, E. M. (1996). Mouse Y-specific repeats isolated by whole chromosome representational difference analysis. Genomics *36*, 349-353.

Nishida, K. M., Saito, K., Mori, T., Kawamura, Y., Nagami-Okada, T., Inagaki, S., Siomi, H., and Siomi, M. C. (2007). Gene silencing mechanisms mediated by Aubergine piRNA complexes in Drosophila male gonad. RNA *13*, 1911-1922.

Nishioka, Y. (1989). Genome comparison in the genus Mus: a study with B1, MIF(mouse interspersed fragment), centromeric and Y chromosomal repetitive sequences. Cytogen Cell Genet *50*, 195-200.

Nishioka, Y., and Lamothe, E. (1986). Isolation and characterization of a mouse Y chromosomal repetitive sequence. Genetics *113*, 417-432.

Norton, A. W., Hosier, S., Terew, J. M., Li, N., Dhingra, A., Vardi, N., Baehr, W., and Cote, R. H. (2005). Evaluation of the 17-kDa prenyl-binding protein as a regulatory protein for phototransduction in retinal photoreceptors. J Biol Chem *280*, 1248-1256.

Oakberg, E. F. (1956a). A description of spermiogenesis in the mouse and its use in analysis of the cycle of the seminiferous epithelium and germ cell renewal. Am J Anat *99*, 391-413.

Oakberg, E. F. (1956b). Duration of spermatogenesis in the mouse and timing of stages of the cycle of the seminiferous epithelium. Am J Anat *99*, 507-516.

Odorisio, T., Mahadevaiah, S. K., McCarrey, J. R., and Burgoyne, P. S. (1996). Transcriptional analysis of the candidate spermatogenesis gene *Ube1y* and of the closely related *Ube1x* shows that they are coexpressed in spermatogonia and spermatids but are repressed in pachytene spermatocytes. Dev Biol *180*, 336-343.

Oh, B., Hampl, A., Eppig, J. J., Solter, D., and Knowles, B. B. (1998). SPIN, a substrate in the MAP kinase pathway in mouse oocytes. Mol Reprod Dev *50*, 240-249.
Ohno, S. (1967). Sex Chromosomes and Sex-linked Genes (New York, Springer-Verlag).

Ohta, T. (2002). Near-neutrality in evolution of genes and gene regulation. Proc Natl Acad Sci U S A *99*, 16134-16137.

Oka, A., Mita, A., Sakurai-Yamatani, N., Yamamoto, H., Takagi, N., Takano-Shimizu, T., Toshimori, K., Moriwaki, K., and Shiroishi, T. (2004). Hybrid breakdown caused by substitution of the X chromosome between two mouse subspecies. Genetics *166*, 913-924.

Okada, Y., Scott, G., Ray, M. K., Mishina, Y., and Zhang, Y. (2007). Histone demethylase JHDM2A is critical for Tnp1 and Prm1 transcription and spermatogenesis. Nature.

Owusu-Daaku, K. O., Butler, R. D., and Wood, R. J. (2007). Meiotic drive by the Y-linked D gene in Aedes aegypti (L.) (Diptera: Culicidae) is associated with disruption of spermiogenesis, leading to premature senescence of spermatozoa. Arthropod Struct Dev *36*, 233-243.

Palmer, D. K., O'Day, K., and Margolis, R. L. (1990a). The centromere specific histone CENP-A is selectively retained in discrete foci in mammalian sperm nuclei. Chromosoma *100*, 32-36.

Palmer, M. S., Berta, P., Sinclair, A. H., Pym, B., and Goodfellow, P. N. (1990b). Comparison of human *ZFY* and *ZFX* transcripts. Genetics *87*, 1681-1685.

Parra, M. T., Viera, A., Gomez, R., Page, J., Carmena, M., Earnshaw, W. C., Rufas, J. S., and Suja, J. A. (2003). Dynamic relocalization of the chromosomal passenger complex proteins inner centromere protein (INCENP) and aurora-B kinase during male mouse meiosis. J Cell Sci *116*, 961-974.

Partridge, L., and Hurst, L. D. (1998). Sex and conflict. Science *281*, 2003-2008.

Peschon, J. J., Behringer, R. R., Brinster, R. L., and Palmiter, R. D. (1987). Spermatid-specific expression of protamine 1 in transgenic mice. Proc. Natl. Adac. Sci. U S A *84*, 5316-5319

Peters, A. H., Mermoud, J. E., O'Carroll, D., Pagani, M., Schweizer, D., Brockdorff, N., and Jenuwein, T. (2002). Histone H3 lysine 9 methylation is an epigenetic imprint of facultative heterochromatin. Nat Genet *30*, 77-80.

Pittman, D. L., Cobb, J., Schimenti, K. J., Wilson, L. A., Cooper, D. M., Brignull, E., Handel, M. A., and Schimenti, J. C. (1998). Meiotic prophase arrest with failure of chromosome synapsis in mice deficient for Dmc1, a germline-specific RecA homolog. Mol Cell *1*, 697-705.

Piwien Pilipuk, G., Galigniana, M. D., and Schwartz, J. (2003). Subnuclear localization of C/EBP beta is regulated by growth hormone and dependent on MAPK. J Biol Chem *278*, 35668-35677.

Platero, J. S., Csink, A. K., Quintanilla, A., and Henikoff, S. (1998). Changes in chromosomal localization of heterochromatin-binding proteins during the cell cycle in Drosophila. J Cell Biol *140*, 1297-1306.

Plath, K., Fang, J., Mlynarczyk-Evans, S. K., Cao, R., Worringer, K. A., Wang, H., de la Cruz, C. C., Otte, A. P., Panning, B., and Zhang, Y. (2003). Role of histone H3 lysine 27 methylation in X inactivation. Science *300*, 131-135.

Plath, K., Talbot, D., Hamer, K. M., Otte, A. P., Yang, T. P., Jaenisch, R., and Panning, B. (2004). Developmentally regulated alterations in Polycomb repressive complex 1 proteins on the inactive X chromosome. J Cell Biol *167*, 1025-1035.

Prado, V. F., Lee, C.-H., Zahed, L., Vekemans, M., and Nishioka, Y. (1992). Molecular characterization of a mouse Y chromosomal repetitive sequence that detects transcripts in the testis. Cytogen Cell Genet *61*, 87-90.

Qi, D., Jin, H., Lilja, T., and Mannervik, M. (2006). Drosophila Reptin and other TIP60 complex components promote generation of silent chromatin. Genetics *174*, 241-251.

Quintana-Murci, L., and Fellous, M. (2001). The Human Y Chromosome: The Biological Role of a "Functional Wasteland". J Biomed Biotechnol *1*, 18-24.

Raefski, A. S., and O'Neill, M. J. (2005). Identification of a cluster of X-linked imprinted genes in mice. Nat Genet *37*, 620-624.

Reynard, L. N., Turner, J. M., Cocquet, J., Mahadevaiah, S. K., Touré, A., Hoog, C., and Burgoyne, P. S. (2007). Expression Analysis of the Mouse Multi-Copy X-Linked Gene Xlr-Related, Meiosis-Regulated (Xmr), Reveals That Xmr Encodes a Spermatid-Expressed Cytoplasmic Protein, SLX/XMR. Biol Reprod *77*, 329-335.

Rice, W. R. (1984). Sex chromosomes and the evolution of sexual dimorphism. Evolution *38*, 735-742

Rice, W. R., and Friberg, U. (2008). Genetics. Functionally degenerate--Y not so? Science *319*, 42-43.

Richler, C., Ast, G., Goitein, R., Wahrman, J., Sperling, R., and Sperling, J. (1994). Splicing components are excluded from the transcriptionally inactive XY body in male meiotic nuclei. Mol Biol Cell *5*, 1341-1352.

Roest, H. P., van Klaveren, J., de Wit, J., van Gurp, C. G., Koken, M. H., Vermey, M., van Roijen, J. H., Hoogerbrugge, J. W., Vreeburg, J. T., Baarends, W. M., *et al.* (1996). Inactivation of the HR6B ubiquitin-conjugating DNA repair enzyme in mice causes male sterility associated with chromatin modification. Cell *86*, 799-810.

Rohozinski, J., Agoulnik, A. I., Boettger-Tong, H. L., and Bishop, C. E. (2002). Successful targeting of mouse Y chromosome genes using a site-directed insertion vector. Genesis *32*, 1-7.

Rohozinski, J., and Bishop, C. E. (2004). The mouse juvenile spermatogonial depletion (jsd) phenotype is due to a mutation in the X-derived retrogene, mUtp14b. Proc Natl Acad Sci U S A *101*, 11695-11700.

Ross, M. T., Grafham, D. V., Coffey, A. J., Scherer, S., McLay, K., Muzny, D., Platzer, M., Howell, G. R., Burrows, C., Bird, C. P., *et al.* (2005). The DNA sequence of the human X chromosome. Nature *434*, 325-337.

Rougeulle, C., Chaumeil, J., Sarma, K., Allis, C. D., Reinberg, D., Avner, P., and Heard, E. (2004). Differential histone H3 Lys-9 and Lys-27 methylation profiles on the X chromosome. Mol Cell Biol *24*, 5475-5484.

Rousseaux, S., Caron, C., Govin, J., Lestrat, C., Faure, A. K., and Khochbin, S. (2005). Establishment of male-specific epigenetic information. Gene *345*, 139-153.

Rozen, S., Skaletsky, H., Marszalek, J. D., Minx, P. J., Cordum, H. S., Waterston, R. H., Wilson, R. K., and Page, D. C. (2003). Abundant gene conversion between arms of palindromes in human and ape Y chromosomes. Nature *423*, 873-876.

Russell, L. D., Ettlin, R. A., Sinha Hikim, A. P., and Clegg, E. D. (2000). Histological and histopathological evalution of the testis. Cache River Press.

Saifi, G. M., and Chandra, H. S. (1999). An apparent excess of sex- and reproduction-related genes on the human X chromosome. Proc Biol Sci *266*, 203-209.

Sanders, S. L., Portoso, M., Mata, J., Bahler, J., Allshire, R. C., and Kouzarides, T. (2004). Methylation of histone H4 lysine 20 controls recruitment of Crb2 to sites of DNA damage. Cell *119*, 603-614.

Sandstedt, S. A., and Tucker, P. K. (2004). Evolutionary strata on the mouse X chromosome correspond to strata on the human X chromosome. Genome Res *14*, 267-272.

Schimenti, J. (2005). Synapsis or silence. Nat Genet *37*, 11-13.

Schneider-Gädicke, A., Beer-Romero, P., Brown, L. G., Nussbaum, R., and Page, D. C. (1989). The ZFX gene on the human X chromosome escapes X-inactivation and is closely related to ZFY, the putative sex determinant on the Y chromosome. Cell *57*, 1247-1258.

Schultz, N., Hamra, F. K., and Garbers, D. L. (2003). A multitude of genes expressed solely in meiotic or postmeiotic spermatogenic cells offers a myriad of contraceptive targets. Proc Natl Acad Sci U S A *100*, 12201-12206.

Shahjahan, R. M., Rendon, P. A., Cook, L. M., and Wood, R. J. (2006). Male biased sex ratio in the Mediterranean fruit fly Ceratitis capitata, an example of Y-chromosome meiotic drive. Heredity *96*, 464-470.

Shamovsky, I., Ivannikov, M., Kandel, E. S., Gershon, D., and Nudler, E. (2006). RNA-mediated response to heat shock in mammalian cells. Nature *440*, 556-560.

Shannon, M., and Handel, M. A. (1993). Expression of the *Hprt* gene during spermatogenesis: implications for sex-chromosome inactivation. Biol Reprod *49*, 770-778.

Shestakova, E. A., Mansuroglu, Z., Mokrani, H., Ghinea, N., and Bonnefoy, E. (2004). Transcription factor YY1 associates with pericentromeric gamma-satellite DNA in cycling but not in quiescent (G0) cells. Nucleic Acids Res *32*, 4390-4399.

Shibata, N., Tsunekawa, N., Okamoto-Ito, S., Akasu, R., Tokumasu, A., and Noce, T. (2004). Mouse RanBPM is a partner gene to a germline specific RNA helicase, mouse vasa homolog protein. Mol Reprod Dev *67*, 1-7.

Shima, J. E., McLean, D. J., McCarrey, J. R., and Griswold, M. D. (2004). The murine testicular transcriptome: characterizing gene expression in the testis during the progression of spermatogenesis. Biol Reprod *71*, 319-330.

Siegel, J. N., Turner, C. A., Klinman, D. M., Wilkinson, M., Steinberg, A. D., MacLeod, C. L., Paul, W. E., Davis, M. M., and Cohen, D. I. (1987). Sequence analysis and expression of an X-linked, lymphocyte-regulated gene family (XLR). J Exp Med *166*, 1702-1715.

Silva, J., Mak, W., Zvetkova, I., Appanah, R., Nesterova, T. B., Webster, Z., Peters, A. H., Jenuwein, T., Otte, A. P., and Brockdorff, N. (2003). Establishment of histone h3 methylation on the inactive X chromosome requires transient recruitment of Eed-Enx1 polycomb group complexes. Dev Cell *4*, 481-495.

Silver, D. P., Dimitrov, S. D., Feunteun, J., Gelman, R., Drapkin, R., Lu, S. D., Shestakova, E., Velmurugan, S., Denunzio, N., Dragomir, S., *et al.* (2007). Further evidence for BRCA1 communication with the inactive X chromosome. Cell *128*, 991-1002.

Simpson, E. M., and Page, D. C. (1991). An interstitial deletion in mouse Y chromosomal DNA created a transcribed Zfy fusion gene. Genomics *11*, 601-608.

Singh, L., Wadhwa, R., Naidu, S., Nagaraj, R., and Ganesan, M. (1994). Sex- and tissue-specific Bkm(GATA)-binding protein in the germ cells of heterogametic sex. J Biol Chem *269*, 25321-25327.

Siruntawineti, J., Yamagata, K., Nakanishi, T., and Baba, T. (2002). Occurrence of small, round vesicles in the acrosome of elongating spermatids from a mous mutant line with partial deletion of the Y chromosome. J Reprod Dev *48*, 513-521.

Skaletsky, H., Kuroda-Kawaguchi, T., Minx, P. J., Cordum, H. S., Hillier, L., Brown, L. G., Repping, S., Pyntikova, T., Ali, J., Bieri, T., *et al.* (2003). The male-specific region of the human Y chromosome is a mosaic of discrete sequence classes. Nature *423*, 825-837.

Skinner, M. K., Norton, J. N., Mullaney, B. P., Rosselli, M., Whaley, P. D., and Anthony, C. T. (1991). Cell-cell interactions and the regulation of testis function. Ann N Y Acad Sci *637*, 354-363.

Small, C. L., Shima, J. E., Uzumcu, M., Skinner, M. K., and Griswold, M. D. (2005). Profiling gene expression during the differentiation and development of the murine embryonic gonad. Biol Reprod *72*, 492-501.

Solari, A. J. (1974). The behaviour of the XY pair in mammals. Int Rev Cytol *38*, 273-317.

Stapleton, W., Das, S., and McKee, B. D. (2001). A role of the Drosophila homeless gene in repression of Stellate in male meiosis. Chromosoma *110*, 228-240.

Styrna, J., Bilinska, B., and Krzanowskaa, H. (2002). The effect of a partial Y chromosome deletion in B10.BR-Ydel mice on testis morphology, sperm quality and efficiency of fertilization. Reprod Fertil Dev *14*, 101-108.

Styrna, J., Imai, H. T., and Moriwaki, K. (1991a). An increased level of sperm abnormalities in mice with a partial deletion of the Y chromosome. Genet Res *57*, 195-199.

Styrna, J., Kilarski, W., and Krzanowska, H. (2003). Influence of the CBA genetic background on sperm morphology and fertilization efficiency in mice with a partial Y chromosome deletion. Reproduction *126*, 579-588.

Styrna, J., Klag, J., and Moriwaki, K. (1991b). Influence of partial deletion of the Y chromosome on mouse sperm phenotype. J Reprod Fertil *92*, 187-195.

Styrna, J., and Krzanowska, H. (1995). Sperm select penetration test reveals differences in sperm quality in strains with different Y chromosome genotype in mice. Arch Androl *35*, 111-118.

Sun, Y., Xu, Y., Roy, K., and Price, B. D. (2007). DNA damage-induced acetylation of lysine 3016 of ATM activates ATM kinase activity. Mol Cell Biol *27*, 8502-8509.

Sutcliffe, M. J., and Burgoyne, P. S. (1989). Analysis of the testes of H-Y negative XOSxr^{b} mice suggests that the spermatogenesis gene (*Spy*) acts during the differentiation of the A spermatogonia. Development *107*, 373-380.

Szot, M., Grigoriev, V., Mahadevaiah, S. K., Ojarikre, O. A., Tour, A., Von Glasenapp, E., Rattigan, A., Turner, J. M., Elliott, D. J., and Burgoyne, P. S. (2003). Does Rbmy have a role in sperm development in mice? Cytogenet Genome Res *103*, 330-336.

Tam, P. P. L., and Snow, M. H. L. (1981). Profiferation and migration of primordial germ cells during compensatory growth in mouse embryos. J Embryol exp Morph *64*, 133-147.

Tang, Q. Q., and Lane, M. D. (1999). Activation and centromeric localization of CCAAT/enhancer-binding proteins during the mitotic clonal expansion of adipocyte differentiation. Genes Dev *13*, 2231-2241.

Tao, Y., Araripe, L., Kingan, S. B., Ke, Y., Xiao, H., and Hartl, D. L. (2007a). A sex-ratio meiotic drive system in Drosophila simulans. II: an X-linked distorter. PLoS Biol *5*, e293.

Tao, Y., Masly, J. P., Araripe, L., Ke, Y., and Hartl, D. L. (2007b). A sex-ratio meiotic drive system in Drosophila simulans. I: an autosomal suppressor. PLoS Biol *5*, e292.

Taylor, J. E., and Jaenike, J. (2002). Sperm competition and the dynamics of X chromosome drive: stability and extinction. Genetics *160*, 1721-1731.

Touré, A., Clemente, E. J., Ellis, P., Mahadevaiah, S. K., Ojarikre, O. A., Ball, P. A., Reynard, L., Loveland, K. L., Burgoyne, P. S., and Affara, N. A. (2005). Identification of novel Y chromosome encoded transcripts by testis transcriptome analysis of mice with deletions of the Y chromosome long arm. Genome Biol *6*, R102.

Touré, A., Clemente, E. J., Ellis, P., Mahadevaiah, S. K., Ojarikre, O. A., Ball, P. A. F., Reynard, L., Loveland, K. L., Burgoyne, P. S., and Affara, N. A. (2005). Identification of novel Y chromosome encoded transcripts by testis transcriptome analysis of mice with deletions of the Y chromosome long arm. Genome Biology *6*, R102.

Touré, A., Grigoriev, V., Mahadevaiah, S. K., Rattigan, A., Ojarikre, O. A., and Burgoyne, P. S. (2004a). A protein encoded by a member of the multicopy Ssty gene family located on the long arm of the mouse Y chromosome is expressed during sperm development. Genomics *83*, 140-147.

Touré, A., Szot, M., Mahadevaiah, S. K., Rattigan, A., Ojarikre, O. A., and Burgoyne, P. S. (2004b). A new deletion of the mouse Y chromosome long arm associated with loss of *Ssty* expression, abnormal sperm development and sterility. Genetics *166*, 901-912.

Tsuchiya, K., Reijo, R., Page, D. C., and Disteche, C. (1995). Gonadoblastoma: molecular definition of the susceptibility region on the Y chromosome. Am J Hum Genet *57*, 1400-1407.

Tulsiani, D. R. (2003). Glycan modifying enzymes in luminal fluid of rat epididymis: are they involved in altering sperm surface glycoproteins during maturation? Microsc Res Tech *61*, 18-27.

Turner, J. M. (2007). Meiotic sex chromosome inactivation. Development *134*, 1823-1831.

Turner, J. M. (2000). An investigation into the role of sex chromosome synapsis in meiotic sex chromosome inactivation and fertility. University College London pHD thesis.

Turner, J. M., Aprelikova, O., Xu, X., Wang, R., Kim, S., Chandramouli, G. V., Barrett, J. C., Burgoyne, P. S., and Deng, C. X. (2004). BRCA1, histone H2AX phosphorylation, and male meiotic sex chromosome inactivation. Curr Biol *14*, 2135-2142.

Turner, J. M., Mahadevaiah, S. K., Ellis, P. J., Mitchell, M. J., and Burgoyne, P. S. (2006). Pachytene asynapsis drives meiotic sex chromosome inactivation and leads to substantial postmeiotic repression in spermatids. Dev Cell *10*, 521-529.

Turner, J. M., Mahadevaiah, S. K., Fernandez-Capetillo, O., Nussenzweig, A., Xu, X., Deng, C. X., and Burgoyne, P. S. (2005). Silencing of unsynapsed meiotic chromosomes in the mouse. Nat Genet *37*, 41-47.

Turner, J. M. A., Mahadevaiah, S. K., Benavente, R., Offenberg, H. H., Heyting, C., and Burgoyne, P. S. (2000). Analysis of male meiotic "sex-body" proteins during XY female meiosis provides new insights into their functions. Chromosoma *109*, 426-432.

Turner, J. M. A., Mahadevaiah, S. K., Elliott, D. J., Garchon, H. J., Pehrson, J. R., Jaenisch, R., and Burgoyne, P. S. (2002). Meiotic sex chromosome inactivation in male mice with targeted disruptions of Xist. J Cell Sci *115*, 4097-4105.

Vallender, E. J., and Lahn, B. T. (2004). How mammalian sex chromosomes acquired their peculiar gene content. Bioessays *26*, 159-169.

van der Heijden, G. W., Derijck, A. A., Posfai, E., Giele, M., Pelczar, P., Ramos, L.,
Wansink, D. G., van der Vlag, J., Peters, A. H., and de Boer, P. (2007). Chromosome-wide nucleosome replacement and H3.3 incorporation during mammalian meiotic sex chromosome inactivation. Nat Genet *39*, 251-258.

Vincent-Salomon, A., Ganem-Elbaz, C., Manie, E., Raynal, V., Sastre-Garau, X., Stoppa-Lyonnet, D., Stern, M. H., and Heard, E. (2007). X inactive-specific transcript RNA coating and genetic instability of the X chromosome in BRCA1 breast tumors. Cancer Res *67*, 5134-5140.

Vollrath, D., Foote, S., Hilton, A., Brown, L. G., Beer-Romero, P., Bogan, J. S., and Page, D. C. (1992). The human Y chromosome: A 43-interval map based on naturally occurring deletions. Science *258*, 52-59.

Voolstra, C., Tautz, D., Farbrother, P., Eichinger, L., and Harr, B. (2007). Contrasting evolution of expression differences in the testis between species and subspecies of the house mouse. Genome Res *17*, 42-49.

Wang, P. J. (2004). X chromosomes, retrogenes and their role in male reproduction. Trends Endocrinol Metab *15*, 79-83.

Wang, P. J., McCarrey, J. R., Yang, F., and Page, D. C. (2001). An abundance of X-linked genes expressed in spermatogonia. Nat Genet *27*, 422-426.

Wang, P. J., Page, D. C., and McCarrey, J. R. (2005a). Differential expression of sex-linked and autosomal germ-cell-specific genes during spermatogenesis in the mouse. Hum Mol Genet *14*, 2911-2918.

Wang, P. J., and Pan, J. (2007). The role of spermatogonially expressed germ cell-specific genes in mammalian meiosis. Chromosome Res *15*, 623-632.

Wang, X. L., Mei, J., Sun, M., Hong, Y. H., and Gui, J. F. (2005b). Identification of three duplicated Spin genes in medaka (Oryzias latipes). Gene *350*, 99-106.

Wang, X. L., Sun, M., Mei, J., and Gui, J. F. (2005c). Identification of a Spindlin homolog in gibel carp (Carassius auratus gibelio). Comp Biochem Physiol B Biochem Mol Biol *141*, 159-167.

Ward, I., Kim, J. E., Minn, K., Chini, C. C., Mer, G., and Chen, J. (2006). The tandem BRCT domain of 53BP1 is not required for its repair function. J Biol Chem.

Ward, M. A., and Burgoyne, P. S. (2006). The Effects of Deletions of the Mouse Y Chromosome Long Arm on Sperm Function - Intracytoplasmic Sperm Injection (ICSI) - Based Analysis. Biol Reprod *74*, 652-658.

Wassarman, P. M., Jovine, L., Litscher, E. S., Qi, H., and Williams, Z. (2004). Egg-sperm interactions at fertilization in mammals. Eur J Obstet Gynecol Reprod Biol *115 Suppl 1*, S57-60.

Waters, P. D., Wallis, M. C., and Marshall Graves, J. A. (2007). Mammalian sex--Origin and evolution of the Y chromosome and SRY. Semin Cell Dev Biol *18*, 389-400.

Welshons, W. J., and Russell, L. B. (1959) The Y-chromosome as the bearer of male determining factors in the mouse. Proc Natl Acad Sci U S A *45,* 560-566.

Willingham, A. T., Orth, A. P., Batalov, S., Peters, E. C., Wen, B. G., Aza-Blanc, P., Hogenesch, J. B., and Schultz, P. G. (2005). A strategy for probing the function of noncoding RNAs finds a repressor of NFAT. Science *309*, 1570-1573.

Wu, C. I., and Xu, E. Y. (2003). Sexual antagonism and X inactivation--the SAXI hypothesis. Trends Genet *19*, 243-247.

Wykes, S. M., and Krawetz, S. A. (2003). The structural organization of sperm chromatin. J Biol Chem *278*, 29471-29477.

Wylie, C. C., and Heasman, J. (1993). Migration, proliferation, and potency of primordial germ cells. Seminars in Developmental Biology *4*, 161-170.

Wyrobek, A. J. (1979). Changes in mammalian sperm morphology after X-ray and chemical exposures. Genetics *92*, s105-119.

Xian, M., Azuma, S., Naito, K., Kunieda, T., Moriwaki, K., and Toyoda, Y. (1992). Effect of a partial deletion of Y chromosome on in vitro fertilizing ability of mouse spermatozoa. Biol Reprod *47*, 549-553.

Yang, F., De La Fuente, R., Leu, N. A., Baumann, C., McLaughlin, K. J., and Wang, P. J. (2006). Mouse SYCP2 is required for synaptonemal complex assembly and chromosomal synapsis during male meiosis. J Cell Biol *173*, 497-507.

Yasuhara, J. C., and Wakimoto, B. T. (2006). Oxymoron no more: the expanding world of heterochromatic genes. Trends Genet *22*, 330-338.

Yoshida, K., Kondoh, G., Matsuda, Y., Habu, T., Nishimune, Y., and Morita, T. (1998). The mouse RecA-like gene Dmc1 is required for homologous chromosome synapsis during meiosis. Mol Cell *1*, 707-718.

Yoshinaga, K., and Toshimori, K. (2003). Organization and modifications of sperm acrosomal molecules during spermatogenesis and epididymal maturation. Microsc Res Tech *61*, 39-45.

Yuan, L., Liu, J.-G., Zhao, J., Brundell, E., Daneholt, B., and Höög, C. (2000). The murine *SCP3* gene is required for synaptonemal complex assembly, chromosome synapsis, and male fertility. Mol Cell *5*, 73-83.

Zalensky, A. O., Siino, J. S., Gineitis, A. A., Zalenskaya, I. A., Tomilin, N. V., Yau, P., and Bradbury, E. M. (2002). Human testis/sperm-specific histone H2B (hTSH2B). Molecular cloning and characterization. J Biol Chem *277*, 43474-43480.

Zhang, H., Liu, X. H., Zhang, K., Chen, C. K., Frederick, J. M., Prestwich, G. D., and Baehr, W. (2004). Photoreceptor cGMP phosphodiesterase delta subunit (PDEdelta) functions as a prenyl-binding protein. J Biol Chem *279*, 407-413.

Zofall, M., and Grewal, S. I. (2006). Swi6/HP1 recruits a JmjC domain protein to facilitate transcription of heterochromatic repeats. Mol Cell *22*, 681-692.